



## City Research Online

### City, University of London Institutional Repository

---

**Citation:** McNamara, A.M. (2001). Influence of heave reducing piles on ground movements around excavations. (Unpublished Doctoral thesis, City University London)

This is the accepted version of the paper.

This version of the publication may differ from the final published version.

---

**Permanent repository link:** <https://openaccess.city.ac.uk/id/eprint/8280/>

**Link to published version:**

**Copyright:** City Research Online aims to make research outputs of City, University of London available to a wider audience. Copyright and Moral Rights remain with the author(s) and/or copyright holders. URLs from City Research Online may be freely distributed and linked to.

**Reuse:** Copies of full items can be used for personal research or study, educational, or not-for-profit purposes without prior permission or charge. Provided that the authors, title and full bibliographic details are credited, a hyperlink and/or URL is given for the original metadata page and the content is not changed in any way.

INFLUENCE OF HEAVE REDUCING PILES  
ON  
GROUND MOVEMENTS AROUND EXCAVATIONS

by

Andrew Martin McNamara

A dissertation submitted for the Degree of  
Doctor of Philosophy

City University, London  
Geotechnical Engineering Research Centre  
Department of Aeronautical Civil and Mechanical Engineering

May 2001

## CONTENTS

Page No.

LIST OF TABLES	vii
LIST OF FIGURES	viii
ACKNOWLEDGEMENTS	xxiii
DECLARATION	xxiv
ABSTRACT	xxv
LIST OF SYMBOLS	xxvi

## CHAPTER 1 INTRODUCTION

1.1	Background	1
1.2	Methodology	3
1.3	Experimental work	3
1.3.1	Centrifuge modelling	3
1.3.2	Numerical modelling	5
1.4	Summary of the thesis	5

## CHAPTER 2 LITERATURE REVIEW

2.1	Mechanisms of ground movement	7
2.2	Vertical stress relief	8
2.3	Earth pressure at rest	9
2.4	Horizontal stress relief and ground movements associated with wall installation	11
2.5	Field studies of ground movement associated with excavation	16
2.6	Numerical studies of ground movement	22
2.7	Centrifuge modelling	25
2.8	Enhanced soil stiffness below excavation formation	27

2.9	Case study of a 24m deep excavation incorporating top down construction at the site of the former Knightsbridge Crown Court	30
2.9.1	Introduction	30
2.9.2	Numerical analyses	31
2.9.3	Comparison with field measurements	33
2.10	Summary	36

### CHAPTER 3 CENTRIFUGE MODEL TESTING

3.1	Principles of centrifuge modelling	38
3.2	Scaling laws	39
3.3	Errors in centrifuge modelling	41
3.3.1	Radial acceleration field	41
3.3.2	Grain size effects	42
3.4	Boundary effects	43
3.5	The geotechnical centrifuge	44
3.6	Model design requirements	45
3.7	Apparatus design development	46
3.8	Model piles	54
3.9	Stress history of soil used in tests	57
3.10	Sample preparation	59
3.11	Model making	61
3.12	Testing	64
3.13	Digital image analysis	66
3.14	Summary	67

### CHAPTER 4 EXPERIMENTAL WORK

4.1	Details of tests	68
-----	------------------	----



4.2	Observations and results	72
4.2.1	Tests AM10, AM11 and AM12	72
4.2.2	Tests AM2, AM9 and AM14	74
4.2.3	Tests AM6 and AM15	78
4.2.4	Tests AM7 and AM13	80
4.2.5	Tests AM5 and AM17	83
4.2.6	Test AM19	84
4.3	Retaining wall displacements	85
4.4	Comparison of image processing and LVDT measurements of retained surface displacements	86
4.5	Pore pressures	90
4.6	Prop loads	91
4.7	Summary	92
4.7.1	Deep embedment walls	92
4.7.2	Shallow embedment walls	93

## CHAPTER 5 NUMERICAL ANALYSIS

5.1	Introduction	94
5.2	Details of preliminary finite element analyses to assist in determining a suitable stress history for the centrifuge model tests	95
5.3	Observations and results of a series of finite element analyses of the centrifuge model tests	99
5.3.1	Datum analyses in which the duration of the simulated excavation was varied	100
5.3.2	A shallow embedded wall	101
5.3.3	The effect of prop stiffness	102
5.3.4	The effect of piles on vertical displacements at excavation formation level and retained ground surface	104
5.3.5	Horizontal and retaining wall displacements	106

5.4	Discussion	108
5.5	Summary	109

## CHAPTER 6 DISCUSSION

6.1	Introduction	112
6.2	The development of heave during the simulated excavation	113
6.2.1	Soil behaviour on unloading	113
6.2.2	Test results from deeply embedded walls	115
6.2.3	Test results from shallow embedded walls	118
6.3	Settlement at the retained ground surface	120
6.3.1	Introduction	120
6.3.2	Test results	121
6.4	Prop loads and horizontal displacements	123
6.4.1	Introduction	123
6.4.2	Test results	124
6.5	Consideration of the test results within the context of existing frameworks	126
6.6	Consideration of the test results with field monitoring data and associated numerical analyses predictions	128
6.7	Summary	129

## CHAPTER 7 SUMMARY, CONCLUSIONS AND RECOMMENDATIONS FOR FURTHER WORK

7.1	Introduction	131
7.2	Experimental procedure	131
7.3	Conclusions	133
7.4	Limitations and implications of the results	136
7.5	Recommendations for further research	137

References

138

Tables

Figures

## LIST OF TABLES

Table 2.1	Summary of finite element analyses carried out prior to construction of a deep basement at the site of the former Knightsttsbridge Crown Court including predictions of maximum vertical and horizontal displacements.
Table 3.1	Scale factors for centrifuge tests on model diaphragm walls. (after Powrie 1986).
Table 4.1	Summary of experimental work.
Table 4.2	Details of tests conducted showing development of experimental technique and with comments on performance of apparatus.
Table 4.3	Comparison of spring stiffness of props in centrifuge tests with numerical analyses and excavations in London Clay.
Table 5.1	Details of values assigned to soil parameters used in numerical analyses.
Table 5.2	Details of numerical analyses of centrifuge model tests carried out by Kopsalidou (2000).

## LIST OF FIGURES

- Figure 2.1 Typical patterns of magnitude of displacement behind retaining walls (Burland et al, 1979).
- Figure 2.2 Soil response to unloading caused by excavation (Burland et al, 1979).
- Figure 2.3 Influence of stress history on  $K_0$  (Burland et al, 1979).
- Figure 2.4 Influence of stress history on  $K_0$  (Mayne and Kulhawy, 1982).
- Figure 2.5 Influence of stress history on  $K_0$  and  $\sigma'_h$  in heavily overconsolidated clay (Burland et al, 1979).
- Figure 2.6 Stress changes with time caused by bored pile installation (Anderson et al, 1985).
- Figure 2.7 Stress changes during diaphragm wall installation (Symons and Carder, 1993).
- Figure 2.8 Stress changes during bored pile wall installation (Symons and Carder, 1993).
- Figure 2.9 Change in total horizontal stress with time of distribution of the total horizontal stress in the soil 0.6m from the diaphragm wall at Bell Common at various stages of excavation (Tedd et al, 1984).
- Figure 2.10 Distribution of the total horizontal stress in the soil with distance from back of the wall (Tedd et al, 1984).
- Figure 2.11 Mobilised friction angle  $\phi'_{mob}$  against shear strain  $\epsilon_s$ , during trench excavation and concreting (a) tests with low in-situ  $K_0$ , and (b) tests with high in-situ  $K_0$  (Pantelidou, 1994).
- Figure 2.12 Horizontal displacements along the wall/soil interface following completion of the wall: comparison between plane strain and 3D analysis with 5m panels (Gourvenec and Powrie, 1999).
- Figure 2.13 Changes in pore water pressure during excavation under bentonite slurry and concreting: plain strain trench with full height groundwater level (Powrie and Kantartzi, 1996).
- Figure 2.14 Influence of retaining wall installation on pore pressure (Symons and Carder, 1993).

- Figure 2.15 Magnitude, distribution and development of surface movement behind the wall:  
a) Stages of construction  
b) Horizontal movement towards excavation  
c) Vertical movement  
d) Movement recorded at surface station 2-6 m from back of wall (Tedd et al, 1984).
- Figure 2.16 a) Progress of excavation  
b) Horizontal movements of wall and ground (Sills et al, 1977).
- Figure 2.17 Typical pile probe operation carried out prior to piling
- Figure 2.18 Measured settlements caused by the installation of concrete diaphragm walls (Rampello et al 1998).
- Figure 2.19 Magnitude of settlement expected next to braced excavations (Burland et al, 1979 after Peck, 1969).
- Figure 2.20 Horizontal surface movement caused by excavation in front of wall (stiff clay) (Carder, 1995).
- Figure 2.21 Surface settlement caused by excavation in front of wall (stiff clay) (Carder, 1995).
- Figure 2.22 Details of a 19.7 m deep top down excavation in Taipei (Ou et al, 2000).
- Figure 2.23 a) Observed wall deflections and ground surface settlements in the main observation section  
b) Conditions of construction between stages 4B and 5 (Ou et al, 2000).
- Figure 2.24 Vectors of the soil movements from stages 5 to stage 13 (Ou et al, 2000).
- Figure 2.25 Cross section through 3 storey top down excavation (Nash et al, 1996).
- Figure 2.26 a) Main stages of construction  
b) Movements vs time (Nash et al, 1996).
- Figure 2.27 Heave beneath an excavation  
a) During excavation  
b) Following completion of excavation (Nash et al, 1996).
- Figure 2.28 Section through the excavation at the Shell Centre on the South Bank showing displacements of the tunnel crowns (Burford, 1988).
- Figure 2.29 Long term uplift of selected points in the crown of the southbound tunnel beneath the Shell Centre (Burford, 1988).
- Figure 2.30 North-South section through British Library (Simpson, 1992).

- Figure 2.31 Tunnel movements at British Library.  
a) East-west section  
b) Heave profile along line of tunnel (Raison, 1988).
- Figure 2.32 Rate of heave in tunnel at the site of British Library (Raison, 1988).
- Figure 2.33 Palace of Westminster: location plan (Burland et al, 1979).
- Figure 2.34 Summary of observed settlements (St John, 1985).
- Figure 2.35 Central YMCA: Influence of perimeter berm on wall movement (Burland et al, 1979).
- Figure 2.36 Strong ground anchored excavation at Neasden (Sills et al, 1977).
- Figure 2.37 Magnitude of settlement behind the retaining wall at Bell Common (Tedd et al, 1984).
- Figure 2.38 Measurement of near surface vertical displacements in front of the retaining wall at Bell Common (Tedd et al, 1984).
- Figure 2.39 Sketch of the 3-SKH model in triaxial stress space (Stallebrass and Taylor, 1997).
- Figure 2.40 Plan on site at 60 Victoria Embankment (St John et al, 1993).
- Figure 2.41 Settlements versus distance from excavation (St John et al, 1993).
- Figure 2.42 Cross section through multi-propped retaining wall centrifuge model (Powrie et al, 1984).
- Figure 2.43 Schematic diagram of the 3D in-flight excavator (Loh et al, 1998).
- Figure 2.44 Typical patterns of treated soil mass used in excavation  
a) Block type  
b) Column type  
c) Wall type (Ou et al, 1996).
- Figure 2.45 Comparison of measured wall deflections and computed wall deflections from both RAS and EMS methods (Ou et al, 1996).
- Figure 2.46 Variation of maximum horizontal wall displacement with increase in  
a) Treated depth H  
b) Treated width B  
for various treated areas, (Xie et al, 1999).

- Figure 2.47 Variation of maximum ground surface settlement with increase in treated depth  $H$  treated width  $B$ , for various treated areas, (Xie et al, 1999).
- Figure 2.48 Layout of centrifuge modelling test (Ohishi et al, 1999).
- Figure 2.49 Ground displacements at the end of excavation showing comparison between unimproved (case 1) and improved (case 2) soil (Ohishi et al, 1999).
- Figure 2.50 General geometry of excavation at Aldersgate Street, London (Ferne et al, 1991).
- Figure 2.51 Detail of typical pin pile (Ferne et al, 1991).
- Figure 2.52 Site of the former Knightsbridge Crown Court showing the outline of the diaphragm wall and the pile layout.
- Figure 2.53 Typical section through the top down basement construction at the site of the former Knightsbridge Crown Court showing the general construction sequence and a typical borehole.
- Figure 2.54 Normalised settlement around the top down excavation at the former Knightsbridge Crown Court site at completion of basement excavation.
- Figure 2.55 Horizontal displacements of the retaining wall at the site of the former Knightsbridge Crown Court measured using inclinometers at key stages during the excavation.
- Figure 2.56 Comparison of horizontal wall movements at the site of the former Knightsbridge Crown Court with field measurements of other excavations in stiff clay. (after Carder, 1995).
- Figure 3.1 Inertial stresses in a centrifuge model compared with gravitational stresses in a corresponding prototype (after Taylor, 1995).
- Figure 3.2 Stress variation with depth in centrifuge model compared with a corresponding prototype (after Taylor, 1995).
- Figure 3.3 Geometry of a typical model on the Acutronic 661 geotechnical centrifuge at City University, London showing components of induced acceleration (after Grant, 1998).
- Figure 3.4 Schematic diagram of the Acutronic 661 geotechnical testing facility at City University, London - capacity 40g.tonnes, radius 1.8m to swing base in flight (after Grant, 1998).



- Figure 3.5 General arrangement of main apparatus prior to modification after test AM1.
- Figure 3.6 Elevation on manifold unit showing location of hydraulic cylinders, oil reservoir and oilways.
- Figure 3.7 Section A-A through manifold unit showing hydraulic oilways.
- Figure 3.8 Plan B-B on manifold unit showing position of hydraulic oil reservoir and oilways for hydraulic cylinders.
- Figure 3.9 Plan and section through tapered aluminium plate used to separate the membranes containing compressed air and dense fluid.
- Figure 3.10 Details of phosphor bronze piston used to pressurise hydraulic oil reservoir.
- Figure 3.11 Details of connection of three plug valves to proportional rotary solenoids.
- Figure 3.12 Details of transducer block bolted to top of manifold apparatus to enable measurement of oil pressure in hydraulic cylinders.
- Figure 3.13 Details of model retaining wall and method of securing cast silicone rubber seals into rebates.
- Figure 3.14 Detail of cast silicone rubber seal in model retaining wall and against strongbox wall.
- Figure 3.15 Detail of typical waling used to support retaining wall at three levels.
- Figure 3.16 Detail of clevis eye and pin used to connect waling to hydraulic piston.
- Figure 3.17 Imposed horizontal and vertical total stresses acting within excavation during consolidation on the centrifuge.
- Figure 3.18 General arrangement of main apparatus following modification after test AM1.
- Figure 3.19 General view of the model showing key components of the apparatus.
- Figure 3.20 Curing exotherm measured during trial pile casting in kaolin using Sika Biresin G27 polyurethane ‘fastcast’ resin.
- Figure 3.21 Comparison of tensile and compressive tests on piles used in test AM13 and made from Sika Biresin G27 mixed 50:50 w/w with aluminium trihydrate (ON) filler.
- Figure 3.22 Detail of tool used for forming model pile bores.

- Figure 3.23 Detail of template used to position and bore piles.
- Figure 3.24 Variation of overconsolidation ratio with depth in model.
- Figure 3.25 Theoretical vertical and horizontal total stress distribution over depth of excavation.
- Figure 3.26 Variation of  $K_0$  with depth over height of model.
- Figure 3.27 Stress history of a typical model following one dimensional compression and swelling in consolidation press and additional swelling during consolidation on the centrifuge prior to the simulated excavation stage of test.
- Figure 3.28 Consolidation press used for sample preparation prior to model making.
- Figure 3.29 Method of ensuring correct positioning of pore pressure transducers within model.
- Figure 3.30 A typical soil sample immediately after removal from the consolidation press.
- Figure 3.31 Top surface of the sample was trimmed to the approximate level using a 50mm diameter brass tube cutter.
- Figure 3.32 Final trimming to level was carried out using an extruded aluminium box section guided with a 150mm wide shelf angle bolted to the strongbox.
- Figure 3.33 Clay ramp behind position of retaining wall to prevent loss of liquid paraffin into the excavation during consolidation on the centrifuge.
- Figure 3.34 Jig used for forming excavation and trench for embedded wall.
- Figure 3.35 Initial removal of soil for excavation.
- Figure 3.36 Trimming of excavation using aluminium box section cutter.
- Figure 3.37 Method of cutting trench below excavation formation level for embedded wall.
- Figure 3.38 Track guided cutting tool in use.
- Figure 3.39 Completed excavation and trench.
- Figure 3.40 Pile cutting template bolted into position on excavation jig.
- Figure 3.41 Forming pile bores using stainless steel tube cutter.
- Figure 3.42 Dispensing polyurethane 'fastcast' resin into pile bores.

- Figure 3.43 Installing prop module apparatus into the strongbox.
- Figure 3.44 Tightening the drainage fitting into the backwall of the strongbox.
- Figure 3.45 Detail of drainage fitting for polyethylene bag at base of excavation.
- Figure 3.46 A completed model with image processing targets for single camera.
- Figure 3.47 LVDTs for measurement of retained surface displacement and wall rotation.
- Figure 3.48 Method of positioning LVDTs to enable measurement of wall rotation.
- Figure 3.49 Drainage reservoir for storage of zinc iodide solution together with two valves, connected in parallel, to control drainage.
- Figure 3.50 Model on centrifuge swing and ready for spin up.
- Figure 3.51 Non linear distribution of total horizontal stress over depth of excavation and comparison between theoretical and imposed total horizontal stress distribution over depth of excavation.
- Figure 3.52 Position of cameras used for image processing.
- Figure 4.1 General details of the modified apparatus used to ensure negligible horizontal wall movement in test AM10, AM11 and AM12.
- Figure 4.2 Settlement profile behind wall on completion of excavation during tests using 'fixed' wall.
- Figure 4.3 Settlement profile behind wall 60 minutes after completion of excavation during tests using 'fixed' wall.
- Figure 4.4 Formation displacements, measured using image processing, at end of excavation during tests using 'fixed wall'.
- Figure 4.5 Horizontal displacements, measured immediately behind and below the retaining wall using image processing, at end of excavation during tests using 'fixed wall'.
- Test AM10, no piles.
  - Test AM12, 5 piles.
  - Test AM11, 10 piles.
- Figure 4.6 Contours of horizontal movement, 30 minutes after completion of simulated excavation.
- Test AM10, no piles.
  - Test AM12, 5 piles.
  - Test AM11, 10 piles.

- Figure 4.7      Contours of vertical movement, 30 minutes after completion of simulated excavation.
- Figure 4.8      Settlement behind retaining wall at completion of simulated excavation for tests AM9 and AM14.
- Figure 4.9      Formation displacements measured using image processing at end of simulated excavation for tests AM9 and AM14.
- Figure 4.10     Horizontal displacements, measured immediately behind and below the retaining wall using image processing, at end of simulated excavation for tests AM9 and AM14.
- Figure 4.11     Prop loads measured during and after simulated excavation stage of test AM9.  
                     a) Prop loads measured during simulated excavation stage.  
                     b) Prop loads measured during and subsequent to simulated excavation.
- Figure 4.13     Graph of displacement of hydraulic cylinder pistons with increasing load in apparatus test.
- Figure 4.14     Graph of displacement of hydraulic cylinder pistons with time under constant load (also shown) in apparatus check.
- Figure 4.15     Contours of horizontal movement after 15 minutes.  
                     a) Test AM9, no piles.  
                     b) Test AM14, no piles.
- Figure 4.16     Contours of vertical movement after 15 minutes.  
                     a) Test AM9, no piles.  
                     b) Test AM14, no piles.
- Figure 4.17     Layout of piles in tests AM6 and AM15.
- Figure 4.18     Comparison of settlement behind retaining wall at completion of simulated excavation between tests AM6 and AM15 and AM9 and AM14.
- Figure 4.19     Comparison of excavation formation displacements measured using image processing at end of simulated excavation between tests AM6 and AM15 and AM9 and AM14.
- Figure 4.20     Comparison between horizontal displacements, measured immediately behind and below the retaining wall using image processing, at end of simulated excavation for tests AM9 and AM14 and tests AM6 and AM15.
- Figure 4.21     Test AM15-contours of horizontal movement after 15 minutes.

- Figure 4.22 Test AM15-contours of vertical movement after 15 minutes.
- Figure 4.23 Prop loads, determined from oil pressure transducers, during and after the simulated excavation stages of tests AM6 and AM15.
- Figure 4.24 Layout of piles in tests AM7 and AM13.
- Figure 4.25 Comparison of settlement behind retaining wall at completion of simulated excavation for tests with and without piles at excavation formation.
- Figure 4.26 Comparison of excavation formation displacements measured using image processing at end of simulated excavation for tests with and without piles at excavation formation.
- Figure 4.27 Comparison of horizontal displacements immediately behind and beneath the retaining wall measured using image processing at end of simulated excavation for tests with and without piles at excavation formation.
- Figure 4.28 Comparison of settlement behind retaining wall at completion of simulated excavation between tests AM5 and AM17.
- Figure 4.29 Heave measured using image processing at end of simulated excavation for tests AM5 and AM17.
- Figure 4.30 Formation displacements measured using image processing at end of simulated excavation for test AM5 in comparison with measurements for other tests.
- Figure 4.31 Horizontal displacements measured immediately behind and beneath the retaining wall in tests AM5 and AM17.
- Figure 4.32 Comparison of settlements behind the retaining wall in test AM19 with those seen in deep and shallow embedded walls without piles.
- Figure 4.33 Comparison of settlements behind the retaining wall in test AM19 with those seen in tests on more deeply embedded walls with piles.
- Figure 4.34 Comparison of heave measured at excavation formation level in test AM19 with that measured in tests on more deeply embedded walls with piles and shallow embedded walls without piles.
- Figure 4.35 Comparison of horizontal displacements measured in test AM19 with those measured in tests on more deeply embedded walls without piles.
- Figure 4.36 Part elevation on model showing arrangement of LVDTs and image processing targets used to measure wall rotation.

- Figure 4.37 Horizontal wall movement with 40mm embedment walls during simulated excavation stage of typical tests.  
a) Displacements at toe of wall.  
b) Displacements of wall at retained ground surface.
- Figure 4.38 Schematic diagram showing positions of LVDTs
- Figure 4.39 Typical images taken from sequence during test AM15 showing the field of vision of the image processing cameras. A substantial area of overlap between the two cameras in the area behind the retaining wall allowed comparison of displacements measured from each camera.  
a) Image from Teli camera.  
b) Image from Pulnix camera.
- Figure 4.40 Comparison between displacements measured using Teli and Pulnix image processing cameras during test AM17.
- Figure 4.41 Comparison between vertical displacements, measured at the retained soil surface with LVDTs, and with image processing 15mm below the retained soil surface at 0.25H and 0.5H behind the retaining wall during the simulated excavation stage of a typical test (test AM19).  
a) 0.25H behind retaining wall.  
b) 0.5H behind retaining wall.
- Figure 4.42 Comparison between vertical displacements, measured at the retained soil surface with LVDTs, and with image processing 15mm below the retained soil surface at 0.25H and 0.5H behind the retaining wall during and subsequent to the period of the simulated excavation stage of a typical test (test AM19).  
a) 0.25H behind retaining wall.  
b) 0.5H behind retaining wall.
- Figure 4.43 Positions of Druck PDCR81 pore pressure transducers.
- Figure 4.44 Excess pore pressures measured during simulated excavation stage of test AM13.
- Figure 4.45 Excess pore pressures measured during simulated excavation stage of test AM19.
- Figure 4.46 Dissipation of excess pore pressures following simulated excavation during test AM13.
- Figure 4.47 Response of pore pressure transducers below excavation formation level during reduction of the supporting air pressure during the simulated excavation stage of two sets of tests using; very stiff propping (a and b); conventional propping (c and d).

- Figure 4.48 Development of prop forces during simulated excavation stage of test AM7.
- Figure 4.49 Prop forces measured in test AM7.
- Figure 5.1 Primary mesh used in preliminary finite element analyses.
- Figure 5.2 Secondary mesh used in preliminary finite element analyses.
- Figure 5.3 Key stages in modelling the stress history of the sample prior to the excavation sequence showing how the true effective stress is maintained throughout the analysis by gravity manipulation and the imposition of an artificial hydrostatic pore pressure distribution.
- Figure 5.4 Finite element analyses predictions of excavation formation displacement for a range of preconsolidation pressures.
- Figure 5.5 Comparison of formation displacement predicted by preliminary finite element analyses with results of centrifuge test AM9 and test AM14.
- Figure 5.6 Typical sequence of events modelled in finite element analyses.
- Figure 5.7 Variation in excavation support pressure during centrifuge model tests AM9 and AM14.
- Figure 5.8 Comparison of heave at excavation formation level in FEA and centrifuge tests in which piles were not modelled.
- Figure 5.9 Comparison of settlement behind retaining wall at completion of simulated excavation between centrifuge model tests AM9 and AM14 and finite element analysis RUN1.
- Figure 5.10 Comparison of formation displacements at end of excavation for centrifuge tests on shallow embedded walls and FEA on deep and shallow embedded walls.
- Figure 5.11 Variation in excavation support pressure during centrifuge model tests AM9, the excavation sequence of which was used in the FEA, and centrifuge model tests AM5 and AM17 on shallow embedment walls.
- Figure 5.12 Comparison of settlement behind retaining wall at completion of simulated excavation between centrifuge model tests AM5 and AM17, with shallow embedded walls, and finite element analyses RUN1 and RUN2.
- Figure 5.13 Comparison of wall displacement predictions between finite element analyses RUN 1 and RUN 5 in which prop stiffness was varied.

- Figure 5.14 Comparison of displacement at excavation formation level between finite element analyses RUN 1 and RUN 5 in which prop stiffness was varied.
- Figure 5.15 Comparison of displacement retained ground surface between finite element analyses RUN 1 and RUN 5 in which prop stiffness was varied.
- Figure 5.16 Comparison of heave measured in centrifuge model tests with and without piles with that predicted by FEA.
- Figure 5.17 Comparison of settlement behind retaining wall at completion of simulated excavation between centrifuge model tests AM13, AM14 and AM15 and finite element analyses RUN1, RUN6 and RUN7.
- Figure 5.18 Comparison between the finite element analysis RUN 1 prediction of horizontal displacement behind the retaining wall and that measured using image analysis in centrifuge test AM9 and AM14.
- Figure 5.19 Comparison between contours of horizontal displacement in finite element analysis and centrifuge test.  
a) Contours of horizontal displacement from finite element analysis RUN 1.  
b) Contours of horizontal displacement from centrifuge test AM14 at completion of simulated excavation.
- Figure 5.20 Comparison of horizontal displacements measured behind the retaining wall in centrifuge model tests with FEA predictions of wall displacement for tests with varying numbers of piles.
- Figure 5.21 Comparison of wall displacement predicted by finite element analysis RUN 1 and centrifuge test AM14.
- Figure 5.22 Comparison of heave in centrifuge model test AM14, in which no piles were used, with the predictions of preliminary finite element analyses carried out prior to model testing and a more detailed analysis.
- Figure 6.1 Generation of excess pore pressures during the simulated excavation stage of a typical test (AM13).
- Figure 6.2 Development of excavation formation displacements during the simulated excavation stage of a typical test (AM14).
- Figure 6.3 Development of heave during simulated excavation in test AM14.
- Figure 6.4 Contours of vertical displacement at key stages during test AM14  
a) At completion of simulated excavation.  
b) After 15 minutes.  
c) After 30 minutes.



- Figure 6.5 Comparison of vertical displacements in the soil below excavation formation level in tests AM13, AM14 and AM15, measured using image processing on completion of the simulated excavation.
- a) Test AM14, no piles.
  - b) Test AM15, 5 piles.
  - c) Test AM13, 10 piles.
- Figure 6.6 Relative times for the simulated excavation stage of tests AM13, AM14 and AM15.
- Figure 6.7 Comparison of vertical displacements in the soil below excavation formation level in tests AM13, AM14 and AM15, measured using image processing 20 minutes after completion of the simulated excavation following some consolidation.
- a) Test AM14, no piles.
  - b) Test AM15, 5 piles.
  - c) Test AM13, 10 piles.
- Figure 6.8 Comparison between displacements beneath excavation formation level in tests with and without piles immediately after completion of simulated excavation and 20 minutes later when some consolidation had taken place.
- a) Test AM14, no piles.
  - b) Test AM15, 5 piles.
  - c) Test AM13, 10 piles.
  - d) Test AM14, no piles.
  - e) Test AM15, 5 piles.
  - f) Test AM13, 10 piles.
- Figure 6.9 Comparison of vertical displacements at pile positions in tests AM13 and AM15.
- a) displacements at completion of excavation.
  - b) displacements 20 minutes after completion of excavation.
- Figure 6.10 Comparison of vertical displacements in the soil below excavation formation level in tests AM17 and AM19, measured using image processing on completion of the simulated excavation.
- a) Test AM17, no piles.
  - b) Test AM19, 10 piles.
- Figure 6.11 Comparison of vertical displacements below excavation formation level in tests AM15 AM13, (with 40mm wall embedment) and test AM19, (with 25mm wall embedment), measured using image processing on completion of the simulated excavation.
- a) Test AM15, 5 piles.
  - b) Test AM13, 10 piles.
  - c) Test AM17, no piles.

- Figure 6.12 Comparison of vertical displacements below excavation formation level in tests AM15 AM13, (with 40mm wall embedment) and test AM19, (with 25mm wall embedment), measured using image processing on completion of the simulated excavation.
- a) Test AM15, 5 piles.
  - b) Test AM13, 10 piles.
  - c) Test AM19, 10 piles.
- Figure 6.13 Comparison of vertical displacements in the soil below excavation formation level in tests AM17 and AM19, measured using image processing 20 minutes after completion of the simulated excavation.
- a) Test AM17, no piles.
  - b) Test AM19, 10 piles.
- Figure 6.14 Comparison between displacements beneath excavation formation level in tests with and without piles immediately after completion of simulated excavation and 20 minutes later when some consolidation had taken place.
- a) Test AM17, no piles.
  - b) Test AM19, 10 piles.
  - c) Test AM17, no piles.
  - d) Test AM19, 10 piles.
- Figure 6.15 Comparison of excavation formation displacements between tests AM17 and AM19 following a 60 minute period of consolidation after the simulated excavation stage of the test.
- Figure 6.16 Comparison of approximate retained surface settlements attributable to horizontal movement of the retaining wall at the end of the simulated excavation stage of typical tests.
- Figure 6.17 Horizontal displacements of retaining wall at the end of simulated excavation in tests AM10, AM11 and AM12 in which the retaining wall was effectively fixed horizontally owing to the use of modified apparatus.
- Figure 6.18 Variation of total retaining wall support pressure normalised by total imposed fluid pressure with reduction in height of fluid in a typical test (test AM15). Also shown, to demonstrate the development of the total prop force, is the reduction in fluid pressure during the simulated excavation stage of the test.
- Figure 6.19 Comparison of horizontal displacements behind the retaining wall measured using image processing at completion of the simulated excavation stage of test AM13, AM14 and AM15.
- Figure 6.20 Comparison of development of total prop force during simulated excavation in tests AM13, AM14 and AM15.

- Figure 6.21 Development of total prop load during and after the simulated excavation stage of a typical test (test AM15).
- Figure 6.22 Normalised settlement behind the retaining wall at the end of simulated excavation in tests AM10, AM11 and AM12 shown in the context of expected settlements for excavation in various soils from field monitoring data by Peck (1969).
- Figure 6.23 Normalised settlement behind the retaining wall at the end of simulated excavation in tests AM10, AM11 and AM12 shown in the context of expected settlements for excavation in stiff clay from field monitoring data by Carder (1995).
- Figure 6.24 Normalised settlement behind the retaining wall at the end of simulated excavation in tests AM13, AM14 and AM15 shown in the context of expected settlements for excavation in stiff clay from field monitoring data by Carder (1995).
- Figure 6.25 Comparison of normalised displacements in centrifuge model tests with predicted and measured normalised displacements at the site of the former Knightsbridge Crown Court.
- Figure 6.26 Relative geometry of the basement at the site of the former Knightsbridge Crown Court formed using top down construction and the centrifuge model.
- Figure 7.1 Trend lines showing the influence of piles on the magnitude of maximum settlement at ground level upon completion of excavation as suggested by results of centrifuge tests.
- Figure 7.2 Trend lines showing the influence of piles on the magnitude of maximum horizontal displacement behind the retaining wall upon completion of excavation as suggested by results of centrifuge tests.

## ACKNOWLEDGEMENTS

I have been fortunate that my involvement with the Geotechnical Engineering Research Centre at City University has enabled me to work closely with a group of highly dedicated people who have always been willing to provide help, support and encouragement whenever needed.

I acknowledge, with many thanks, the help and guidance of my supervisor, Professor Neil Taylor, who has been so generous with his time and contributed much to my understanding. Without his attention to detail, commitment and good humour, especially when faced with difficult problems, I could not have completed this research. He has been an unending source of practical ideas and solutions and has patiently guided me in the right direction at all times.

I have benefitted greatly from the skills and technical knowledge of Dr Sarah Stallebrass who has always been willing to help with problems and discuss ideas. She has enthusiastically provided guidance whilst I was carrying out the finite element analyses and other difficult work and her encouragement throughout has been invaluable and very much appreciated.

Thanks are also due to Professor John Atkinson, who has given much encouragement and has always been helpful in providing clear explanation of many geotechnical issues, and Dr Richard Grant who showed me how to conduct successful tests at the beginning.

The experimental work required considerable input and dedication of the highly skilled technical staff. Thanks are therefore due to Mr Keith Osborne, Mr Lloyd Martyka and Mr Reg Allen for manufacturing and assembling the apparatus and providing much needed assistance, often at short notice, during model preparation and testing.

I am grateful that, during various stages of the project, I have received useful information, ideas and guidance from Mr Rab Fernie and Mr Rob Dickson of Cementation Foundations Skanska and Dr Hugh St John of the Geotechnical Consulting Group. The interest of these and others including Mr T Balakumar and Mr Simon Simpson of Skanska Construction has been a source of great encouragement. In addition, financial support from Skanska, throughout the project, and for the last three months from the GERC are gratefully acknowledged as an addition to funding from the Engineering and Physical Science Research Council.

Work at the GERC has been made an enjoyable experience by all of the members of the group who created an atmosphere of friendship and good humour at all times. Thanks are therefore due to Ms Beatrice Baudet, Dr Peter Ingram, Dr Ulrich Klotz and Dr Matthew Coop.

Thanks go to my family, especially my parents, for their continual support, and particular thanks also to my brother, Stephen, for drawing many of the figures. Finally, thanks to Lorraine who has always provided encouragement and has worked hard to shield me from all but the worst excesses of two very demanding boys; Daniel and Sam. This thesis could not have been completed without her help and understanding.

## DECLARATION

I grant powers of discretion to the University Librarian to allow this thesis to be copied in whole or in part without further reference to me. This permission covers only single copies made for study purposes, subject to normal conditions of acknowledgement.

## ABSTRACT

The research concerns the influence of piles, installed beneath deep excavations, as a means of reducing movements in the surrounding ground. The work focussed on the use of piles installed as a part of top down basement construction, a technique used in conjunction with deep excavations in urban areas. The investigations sought to explore the effectiveness of bored piles as a means of enhancing the stiffness of the soil beneath the excavation and so reducing the spread of movements to the surrounding ground.

Experimental data were obtained from a series of 19 centrifuge model tests undertaken at 100g. The plane strain models consisted of a pre-formed excavation temporarily supported by fluid pressures acting at formation level and against the retaining wall. The fluid support was removed as the test proceeded and successive levels of props were advanced against the retaining wall using pressurised hydraulic cylinders as jacks. Ground movements were measured using a combination of transducers and analysis of digital images from a camera viewing the front of the model seen through the Perspex side of the model container. These systems gave ground surface, formation level and wall displacement profiles as well as overall patterns of movement.

The general model behaviour was characterised in a series of datum tests. These established the magnitude of displacements generated with ground support provided by the retaining wall alone in key positions throughout the model. Following this the overall stiffness of the soil below excavation formation level was enhanced by the introduction of either one or two rows of cast in situ piles installed at distances of 3 and 6 pile diameters from the retaining wall during model making. Direct comparison was then made between the various test results. These procedures were repeated in a small number of additional tests in which the retaining wall embedment depth was reduced.

The use of piles was found to reduce both horizontal movements and settlement behind the retaining wall. Maximum reductions in settlement behind the retaining wall were found to be about 55%. The influence of piles on settlement was limited to a distance of about two times the excavation depth behind the retaining wall. Maximum reductions in horizontal displacement, near to the retaining wall, were about 70%. The effectiveness of the piles in reducing ground movement diminished with increasing prop stiffness such that when lateral displacement of the retaining wall was effectively prevented maximum movements were reduced by 40% (settlement) and 50% (horizontal). The piles were found to create a general stiffening effect that reduced horizontal movement at the toe of the retaining wall and led to reductions in overall prop load. Additionally the piles provided restraint against heave movements at the excavation formation and therefore also acted in tension. As a result the soil mass around the piles tended to behave as a block. This behaviour was observed for excavations in which both one and two rows of piles were used despite the relatively discrete nature of the elements. With increasing time after completion of the excavation the block behaviour became less well defined although the effect was better maintained when the greater number of piles were used.

Finite element analyses of the centrifuge models also predicted reductions in displacement when piles were modelled at excavation formation level although the magnitude of reduction was less than that observed in the centrifuge tests.

## LIST OF SYMBOLS

$a$	Radial acceleration
$c_v$	Coefficient of consolidation
$d$	Displacement
$d_{\max}$	Maximum settlement in centrifuge test
$d_p$	Particle size
$g$	Acceleration due to gravity
$h$	Height
$h_m$	Depth in model
$h_p$	Depth in prototype
$l$	Lateral displacement
$l_{\max}$	Maximum lateral displacement in centrifuge test
$m$	Exponent of $R_0$ in relationship for $G'_{\max}$
$n$	Overconsolidation ratio or exponent of $p'$ in relationship for $G'_{\max}$
$p'_r$	Reference pressure in relationship for $G'_{\max}$ ( $p'_r = 1\text{ kPa}$ )
$r$	Radius
$s_u$	Undrained shear strength
$t$	Time
$t_m$	Time in model
$t_p$	Time in prototype
$u$	Pore pressure
$x$	Distance behind retaining wall
$A$	Coefficient of $p'$ in relationship for $G'_{\max}$
$E_c$	Young's modulus for concrete
$E_a$	Young's modulus for aluminium
$E_p$	Young's modulus for model piles
$H$	Depth of excavation
$I$	Moment of inertia
$K_0$	Coefficient of earth pressure at rest

$K_p$	Coefficient of passive earth pressure
$L$	Drainage path length
$N$	Gravity scaling factor
$S$	Ratio of size of yield surface to bounding surface for the 3-SKH model
$T$	Ratio of size of history surface to bounding surface for the 3-SKH model
$T_v$	Time factor for consolidation
$\delta$	Displacement
$\gamma_s$	Unit weight of soil
$\gamma_w$	Unit weight of water
$\kappa$	Gradient of unload-reload line in $v:\ln p'$ space
$\lambda$	Gradient of normal compression line in $v:\ln p'$ space
$\nu'$	Poisson's ratio
$\rho$	Density
$\sigma'_h$	Horizontal effective stress
$\sigma'_v$	Vertical effective stress
$\sigma_{vm}$	Vertical stress acting in model
$\sigma_{vp}$	Vertical stress acting in prototype
$\phi'$	Friction angle
$\psi$	Exponent in the hardening modulus for the 3-SKH model
$\omega$	Angular velocity (radians/second)
$\Gamma$	Specific volume on the critical state line when $p'=1\text{kPa}$
$M$	Stress ratio at critical state ( $q'/p'$ )

#### Abbreviations

3-SKH	3-Surface Kinematic Hardening (model)
cS	Centistoke
ppt	Pore pressure transducer
rc	Reinforced concrete



rpm	Revolutions per minute
CCD	Charge coupled device
CRISP	Critical State Program
FEA	Finite element analysis
LVDT	Linearly variable differential transformer (displacement transducer)
OCR	Overconsolidation ratio
PC	Personal computer

The research undertaken concerns the influence of piles, installed beneath deep excavations, as a means of reducing movements in the surrounding ground. The work focussed on the use of piles installed as a part of top down basement construction which is a technique commonly used in conjunction with very deep excavations in urban areas. The investigations sought to explore the effectiveness of bored piles as a means of enhancing the stiffness of the soil beneath the excavation and so reducing the spread of movements to the surrounding ground.

### 1.1 Background

Redevelopment of high value land in urban areas is driven by economical viability which frequently dictates that any new building should maximise the lettable floor area. Planning restrictions on building height in London have curtailed construction of very tall buildings and, in recent years, this has resulted in an increased requirement for deep basements. Large stress changes caused by construction of deep basements inevitably results in movements of the surrounding ground. The magnitude and extent of the ground movements are dependent upon many factors including the nature of the soil, the construction methods employed and the time involved in carrying out the excavation work. Predicting and controlling these movements therefore involves complex design processes and a detailed understanding of the construction process.

Deep excavations have the potential to cause very large displacements in the surrounding ground with consequent damage to existing structures and buried services. The allowable surface settlement around a typical excavation is thus commonly set at less than 20mm, regardless of the depth of excavation, in order to reduce the risk of serious building damage. This means that for increasingly deep excavations, where there is a much greater potential for ground movement, extremely onerous constraints are often imposed. There is also a need to be able to predict, with some degree of accuracy, the effect of basement construction on the surrounding structures. Nevertheless, owing to the complicated stress changes and site specific complications

that are entailed in deep basement construction even the most sophisticated of the current numerical analyses tools are incapable of providing very accurate predictions of ground movement. From the point of view of economy in construction and confidence in design there is a growing need to be able to control and more accurately quantify displacements. This will enable more expeditious construction and can be achieved by gaining a better understanding of the soil response to unloading and developing ways in which displacements can be controlled and reduced.

Control of movements around deep basement excavations both during and after construction are known to be highly dependent upon the design of the perimeter wall and the excavation and propping sequence adopted. Over the years new techniques such as the use of embedded retaining walls have been developed that have both hastened the operations involved in construction and also enabled much greater control of ground movements in the area behind the retaining wall. However, there is further potential for the implementation of existing technology in the form of a new technique that may enable closer control of ground movements and the development of this is therefore an attractive proposition.

The use of heave resisting piles in minimising deep-seated movements beneath an area to be excavated is relatively recent and the effectiveness of such measures cannot yet be quantified with sufficient accuracy by finite element analysis owing to limitations of the models used, the complex nature of the problem and the requirement for extensive simplification into two dimensions for the majority of analyses undertaken.

Whilst the ground movements cannot be eliminated it would be useful to understand the role of heave reducing piles in limiting movement and how, and in what circumstances, their performance can be maximised. A potentially useful method of investigating the problem is via small scale physical model tests undertaken preferably in the centrifuge where realistic profiles of in situ stress can be created. However, when considered in the context of the large scale deep excavations often encountered in practice the, magnitude of displacements involved are extremely small. This presents two problems: firstly in achieving reductions of movement at all and secondly of practical

considerations, since any reduction in movement must be both measurable and consistent at small scale in the centrifuge.

## 1.2 Methodology

The aim of the research is to improve understanding of the development and control of deep-seated ground movements around excavations. In achieving this centrifuge model testing techniques and some data from finite element analyses have been used to explore the effectiveness of piles in reducing these movements for top down construction in overconsolidated clay. The following are listed as the main features and achievements of the research and form the basis for the discussion and conclusions:

- i) Apparatus was developed to enable the stress changes associated with a 12m deep prototype top down excavation to be accurately reproduced in the geotechnical centrifuge at City University.
- ii) The results of the centrifuge model tests have been compared with a limited amount of field data from a project in which the techniques investigated have been used as well as data from a parametric study using finite element analyses in an attempt to relate the model testing to field problems and to help establish guidance for future designs.
- iii) The centrifuge test results have further been compared within existing frameworks of expected settlements around excavations to compare the performance of the apparatus.

## 1.3 Experimental work

### 1.3.1 Centrifuge modelling

The model apparatus was capable of simulating an excavation process, including top down construction, of a twelve metre deep prototype in plane strain. Two series of tests were conducted using the same very stiff retaining wall. In one set of tests the

apparatus set up virtually prevented horizontal displacement of the retaining wall into the excavation. This meant that almost all of the movements that occurred resulted from heave of the excavation base and enabled displacement caused by flexibility in the wall or propping system to be ignored. The other set of tests, that constituted the main part of the testing programme, involved the use of apparatus with three levels of propping used to support the very stiff retaining wall and enabled realistic simulation of a basement excavation incorporating top down construction techniques.

A total of 19 model tests were conducted under conditions of plane strain and consisted of a pre-formed excavation supported by fluid pressures acting at formation level and against the retaining wall. During the simulated excavation sequence of the tests the fluid pressures were gradually reduced, thereby mimicking as near as possible the stress change caused by excavation. As the removal of fluid support proceeded successive levels of props were advanced against the retaining wall using pressurised hydraulic cylinders as jacks. Measurements were made of displacements at the retained ground surface and rotation of the retaining wall using displacement transducers. Images of the model were grabbed throughout the tests and subsequently analysed using specialised software. This enabled the displacement of targets embedded in the surface of the clay throughout the model to be tracked thereby allowing movements at formation level to be measured and comparison of retained surface displacements to be made with measurements from the displacement transducers. In addition, overall patterns of movement were determined from the image processing data.

The general model behaviour was characterised in a series of datum tests that established the magnitude of displacements in key positions throughout the model that could be expected to be reduced by the implementation of the new technique. Following this the overall stiffness of the soil below excavation formation level was enhanced by the introduction of either one or two rows of piles installed during model making. Direct comparison was then made between the results. These procedures were repeated in a small number of additional tests in which the retaining wall embedment depth was reduced.

Two series of finite element analyses were conducted. These sought to model the behaviour of the centrifuge model tests using SSCRISP (Stallebrass 1992) a modified version of the CRISP (Critical State Program) incorporating the 3-Surface Kinematic Hardening (3-SKH) constitutive soil model, a non linear elasto-plastic model capable of modelling the behaviour of overconsolidated clay within the framework of critical state soil mechanics.

### 1.3.2 Numerical modelling

A total of eleven analyses were conducted, four of which were relatively simple and formed part of the pre centrifuge testing work that contributed to the design and development of the centrifuge apparatus. The remaining analyses were conducted as a parametric study by another student at City University and the results have been analysed and used to help explain and elaborate upon the centrifuge test results. The numerical modelling was especially useful in determining parameters for model design and gave useful insights into boundary effects.

### 1.4 Summary of the thesis

The thesis details the approach to the research, describes the development of the model testing apparatus and explains and interprets the model response in the series of tests conducted. There are many important studies focussing on ground movements around excavations in the literature. This has enabled a comprehensive literature review to be undertaken in Chapter 2 that establishes the background to the problem and explains the factors that may influence the magnitude of displacements around excavations.

The design development of the centrifuge testing apparatus was undertaken over a rather extended period owing to its complexity. Significant time was spent on preliminary experimental work to determine the performance of materials and methods that were novel in terms of centrifuge testing. This work is described in detail in Chapter 3 where the solutions to the practical problems that were encountered are described.

Model testing was carried out over a period of about 18 months with modifications to the apparatus becoming necessary during this time. In Chapter 4 the results from all of the tests are presented in a manner that enables a stage by stage understanding of the influence of changes in the test procedure. The results are presented in an unprocessed form that shows all test results unless truly typical behaviour justified the omission of repeated results. The general quality of data from the instrumentation and image processing is assessed and discussed and explanations given of problems that may have influenced the test results.

The two sets of numerical analyses are described and explained in Chapter 5. The results are discussed in detail and comparison made with the test results described in Chapter 4. In Chapter 6 the results of the centrifuge tests are compared and discussed in the context of data from the numerical analyses described in Chapter 5, with reference to field monitoring data from the literature review and a recent case study. Trends in the data are identified and analysed and the significance of the test results highlighted.

In Chapter 7 final conclusions are drawn with reference to the applicability and accuracy of the results. Recommendations are made for further research that will enable a better understanding of the influence of piles in reducing ground movements around excavations. The implications of the results of this research to help solve design problems faced by industry are discussed.

## 2.1 Mechanisms of ground movement

Peck (1969) wrote that “substantial upward movements of the bottom of excavations in stiff clays have been reported in the literature” and stated that Cooling (1948) observed movements of three inches at Waterloo Bridge. At the time these movements were attributed to artesian pressure in pervious horizontal partings beneath the excavation despite there being no evidence to confirm this.

Cooling had observed ground response to a deep excavation the mechanisms of which are now well understood and were subsequently clearly explained by Burland et al (1979). However, these excavation induced ground movements are notoriously difficult to quantify owing to the many variables involved. This is further complicated by the fact that there are two modes of deformation that combine to generate displacements at the retained ground surface and at the excavation formation. Padfield and Mair (1984) referred to movements around excavations as being global and local, the former caused mainly by vertical unloading and the latter by plastic deformations in the active and passive zones. Whilst the local movements could be controlled to a certain extent by the adoption of a stiff wall and propping system in conjunction with good workmanship, the global movements were much more difficult to control since they were influenced little by the stiffness of the wall or propping system but much more by vertical unloading associated with the excavation process. Peck (1969) stated that the characteristics of the surrounding soil control the deep seated global movements with which this research is concerned.

Burland et al (1979) described ground movements resulting from relief of horizontal and vertical stress. They stated that the movements resulting from horizontal stress relief were directly related to the mode of deformation of the retaining wall. Therefore movements associated with cantilever walls could be expected to be quite different from those associated with propped walls. Not surprisingly the horizontal component of movement is likely to be greater than the settlement for a cantilevered wall whilst for a



similar structure propped near to the surface, and allowed to deflect at depth, settlements would normally greatly exceed horizontal surface displacements as shown in Figure 2.1.

## 2.2 Vertical stress relief

Vertical stress relief can instigate the deep seated movements and Burland et al (1979) describe it as a vertical unloading leading to heave within the confines of the excavation and settlement outside in the short term. However, in the long term, with the excavated ground remaining unloaded, the ground continues to heave or swell under the excavated area and the effects continue to spread to the ground outside the excavation if there is a net long-term stress relief at the base of the excavation. This is because, in the long term, drainage occurs. The effect of these processes are illustrated in Figure 2.2. The heave movement, combined with horizontal movements caused by wall displacements resulting from wall deformation depicted in Figure 2.1, can cause the movements shown in Figure 2.2b.

Clough and O'Rourke (1990) stated that in overconsolidated clay with high in situ lateral stresses movements induced by the excavation will extend further from the retaining wall than in other soils. This had also been noted by St John (1975) who found that the results of three dimensional finite element analyses on an excavation indicated that, close to the excavation, the predominant surface movement was heave with settlements occurring at greater distances and as  $K_0$  increased so the region of settlement increased. Clearly then, stress history plays an important part in influencing the magnitude and pattern of ground movements. Notwithstanding this, geometry is also important since it was observed that corners provide a stiffening effect which restrain horizontal movements. However, whilst the precise effects of stress history may be difficult to determine, those associated with geometry can be considered very much more complicated since they are by their very nature site specific.

Even when the sides of the excavation are prevented from moving horizontally settlements and heave can occur depending upon time and whether there is a net vertical unloading. Peck (1969) suggested that movements are inevitable unless the entire

basement could be constructed before removal of any soil. However, this overlooked the vertical unloading that would occur during the subsequent excavation and therefore, even if such a situation were possible, some movement would still be expected.

### 2.3 Earth pressure at rest

Whilst the concept of earth pressure at rest may be simple to understand, as the ratio

$$K_0 = \frac{\sigma'_h}{\sigma'_v} \quad 2.1$$

the manner in which it may change as a result of variations in vertical effective stress owing to subsequent erosion of overlying sediments or variations in pore water pressure is relatively complex, (Pantelidou 1994). This is described by Burland et al (1979) and by Mayne and Kulhawy (1982) by way of similar diagrammatic representations as shown in Figures 2.3 and 2.4 respectively.

The steep slope of the unloading path in Figures 2.3 and 2.4 indicates horizontal stresses becoming locked in and, as  $\sigma'_v$  reduces,  $K_0$  approaches  $K_p$ . Indeed, Peck (1969) suggests that heave at the base of excavations in stiff clay may be associated with passive failure and the dramatic stress reduction associated with deep excavations may very well lead to such a situation but this would clearly be governed by plastic straining associated with dissipation of excess pore pressures. In Figure 2.3 the reloading path is very much steeper than the unloading path AB at B. Burland et al (1979) suggest that this results from elastic behaviour during the re-loading cycle where:

$$\frac{\sigma'_h}{\sigma'_v} = \frac{\nu'}{1 - \nu'} \quad 2.2$$

where  $\nu'$  is the Poisson's ratio for the soil skeleton.

Mayne and Kulhawy (1982) collected data from 170 different soils and statistically analysed them to determine values for  $K_0$ . They concluded that within the limits imposed by conditions of passive failure for overconsolidated clays

$$K_0 = (1 - \sin \phi') \text{OCR}^{\sin \phi'} \quad 2.3$$

where  $\phi'$  is the friction angle and OCR is the overconsolidation ratio

Passive failure could then be expected at OCR = 25 according to Skempton (1961) or at OCR = 20 according to Brooker and Ireland (1965). Al-Tabbaa (1987) carried out tests on spesswhite kaolin and suggested

$$K_0 = 0.69n^{0.464} \quad 2.4$$

where  $n = \text{OCR}$  which agrees well with the findings of Mayne and Kulhawy. The influence of stress history on the relationship between  $\sigma'_h$  and  $\sigma'_v$  is therefore of fundamental importance and the resulting ratio,  $K_0$  is extremely sensitive to change in  $\sigma'_v$ . The effect of such change is illustrated by Burland et al (1979) as shown in Figure 2.5.

The solid lines in Figure 2.5a show the variation of  $\sigma'_h$  and  $\sigma'_v$  with depth for a deposit that has had 170 m of overlying sediment removed. The water table is at the ground surface giving a hydrostatic distribution of pore water pressure. Corresponding distributions of  $K_0$  with depth are shown in Figure 2.5b. A limiting value of  $K_p = 3.5$  is assumed since  $K_0$  would tend to infinity at very low values of  $\sigma'_v$ . This means that the soil is at passive failure in the top 4 m. The chain dotted line indicates the stress changes caused by a surcharge of 100kPa applied to the surface and allowed to come into equilibrium. Whilst  $\sigma'_v$  increases uniformly with depth by 100kPa,  $\sigma'_h$  increases by only 18kPa except near to the surface where the soil is on the virgin compression line. A similar effect can be seen if  $\sigma'_v$  is increased by a general reduction in pore water pressure. Thus a relatively small change in vertical effective stress has resulted in a very large change in  $K_0$ , but only a small change in absolute magnitude of  $\sigma'_h$ .

Burland et al (1979) concluded that the distribution of  $K_0$  with depth is extremely sensitive to stress history and that although it is quite common to assume a unique value of  $K_0$  for a particular heavily overconsolidated deposit this should not be regarded as likely. However, a fairly unique value for  $\sigma'_h$  was thought to be more probable since this is relatively insensitive to changes in  $\sigma'_v$ .

## 2.4 Horizontal stress relief and ground movements associated with wall installation.

In highly overconsolidated soils, where horizontal stresses are locked in, it may be reasonable to assume that a reduction of these stresses will be associated with installation of an embedded wall. It is widely recognised that the stress changes associated with the installation of an embedded wall are complex, particularly so in cases where slurry trench techniques associated with diaphragm wall installation are used. They are described in detail by Pantelidou (1994). Anderson et al (1985) carried out laboratory tests on bored cast in situ piles in normally consolidated and overconsolidated clays and found that during excavation  $\sigma'_h$  reduced dramatically but recovered 90% of the initial “at rest” effective stress after only 30 days as shown in Figure 2.6. It was noted that the time required for recovery was very dependent on any delay between excavation and concreting, since this resulted in deterioration of the soil. However, they concluded that it was probable that  $K_0$  values would eventually be re-established even if there was considerable delay between boring and concreting.

Powrie and Li (1991) carried out finite element analyses of an in situ wall retaining 9m of stiff overconsolidated boulder clay and concluded that both in situ soil stiffness and the assumed pre-excavation lateral earth pressures have an important influence on the behaviour of the wall. Upon excavation, prop loads and bending moments in the retaining wall were found to be dependent on the assumed pre-excavation lateral earth pressures. However, higher pre-excavation lateral earth pressure resulted in reduced bending moments because the soil stiffness was increased. The effect of reducing soil stiffness by a factor of approximately 2 led to increased displacements by a factor of almost 2 and increased wall bending moments by as much as 15%. The importance of determining a reasonable estimate for soil stiffness can therefore not be overstated. On reducing the prop stiffness from one that was rigid to a value of  $2.8 \times 10^5 \text{ kN/m}$  the long term effect was found to be negligible.

Symons and Carder (1993) reported field monitoring for three embedded walls in London Clay. Measurements of earth and water pressures were carried out during the construction of a contiguous bored pile wall and two diaphragm walls where reductions

in  $K_0$  of just 10% and 20% were recorded for the contiguous and diaphragm walls respectively and implied by the horizontal stress changes shown in Figures 2.7 and 2.8.

Tedd et al (1984) carried out extensive monitoring of the secant piled wall at Bell Common Tunnel on the M25 at Epping Forest and recorded a marked reduction in  $\sigma_h$  during wall installation, at a distance 0.6 m behind the wall, as can be seen in Figure 2.9. However, although this initial reduction was found to be limited in its extent, at greater distances behind the wall, a further and gradual reduction in  $K_0$  was observed to accompany successive stages of construction throughout the depth of the retained soil as shown in Figure 2.10. This rapid reduction in stress at distances relatively close to the wall was also observed by Watson and Carder (1994) who reported a comparison of field measurement and numerical analyses on the performance of a propped bored pile retaining wall in London Clay, although overall less than 10% total lateral stress relief was found.

Atkinson et al (1990) found that although such recent stress history has a major influence on the subsequent stress-strain behaviour of overconsolidated soil the effect is limited according to the magnitude of subsequent strains. Upon re-loading, following rotation of the stress path, stiffness reduced rapidly until behaviour became independent of the previous stress path rotation when strains reached the relatively small value of about 0.5%. Observations of ground movements associated with embedded wall installation tend to indicate that the strains associated with these operations may exceed such a value, at least in the region near to the wall. Indeed Pantelidou (1994) found that finite element analyses of a 10m deep excavation retained by a wall with 10m embedment indicated that the majority of overall soil displacement occurring by the end of excavation resulted from the process of wall installation. Evidence that supported this was found in triaxial test results indicating that relatively large strains could result merely from trench excavation, particularly when a high initial  $K_0$  existed (Figure 2.11). Additionally evidence to suggest that the stress changes associated with embedded wall installation play a relatively insignificant role in influencing subsequent behaviour was also given by Pantelidou (1994) and Powrie et al (1998) who found that triaxial test results indicated that uncertainties in the definition of the in situ stresses and previous

stress history of the surrounding soil seemed to have only a minor effect on soil behaviour subsequent to wall installation. Nevertheless, the influence of ground movements associated with embedded wall installation are still important and Clough and O'Rourke (1990) state that they tend to result in localised but significant displacements within 5 to 10m of the retaining wall. Such localised movements have potential for more damage than those occurring over a wider area.

Stewart (1989) suggested that the slurry trench phase of diaphragm wall construction has a significant effect on the surrounding soil in an overconsolidated clay, such that  $K_0$  could be expected to reduce to approximately unity and argued that the data from Bell Common (Tedd et al 1984) implied this. Powrie (1986) also suggested that a reduction in  $K_0$  to between 1.0 and 1.2 was likely and cited the results of a numerical experiment by Potts and Fourie (1984) in support of this. However, Powrie and Kantartzi (1992), Powrie et al (1994) and Richards et al (1998) attempted centrifuge modelling of installation effects but were unable to confirm such an assumption. One of the reasons for this was the complications caused by the extended slurry trench phase time necessary in the centrifuge models. Powrie and Kantartzi (1996) concluded however that comparatively large deformations may result in cases where the groundwater level is high, there is a close source of recharge and the clay is not stiff or may soften quickly.

Gourvenec and Powrie (1999) report three-dimensional finite element analyses on diaphragm wall installation and concluded that the magnitude of ground movements, and the degree and zone of lateral stress reduction, have in the past tended to be overestimated by two dimensional analyses. The installation of diaphragm wall panels was found to be greatly influenced by three dimensional effects which were responsible for reductions in lateral soil movements during installation in comparison to plane strain conditions (Figure 2.12). Panel length was also found to have a profound effect since movements were seen to increase markedly with panel length at aspect ratios of less than three.

Ng and Yan (1999) carried out back analyses of diaphragm wall construction at Lion Yard in Cambridge. They found that horizontal arching behind the wall panels caused

local increases in stress either side and also below the panel under construction although these increases were, to some extent, reduced during subsequent panel construction.

During centrifuge tests, Powrie and Kantartzi (1996) found that pore water pressures were reduced during the excavation stage of embedded wall installation but increased during concreting (Figure 2.13). The combined effect of these processes were said to make only a small impact on the pore pressures and, consequently, the initial groundwater conditions may reasonably be taken as the starting point for soil-structure interaction analysis in which installation of the wall is not considered explicitly. Support for such an assumption was given in field observations by Symons and Carder (1993) which indicated similarly small overall pore pressure changes during the installation of a diaphragm wall (Figure 2.14).

Notwithstanding the incomplete knowledge and consequent assumptions that are necessarily applied regarding embedded wall installation effects, field studies of these movements are of considerable interest from the point of view of their magnitude. These movements, when compared to those attributed to the excavation process appear, in the majority of cases, to be excessive when viewed within the context of overall ground movements associated with a deep excavation. Indeed, Tedd et al (1984) concluded that wall installation caused a surprisingly large proportion of total movements at Bell Common (Figure 2.15). It appears that approximately 20% of horizontal movement occurred during this operation. Of the horizontal ground movement that occurred during the construction stages of an 8m deep excavation at Neasden (Figure 2.16) approximately 30% appears to have taken place immediately following wall installation (Sills et al 1977). This phenomena is one that repeats itself elsewhere, e.g. O'Rourke (1981) and it has generally been assumed that such large movements relate only to the piling work associated with wall installation.

Simpson (1998) suggested that pile probing could be responsible for excessive movement during wall installation. This operation is, more often than not, carried out in an unsupervised manner prior to the commencement of the piling contract, resulting in local unsupported excavations of at least 2m in depth, and sometimes exceeding 5m in depth, being carried out along the line of the embedded wall. The work is carried out

as a necessary operation prior to the commencement of piling works to avoid delays that may be caused by the removal of obstructions during the piling contract. A typical pile probe zone for an urban development is shown in Figure 2.17 and, in common with most operations of this type, no specific controls or method of working were specified to ensure that excessive ground movements did not occur. Such a lack of control during the early stages of construction could well result in excessive movements that have hitherto been thought to result from piled wall installation per se. St John et al (1993) carried out monitoring during the early stages of construction at 60, Victoria Embankment. Larger than anticipated settlements were noted during the installation of the secant piled wall but, interestingly, significant movements were also associated with the removal of obstructions to allow for the main piling. The removal of those obstructions can be assumed to have been supervised if monitoring was ongoing and it therefore seems that the same operations undertaken in different circumstances could very well result in the excessive movements that have been widely observed.

The difficulty in separating the field data on ground movements into one component associated with wall installation and another associated solely with the excavation process (ie not influenced by the previous installation process) makes it impossible to draw satisfactory conclusions regarding the overall influence of each. Moreover, it seems that if it is difficult to establish whether or not wall installation effects have a profound influence on subsequent excavation induced movements it is currently much more difficult to know whether the extent and or magnitude of the resulting movements may be affected.

In the absence of conclusive evidence to the contrary it seems reasonable to assume, and to expect, that a certain amount of reduction in  $\sigma'_h$  is associated with normal installation of an embedded wall and that the magnitude of reduction is governed largely by the type of wall. For instance, excavation for large diaphragm wall panels may cause greater changes in  $\sigma'_h$  in comparison to relatively small excavations for rotary piles since these may in turn be made using continuous flight auger techniques which reduce the likelihood of substantial changes in  $\sigma'_h$ . Additionally, Rampello et al (1998) observed that field studies of ground movements associated with wall



installation reported by Clough and O'Rourke (1990) indicated that even the most rigid in situ diaphragm or secant pile wall cannot be totally effective in preventing loss of ground as shown in Figure 2.18. The likelihood of the occurrence of excessive ground movement during the installation stage of deeply embedded walls is therefore very significant and should not be overlooked. It seems probable however that the measures to limit ground movements resulting from the excavation process, that have been investigated in this project, will in all probability have little or no additional influence on the in situ stress changes that will inevitably occur when an embedded wall is installed. This is because the effect of discrete pile installation in comparison to a piled or diaphragm wall can be considered minor and therefore reasonably neglected.

In conclusion, whilst it appears that wall installation can have significant effects on the overall magnitude of ground movements associated with an excavation there are no strong indications that the stress changes caused by such processes significantly influence the subsequent events. The idea that relatively large changes of in situ stresses can have little influence on soil behaviour during the main excavation is difficult to comprehend but may, nonetheless, be reasonable given the much larger magnitude of changes in stress and the extended periods over which they occur, when the effects of a large scale excavation are considered. The influence of recent stress history to problems involving the use of embedded walls would however appear to complicate the problem of accurate prediction of ground movements. This is because at some distance away from the wall large regions would be affected by substantially reduced levels of strain. The extent of these regions may be difficult to define although the influence of small strain stiffness on ground movements in these areas would almost certainly be significant.

## 2.5 Field studies of ground movement associated with excavations

Apart from stiff bracing and good design and construction procedures, that are well executed, settlements around excavations can only be reduced by decreasing lateral movements of earth supports and heave at the base (Peck 1969). More recently, Clough and O'Rourke (1990) presented a summary of conclusions from a number of instrumented excavations. They confirmed that poor construction techniques over-

excavation, slow installation of props and construction and removal of foundations can all adversely affect the magnitude of ground movements. Additionally, the support system stiffness was found to be important in controlling ground movements but mostly in soft to medium clays. Support spacing was found to be more important than wall stiffness when viewed in the context of overall system stiffness and the stiffness of individual supports was found to have less influence on overall system stiffness than wall stiffness or prop spacing.

In general, and with few exceptions including Carder (1995), there is a lack of field data in the literature regarding settlement profiles behind retaining walls although much information is available on wall deformations. The overall pattern of movements at all the monitored sites is very much in agreement with those suggested for propped walls, by Padfield and Mair (1984), although large variations in magnitude are evident. Peck (1969) gave a summary of magnitude of settlements next to open cut excavations in relation to their depth based on a number of field studies of propped sheet piled or soldier pile excavations; this was subsequently simplified by Burland et al (1979), (Figure 2.19) and Carder (1995). The settlements indicated for various ground conditions ranging from soft to stiff clays could be assumed to be higher than may be expected, with careful control of construction activities, but are often still used as a benchmark against which predictions are made and performance is judged. Indeed Burland et al (1979) suggested that settlements around an excavation within a diaphragm wall in London Clay could be expected to be well within Zone 1 and would seldom be expected to exceed 0.15% of the depth of excavation. More recently, Carder (1995) gave upper bounds for vertical and horizontal movement caused by various embedded wall installation techniques and subsequent excavation, in a range ground stiffness conditions including stiff clay and based on numerous field studies (Figures 2.20 and 2.21). Importantly, information relating to the zone of influence of both installation and excavation induced movement is included and suggests that although the influence of installation movements may extend laterally only 1.5 times the trench depth the same zone was found to extend up to 4 times the trench depth upon excavation. A similar zone of influence was observed by Sills et al (1977). Additionally, at the retained ground surface, predominant displacements were horizontal and about twice the magnitude of the vertical displacements. Similar ratios

of movement were noted by Wood and Perrin (1984) at an 18m deep excavation in Charing Cross Road and also by Cole and Burland (1972) who found that during construction of an 18m deep basement for Britannic House in Ropemaker Street horizontal displacements were two to three times larger than the corresponding vertical displacements and that, additionally, the movements were significantly time related.

By and large, where monitoring work has concentrated on movements behind retaining walls, only surface displacements have been considered since they are relatively easy to monitor and are normally perceived to be most relevant to the surrounding structures. It is obvious, however, that buried services and underground structures may also be affected by the movements referred to by Peck (1969) and because of this the few studies that include information relating to behaviour beneath excavations are of obvious significant value.

Ou et al (2000) made detailed field measurements of ground movements and building response to a 19.7m deep top down excavation in soft layered silty sand and sandy clay in Taipei (Figure 2.22). The observations indicated that volume changes occurred during excavation which is not surprising since a more drained than undrained response could be expected in the short term in such layered ground. The magnitude of displacements was high for a top down excavation with maximum wall displacements of 106mm (Figure 2.23) which were attributed to slow excavation, and construction (about 10 months) owing to the techniques used. Vertical settlements at the ground surface (Figure 2.23) were measured at 12mm up to 50m, three times the excavation depth, from the retaining wall with maximum values found at a distance approximately half the excavation depth from the wall. Unfortunately, and in common with many other data from field monitoring, the retaining wall was complete prior to monitoring work commencing and it is therefore not possible to know what movements this phase of construction may have caused. Significantly for the surrounding buildings, however, was that most of the soil behind the retaining wall was subjected to horizontal or near horizontal extension except near to the wall. This was deduced from inclinometer and extensometer readings that were used to calculate maximum shear strain values of around 0.6%. Overall movements, indicated by displacement vectors, are shown in Figure 2.24. The effect of the excavation on adjacent buildings was found to be

influenced by the type of foundation, length of excavation side, size of foundation and shape of the settlement profile. Importantly, three dimensional or geometry effects were found to be significant and, consequently, a building founded on a raft near a relatively short excavation side should be subjected to a smaller inclination than if the excavation side was very long.

Nash et al (1996) monitored a 10m deep three storey top down basement excavation in Gault clay in the centre of Cambridge (Figure 2.25) and made observations of the soil movements and pore pressure changes beneath the centre of the excavation. Initial movements, associated with the undrained soil response resulting from rapid excavation, were termed heave whereas subsequent movement of pore water leading to reduction in effective stress were referred to as swelling. Measurements of movement were made using an extensometer near to the centre of the site (Figure 2.25). Each stage of excavation was accompanied by immediate upward movements which were seen to continue with time although at a decreasing rate. Significant upward movements were noted in the first stages of excavation resulting in about 32mm of heave by the end of excavation over a period of about 4 months (Figure 2.26). These movements were not however recorded at the depth of the datum magnet of the extensometer, 15m below formation level, until the final stages of excavation were underway. It was suggested that this may be a result of small strain effects leading to a marked variation of stiffness with depth.

A void was left beneath the basement slab, which was suspended to avoid the need to design against swelling pressure, thus enabling the long term effects of swelling at the base of the excavation to be monitored. Maximum movements of 110mm were recorded over about six years although three quarters of this developed subsequent to completion of the excavation. The continuing vertical movements were recorded (Figure 2.27) and observed to plot linearly against log time (Figure 2.26) and this was said to indicate the development of secondary swelling.

The heave affecting tunnels of the Bakerloo Line beneath the Shell Centre on the South Bank (Figure 2.28) continued to increase, at a linear rate with normal time, some 27 years after a 12m deep basement was constructed over an area of 210m x 110m.

Burford (1988) reported monitoring of the tunnel linings that commenced in 1958 and concluded that by 1986, when maximum heave measurements of 50mm had been recorded, there was little indication that the rate of movement was decreasing (Figure 2.29) indicating that time had an important influence on the magnitude of the movements.

Raison (1988) discussed the monitoring at the British Library in Euston (Figure 2.30). The excavation extended to a depth of 25m in the south area and to depths of up to 15m above the Victoria Line tunnels in the central area of the site. Construction of the basement commenced with excavation to a depth of 5m over the entire site followed by local excavation to enable the higher level B1 raft slab and subsequently the B2 raft slab to be constructed. Monitoring was carried out during construction using inclinometers and extensometers as well as level surveys of the tunnels. Heave at the tunnel crown was measured to be 20mm maximum beneath the two deepest excavations for the B2 area (Figure 2.31). The rate of heave was also given (Figure 2.32) and was observed to follow closely the progress of excavation which was relatively slow. The heave was noted not to have taken place at constant volume and that, additionally, large horizontal wall movements that would have to be of the order of 50mm to maintain constant volume conditions were not associated with these displacements. The possibility of cavitation in the pore water during removal of the overburden and consequent reduction in pore pressure was suggested as a cause.

St John (1975) and Tedd et al (1984) provide a significant amount of invaluable data and analyses in comparing ground movements around the area of deep excavations associated with different methods of excavation support. This has followed extensive monitoring of the YMCA and New Palace Yard projects in London (St John, 1975) and Bell Common tunnel on the M25 (Tedd et al, 1984). St John (1975) points out that construction methods influence not only magnitude, but also distribution of movements. At New Palace Yard (Figure 2.33) an 18 m deep top down basement over five levels was constructed. Close control over construction meant that each successive basement slab was formed on plywood shuttering, resting on rough concrete blinding, as the excavation proceeded. A summary of ground surface settlements (Figure 2.34)

expressed as the ratio  $\delta/h$  where positive values of  $\delta$  represent settlement and  $h$ =depth of excavation, revealed that values of settlement at New Palace Yard exceeded those for the YMCA. Burland et al (1979) subsequently wrote on the subject of the 16 m deep YMCA basement which was formed using top down, partial tied back construction. Excavation initially proceeded to a depth 10 metres below ground level whereupon a waling slab was constructed at that level as shown in Figure 2.35. Work then progressed to formation level at 16m below ground level leaving a berm around the perimeter which was subsequently removed in sequence as the basement slab was completed. This appears to be a method that would favour construction progress owing to the provision of a clear working space without temporary propping. Figure 2.35 also shows that following excavation to formation level the wall rotated about the waling slab effectively reducing horizontal displacements near to ground level. The comparison of ground surface displacements between these two sites in (Figure 2.34) is therefore at odds with the hypothesis of Peck (1969) that much stiffer propping will necessarily lead to reduced movements.

St John (1975) and Sills et al (1977) reported on the behaviour of an anchored diaphragm wall supporting an 8m deep excavation at Neasden and concluded that significant movements were time dependent, extending well beyond the anchorage region. Here the anchors extended some 15 m into the ground behind the retaining wall (Figure 2.36) and St John suggests that they contributed little to the control of ground movements. Excavation in front of the walls at Bell Common and reported by Tedd et al (1984) resulted in the occurrence of settlements behind the wall extending for a distance of more than 20m (Figure 2.37) whilst significant heave (Figure 2.38) accompanied successive stages of removal of overburden.

O'Rourke (1981) suggested that it is excavation depth beneath the bottom level of propping that governs wall movement, since deflection depends upon approximately the fourth power of the unsupported depth and proposed that movement may be minimised by limiting excavation below prop level to about 5.5 m although an unsupported wall of such a height may, in any event generate movements that are perceived to be excessive. At New Palace Yard the final depth of excavation to formation level was approximately

4.75 m and this part of the excavation accounted for only 12% of the total horizontal displacement. It therefore seems that there may be limits to the benefits accruing from increased prop stiffness if there is, for instance, close control over construction activities such that excavation does not exceed some predetermined depth below a level of stiff propping.

St John (1975) noted that, in general, an increased toe embedment depth can decrease total movements by reducing flexibility, and that time dependent movement is characterised by increasing settlements behind the retaining wall. However, whilst stiff propping may reduce the overall magnitude of movement the region of influence is extended. Clearly, measures can be taken such that movements can be controlled in their magnitude and extent but not eliminated.

## 2.6 Numerical studies of ground movement

Owing to the complex nature of retaining wall problems, the use of finite element analysis has become more commonplace in predicting ground movements. Indeed there is no shortage of published literature on numerical studies of excavation processes and the influence on the surrounding ground. However, Woods and Clayton (1992) highlighted the many problems associated with relying entirely on such an approach. They listed the choice of constitutive model and associated soil parameters, modelling of wall installation and excavation, and derivation of design output amongst some of the many difficulties facing the modeller. Perhaps most importantly though is their conclusion that there is a need to validate analyses against real problems. Nevertheless, there is often a strong reliance on the results of numerical analyses for the most complex of geotechnical problems. Use of finite element analyses is costly and time consuming although Twine and Roscoe (1997) suggest that good results can be obtained when modelling well researched soil. However, they were of the opinion that the use of numerical methods should generally be limited to excavations that, owing to their size or complexity, fall outside the range of available case histories.

Stallebrass and Taylor (1997) referred to the development and evaluation of a constitutive model for the prediction of ground movements in overconsolidated clay.

Results of numerical analyses that modelled the recent stress history of the soil were compared with the results of previously conducted centrifuge tests in which the stress history of the soil had been carefully controlled. The computations were found to reproduce the main characteristics of the observed ground movement and in particular the surface profile around a stiff circular foundation. The constitutive model that was used described essential features of soil stress-strain response observed in triaxial tests. Subsequent use in finite element analyses had permitted agreement of results with those from centrifuge tests without tuning of parameters. This approach was regarded as fundamentally important to the work in terms of validation referred to by Woods and Clayton (1992).

The model, known as the three-surface kinematic hardening model (3-SKH), was formulated to enable the behaviour of overconsolidated clays to be modelled within the framework of critical state soil mechanics (Schofield and Wroth, 1968). The model described by Stallebrass (1990) incorporates two kinematic yield surfaces, (Figure 2.39) within a conventional Modified Cam-clay state boundary surface as a means of representing the memory of recent loading history and allowing plasticity within the SBS. This arrangement enables realistic soil behaviour to be modelled in a way that is not possible with simpler models.

The model is similar in principle to the ‘bubble’ model developed by Al Tabbaa and Wood (1989) but incorporates an additional kinematic surface that enables the effect of recent stress history to be modelled. If the stress state remains inside the inner yield surface then strains are elastic and stiffness is at its greatest. When the stress state reaches the boundary of the yield surface increasing stress causes the yield surface to translate and move in the direction of the stress path resulting in non linear behaviour and plastic deformation. This behaviour continues until the yield surface aligns with the history surface. At this point additional stress in the same direction as before causes both surfaces to translate and move with subsequent behaviour unaffected by recent stress history. The model has been incorporated into the SSCRISP finite element program (Britto and Gunn, 1987) used in analyses of some of the physical model tests conducted during this project details of which are included in Chapter 5.



Higgins et al (1989) carried out six separate analyses in comparison with the measured performance of the Bell Common tunnel. They concluded that modelling of wall installation was extremely important, as was modelling of construction procedure since the soil in which the wall is formed exhibits a non-linear response. When comparing the parameters used in the analyses, they found that parameters from high quality laboratory tests gave a better estimate of the maximum measured ground surface measurements than those obtained when using parameters from back analysis. Whilst some useful information was undoubtedly gained from the exercise, the merits of fitting analyses to data has to be questioned in the light of the parameters available at design stage if predictions of ground movement are to be made with any confidence.

Similarly Potts and Fourie (1984) carried out a numerical experiment on the behaviour of a propped retaining wall. Despite the many conclusions drawn, there was a need for comparison with data from field measurements, acknowledged by the authors, or validation using physical model testing. However, in soils which were described as having a high  $K_0$  the behaviour of the retaining wall was found to be dominated by the vertical unloading associated with excavation. Additional horizontal restraint in the form of multi-propping was thought to have a small effect on vertical movements which would, in turn, affect surrounding structures and services. Increasing the depth of wall embedment would not reduce prop forces or bending moments.

St John et al (1993) carried out numerical analyses on a 19m deep top down excavation at 60 Victoria Embankment (Figure 2.40). Predictions of the ground movement profile were made with reasonable accuracy, although predicted values of settlement were significantly greater than those measured (Figure 2.41) and the use of judgement and experience was necessary to provide realistic estimates of likely movement. It was concluded that whilst the finite element analyses may have lacked accuracy in quantifying settlements, it enabled a range of construction options to be considered and, as such, proved a valuable design tool.

Simpson (1992) carried out finite element analyses based on a method of relating displacements to the degree of mobilisation of the soil strength (Bolton 1990a and b). The results implied that the use of shorter embedded walls in stiff clays would not lead

to substantially greater ground movements. Not surprisingly, increased prop loads were found to result owing to a reduction in passive resistance in front of the toe of the retaining wall. Whittle and Hashash (1992) found from extensive parametric studies that wall length had a very minor effect on the pre-failure soil deformations and maximum wall deflections. The implication is that the wall embedment below formation affects only excavation stability and subsequent centrifuge model testing by Richards and Powrie (1998) and Richards et al (1998) was found to confirm this. Such findings tend to contradict the suggestion of St John (1975) who argued that an increased toe embedment depth can decrease total movements by reducing flexibility. Whilst increasing toe embedment could clearly be expected to help in reducing movement at the toe of the wall there appears to be a limiting value of depth above which there is no additional benefit in preventing movement.

## 2.7 Centrifuge modelling

Craig (1995) discusses the advent of geotechnical centrifuge modelling, and notes that whilst the first work on geotechnical modelling in the centrifuge was carried out in the USSR by Davidenkov and Pokrovskii in 1932 its use elsewhere was virtually unknown until Mikasa in Japan and Schofield at Cambridge became aware of its potential in the 1960's. As a consequence of this the first papers relating to geotechnical centrifuge work since 1936 were published at the International Society for Soil Mechanics and Foundation Engineering Conference in Mexico, 1969. All of the papers were devoted to slope stability which, notes Craig, is hardly surprising since the centrifuge is ideally suited to studying problems of this nature which involve pore fluid movement associated with gravity-induced hydraulic gradients, and instability resulting from soil self weight.

At the subsequent International Conference in Moscow in 1973 the extent of the Russian expertise in the subject of centrifuge modelling became apparent. Although much of their research had military applications, there was also considerable work of a non military nature that enabled rapid advances in modelling techniques and instrumentation worldwide.

Today the use of geotechnical centrifuge modelling is widespread, but generally only in academic research establishments with the exception of Japan which has the greatest proportion of the world's geotechnical centrifuges used by both industry and academia.

Whilst centrifuge modelling is, in principle, eminently suitable for the study of problems relating to retaining walls the practical difficulties in carrying out an excavation in flight have required the development of innovative techniques. In recent years, Kimura et al (1994) in Japan developed an in-flight excavator that was successfully used in a soft clay model. In the UK, Craig and Yildirim (1976) carried out centrifuge tests on retaining walls, at the University of Manchester, using a series of props that were removed to simulate the excavation process. Following this, significant centrifuge modelling work relating to retaining walls in stiff clays and incorporating techniques involving draining of a dense fluid to simulate excavation in front of the retaining wall was carried out at Cambridge University during the 1980's. Work during that time and subsequently has focussed on a variety of issues including soil pressure distribution, propping, wall embedment depth, and the effects of wall installation and groundwater.

Bolton and Powrie (1987) reported tests that considered the collapse behaviour of diaphragm walls in clay which had important implications for design and construction. They found that the depth of wall embedment required for stability of when retaining large heights of clay (in the order of 10m) would be likely to make the use of cantilever support uneconomical. A flooded tension crack behind a wall was found to have a marked influence on the stability of unpropped walls and the rate of wall movement was controlled by the flow rate of water into the tension crack. The behaviour of diaphragm walls in clay prior to collapse was reported by Bolton and Powrie (1988). A series of centrifuge tests sought to gain information on soil-structure interaction and were used to develop the idea of the use of mobilised soil strength in retaining wall design. From this an approach to design that focussed on displacement criteria rather than factors of safety was suggested. This was achieved by establishing the effective mobilised soil strain in major zones of soil deformation and thereby determining soil or wall displacements. Further and more general details of previous work on retaining walls are also given by Powrie (1995).

Much of the more recent work relevant to this project and relating to the behaviour of embedded walls in stiff clay has been carried out at Queen Mary and Westfield College and Southampton University where attempts have been made to model wall installation effects (Powrie and Kantartzi 1996; Powrie et al 1994; Richards et al 1998). These tests have had some success although the test procedure necessary to construct a wall in flight was extremely complicated, owing to scaling laws which were unfavourable in this instance, problems were experienced with the time taken to allow curing of the materials used to form the model wall. The work by Powrie et al (1994) involved modelling the installation of props (Figure 2.42) using hydraulic locking devices that enabled two levels of props to remain free to move laterally during consolidation but fixed in place following the simulated excavation stage of the test. By selecting suitable fluid densities and excess fluid above the retained soil surface a range of pre-excavation lateral stress profiles were modelled.

Loh et al (1998) observed three dimensional effects during excavation in front of a retaining wall involving the use of a three dimensional in-flight excavator (Figure 2.43). Such effects are notoriously difficult to quantify during the construction of deep basements although the tests confirmed that they play an important part in reducing pressure on retaining walls and propping systems and influence wall movement in comparison to two dimensional tests. Richards and Powrie (1998) carried out tests on a doubly propped retaining wall and concluded that the effects of  $K_0$  on surface settlements were significant and that lowering the groundwater level behind the retaining wall led to large reductions in prop loads and bending moments.

## 2.8 Enhanced soil stiffness below excavation formation

The use of numerical analyses have, in the past, provided mixed results in terms of accuracy in patterns and magnitude of displacements around excavations. Thus there might be a reduced degree of confidence in the use of such techniques to provide accurate results when attempting to study more complex problems than a relatively simple excavation process. Ou et al (1996) carried out finite element analyses of excavations in which soil improvement techniques, such as jet grouting and deep soil mixing in the passive zone near to the retaining wall, were modelled. This was

achieved by determining typical stress-strain relationships for treated soils and carrying out analyses based on a range of patterns of treated soil mass (Figure 2.44). Two different approaches to the analyses were made. The first, known as 'real allocation simulation' (RAS) modelled individual elements in treated zones according to their perceived stiffness. The second, regarded a treated zone as a composite ground mass. Results of both plane strain and 3-dimensional analyses using the different methods were compared with measured wall displacements from a 13m deep excavation in Taipei. Results of the analyses were seen to fall generally within the range of measured horizontal displacements for the wall (Figure 2.45). Consequently, it was concluded that the results of the simplified equivalent material simulation method using either 3-dimensional or plane strain analyses were sufficiently similar to those from the more complicated method of analyses and were therefore valid.

Finite element analyses were also conducted by Xie et al (1999) to investigate the effects of stiffening the ground in the passive zone using ground improvement techniques such as deep mixing and jet grouting (Figure 2.46). These analyses focussed on the effect of stiffening a volume of ground below formation level in front of the wall similar to Ou et al (1996). It was found that the plan extent of the stiffened ground rather than the depth over which it had been stiffened was most influential in reducing heave at the excavation formation (Figure 2.47). Treated soil was thought to behave as an imaginary strut and therefore increasing the width of treated area would result in an overall increase in stiffness. The effects of ground improvement were also seen at the retained ground surface with reductions in settlement resulting from a stiffer formation. However, the width of the treated area of soil was again found to be most influential in controlling settlements with larger areas of treatment leading to progressively smaller displacements, whereas increased depth of improved soil beyond 60% of the excavation depth was not seen to be beneficial.

A series of centrifuge tests was carried out to investigate the effects of ground improvement in front of the retaining wall toe by Ohishi et al (1999). This work involved a simplified approach that modelled the effect of surcharge loading applied to a layer of soil below the excavation formation level (Figure 2.48). The soil in the passive zone was improved by mixing clay, used for the remainder of the model, with

cement and fly ash in unspecified proportions but to give a material with an unconfined compressive strength of 368kPa compared to 60 and 110kPa for two other tests without soil improvement. Draining of a dense fluid to simulate excavation resulted in significant reductions in heave at excavation formation (Figure 2.49) although the effect at the retained ground surface could not be determined owing to the nature of the tests.

Fernie et al (1991) reported on the use of 15m long pin piles to control movements, resulting from the rise in aquifer level beneath London, around a 24m deep excavation. About 30 large diameter piles were used to support vertical load from the structure with diaphragm walls providing additional vertical support at the perimeter, as well as lateral support, and extending to a depth some 33m below ground level, (Figure 2.50 ). Low effective stresses resulting from an upward hydraulic gradient from the sand layer towards the basement meant that there were problems in developing sufficient passive resistance in front of the toe of the wall. One possible solution to this problem was to carry some of the vertical load from the new structure onto the excavated ground, particularly near to the perimeter, although this was not considered possible owing to divisions of responsibility within the design process.

Ground anchorage was seen as the favoured option and the pin pile concept was developed as a means of stiffening the ground in the passive zone near to the retaining wall. This consisted of a regular grid of 254mm diameter, 15.5m long mini piles as shown in Figure 2.51. The piles were designed to resist the heave induced tension that would be expected in the short term but would provide a stiffening effect in front of the wall in the long term.

Insufficient monitoring data are available to enable conclusions to be drawn regarding the effectiveness of the piles in controlling ground movements. However, measured displacements in the short term were said to have been predicted with reasonable accuracy by finite element analysis.

## 2.9 Case study of a 24m deep excavation incorporating heave reducing piles at the site of the former Knightsbridge Crown Court

### 2.9.1 Introduction

The construction of a 24m deep basement at the site of the former Knightsbridge Crown Court led to the use of heave reducing piles at excavation formation level in an attempt to limit ground movements around the site. The close proximity of sensitive buildings, including a retained facade on part of the site perimeter led to extremely onerous design constraints regarding allowable settlement. The requirement to maximise the useable space within a relatively small site footprint resulted in the adoption of a heavily reinforced, but quite slender, 800mm thick diaphragm wall at the basement perimeter. Subsequent excavation was carried out using top down construction techniques with excavation generally progressing two levels prior to construction of successive permanent basement slabs. By and large, temporary propping of the perimeter wall was avoided apart from near to the ground surface. The basement construction sequence and method meant that all piling was carried out from a platform about 2 metres below ground level thereby maximising any benefit that may accrue from the stiffening effects that pile installation may have on the excavation formation.

Details of the site geometry including locations of heave piles are shown in Figure 2.52. A section through the basement including the main excavation and construction stages are shown in Figure 2.53. A comprehensive monitoring exercise was carried out all around the site but tended to focus on the Embassy building, No.3 Hans Crescent, since this structure was regarded as being most at risk owing to its proximity to the re-entrant corner. This assumption proved to be correct and consequently, during the latter stages of the excavation, monitoring tended to be concentrated on this area. Nonetheless, precise levelling data and inclinometers in the diaphragm wall panels provided good general information on ground response to the excavation. The locations of inclinometers and precise levelling studs are shown in Figure 2.52.

### 2.9.2 Numerical analyses

A series of eight detailed finite element analyses were carried out (Geotechnical Consulting Group, 1998) that suggested maximum settlements at ground level behind the retaining wall in the region of about 15mm. Additionally, horizontal wall movements of about 20mm were predicted. Two basic cross sectional geometries were developed for the analyses in order that the wider part of the site may be considered separately from the narrow section. Most of the analyses were plane strain although for the wider part of the site one axi-symmetric analysis was carried out. All of the final analyses modelled piles at formation level as a means of controlling heave but, unfortunately, no detailed information was available from a series of preliminary analyses that were conducted to establish the approach for the final design. However, the results of the preliminary analyses were summarised in the subsequent report (Geotechnical Consulting Group, 1998) and, importantly, the predicted movements were noted to be sensitive to the construction sequence and the potential for the piles to act in tension to reduce heave at the base of the excavation. The assumption that this would in turn lead to reduced movements in the surrounding ground was therefore an important feature of the overall design philosophy.

Maximum vertical and horizontal displacements of 30mm and 60mm respectively were predicted by the preliminary datum analyses without piles. These displacements were predicted to be reduced by just 5mm by modelling a soil zone between the wall panels, below formation level, that was twice as stiff as that in the datum analysis. This could be regarded as a similar approach to that of Ou et al (1996) who carried out analyses using a simplified 'equivalent material simulation' (EMS) as a means of accounting for enhanced stiffness at formation level by deep mixing.

Another approach, that yielded similar results to the stiffened formation, was the direct modelling as 'bar' elements of two rows of piles with 1% cross sectional area of steel. However, subsequent analyses reverted to the stiffened formation technique and further stiffening, to quadruple the value used in the datum analysis, reduced predictions of vertical and horizontal settlement to 22mm and 24mm respectively. Significant reduction over these predictions were made however when allowance for over-



excavation during construction of successive basement slab props was omitted from the analyses. This resulted in maximum predicted displacements of 15mm vertically and 16mm horizontally thereby reducing the original datum predictions by about 50%.

The eight final analyses are summarised in Table 2.1. The main details and magnitude of predicted displacements at the completion of the excavation are included. Three of the analyses, RUN 1, RUN 2 and RUN 3 were carried out for the narrow section of the site near to Basil Street. The analyses concentrated on variations in pile length and prop stiffness, particularly for the lower levels of propping, following a datum analysis, RUN 1, in which two rows of piles extended to a depth of 24m below final excavation formation. Somewhat shorter 14m long piles were used near to the centre of the excavation in RUN 2 although this was found to make minimal difference, the horizontal and vertical displacements being almost identical to RUN 1. In RUN 3 increasing the prop stiffness at the lower levels resulted in an approximately 15% reduction in both the horizontal and vertical displacements.

For the wider part of the site, 5 analyses were carried out although two of these, RUN 6 and RUN 7, were essentially identical since they considered different cross sections that were geometrically very similar whilst maintaining the same design parameters. In RUN 4 four rows of piles were modelled and prop stiffness was similar to that used in RUN 3. Predictions of displacements were also of a similar magnitude to RUN 3 implying that the increased width of the excavation would not necessarily lead to a greater magnitude of movement provided additional piles were provided.

Three axi-symmetric analyses were carried out to simulate the wide section of the site between Hans Crescent and Herbert Crescent. Included in these were RUN 6 and RUN 7 in which displacements were dramatically reduced, probably owing to the effects of hoop stiffness in the pile elements which were modelled as embedded cylindrical walls. Consequently, in RUN 8 the pile stiffness was reduced by about 30% leading to predicted displacements that were very similar in magnitude to those given by the plane strain analyses.

Numerical analysis of such a complicated geometry was clearly not a trivial undertaking and results could not be expected to provide very accurate predictions of displacement. Whilst the problem could not be accurately modelled in plane strain, owing to three dimensional effects, neither could it necessarily be represented more accurately by assuming conditions of axis-symmetry. The complexity of the problem was such that more accurate predictions of movement would probably lie somewhere between the plane strain and axis-symmetry conditions. In view of this, the general predictions of vertical and horizontal displacements at the end of excavation of approximately 15mm and 20mm respectively could be expected to represent probable upper bounds.

### 2.9.3 Comparison with field measurements

Whilst the use of piles at formation level were predicted to have a strong influence on the ground movements behind the wall prop stiffness at low level was also found to be important. Given these results it would seem reasonable to assume that any measures taken to increase the general stiffness near to formation level would be likely to have a beneficial influence from the point of view of reducing ground movements.

The final design used heave reducing piles in the positions shown in Figure 2.52 with lengths varying between 18m to 22m. A plot of settlement against distance from the retaining wall, both normalised by the final excavation depth, is shown in Figure 2.54. The value of excavation depth,  $H$ , used in the normalisation was the maximum excavation depth. This means that all displacements measured during the excavation process, and the positions of the precise levelling studs, were normalised by  $H=24\text{m}$ . The monitoring data included in Figure 2.54 were gathered from numerous survey points situated around the site and should therefore be regarded as a composite plot that is indicative of the general trend of settlement. However, during the final stage of excavation data were only available for the ground around the embassy building. Since this area suffered the greatest magnitude of settlement during the early stages of excavation it is reasonable to assume that data for the latter stage of excavation could be regarded as representing an upper bound for the excavation in general. Also included in Figure 2.54 is the finite element analysis RUN 1 prediction of ground surface settlement. The predicted settlement trough applies specifically to the narrow section of

the site near to Basil Street although the final results of the analyses indicate that the magnitude of predicted settlements is fairly typical elsewhere as well owing to increased numbers of piles in the wider section of the site between Hans Crescent and Herbert Crescent.

When viewed in the context of data presented by Carder (1995) the settlements appear to be well within the upper bound for similar excavations with high stiffness support (Figure 2.21). Indeed, during the early stages of excavation and prior to excavation beyond about 15m depth the displacements were mostly less than 5mm and therefore fairly insignificant. Larger settlements were however seen to accompany the latter stages of the excavation although the overall magnitude failed to reach the upper bound limit suggested by Carder (1995). Furthermore, whilst data for settlement were only available at distances up to about 1.5 times the excavation depth it seems likely, from the magnitude of settlements at the margin of the monitored area, that significant settlements from a point of view of damage to surrounding structures would have been limited to an area within three times the excavation depth. This is slightly less than the four times excavation depth zone proposed by Carder (1995).

Eleven inclinometers were installed during construction of the diaphragm wall and data from three of these have been presented in Figure 2.55. The positions of the inclinometers, which were selected primarily because monitoring data were available throughout the period of the excavation, are shown in Figure 2.52. It should be noted that the monitoring data were processed using specialist software and that the results are conditioned by the following important assumptions:

- i) Prior to excavation below B3 level (-2.00m AOD), the toe of the wall was effectively prevented from moving owing to the substantial depth of embedment below the excavation level.
- ii) Subsequent to excavation below B3 level the top of the wall was prevented from moving owing to the completion of the stiff upper levels of the basement structure.

This means that following the initial excavation the position of the datum was moved from the toe of the wall to the top of the wall and this is characterised on the graphs shown in Figure 2.55 by a change in the apparent displacement profile. This is especially noticeable in the results of inclinometer 9D (Figure 2.55c). Two of the inclinometers (3D and 4D) were located in Landon Place near to the embassy building whilst the third (9D) was in the wall against the rear of Hans Place (see Figure 2.52). Both of the locations could be regarded as representative of potential worst cases owing to their proximity to the re-entrant corner or positioning in a relatively long straight wall. Incomplete sets of data, in terms of measured displacement at the stages of excavation considered, were also available for other inclinometers. However, these suggested that inclinometers 4D and 9D represent maximum displacements around the excavation. Similar maximum values were measured at inclinometer positions 2D and 8D.

Horizontal movements developed at a steady rate with excavation and reached maximum values of approximately 17mm (inclinometers 4D and 9D) at a depth of about 23m. Carder (1995) presented data relating to horizontal wall movement from a number of sites in stiff clay and concluded that maximum displacements for low stiffness support occurs at the ground surface. Increasing the support stiffness (i.e. top down construction) was found to result in the occurrence of maximum displacements at between 0.7 and 0.9 times excavation depth,  $H$ . When plotted on a similar graph of maximum movement against depth to maximum movement, both normalised by the excavation depth (Figure 2.56) the data from Knightsbridge Crown Court suggests maximum displacement at about  $0.95H$  implying a stiff support in comparison to the data considered by Carder (1995). Additionally, the magnitude of maximum displacement compares well with that measured at similar well supported excavations.

The field monitoring has provided a useful source of data that has enabled the performance of a piled formation excavation to be assessed and compared with the predictions of a complex series of numerical analyses. The results of an extensive site monitoring exercise suggest that ground movements were well controlled and that the magnitude of movement predicted by the numerical analyses was realistic but also conservative. The overall magnitude of ground movement resulting from the

excavation was well within that suggested in data from other relevant case studies and overall stiffness was shown to be greater than attained elsewhere. There is no reason to suppose that this overall increase in stiffness was attributable to anything other than the fact that the stiffness of the ground below excavation formation level was enhanced by the introduction of piles.

## 2.10 Summary

Considerable amounts of data relating to ground movements around various types of excavation are published in the literature although there is limited monitoring data on movements associated with the retained soil both at the surface and at depth. These data have, by and large, been compiled from field studies and from numerical analyses whilst a small amount of data are available from physical model testing. From this the basic mechanisms of movement are known and well explained since information on the pattern of ground movements is clear. However, the way in which their magnitude and spread may be controlled is not well understood. The relationship between initial vertical and horizontal effective stress is not simple and is governed by the geological stress history. In addition recent stress history has a significant influence on the magnitude and distribution of ground stiffness that will apply during various stages of construction of an embedded wall adding to the difficulties in making accurate predictions of displacement.

However, there is no clear evidence in the literature to suggest that horizontal stresses are permanently and/or substantially reduced during installation of embedded retaining walls. Indeed some test data implies that no overall reduction is evident. The key to establishing better guidelines for predicting ground movements lies with improving understanding of the mechanisms of movement through a combination of field studies, numerical analyses and physical model testing.

A comprehensive monitoring exercise during construction of a deep excavation, in which piles were used to enhance the stiffness of the ground below excavation formation level, suggests that ground movements were well controlled and that overall stiffness was increased. Prior to construction a series of numerical analyses modelled

the construction process, including the piles, and predicted that the influence of the piles would be to reduce the overall magnitude of displacements. Predicted displacements were reasonable when compared with the results of the field monitoring although the fact that they were somewhat conservative suggests that improvements in predictions would be beneficial.

### 3.1 Principles of centrifuge modelling

The fact that soil behaviour is governed by stress level and stress history, and that as a consequence there is a need to model in situ stresses that change with depth to reproduce both strength and stiffness aspects of soil behaviour, makes the use of a geotechnical centrifuge attractive. The sheer scale of most geotechnical problems by and large precludes the use of full scale testing, and the use of sophisticated numerical analyses can generally only be relied upon to give approximations of behaviour as discussed in Chapters 2 and 5. Physical modelling offers opportunities to correlate other analyses. This is achieved by carrying out a series of tests with known and repeatable boundary conditions and parameters. Physical modelling using a centrifuge involves accelerating a model contained in a strong box at the end of a centrifuge arm to create an inertial radial acceleration field many times greater than the Earth's gravity. In the model, stress increases rapidly with depth from zero at the surface to values that are determined by the soil density and radial acceleration.

Models for clay soils are subjected to a similar stress history to that in the corresponding prototype situation. For a model of scale 1:N of the prototype, the requirement of stress similarity means that the vertical stress at depth  $h_{m(model)}$  should be the same as at  $h_{p(prototype)}$  where

$$h_p = N h_m \quad (3.1)$$

This is achieved by accelerating the model (of scale 1:N) at N times Earth's gravity using a centrifuge which then conveniently gives stress similarity at homologous points throughout the model. Newton's Laws of motion state that in pulling a mass out of its straight flight path around a curve of constant radius,  $r$  (metres) the centrifuge will impose a radial acceleration (towards the centre of rotation) of

$$a = \omega^2 r \quad (3.2)$$

where

$\omega$  = angular velocity (radians/second), Schofield (1980).

The model will experience an equal and opposite inertial acceleration towards the base of the model, and thus the requirement is for:

$$a = Ng \quad (3.3)$$

where  $N$  = gravity scaling factor,  $g$  = acceleration due to gravity ( $9.81\text{m/s}^2$ ). The effect of the radial acceleration is therefore to increase the self weight of the model in the direction of its base. Consequently, it follows that, with care, models can be made with stress profiles that closely resemble a corresponding prototype when subjected to an acceleration field in the centrifuge as indicated in Figure 3.1.

### 3.2 Scaling Laws

Central to the theory of centrifuge modelling is the fact that if an acceleration of  $N$  times the Earth's gravity is applied to a material of density  $\rho$  then the vertical stress  $\sigma_v$  acting at depth  $h_m$  in the model is given by:

$$\sigma_{vm} = \rho N g h_m \quad (3.4)$$

and for the prototype

$$\sigma_{vp} = \rho g h_p \quad (3.5)$$

Therefore if the density of the material in the model is the same as that in the prototype then for stress similarity, i.e.

$$\sigma_{vm} = \sigma_{vp} \quad (3.6)$$

the requirement becomes

$$\rho N g h_m = \rho g h_p \quad (3.7)$$

or

$$h_p/h_m = N \quad (3.8)$$

Hence the scaling law for length is  $1/N$  and affects not only model dimensions but also the geometrical properties of components used in the model. For example, the moment of inertia of a walling is governed by the fourth power of length and scales as  $1/N^4$  in the centrifuge. Powrie (1986) provides a comprehensive list of scaling factors, relevant to retaining wall models, that can all be derived from the scaling relationships for self



weight stress (1:1) and for length (1:N), and these are given in Table 3.1. However care should be taken in applying the scaling laws to geometrical parameters that include dimensions in the out of plane dimension when conducting plane strain model testing.

One scaling factor that is particularly advantageous in small scale physical models is that for consolidation and seepage. The dimensionless time factor  $T_v$  for consolidation is defined as;

$$T_v = \frac{c_v t}{L^2} \quad (3.9)$$

where  $c_v$  = coefficient of consolidation

$t$  = time

$L$  = drainage path length

For the same time factor in model and prototype:

$$\frac{c_{vm} t_m}{L_m^2} = \frac{c_{vp} t_p}{L_p^2} \quad (3.10)$$

since 
$$\frac{L_m^2}{L_p^2} = \frac{1}{N^2} \quad (3.11)$$

thus 
$$t_m = \frac{1}{N^2} \frac{c_{vp} t_p}{c_{vm}} \quad (3.12)$$

Hence the scale factor for time is  $1/N^2$  assuming the same soil is used in model and prototype. This means that, in the centrifuge at 100g, an event lasting for one minute corresponds to about one week at prototype scale. The reduced geometrical scale in the model results in a dramatic speeding up of time related processes allowing the modeller to observe in minutes events that would take months or years at prototype scale.

Despite the advantages offered in relation to the effects of seepage related processes in the reduced scale physical modelling the extremely low permeability of London Clay renders it unfavourable for use in model testing. This is because the time for sample preparation and the time necessary on the centrifuge to achieve conditions of effective stress equilibrium would be very long. In contrast, kaolin is a relatively permeable

coarse grained clay that has measured values for consolidation coefficient in the range  $c_v=2.5\text{mm}^2/\text{s}$  (Bolton and Powrie, 1987) and  $c_v=0.35\text{mm}^2/\text{s}$  (Al Tabbaa, 1987). This allows samples to be prepared in the consolidation press in less than 3 weeks compared to months for London Clay and tested in hours rather than days for models in London Clay. Justification for the use of kaolin, in respect of its behaviour, is discussed later.

### 3.3 Errors in centrifuge modelling

In trying to model a prototype event it is inevitable that some errors will result from the testing procedure and the artificial gravity field. Errors relevant to this project are now discussed.

The Earth's gravity is uniform for the purposes of problems encountered in civil engineering but the centrifuge generates a slightly variable acceleration throughout the model, Taylor (1995). This is because there is variation in radius over the height of the model causing variation in acceleration as can be seen from equation 3.2 and depicted in Figure 3.2. Careful choice of the effective radius used to calculate the average effective inertial acceleration allows the errors of overstress at the model base and the understress near the surface to be minimised. For the tests undertaken an effective radius was taken at a distance of one third the depth of the model. It is important to note that the maximum error in stress profile associated with the variation in radius of the centrifuge model is generally only about 3% of prototype stress.

#### 3.3.1 Radial acceleration field.

Stewart (1989) described the radial acceleration field that acts in a direction that passes through the axis of the centrifuge. The effect of this is to introduce a horizontal component of acceleration into the model. This horizontal component, or error, increases with the distance from the model centreline. It therefore follows that in minimising such effects the orientation of the strongbox should be such that the smallest dimension is in the same plane as the radial acceleration field and that critical measurements be made on or near to the centreline of the model. For the model tests undertaken, with a maximum radius of 1.8m and minimum model dimension of  $\pm 0.1\text{m}$

from the centre line, the maximum horizontal accelerations were approximately 5% of the vertical. Figure 3.3 summarises the components of induced acceleration in a typical model on the Acutronic 661 centrifuge at City University and shows the orientation of the model on the swing.

### 3.3.2 Grain size

The scaling laws in centrifuge modelling apply equally to model dimensions and soil grain size although the need to replicate the stress-strain behaviour implies that it is necessary to test the prototype soil. There is, as a result, a need to consider the effects of using the prototype soil, and particularly a coarse grained clay such as kaolin, for the model. The problem is demonstrated by the fact that the use of a fine sand might be thought of as representing a gravel at 100g. However, Taylor (1995), states that, in this way, a clay could be thought of as representing a fine sand and that since the stress-strain characteristics of clay and fine sand are very different this argument is flawed. Indeed it is generally accepted that, for coarse grained soils, only where grain size exceeds 1/30th of an important model dimension does a significant grain size effect occur; see for example Fuglsang and Ovesen (1988).

As mentioned previously, accepted practice is that speswhite kaolin is generally used for tests on clay soils owing to its relatively high permeability, minimising sample preparation time, and well researched characteristics, e.g. Al Tabbaa (1987). In retaining wall tests Powrie (1986) established the ratio of the particle size of kaolin (2 $\mu$ m) and height of model retaining wall thus:

$$h/d_p = 80/0.002 = 4 \times 10^4$$

where

$h$  = height of retaining wall (mm)

and

$d_p$  = particle size (mm)

This was compared with a similar ratio of particle size : height of prototype retaining wall =  $10000/0.002 = 5 \times 10^6$  for 125g tests. Tests using kaolin clay by Stewart (1989) had the same ratios. Powrie (1986) cited the work of Davis and Auger (1979) which

suggested that these values were sufficiently high to be effectively similar. Richards (1995) also carried out tests on retaining walls, at 100g, using kaolin clay. In those tests the relevant  $h/d_p$  ratios would have been  $5 \times 10^4$  and  $5 \times 10^6$ . For the 100g tests carried out in this project the model retaining wall height of 120mm corresponded to a prototype height of 12000mm implying ratios of  $6 \times 10^4$  and  $6 \times 10^6$  which are not dissimilar. Confidence can therefore be drawn from the previous work and the use of kaolin clay for these tests justified.

### 3.4 Boundary effects

The range of scales at which the prototype may be modelled is controlled not only by the practicalities of instrumentation but also by the boundary effects imposed by the container. These limitations in part dictated the use of a plane strain model for this project since the size of model otherwise required could not have been accommodated on the centrifuge. The strongbox in which the model is contained is manufactured from aluminium plate and has an 80mm thick Perspex window on one side to permit a clear view of the cross section.

Phillips (1995) gives guidance on containers and states that side wall friction is always present to some extent and, consequently, the model should be sufficiently wide so that such effects do not create significant problems. Measurements of movements should, if possible, be taken on the model centreline to minimise the effect. However image analyses necessarily involve movements of the soil immediately behind the Perspex window.

Powrie (1986) and Stewart (1987) coated the inside of the backwall and sidewalls of the strongbox with Molykote 33 silicone grease whilst Adsil, a mould release agent, was used on the inside of the Perspex window. Mair (1979) however used Duckham's 'Keenomax' L3 water pump grease, an off white coloured lithium based product with water resistant properties claiming it much superior to silicone based grease. Duckham's grease was also used for these tests mainly because it was readily available.

The lubrication of the Perspex window presents additional problems that are not easily overcome. The need to provide a low friction surface together with the requirement to enable a clear view for the image processing currently dictates the use of colourless silicone oil.

In modelling the cross section of an excavation one end wall of the strong box represents a line of symmetry and care must also be taken here to ensure that any restraint provided is minimised.

### 3.5 The geotechnical centrifuge.

Schofield and Taylor (1988) describe the Acutronic 661 centrifuge, shown in Figure 3.4, used by the Geotechnical Engineering Research Centre at City University.

The swinging platform at one end of the rotor has overall dimensions of 500mm x 700mm with a usable height of 500mm. A package weight of 400kg at 100g can be accommodated and this capacity reduces linearly with acceleration to give a maximum 200kg at 200g; thus the centrifuge is a 40g/tonne machine. The package is balanced by a 1.45 tonne counterweight that can be moved radially along the centrifuge arm by a screw mechanism. The radius to the swinging platform is 1.8m giving a working radius of between 1.5m and 1.6m requiring an operating speed of approximately 340rpm to give 200g at 1.55m radius. However, for the 100g tests undertaken in this project an operating speed of approximately 240rpm was required.

Four strain gauged sensors are used in the base to detect out-of-balance operation of the centrifuge. The signals from these sensors are monitored continuously and the machine is shut down automatically if the out-of-balance exceeds the pre-set maximum of 15kN. Such a safety feature enables unmanned overnight running of the machine.

A fibreglass clamshell around the centrifuge creates an aerodynamically smooth chamber and a fairing on the leading side of the swing improves performance. A sacrificial block wall surrounds the clamshell and is itself surrounded by a reinforced concrete structure to provide an effective and safe containment.

Electrical and hydraulic connections are available at the swinging platform and are supplied through a stack of slip rings. 55 slip rings are electrical and 5 fluid with 15 bar capacity. Of the electrical slip rings 5 are used to transmit transducer signals, which are converted from analogue to digital by the on-board computer and may be amplified prior to transmission in bits. The remaining slip rings are used for communicating closed circuit television signals, supplying power for lights or operating solenoids or motors as necessary. The fluid slip rings may be used for water, oil, or compressed gas.

### 3.6 Model design requirements

Previous centrifuge work on propped retaining wall behaviour has made use of props that were fixed into position using hydraulic locking units (Richards, 1995). In those tests the props were themselves instrumented to enable horizontal loads to be determined. This was achieved by provision of strain gauges on specially machined shafts that supported knife edge walings. For the tests in this project it was planned to use three levels of props, in close proximity to one another, which would make direct instrumentation such as strain gauges a difficult problem. In an attempt to simplify as much as possible what was expected to develop into complex apparatus, it was considered that miniature hydraulic cylinders could be used to provide prop reactions since they offered the advantage of being able to measure, directly, the prop load by monitoring the oil pressure in them throughout the test. This simple, but potentially less stiff approach could be justified because prop loads were not central to the investigation although any movement resulting from flexibility in the propping system would not be well known.

An in-flight excavator, similar to that used by Kimura et al (1984) to model an unsupported or tied back excavation would, in itself, be a highly complex and difficult piece of apparatus to develop. Also, its use in conjunction with a propping system would have imposed particularly onerous constraints. For instance, the extremely limited space available for apparatus meant that the propping system occupied nearly the entire area of the excavation. In view of this it was obvious that the excavated soil profile should be formed before the test, using specially fabricated templates or jigs to ensure an accurate and repeatable cut profile. The problem of temporary support to a

pre-excavated soil model has, in the past, led to the use of a dense fluid to maintain horizontal total stress reasonably consistent with that in the clay, (Powrie, 1986 and Richards, 1995). Clearly, it would be possible to vary the density of the fluid to provide some pre-determined magnitude of horizontal support that varied hydrostatically over the depth of the excavation. However, this method limited the scope of testing since it would be unreasonable to use a fluid of a density unequal to the specific gravity of the soil in order to avoid the imposition of an incorrect overburden at excavation formation level. Indeed the use of this method, with the constraints imposed by fluid equal in density to the soil model, would imply that  $K_0$ , the coefficient of earth pressure at rest, was unity.

An alternative approach was sought which would allow for the ability to control independently the horizontal (wall) and vertical (excavation support) pressures. This could be achieved by the use of another fluid, contained within a membrane and separated from the dense fluid, to provide a surcharge at excavation formation level that would simulate the overburden removed during model making. Two separate membranes, that contained different fluids, were therefore necessary to enable the ratio of horizontal to vertical stress to be varied.

### 3.7 Apparatus design development

The apparatus required considerable time to develop and became necessarily complex owing to the decision to be able to control independently the horizontal and vertical total stresses in the model excavation. A cross section of the general model apparatus is shown in Figure 3.5, although this was modified slightly after test AM1 to provide additional clearance for swelling at the excavation formation. The design considerations leading towards the arrangement of apparatus used will now be discussed. Previous research on retaining wall problems has relied upon the use of fluid filled rubber bags that were drained in flight to simulate the vertical and horizontal unloading occurring during excavation (Powrie, 1986 and Richards, 1995). Rubber bags manufactured from dipped latex offer little restraint to either wall or fluid owing to their low stiffness and behave as a separating membrane. Whilst this served as a starting point in the apparatus development it quickly became apparent that significant

problems would have to be overcome in order that the top down construction process could be modelled.

The use of two bags, separated by a stiff plate at the junction of formation level and retaining wall offered a solution to the problem. At first it was intended that each bag would be filled with aqueous fluids of different densities. However, compressed air could be used to pressurise the bag used to impose vertical total stress. This simplified the apparatus since it gave the advantage of reducing stress without the need for draining fluid into a reservoir and the added complications and uncertainty that such an operation involves.

Previous similar work, using dense fluids to simulate unexcavated earth pressure against an embedded retaining wall, have made use of a solution of zinc chloride; Powrie (1986), Stewart (1989) and Richards (1995). Crystals of this compound have an extremely high solubility in water leading to the ability to produce dense fluids of relatively low viscosity. Unfortunately the solution is highly corrosive and mildly carcinogenic and it was thought prudent to use an alternative, if available. Several dense fluids such as tetrabromoethane and thallium formate (Clerici solution) were considered but these too would have proved excessively toxic. Eventually zinc iodide was selected. Although relatively expensive, crystals of this compound offer similar solubility in water to zinc chloride and the solution is much less hazardous.

Early experiments concentrated on the behaviour of a rubber bag whilst draining the fluid it contained. It was considered important that rubber was not trapped between the prop and the wall, since this would add an undesirable flexibility to the propping system. It was hoped that, as the fluid drained, the rubber bag would collapse, under its enhanced self weight, enabling a clear space for the props to advance against the wall. Bags were initially manufactured from dipped latex and simple tests performed whereby water was drained whilst the behaviour of the unsupported latex bag observed. It soon became apparent that a thinner material was required to reduce stiffness and alternative bags were manufactured from 0.5mm thick neoprene sheet with joints bonded with latex solution.



The use of water during the trial testing, instead of the more dense fluid that would be needed for the main series of tests, led to problems with the free rubber, above fluid level, becoming partially submerged in the water. This was because of the similarity in density of the bag material and water and resulted in leakage. A more dense fluid was necessary to ensure that the rubber was able to float on the surface. Zinc iodide solution could have been used, but an inexpensive alternative was preferable for these proving tests. Sugar solution with a specific gravity of 1.3 was used although it resulted in a quite concentrated and very glutinous solution that tended to clog the drainage pipe as sugar crystals began to form. However, the tests showed that whilst large areas of rubber bag collapsed and floated on the fluid surface, others remained upright. This would clearly be unacceptable since there was a strong possibility of rubber becoming trapped between the prop and the wall. It was therefore concluded that an alternative approach was needed.

Another, more elaborate, system was tried based on a number of individual sealed bags which, owing to the fact that they were sealed, would effectively implode as fluid was drained from them. However, this too failed to work satisfactorily since sufficient fluid could not be drained to effectively collapse the bags.

It was concluded that, because the bag material could not be relied upon to collapse completely during fluid draining, a stiffer, but much thinner, membrane could be used that could be allowed to become trapped between the prop and wall. The implication of this was that a much larger bag, or box, would be required that would envelop the mechanical prop apparatus so that it would become immersed in zinc iodide solution. Aluminium or copper foils were considered first and attempts were made to form a container from 50 $\mu$ m thick aluminium foil. This particular gauge of foil is malleable and is used in the manufacture of food packaging containers, but was too difficult to form into the required profile without puncturing. Besides, the resulting box shaped bag proved to be relatively stiff and would almost certainly provide unacceptable restraint to the wall.

A different sheet material that was strong, and yet lacked stiffness, was required. Polyethylene was available and initial tests confirmed that it could be easily and accurately heat sealed to form a simple container and was flexible enough to resist puncture, even at a relatively thin gauge. Calculations showed that deformation resulting from compression of a 125 $\mu$ m thick polyethylene membrane trapped between waling and retaining wall would be only 20 $\mu$ m at prototype scale for a waling load of 1000kN/m run. This value was approximately 80 times smaller than the deformation calculated for a membrane manufactured from 500 $\mu$ m rubber.

Draining of the polyethylene bag required a different approach to that previously used for rubber bags and a special aluminium fitting incorporating an 'O' ring seal was manufactured for preliminary tests in the centrifuge. These confirmed that polyethylene as a material was capable of withstanding the pressure expected and also confirmed the viability of the new technique. Following further experimentation the use of bags with a single heat sealed seam at each corner was determined to be most reliable but the ability to produce only a simple geometry governed the design of the main apparatus. Furthermore, reliable heat sealing of seams proved to be difficult and became a problem which returned during the main testing programme and directly led to the failure of one test.

Having decided on the use of polyethylene bags work focused on the design of the mechanical components of the apparatus most of which are shown on the cross section in Figure 3.5. Since it had been decided to submerge the entire propping system in the fluid filled polyethylene bag, it was desirable to maximise the volume of the apparatus in order to minimise the volume of fluid required. This led to the use of a solid block of aluminium that could be used not only as a manifold for the hydraulic cylinders, but could also incorporate a reservoir for the hydraulic oil used to actuate them provided that sufficient head could be generated. This solution was particularly attractive since it enabled the main experimental apparatus to be manufactured as a single 'prop module' that could be quickly and easily incorporated into the model. Details of the prop manifold unit are given in Figures 3.6, 3.7 and 3.8. A tapered cantilever plate, bolted to the underside of the manifold, Figure 3.9, separated the polyethylene bag from the

rubber bag at formation level and was sealed using 'O' rings to prevent leakage from the bag where the bolts passed through the plate.

Miniature hydraulic cylinders were obtained from Enerpac. These have a maximum stroke of 19 mm and can apply a force of 11.3kN when pressurised to 350bar. The hexagon heads used for tightening the cylinders into the manifold were 36mm across flats and had to be turned down to enable them to be installed at 35mm centres. Apart from this the only further modification necessary to these components was removal of the return springs.

A 150mm deep by 25mm diameter reservoir was bored into the manifold block away from the hydraulic cylinders. The reservoir capacity required to advance each cylinder piston 10 mm was only 10 ml and so the reservoir, although relatively small, had ample capacity. The reservoir became pressurised during testing by means of a 100mm long phosphor bronze piston sealed with double 'O' rings against the reamed bore, Figure 3.10. This heavy weight was capable of generating approximately 8 bar in the centrifuge at 100g.

The need to control oil flow into three hydraulic cylinders in close proximity to one another meant that three valves were necessary. In the past normally closed solenoid valves have been used for similar applications in the centrifuge and have proved reliable at accelerations up to 100g. Unfortunately, those that were readily available were too large to be incorporated into the apparatus and, additionally, concerns over their ability to resist a potentially high back pressure precluded their use. Since suitable 'off the shelf' alternatives were not available three motorised valves were made from components available commercially. They consisted of low friction manual plug valves coupled to rotary solenoids to enable actuation. The plug valves were manufactured by Hoke from stainless steel (model no.7312G2Y) and had 2.63 mm diameter orifices. Such a small orifice was considered advantageous since it would lead to greater control and smooth movement of the walings as they were advanced against the retaining wall. However, after overall size, the main criteria in selecting the valves was low actuating torque and a capacity to operate at potentially high (20.7MPa) pressure. Measurements were made of the torque required to open and close the valves at a range of pressures up

to the expected operating pressure on the supply side of the valve and these data were used to select appropriate solenoids. After some trials 50mm diameter proportional rotary solenoids, supplied by Emessem Solenoid Co Ltd, were selected as being most suitable owing to their compact nature. The solenoids were rated at 24V and operated on Direct Current which if reversed provided contra-rotation thus allowing the valves to be turned on and off. However, the torque generated at such a voltage was not sufficient to provide the instantaneous on/off that was desirable to control waling movement and jacking force against the retaining wall. Since each valve was only required to be used for the short period of once on and once off during a test it was decided to increase the input voltage to 70V to ensure rapid actuation. This combination of valve and solenoid provided an extremely compact arrangement which formed part of the main apparatus although positioned outside the strongbox in such a way as to minimise pipework. Support for the valves was from two machined aluminium arms that were bolted to the top of the manifold shown in Figure 3.5. The general arrangement of the valve and actuation components is shown in Figure 3.11.

When the manifold was complete and the hydraulic cylinders and valves installed the apparatus was bled. A light hydraulic oil was used to minimise the possibility of air entrapment but bleeding was very difficult and time consuming. With hindsight, the provision of bleed nipples in some positions would have been beneficial since the stiffness of the entire propping system was reliant upon successful bleeding of the hydraulic system. The performance of the apparatus could only be tested by spinning in the centrifuge at 100g and this was carried out using a dummy retaining wall against which the props could react when advanced. At this time the oil pressure in the hydraulic system was not measured but the capability for doing so, was available via the three Druck 810 pressure transducers mounted within a specially manufactured block bolted to the manifold and detailed in Figure 3.12. The trial test of the apparatus was successful and each of the three props were advanced and locked into position. It was clear that it would be possible to measure changes in oil pressure resulting from movements of the wall and, from these, prop loads could be determined.

The model wall had a stiffness that corresponded to a prototype concrete wall approximately 1.35m thick. It was manufactured from 10mm thick aluminium plate and

was sealed against the back wall of the strongbox and the Perspex window using cast silicone rubber seals retained in place with pins as shown in Figures 3.13 and 3.14 (Powrie 1986). Clearly, to ensure that a good seal could be maintained between the retaining wall and the strongbox there must be contact but not to the extent that excessive friction could be generated that might provide restraint to the wall. With this in mind the overall width of the wall, including the seals, was therefore made slightly greater than the width of the strongbox but with provision for silicone grease to be applied to a recess formed in the surface of the soft cast silicone rubber. The purpose of this was to minimise friction whilst enhancing the water retaining effects. The height of the wall was such that for most of the tests a 10mm high upstand protruded above the clay surface. This served in part to ensure that liquid paraffin, used to prevent the retained soil surface from drying during the consolidation period of the test, did not leak into the pre-formed excavation.

Owing to the requirement to maintain stiffness throughout the propping system it was decided to provide walings that would have equivalent stiffness to a reinforced concrete slab of a realistic prototype thickness. With this in mind the following assumptions were made:

- i) Top down flat slab construction incorporating 300mm thick rc slab.
- ii) Young's modulus for concrete  $E_c = 25\text{kN/mm}^2$ .
- iii) Load from earth pressure spreads through the retaining wall and slab at  $45^\circ$  giving an effective deep beam depth of 9.2m.

Hence, the stiffness  $E_c I = 25 \times 10^6 \times \frac{0.3 \times 9.2^3}{12} = 486.7 \times 10^6 \text{kNm}^2$

A beam of similar stiffness made from aluminium ( $E_a = 70\text{kN/mm}^2$ ) required  $I = 6.95\text{m}^4$ . The profile adopted had  $I = 7.45\text{m}^4$  at prototype scale and could therefore be regarded as very stiff. It was considered advantageous to minimise both weight and dimensions of all components in the model apparatus but particularly the walings since, under their enhanced self weight, they may impose excessive lateral load on the hydraulic cylinders. In view of this the use of alternative materials was given consideration. However, of the materials that were possibly suitable, steel would have resulted in an excessively heavy component for the minimum size that could be

machined, whilst magnesium, although offering some weight saving, would require unacceptably large overall dimensions to provide the necessary stiffness. Aluminium offered the best solution since the size necessary to achieve the required stiffness could be machined easily from 25mm thick plate and the weight could be kept to within reasonable limits. The resulting walings, shown in Figure 3.15 were very stiff, being 4m deep by 2.5m wide at prototype scale and were more than capable of providing a similar stiffness to the reinforced concrete slab that they were intended to model.

The area of contact between the waling and the retaining wall was limited to a 3mm wide nib that protruded 1.5mm beyond the waling flange representing the previously mentioned 300mm deep slab at prototype scale. The walings were connected to the hydraulic cylinders by means of a single bolt through a clevis eye, Figure 3.16, to form a pin joint that allowed a small degree of rotation, thereby permitting a capability for self adjustment and ensuring correct alignment with the retaining wall. The walings were prevented from rotating about the axis of the hydraulic cylinders by guide pins that were mounted in the manifold block above each waling.

Beneath the main apparatus, support to the pre-excavated formation was required. A specially manufactured dipped latex bag was used that, when supplied with compressed air at the appropriate pressure, imposed a stress at formation level equivalent to that of the total stress prior to excavation. However, the pressure required was approximately 20kPa less than that resulting from the fluid (Figure 3.17) contained within the polyethylene bag and a stiff plate was therefore necessary to both separate the membranes and support the excess weight of the polyethylene bag. It was recognised that the plate must neither interfere with the wall nor prevent movement of the excavation formation. A clearance of 2mm both horizontally and vertically at the junction of the retaining wall and formation level was therefore allowed for movement. This led to the design of the tapered plate (Figure 3.9) that clamped the polyethylene bag to the underside of the main apparatus. Initially, the plate was designed to support the entire pressure from either the polyethylene bag or the rubber bag since, in the case of a failure of one or the other, it would be subjected to very high bending stresses. To provide such support a 9.6mm thick aluminium plate would be necessary but this could be reduced to 2mm thickness near to the retaining wall. Clearance of 2mm underneath

the taper was maintained, although the heave of the excavation formation during test AM1 caused the rubber bag to become trapped beneath the tapered section of the plate. The tapered plate was subsequently replaced with a 1.6mm thick stainless steel plate which could not withstand the effects of a failure of either the polyethylene or the rubber bag but was nonetheless adequate to resist the variation in pressure between the two membranes. The modified apparatus incorporating the stainless steel plate is shown in Figure 3.18 and a three dimensional representation of the key features of the model and apparatus are shown in Figure 3.19.

### 3.8 Model piles

The position, depth and layout of the model piles was difficult to determine since the mechanism involved in their contribution to reduction of ground movements was not known. Consultation with industry resulted in the use of an embedment depth equivalent to the depth of the excavation, (Ferne, 1998). The depth of clay in the model was limited to 300mm. An embedded pile length of 120mm, equal to the depth of the excavation, was deemed acceptable since there would be a thick layer of clay between the toe of the piles and the base of the model. A fairly arbitrary positioning was eventually adopted owing to the assumption that the piles would merely provide a general stiffening effect to the formation rather than acting purely in tension and thereby anchoring down the excavated surface. This was based on the fact that the movements to be resisted were known to be very deep seated and would certainly extend well beyond the depth of any piles that could be used for this purpose. No guidance was available as to positioning for optimum pile performance although it was felt prudent to maintain a standard three pile diameter spacing between the model wall and the piles to minimise the effect on the wall. Furthermore, the individual piles that would stiffen the formation should also be similarly spaced and this led to the question of pile diameter. Several options were considered ranging from many fairly small (11mm diameter) piles to few large (22mm diameter) piles. The use of large diameter piles was ruled out since it was felt that their use may prevent the observation of plane strain effects near to the window owing to the spacing required. Besides, positioning such large piles in a relatively small area would impose significant restrictions if it was found to be necessary to vary the layout in some tests. Smaller diameter piles were

therefore preferred owing to the flexibility they offered as far as positioning was concerned. In addition, with the spacing regime, they could be positioned close enough to the window to minimise boundary effects whilst allowing confidence that reasonably plane strain behaviour would be observed.

A sample of Blagdenite 88-2517 unsaturated polyester resin was obtained from Blagden Chemicals for some preliminary tests to ascertain the viability of cast in situ piles. The main criteria surrounding the use of cast in situ piles were the availability of a resin that would be pourable at room temperature and cure without excessive exotherm whilst providing good resistance to shrinkage and fast setting. The resin supplied required approximately 1% by weight of a medium activity MEKP (methyl ethyl ketone peroxide) catalyst and a sample of Butanox M50 was obtained from Akzo-Nobel Chemicals Ltd for this purpose. It was hoped that the combination of these two components would give reasonable gelation and curing times. However, in order to reduce the effects of shrinkage and curing exotherm, as far as possible, a small amount of calcium carbonate, filler that had been supplied with the resin, was added. Mixing involved the addition of 50g of filler to 100g of resin and stirring until all agglomerates of filler were completely broken down. The catalyst was then added to the resin and the liquid poured into the pile hole. The resin was of a readily pourable consistency but curing proved slow and shrinkage at about 4% was unacceptably high. The addition of more filler to subsequent mixes did little to reduce the effects of shrinkage but resulted in a much more viscous fluid that was difficult to place without entrapping air bubbles.

Another, faster setting and more stable material was required and a polyurethane resin was obtained. Sika Biresin G27, a two part “fast cast” resin used commercially for complex and rotational mouldings was supplied by Mason Chemicals. This product consisted of two parts that were mixed first with filler, in a similar manner to that used for the polyester resin, and then together to form a pourable fluid with a pot life of about 2 minutes whilst curing would take about 20 minutes. The initial tests on this material made use of calcium carbonate filler and, subsequently, silica sand, mixed in similar proportions to the tests on the polyester resin. However, both the calcium carbonate and the sand were found to be excessively dense and tended to separate during curing leading to a concentration of filler in the base of the pile and solid resin near to the top.



This would clearly be unacceptable for the main testing programme but for these tests, a method of dispersing the resin/filler mixture into the pile holes through a polyethylene bag funnel enabled the formation of piles that were reasonably homogeneous. The piles were observed to shrink less than 1% during curing and a temperature sensor embedded in a pile hole measured curing exotherm to be within acceptable limits (Figure 3.20 ). Having established the feasibility of casting the piles in situ an alternative filler, that was more suited to the polyurethane resin was sought and a sample of aluminium trihydrate (ON) filler was obtained from Mason Chemicals. The addition of this filler to the resin at a rate of 100g filler to 100g resin resulted in an easily pourable fluid that filled the pile holes leaving few, if any, voids and shrinkage on curing was found to be unaffected by the change in filler type. Consequently, this combination and type of resin and filler was considered suitable for the main series of tests from a practical point of view, and all tests conducted that incorporated piles used this material.

A series of tensile and compressive tests were subsequently carried out on samples of resin obtained from piles cast in test AM13. In these tests several 10mm high x 11.8mm diameter cylinders were subjected to compression tests whilst two 49mm long x 8mm diameter samples were prepared for tensile tests. Difficulties existed over determining the most appropriate mode of testing since it was thought that the piles were subjected partially to tension but also to bending. The simple tests that could be performed on tensile and compressive specimens were considered adequate to provide an approximate value of stiffness adequate for the purposes of carrying out the numerical analyses. The samples were tested well beyond the maximum strain that they may be expected to achieve during the tests and from the graph shown in Figure 3.21 the stiffness,  $E_p$ , was determined to be approximately 800MPa. The density of the pile material was found to be about 1200kg/m<sup>3</sup>. Whilst this was about half of the density that could be assumed for concrete it was nonetheless still considered appropriate to use such a light weight material. This was because piles formed from the material could not provide any support to the excavation formation as a result of their self weight and therefore any pattern of reduction in displacements resulting in tests with piles could be assumed to be a result of stiffening effects only.

In order to minimise, as far as possible, disturbance of the soil model a method was developed whereby the cast in situ piles could be installed. The soil sample was to be quite soft and it was thought that a method of forming the pile bores, by use of a thin walled hypodermic steel tube, could be developed relatively easily. The available range of tube size was limited, especially for very thin walled varieties, and this in part contributed to the selection of ½" (12.7mm) diameter piles which, in turn, largely predetermined their location. Tube of this diameter was supplied with a wall thickness of 0.01" (0.25mm) and was used initially to make a sleeve (Figure 3.22) which was advanced to the required depth through a template (Figure 3.23), manufactured from 40mm thick aluminium plate, into the clay. The template contained two rows of 5 holes, reamed to enable the tube to pass through whilst ensuring verticality. A drill bit modified to form an auger was then inserted into the bore of the tube and rotated to enable the clay to be removed. However it was found that the holes could be formed equally well by inserting the thin walled tube, rotating it through 90 degrees, and then withdrawing it together with a core of clay. The depth of the piles could be controlled accurately using a collar, Figure 3.22, that was clamped to the tube at the required position by means of tightening a nylon grub screw and acting as a stop to prevent excess penetration.

### 3.9 Stress history of soil used in the tests

Much of the previous model testing of retaining walls has been carried out on very stiff samples that were consolidated to 1250kPa and then allowed to swell to 80kPa, eg Powrie (1986) and Richards (1995). However, for this project, owing to the stiffness of the wall and propping employed it was considered preferable to use a less stiff soil principally to ensure that measurable movements were achieved. A preconsolidation pressure of 500kPa followed by swelling to 250kPa was used for all tests giving an overconsolidation ratio variation with depth as shown in Figure 3.24. The distribution of pore pressure throughout the model was known and the consequent theoretical vertical and horizontal total and effective stresses are shown in Figure 3.25 leading to a variation of  $K_0$  with depth as shown in Figure 3.26 calculated from:

$$K_0 = (1 - \sin \phi') OCR^{\sin \phi'} \quad (3.13)$$

At the end of preparation in the consolidation press the effective stress and total stress throughout the depth of the sample were equal at 250kPa. Therefore, when removed from the press the soil samples were subjected to high negative pore pressures as the load was removed and the total stress was essentially zero. Closing the base drainage valves and sealing the most exposed surfaces of the clay prior to and during model making sought to minimise dissipation of these pressures such that the effective stress remained as close to 250kPa as possible.

Once on the centrifuge swing the model underwent a further period of consolidation under its enhanced self weight. This resulted in additional swelling throughout the depth of the model although the degree of swelling of any element was dependent upon its depth within the model. Figure 3.27 shows the idealised stress path that may be assumed, at various levels in the model, if there was no loss of suction from the sample during model making. Indication of any loss of suction could be gained from pore pressure readings immediately after spin up of the centrifuge but not before this time owing to the limitations of the pore pressure transducers, to measure large suctions. The pore pressure transducers were necessarily positioned near to the wall and therefore close to surfaces that were not sealed during model making. Whilst every care was taken to carry out the model making quickly, to prevent excessive drying of the clay surfaces, the exposed boundaries would undoubtedly have been affected by loss of moisture near to the transducers. Consequently, and not surprisingly, the pore pressure transducer readings immediately after spin up of a typical test, indicated dissipation of negative pore pressures of up to 220kPa. Clearly, the pore pressures were then significantly less than the expected hydrostatic values and this would have affected the stress path near to the retaining wall but to a lesser extent further away where suctions should have been better maintained. During test AM17 for instance, where three pore pressure transducers were positioned throughout the depth of the model and distant from the retaining wall, dissipation of suction to about half the value assumed in the idealised stress path was indicated. Grant (1998) experienced similar changes on a series of tests that required minimal time for model making and it therefore seems that such changes were unavoidable. The implications of measured pore pressures being lower than the predicted values is discussed in Section 5.2.

### 3.10 Sample preparation.

In common with normal practice the clay samples for the tests were prepared from a slurry at a water content of approximately twice the liquid limit. For speswhite kaolin this is about 120%.

Mixing was carried out in a large paddle mixer using distilled water and kaolin in dry, powdered form or, when available, selected material salvaged from previous tests. Mixing was continued until a uniform slurry was achieved which often took in excess of four hours, particularly when recycled clay was used. The volume required to provide sufficient slurry for consolidation to a 300mm thick sample was greater than could be accommodated in the mixer bowl thus necessitating two separate mixes. As a consequence, slurry mixing, preparation of the strongbox, and commencement of consolidation typically required a full day. Prior to use the strongbox was prepared by thorough cleaning and all ports used for insertion of transducers were plugged. The anodised aluminium surfaces of the strongbox were coated with Duckham's water pump grease and the base lined with a 3mm thick porous plastic sheet over which a filter paper was placed. The base of the strongbox had a herringbone pattern of drainage channels machined into the aluminium surface and connected to drainage taps at each end of the box. The channels and porous plastic sheet provided an effective drainage system that, when separated from the clay by the filter paper, prevented the loss of clay particles.

Since it was required to prepare a consolidated sample 300mm thick in a strongbox only 375mm deep, from slurry of water content 120%, an extension to the box was necessary. The extension was 300mm deep with the same plan dimensions as the strongbox. It was bolted to the top of the strongbox and sealed using an 'O' ring with a liberal coating of silicone grease. The performance of the seal was often less than adequate and extreme care was necessary to ensure that the extension was placed properly and bolted tightly to prevent leakage of clay slurry.

Although the slurry was at a high water content when mixed it was quite viscous and could not have been poured without special equipment. It was, therefore, carefully

placed into the strongbox, using a scoop, to prevent entrapment of air. When the required amount of slurry was in place and the top levelled a filter paper and porous plastic sheet were placed to enable top drainage. The sample was placed in a consolidation press (Figure 3.28) which had a loading platen that fitted tightly within the strongbox. Loading through the platen was by a hydraulic ram the pressure in which was controlled by computer and movement of the ram was measured using a LVDT. Increments of loading commenced at 5kPa and increased fairly rapidly to 50kPa within half an hour. Owing to the time taken to prepare the sample prior to consolidation commencing, the pressure of 50kPa was usually the maximum achieved during the first day. In general, the pressure was approximately doubled each day over the following two days and increased to full pressure on the third day. However, leakage around the extension seal resulted in a much slower increase in pressure for many of the tests.

Consolidation at 500kPa continued for approximately one week whereupon vertical ram movement indicated by the LVDT was negligible. The pressure at the platen was then reduced to 250kPa to commence swelling. Extreme care and familiarity with the software were necessary to ensure that the reduction in pressure was carried out in a controlled manner. The sample was left to swell for at least 24 hours during which time pore pressure transducers were de-aired and calibrated. Care was taken to ensure that the ends of the drainage pipes were kept submerged in water to prevent air from entering the sample. Special equipment was used to install pore pressure transducers through ports in the back wall of the strongbox. This consisted of a stainless steel tube cutter that was used to remove cores of clay slightly larger in diameter than the 6mm diameter of the pore pressure transducer head. The cutter was guided using a reamed ferrule that screwed into the ports and thus ensured that the transducers were positioned at the correct level (Figure 3.29). The porous stones of the transducers were coated with a small amount of clay slurry and then advanced into the model and gently pushed against the end of the cored holes. The purpose of the slurry was to prevent entrapment of air around the stone since the surface against which the stone would otherwise be embedded could not be assumed to be even. Further clay slurry was applied around the transducer cable using a modified skeleton gun, typically used for applying mastic sealant. This procedure ensured that no voids were left as a result of transducer

installation. The sample was now ready for model making but was left for at least 24 hours to ensure full consolidation around the pore pressure transducers.

### 3.11 Model making

The drainage taps at the base of the strong box were closed and all water that had collected above the loading platen mopped to prevent it re-entering the clay when the platen was raised. The strongbox was removed from the consolidation press and the extension and the front, aluminium, wall removed. The exposed vertical surface was very lightly scraped to remove water pump grease (Figure 3.30) and expose the white kaolin surface that was necessary to ensure good image analysis. This surface was then immediately sealed with liquid paraffin or silicone oil to prevent drying.

The top surface of the model was reduced using a circular tube cutter (Figure 3.31) and trimmed to the required level using an extruded aluminium box section cutting tool guided by a 150mm wide aluminium shelf angle bolted to the strongbox as shown in Figures 3.32. When the required level was achieved this surface too was sealed with liquid paraffin after a silicone grease bead had been applied around the edges of the top surface of the model. An approximately 10mm high ramp of unexcavated clay was left immediately behind the position of the retaining wall (Figure 3.33). The purpose of both the grease bead and the clay ramp were to prevent the loss of liquid paraffin from the clay surface during consolidation on the centrifuge. About 200ml of liquid paraffin was poured onto the top surface of the model immediate prior to spin-up to prevent drying of the retained surface during consolidation of the model in the centrifuge. Without such measures there would be a danger of seepage of this fluid down the sides of the model or behind the wall and possibly into the excavation.

A more elaborate jig (see Figure 3.34) than the simple shelf angle was used to form the remainder of the cut faces that completed the model. Originally it was envisaged that the soil profile could be formed using a wire cutter, guided by templates bolted to front and back of the strongbox. However this proved impracticable as it would have prevented the insertion of pore pressure transducers through the back wall since this

would have to be removed to allow for the template. Instead it was decided to shape the model entirely from the front of the strongbox.

The main vertical and horizontal surfaces were formed using the same tools used previously for the top surface (Figures 3.35 and 3.36) but the trench for the retaining wall toe embedment required a special tool (see Figure 3.37). This cutter was guided on a track, shown in Figure 3.38, and had an adjustable blade that allowed the depth of cut to be varied with each pass. A cutting depth of about 5mm was suitable for the relatively soft sample tested and this was found to provide a very smooth and clean trench (Figure 3.39). Thus for a 40mm wall embedment depth eight passes of the cutter were necessary. The cutting blade was of hardened steel and over sized by 0.01mm to give clearance for the model wall to be inserted whilst ensuring the minimum amount of movement during testing.

When piles were used an additional operation was introduced into the sequence and, because of this, the cutting jig for the excavation was modified to allow the pile template to be bolted accurately into position (Figure 3.40). Once the holes for the piles had been formed (Figure 3.41) using the apparatus previously described (Figures 3.22 and 3.23) the resin could be poured. The constituent ingredients of the pile material were usually pre-measured, on the day preceding the test, to save time during model making. This meant that it was only necessary to combine the contents of a few jars and then mix to produce a resin of the required specification. The resulting liquid was transferred into syringes and quickly dispensed into the pile bores (Figure 3.42). This method was found to be extremely effective and produced consistent piles with few visible imperfections. However, during the time taken to place the piles the surfaces of both the excavation formation and that behind the retaining wall and trench were exposed and susceptible to drying. To reduce this effect as far as possible, a piece of polyethylene sheet, cut to size, was placed against the vertical surface although no similar protection was possible for the excavation formation owing to the need to install the piles.

Black plastic marker beads for the image processing were pressed into the vertical surface, generally on a 10mm grid, through a Perspex template using a brass rod with a

shoulder stop to ensure correct embedment. During the early tests about 400 marker beads were used and this operation, consisting of placing each target individually in the template and then pressing into the model typically needed about  $\frac{3}{4}$  hour to complete. For later tests, in which two image processing cameras were used, the number of targets required increased to about 900. Clearly it would take a very long time to place the targets in the template and then embed them in the model using the established method. The targets were therefore pre-placed into the template where they were held in place by adhesive tape. This operation was carried out on a day preceding the test leaving only embedment of the targets into the clay model to be completed during model making. This considerably reduced the model preparation time and it was found that 900 targets could be placed in less than 15 minutes.

At this stage the model was complete and required only the apparatus to be placed. The rubber bag at excavation formation level was positioned and the air supply fitting clamped through the end wall of the strongbox. The main prop module apparatus was then installed (Figure 3.43). Great care was necessary to achieve success in this operation owing to the delicate nature of the polyethylene membrane. If there were any doubts regarding possible damage to the membrane during this operation the apparatus was removed and the bag replaced. When in position the apparatus was secured by two bolts through the end wall of the strongbox above the level of the polyethylene membrane. Finally, the dense fluid drainage connection was carefully tightened into the back wall of the strongbox (Figure 3.44 and 3.45). Before the model wall was positioned the cast silicone rubber seals were filled with silicone grease to limit friction against the Perspex window and the back wall of the strongbox and also to provide a good seal against groundwater flow into the excavation. The wall was slid into place taking care not to pinch either the rubber or polyethylene membranes (Figure 3.46).

When the apparatus had been placed and fixed into position the Perspex window, incorporating the image processing control targets, was bolted in place. The window was first lubricated using a high viscosity, clear, silicone oil. A rack containing LVDTs, to record vertical displacements of the ground surface behind the retaining wall as well as providing a means of direct measurement of wall rotation, was bolted on top of the strongbox (Figure 3.47 and 3.48). Prior to the model being weighed and placed



on the swing the reservoir and drainage control valve were positioned, at the edge of the platform, since there was insufficient room to permit locating these components prior to loading the strongbox.(Figure 3.49).

### 3.12 Testing

Once the model was on the swing a significant amount of work remained to be carried out before the test could begin. This was of a standard nature involving connection of power supplies and transducers as well as compressed air, fluid drainage reservoir, solenoid valve and standpipe to maintain a constant groundwater level in the model. Positioning of lights and cameras to enable good image processing data was critical although experience gained in early tests led to a satisfactory set up that was used very successfully in the main testing programme. When complete, all cables were securely fastened and the polyethylene bag was filled with zinc iodide solution. About 200ml of liquid paraffin was poured onto the retained surface of the model to prevent drying during the consolidation stage on the centrifuge. The model was then ready for spin up (Figure 3.50).

Since the vertical total stress at the excavation formation level was maintained and controlled using a rubber bag supplied with compressed air it was necessary, during spin-up, to increase the pressure incrementally with the centrifuge speed. This ensured that the vertical and horizontal total stresses were in the correct ratio at all times. Whilst the required pressure in the rubber bag could be determined easily the fluid density in the polyethylene bag was more difficult to match to the horizontal stress expected owing to the non-linear variation of stress with depth. Zinc iodide solution mixed to a specific gravity of 1.91 was used to give a hydrostatic pressure of 228kPa acting horizontally at excavation formation level. This required pressure was calculated assuming a saturated bulk unit weight for the kaolin of  $17.44\text{kN/m}^2$ , an average  $K_0$  of 1.2 and that the pore water pressure was hydrostatic with the water table 5mm below the top surface of the model. However, since the theoretical horizontal stress distribution is not linear the total horizontal stress resulting from the fluid pressure was probably not equal to that from the retained soil. This is demonstrated in Figure 3.51 which shows a comparison between the theoretical and imposed pressure distributions. Indeed, during

consolidation on the centrifuge, the level of zinc iodide was, on occasion, noted to rise fractionally. This was a result of the wall moving forward slightly into the excavation (indicating that the support pressure was a little low) and reducing the plan area of the fluid.

When the model reached 100g it was left, at least overnight but more often for about 30 hours, for the pore pressures to come into equilibrium. The excavation stage of the tests was therefore usually carried out two days after removal of the sample from the consolidation press. The depth of the clay model and the ability to control the boundary pore pressure at the base only made consolidation a very slow process and increased the likelihood of instrument failure. The progress of each pore pressure transducer toward their expected equilibrium value was therefore closely monitored and the rate of increase used as a guide when assessing the most favourable time for the test. Clearly, there would be little point in risking a successful test by leaving the model to consolidate over a second night in order to achieve only a very small change in pore pressure.

All tests were relatively complicated and four or five people were required to execute them successfully owing to the need for operation of mechanical components whilst draining zinc iodide solution, adjusting air pressure to the excavation formation and logging data from the image processing. The procedure for most of the tests was as follows:

- i Advance top prop and lock into position.
- ii Drain fluid to level of middle prop whilst simultaneously reducing air pressure at formation to suit rate of drainage.
- iii Advance middle prop and lock into position
- iv Drain fluid to level of bottom prop whilst simultaneously reducing air pressure at formation to suit rate of drainage.
- v Advance bottom prop and lock into position.
- vi Drain remainder of fluid whilst simultaneously reducing air pressure at formation to suit rate of drainage.

The duration of the tests was mainly controlled by the rate of fluid drainage and the air pressure was therefore manually adjusted to maintain the vertical total stress acting at formation relative to the unexcavated height. Although the procedure was involved and labour intensive the test itself was typically completed in less than 8 minutes.

### 3.13 Digital image analysis

The image processing system used in conjunction with these tests was developed as a joint research project with the Engineering Surveying Research Centre at City University and is described in detail by Taylor et al (1998) and Grant (1998). The system relies on the capture of images using a CCD (charge coupled device) camera and tracking the movement of targets in the image plane on the pixel board of the camera. Most of the tests undertaken in this project used one camera although a few later tests made use of two separately recorded cameras to enable a greater area of the model to be viewed. This later arrangement gave the added benefit of allowing comparison of measurements between the two cameras (which were from different manufacturers and specification) where the fields of vision were coincident.

The video output from each CCD camera were relayed through the slip rings. Each camera was connected to a PC with a frame grabber card and discrete images were grabbed and stored at 5 second intervals, during spin up of the centrifuge, and at 20 minute intervals during re-consolidation prior to the simulated excavation. In most tests the frequency of grabbing was increased to 1 per second during, and for the period immediately after, the simulated excavation stage although later in the series of tests, when two cameras were used, it was found that, to maintain some form of correlation, slower image grabbing, at two second intervals, was needed. In order to relate correctly the sequence of images to the corresponding points in the test the epoch numbers of selected individual images were manually recorded against, and subsequently matched to, the sample count recorded by the data logger used to record information from the pore pressure transducers and LVDTs. This system, although laborious, has been found to be reliable.

The work carried out by Grant (1998) used a single camera to view a tunnel lining in the centre of the strongbox. Positioning of the camera presented no particular problems for this application since the area of interest was clearly visible. The main area of interest in these tests however was the excavation formation at one end of the strongbox. In order to bring this area into the field of view of the camera it was necessary to manufacture a special bracket that allowed the camera to be moved to a new location inside the windshield of the centrifuge and positioned at an oblique angle to the model (Figure 3.52). Images taken at such angles were subject to much more distortion than had previously been the case. However, this was calibrated out by the image processing software.

Although the new camera position allowed the entire excavation formation to be seen a large part of the retained surface was, as a consequence, excluded from the field of view. This problem was eventually overcome in test AM15 when a second camera was introduced to view the remainder of the model from the reverse angle (Figure 3.52). This presented some practical problems regarding synchronisation between the two PCs used for image grabbing and the data logger although these were relatively easily overcome, again by the manual recording of epoch numbers of the images against sample count from the data logger.

### 3.14 Summary

The basic principles of centrifuge modelling have been explained and, in particular, the errors and scaling laws applicable to this project have been highlighted. The centrifuge facility, at City University, including the data acquisition instrumentation and image processing, has been briefly described and the requirements surrounding design development of the model apparatus and the special equipment required for model making has been included together with figures based on apparatus fabrication drawings. Details of the soil stress history, sample preparation and model making for the main testing programme have been described and illustrated with photographs where appropriate.

#### 4.1 Details of tests

This chapter describes in detail the tests that were conducted and their basic results. Two basic tests were performed and, in each of these, the apparatus used was as described in Chapter 3. Time constraints dictated that variations focussed largely on the number of piles in the model although the depth of embedment of the retaining wall was also varied in some of the tests. The general details of the tests conducted are presented in Table 4.1 and this is elaborated upon in Table 4.2 where the development of the experimental technique and comments on apparatus performance are made.

In all tests instrumentation consisted of varying numbers of LVDTs and miniature pore pressure transducers. Image processing was also used to provide independent measurement of retained surface settlements as well as subsurface displacements. Later tests made much more use of additional instrumentation in the form of pore pressure transducers and, of these, a few included increased use of image processing. This was made possible by provision of a secondary camera to view an area of the plane strain model that had been hitherto out of sight. The general test arrangement described in Chapter 3 was however varied for a set of three tests: AM10, AM11, and AM12 which was carried out to confirm that the reductions in ground movements seen during early tests in which piles had been used were not influenced by variations in prop stiffness. This series of tests using modified apparatus was devised following problems during test AM9 when it was apparent that the hydraulic props were significantly less stiff than had been intended.

Test AM1 was the first attempt to model an excavation process with the newly developed apparatus. This test was intended to provide a datum, without piles, against which the results from subsequent tests could be compared. Whilst the individual pieces of special equipment had been tested to assess their suitability for model making it was inevitable that unforeseen problems would arise during preparations for early tests. This meant that the time for model making and time spent on the centrifuge swing

prior to spin up was about 12 hours. The time for model making and work on the swing was substantially reduced in subsequent tests, the shortest of which was about 5 hours between removal from the consolidation press and spin up for test AM17 when special efforts were made to prepare all items of apparatus and equipment prior to the day of the test. Typically, however, a period of about 7 hours was required for this work.

The polyethylene membrane used to contain the dense fluid was known to be fragile and a potential source of weakness in the apparatus. It was therefore not surprising that several of the tests had to be abandoned owing to leakage from punctured bags. For this reason no data were available for tests AM3, AM4, AM8, or AM16, all of which were abandoned either just before or immediately after spin up on the centrifuge. In all tests the dense zinc iodide solution was added to the model immediately prior to spin up. The principal purpose of this was to avoid having to work on the model in close proximity to the solution, which, although not particularly hazardous, was moderately corrosive. The first experience of a leak was during filling of the bag for test AM1 when it became apparent that the bag had been punctured and seepage of the fluid into the model was evident. Nonetheless it was decided that the test should proceed so that, if nothing else, the apparatus could be fully tested. The model was spun up to 100g and the test performed immediately, without waiting for any consolidation to take place, since there was a constant, and fairly rapid, loss of fluid from the bag. The apparatus was seen to perform well although no meaningful data were collected. The centrifuge was stopped shortly after the experiment was performed when it was evident that heave, at the base of the excavation, had reached the tapered plate that separated the two membranes. Despite the failure of the polyethylene bag useful information was nonetheless gained from this test and it enabled the apparatus to be modified, by replacing the tapered aluminium plate with a modified stainless steel plate, prior to test AM2.

It was originally envisaged that all tests would be essentially the same to enable direct comparison of results. However, the successful execution of the tests conducted relied upon the satisfactory performance of several components working in less than ideal conditions. Failure of one of the props to attract load during test AM9 seemed to indicate that air may be trapped in the hydraulic system. The propping system was

intended to be very stiff and the difficulty experienced in bleeding air during apparatus assembly was known to be the possible source of a problem. The fact that the props could not, at that time, be relied upon to be as stiff or as consistent as had once been hoped led to the development of a simplified version of the apparatus which was used until the hydraulic system could be satisfactorily bled and the prop stiffness demonstrated to be adequate by means of measurement of piston displacement over time whilst under constant load.

In tests AM10, AM11 and AM12 the wall was effectively fixed in position, to prevent horizontal displacement, by means of two aluminium plates that fitted tightly between the apparatus and the retaining wall, Figure 4.1. These could be virtually guaranteed to provide stiff support to the wall whilst still permitting vertical displacement because the horizontal support allowed the wall to remain free to move in this plane. Since the wall would always be propped the use of a fluid filled polyethylene membrane was unnecessary and this omission simplified these tests considerably. Only an air filled rubber bag, at excavation formation level, was necessary to provide the correct pre-excavation total stress. The tests were therefore conducted, very simply, by gradually reducing the pressure in the rubber bag to simulate the reduction of total stress caused by the excavation process.

By and large tests AM10, AM11, and AM12 were successful and, in view of their simplicity, were low risk as far as apparatus failure was concerned. However, even these tests were not free from problems. In both AM10 and AM12 the rubber bag, that provided support at formation level, burst during or soon after spin up. This was because there was inadequate support between the plate that would normally separate the two membranes and the retaining wall. The absence of the fluid filled bag had created a small gap that the thin rubber membrane was unable to bridge when under pressure. In both instances the apparatus was carefully removed from the strongbox, with the model remaining on the swing, and the rubber bag replaced. This approach, whilst relatively quick to perform, necessitated the removal of one of the image processing targets that were fixed to wall. However, the alternative, involving complete removal of the model from the swing and partial dismantling of the strongbox, to enable access to the damaged bag, would have taken considerably longer and would quite

probably cause damage to the model hence the compromise was made. A small packing piece was introduced to provide additional support to the rubber bag during subsequent spin up for each test.

During the 30 hour consolidation period on the centrifuge, prior to the simulated excavation stage of the test, the excavation void partially filled with water. This was because the absence of the fluid filled polyethylene bag, used in the main tests, resulted in the excavation becoming a reservoir for the water supplied to the base of the model by the stand pipe. The quantity of water that entered the void past the rubber bag supporting the formation appeared substantial owing to the level that was visible against the Perspex window of the strongbox. However, the volume was found to be quite small following reduction of air pressure at formation when the level dropped substantially.

Clearly, the level of water that accumulated in the excavation during consolidation would have affected the effective stress in the vicinity of the formation level. It is reasonable to assume that during the conventional tests, when a dense fluid filled polyethylene bag occupied the excavation void during consolidation, the same groundwater level would be imposed throughout the soil model and the area of the excavation. This is because only a small amount of water would be needed to fill small voids in the excavation where the bags did not quite fit into the corners. However, owing to the large void in the area of the excavation during the simplified tests, flow of water into the model was insufficient to achieve a level equivalent to that in the soil model. Consequently, a lower pore pressure existed inside the excavation at the end of consolidation and resulted in an increased  $\sigma_v'$  of slightly varying amounts in the simplified tests. The excavation formation level could therefore be expected to be somewhat stiffer in the period during and immediately following excavation for the simplified tests but may not have been very uniform with the centre being stiffer than the edges. Nonetheless, the consequence of the additional water directly on the unsupported formation led to fairly rapid softening and disproportionate heave displacements in comparison to the standard tests where a fluid filled bag was used.



Although very much simplified in comparison to the main test series, these tests were extremely useful in establishing, beyond doubt, that piles could be seen to contribute to the control of ground movements. This was made possible owing to the simplifications made to the apparatus which enabled the excavation simulation to be carried out in a very much more controlled and consistent manner than had hitherto been possible. The simplified method therefore contrasted with some of the conventional propped wall tests where the time taken to complete the excavation varied between 6 and 20 minutes. Such variation in time should be borne in mind when interpreting the results since at prototype scale this amounted to more than 3 months.

## 4.2 Observations and Results

### 4.2.1 Tests AM10, AM11 and AM12

The tests essentially sought to eliminate the effects on ground movement of horizontal wall movement associated with varying stiffness of propping. They showed that the introduction of piles had beneficial effects in reducing both horizontal and vertical displacements behind the retaining wall.

Figure 4.2 shows a plot of the retained surface settlements measured immediately after completion of the excavation. Near to the retaining wall the settlement was about 50% more for test AM10, the excavation without piles, than for test AM11, with 10 piles. Slightly less reduction in displacement was observed in test AM12 where 5 piles were used. Further away from the wall, at a distance equal to about twice the excavation depth there was no clear distinction between settlements in the three tests although all displacements were very small.

One hour after the completion of the excavation, i.e. allowing for some dissipation of excess pore pressures, the settlements observed in the three tests were well established (Figure 4.3). Near to the retaining wall the displacements observed in both of the tests with piles were about 80% of those seen in test AM10. There was a less clear distinction further away from the wall but the greatest settlements were seen in test AM11 where 10 piles were used. The displacements at the retained ground surface

were no longer so limited in their extent and small movements were recorded at a horizontal distance up to 3 times the excavation depth. The settlement profiles indicate that after a relatively long period of time the use of piles had the effect of reducing displacements near to the wall. Further away from the excavation there was no strong indication that overall displacements had been reduced by the introduction of piles. However, the effect of limiting maximum settlement would nonetheless be beneficial since it would ensure reduced variation in displacement (i.e. less differential settlement) over the area behind the retaining wall

At the completion of excavation the heave measured by image processing at the excavation formation clearly showed a progressive reduction as more piles were introduced, (Figure 4.4). The reduction in heave was most pronounced at the pile positions although a general reduction was observed across the entire formation. In broad terms the displacements were halved by the introduction of 5 piles in test AM12 and reduced by two-thirds with 10 piles in test AM11. The effect of friction on the end wall of the strongbox probably led to the slight reduction in heave measured close to this boundary in test AM10. The excavation process, particularly for these simplified tests, which was carried out in about two minutes could be regarded as undrained. It is perhaps surprising therefore that the results obtained from the heave measurements are not in more close agreement with the corresponding settlements observed in Figure 4.2.

Horizontal displacements (Figure 4.5), measured immediately behind and below the wall using image processing, also reflected the general trend of reduced movement with increasing use of piles. Maximum displacements in tests AM10 and test AM12 were observed around the toe of the wall, at a depth of 160mm below ground level. This indicates that some forward translation of the wall had occurred since at the ground surface the retaining wall had moved into the retained soil. In test AM11, however, movement was of a generally constant amount over the height of the wall with no rotation being observed. Near to the strongbox base displacements were negligible although this was probably a result of frictional effects at the boundary.

It was found that the ability to see the effects of the piles on displacements throughout the model could be achieved by using the image processing data to draw contours of

horizontal and vertical displacement. The magnitude of the movements that occurred immediately upon completion of the excavation simulation were however too small to enable meaningful contours over the entire area of the model. This was because at such an early stage most of the measurable displacements were at the excavation formation level and those elsewhere were too small to be resolved using image processing. The effects of the piles could be seen more clearly some time after the excavation had been completed, (Figures 4.6 and 4.7a-c). For tests AM10, AM11 and AM12 contours of horizontal and vertical movement were plotted for the stage 30 minutes after commencement of the excavation process. The contours were based on the difference in x and y coordinates for each of the image processing targets within the field of view of the camera. With increasing use of piles, the contours clearly show that both vertical and horizontal displacements were reduced and that the reduction in movement could be seen throughout the model.

#### 4.2.2 Tests AM2, AM9, and AM14,

A successful test without piles was most important to establish a datum against which other test results could be compared. Such a test was therefore repeated three times before there was satisfaction with both the test procedure and the consistency of the results. Following test AM1 the apparatus was modified slightly to enable more room for the unsupported excavation formation to heave. However, during the early test AM2, instrumentation was minimal with only two pore pressure transducers in the model and seven LVDTs to measure surface displacement. In recent previous testing, particularly with tunnels, use had also been made of image processing (Grant, 1998). In those tests, most of the activity within the model had been near to the centre of the strongbox window and the camera had been positioned accordingly. However, for these retaining wall experiments the excavation was positioned at the right hand side of the strongbox and thus partially outside the field of view of the camera. Clearly an alternative approach was necessary but in the meantime the tests proceeded in the knowledge that only limited data would become available from image processing. In general therefore the success of test AM2 merely proved that the test procedure was possible, and confirmed that further work was necessary to enable image processing to

be of use. The test was also useful, however, in demonstrating that the addition of pore pressure transducers around the retaining wall may be beneficial.

The datum test was not repeated again until test AM9 when more instrumentation was available. The procedures for model making and consolidation were, by that time, well established and it was known that, if a test was conducted with care, success could reasonably be expected. However, during testing, the drain valve initially failed to open leading to a delay in commencing the excavation following installation of the top prop. This problem was relatively quickly overcome and the excavation stage of the test then proceeded normally.

Relatively large settlements were recorded, at the retained ground surface, reaching a maximum value at a distance behind the wall equal to approximately half the excavation depth, i.e.  $0.5H$  (Figure 4.8). Indeed the magnitude of the settlements, that were recorded for test AM9, following simulated excavation were greater than for any other test. These large displacements were also reflected in the excavation formation where heave, measured by image analysis, is shown in Figure 4.9. Maximum heave was seen to occur at about 50mm from the face of the retaining wall and this, as in all previous tests, reduced towards the end wall of the strongbox. Two image processing targets indicated markedly lower displacement values probably as a result of excessive friction against the window. Horizontal displacements measured along a line immediately behind and below the retaining wall were also greater for test AM9 indicating good correlation between the data, (Figure 4.10).

Prop forces are discussed fully in Section 4.5 but those associated with test AM9 (Figures 4.11a and b) are mentioned at this point owing to the fact that their significant difference in comparison with those measured in other tests identified a problem with the apparatus that led to a series of three simplified tests AM10, AM11 and AM12. Following their initial installation the middle and bottom props in test AM9 attracted very much lower values than could be expected given the experience of previous tests. In most other tests a prop force of about 100N was measured upon installation and a force of this magnitude was generally maintained or increased as the test progressed. Indeed the force in the middle prop reduced at the time the bottom prop was installed

and failed to recover subsequent to completion of the simulated excavation. Most of the load was carried by the top prop in which a much higher than usual force was recorded. Furthermore, when the test was stopped a rupture line was clearly visible emanating from the toe of the wall. Close inspection of the model revealed that the line rose behind the wall but stopped some 80mm below the retained ground surface about 35mm behind the wall, (Figure 4.12). The toe of the wall had itself rotated into the excavation leaving a clear gap, immediately behind the Perspex window, measuring nearly 2mm at the base. Clearly, the two lowest levels of propping had failed to provide adequate support to the wall.

After the test the model was dismantled and the prop assembly was removed and set up on the bench with constant loads applied to the hydraulic cylinders. Displacement was measured over time and confirmed the assumption that air was trapped in the hydraulic system. The reason for this was found to be that in handling the apparatus, which was relatively heavy, it was possible to accidentally pull on the walings which, in turn, would allow air to enter the hydraulic cylinders and become trapped behind the piston. Removal of the return springs from the pistons had made this problem possible and care was obviously necessary in handling the apparatus to prevent a recurrence.

The sealing system was replaced where zinc iodide solution was found to have corroded some components and the apparatus was refilled with hydraulic oil, bled and re-tested. Testing of the apparatus involved loading the hydraulic cylinder pistons incrementally with weights to apply a force of around 100N per cylinder. Piston displacements were measured during the period of loading using LVDTs (Figure 4.13) and enabled the stiffness of the propping system to be determined from a reasonably linear section of the graph as  $350 \times 10^3 \text{ N/m}$  in terms of spring stiffness assuming that the wall and walings were essentially incompressible. Over a model width of 200mm this provides a stiffness of  $1.75 \times 10^6 \text{ N/m}$ .

The prop stiffness is not known for the tests that were conducted prior to the apparatus load test although it could probably be approximated from prop load and displacement data gained during tests. However, relatively small differences in horizontal displacement between pre and post bleeding tests suggests that the influence, although

noticeable, was small. Comparative spring stiffness for the centrifuge model tests, numerical analyses and basement excavations in London Clay are given in Table 4.3 and indicate that the stiffness of the centrifuge apparatus props was relatively low.

The maximum applied force was maintained over a period of about 20 hours (Figure 4.14) and displacement under constant loading can be seen to continue on all props at a maximum rate of approximately 10µm/hour. The additional displacement with time was probably caused by minor leaks in the hydraulic system and was at a sufficiently low rate as to be regarded acceptable in view of the typical test duration. Therefore, following the loading tests, there was confidence that the apparatus was performing well and that the props could be relied upon to provide stiff support. The retaining wall testing then resumed using the conventional apparatus set up for test AM13 the results of which are reported in Section 4.2.4.

Following good performance in test AM13 a third attempt at a successful datum test was undertaken in test AM14. No problems were encountered during the sample preparation, model making or test procedure and the test was regarded as a complete success in this regard.

The displacements measured during the test were in good agreement with those in test AM9 (see Figures 4.8-4.10 inclusive) in as much as they were of a large order of magnitude in comparison to the previously conducted tests that had included piles. Both vertical and horizontal surface displacements were generally less in test AM14 but of a similar magnitude to test AM9 which seemed reasonable given the difference in conditions imposed in the two tests. The settlement profile behind the retaining wall (Figure 4.8) indicated displacements near to the wall that were very similar to those shown in test AM9. However, with increasing distance from the wall, the values recorded in test AM14 reduced to less than half of the corresponding amount in test AM9. In contrast, the magnitude of horizontal displacements (Figure 4.10) were seen to be of a similar order at depth, below the retaining wall, and less in agreement near to the surface where the displacement measured in test AM14 was a fairly consistent amount

less than test AM9. Heave measured at excavation formation level (Figure 4.9) followed a similar profile to that for test AM9 although this too was less pronounced.

Prop loads measured during and after the excavation stage of test AM14 were higher than those measured in previous similar tests. This was expected since the hydraulic system had been bled making the props stiffer. However the bottom prop attracted an unexpectedly high load in comparison to earlier tests and the oil pressure transducer very quickly became out of range owing to high amplification of the output. As a consequence no data were available for the load in the bottom prop for most of the post-excavation period of the test.

Contours of both horizontal (Figure 4.15a,b) and vertical (Figure 4.16a,b) movement after 15 minutes were plotted for tests AM9 and AM14. The relatively small number of image processing targets used during test AM2 precluded such a representation of the data for that test. Patterns of overall movement and the location of maximum movement were similar for both tests but the greatest heave displacements at excavation formation level were seen in test AM9 (Figure 4.9), and this test also showed greater settlements than test AM14 (Figure 4.8) over the same period. Horizontal movements in the two tests were similar in magnitude despite the lack of stiffness of the lower props in test AM9.

#### 4.2.3 Tests AM6 and AM15

Tests AM6 and AM15 both incorporated 1 line of 5 piles in the excavation formation close to the retaining wall (Figure 4.17). Test AM6 was the first test in which model piles were used and, whilst the test could be considered relatively successful, a sudden and unexpected drop in air pressure was experienced in the period immediately before the excavation was simulated. The air pressure reduced to a minimum recorded pressure of 158kPa over a period of about 8 minutes before the full pressure of 210kPa was restored. Such a reduction, in terms of total stress acting at excavation formation level, corresponded to premature excavation of about 3m. The pore pressure transducers responded to the drop in support pressure in the manner expected. However, in terms of the influence on ground movements, there was only a small effect

since the rate and magnitude of movement were known, from experience of previous tests, to increase substantially only after considerably more excavation was complete.

Nonetheless the test was repeated in test AM15 when additional image processing was available to enable a greater area behind the retaining wall, and in particular the surface, to be viewed. The provision of a secondary camera also enabled an independent check of the image processing used elsewhere, and in particular, the measurement of heave at excavation formation. This was made possible by comparison of measurements in an area within the field of view of both cameras and is discussed in greater detail in Chapter 3.

Similar duration for the excavation simulation allowed a direct comparison to be made between the two tests. Reasonable agreement was obtained from the settlements measured by the LVDTs although, near to the retaining wall, larger displacements were measured in test AM15 than in test AM6. The range of displacements that were recorded in the two tests was small, however, and values were considerably less than those measured during tests AM9 and AM14 where no piles were used. This is shown in the plot of settlement against excavation depth, (Figure 4.18). Similarly, heave measured at formation level using image processing, (Figure 4.19) revealed a marked reduction in displacement, particularly near to the retaining wall where the piles were positioned. Additionally, as with settlement, quite good consistency was achieved between results for the two tests particularly when the magnitude of displacements are compared with those for tests AM9 and AM14. Heave measured in test AM15, (Figure 4.19) was generally greater than that in test AM6, particularly close to the wall although the slight loss of pressure at formation level prior to the simulated excavation stage of the test would account for some of the difference.

Horizontal displacements measured immediately behind and below the retaining wall were of similar magnitude at depth. Near to the bottom of the strongbox virtually no movement occurred indicating that boundary effects were influencing movements. Behind the retaining wall consistently smaller horizontal displacements were measured in tests AM6 and AM15 than in tests AM9 and AM14 where piles had not been used and the range of maximum displacements were reduced by about 50% (Figure 4.20).



Contours of movement were plotted for test AM15 but not test AM6. This was because the amount of image processing data available for test AM6 prevented meaningful interpretation in this form. The use of two cameras during test AM15, however, enabled two composite contour plots (Figures 4.21 and 4.22) to be made incorporating data from both cameras and covering most of the area of the model. The contours indicate that the piles influenced not only movements generated at the retained surface and excavation formation but also areas remote from the excavation when compared with tests AM9 and AM14 (Figures 4.15 and 4.16). An overall reduction in movement therefore resulted from the use of piles.

As stated previously, general observations on prop loads are made in Section 4.4 since most tests followed a similar pattern. However, the loads seen in tests AM6 and AM15 were significantly different, (Figure 4.23) with much higher loads being measured in test AM15 than in test AM6. The middle prop, in both tests, carried most of the horizontal load whilst the top props carried only a small amount of load and only during the early stages of excavation. The installation of the lower levels of propping had a marked influence on the top props where load, subsequent to lower prop installation, consistently reduced throughout the remainder of the test. The bottom prop in AM6 carried load immediately upon installation but this soon reduced, in a similar way to the top prop. Clearly, most of the horizontal support was being provided by only one or two props with the top props being largely superfluous.

#### 4.2.4 Tests AM7 and AM13

In tests AM7 and AM13 two rows of 5 piles were incorporated into the model in an attempt to determine if additional piles would assist in reducing movements further (Figure 4.24). AM7 was only the second test undertaken with piles and, in order to reduce model making time as much as possible, the three constituents of the pile resin were weighed out on the day preceding the test and stored overnight. Half of the aluminium hydroxide filler was mixed with each of the Part A and Part B components. It was intended that these two components would then be mixed in equal proportions to produce the resin. Unfortunately, when the components were mixed together and poured into the pile holes the resin foamed and failed to harden properly. The resulting

substance was very different from the properly cured resin but it was impossible to remove. One pile in particular was very spongy and this was re-augered to allow some correctly mixed resin to be placed. This operation was, however, only partially successful and the finished pile at that position bore little resemblance dimensionally to the other piles in the model.

Sample preparation for test AM13 was made difficult since the load cell, used to monitor and control pressure on the sample during consolidation, failed shortly after the sample was placed in the consolidation press. Consolidation pressure during test AM13 and, indeed all subsequent tests, was therefore controlled using an oil pressure transducer that hitherto had primarily been used to monitor pressure in the hydraulic cylinder above the loading platen. The use of this transducer required a minor amendment to the computer control program but any reduction in accuracy resulting from an indirect measurement of pressure was estimated to be small and probably limited to the weight of the ram and friction in the seals. Furthermore the use of this transducer could be justified owing to the fact that, prior to failure of the load cell, it was common for the oil pressure transducer to be used as an independent check of pressure on the sample at any particular time. The normal ratio between pressure measured using the transducer and that of the load cell was therefore well known. The transducer was successfully used to control both the compression and swelling stages of sample preparation

In contrast with test AM7, the model making operation in test AM13 proceeded well as the experience gained during testing in the intervening period meant that the techniques necessary for successfully incorporating piles were well established. Following spin up and reconsolidation on the centrifuge the excavation simulation stage of the test was undertaken. Drainage of the dense fluid from the model during this stage was much slower than with previous tests. The cause of this was found to be a restriction in one of the polyethylene drainage pipes that had been partially crushed during tightening of a union whilst assembling the apparatus. The effect of this was to slow the excavation stage of the test such that a period of about 18 minutes was necessary to complete the drainage of fluid from the model in comparison to between 7 and 9 minutes for most of the other conventional tests.

Despite the difficulties experienced in model making during test AM7 the retained ground surface settlements measured during the two 10 pile tests, (Figure 4.25) were not significantly different in magnitude at the end of the excavation stage. This was especially the case close to the retaining wall. The profile of the settlement trough in AM7 was slightly different in comparison with other tests since the maximum displacement occurred at a distance, from the back of the retaining wall, equal to  $H$ , the depth of the excavation, rather than  $0.5H$ . Away from the retaining wall, at a distance greater than  $2H$ , there was no clear distinction between those tests that included piles and those that did not.

Similarly, heave measured at excavation formation was generally very similar in tests AM7 and AM13, (Figure 4.26) and also comparable in magnitude to tests AM6 and AM15. By and large displacements were very much reduced in comparison to tests AM9 and AM14. In general, a marked reduction in heave was seen around the pile positions in tests AM7 and AM14, even where the piles were defective. However, there was no indication that discernible benefit may accrue from the use of additional piles since values of both settlement and heave were similar to those seen in tests AM6 and AM15 in which 5 piles were used.

Horizontal displacements immediately behind and below the retaining wall were also of a similar order in both tests (Figure 4.27) and considerably less than those measured in the tests where no piles were used. In terms of proportion, the maximum displacement measured in AM7 and AM13 was about a third of that in tests AM9 and AM14 where no piles were used and around half of that measured in test AM6 and AM15. In general, similar reductions in displacement were seen with 5 or 10 piles. A less well defined deviation in movement over the height of the model was apparent when piles were used since horizontal movement was seen to reduce substantially at depth in all tests appearing to be influenced by boundary effects caused by the relatively close proximity of the base of the strongbox.

#### 4.2.5 Tests AM5 and AM17

The retaining wall in tests AM5 and AM17 had only 25mm embedment and no piles at excavation formation level. The purpose of these tests was to investigate the effect of wall embedment on movements both in front of and behind the retaining wall but, in particular, in relation to the use of piles.

Model making for test AM5 progressed well but a slight leak of zinc iodide solution into the model was evident upon spin up. The fluid loss was very slow but, considering the time required to establish pore pressure equilibrium, it was clear that an almost total loss of fluid would have occurred if the model was left spinning for the minimum time of about 18 hours necessary to establish conditions of pore pressure equilibrium. It was decided that the centrifuge should be stopped, the base drain closed, and the model left on the swing overnight. The following morning the model was removed from the swing and partially dismantled to allow access to remove the apparatus. The excavation formation and trench had clearly swelled overnight, by approximately 3mm, and to such an extent that it was necessary to trim the excavation. The polyethylene bag was carefully removed from the apparatus and inspected for leaks although it appeared sound. It was concluded that one or more of the bolts that were sealed with 'O' rings, and used to tighten the membrane separation plate through the bottom of the polyethylene bag, had been the cause of the leak. Nonetheless a new bag was placed on the apparatus and the bolts fully tightened before the apparatus was replaced in the model. On spin up a small drop in pressure measured by the transducer immersed in the dense fluid was thought to be a result of 'bedding in' and was seen to reduce with time.

Test AM17 was conducted nearly a year after test AM5 and the techniques involved in sample preparation, model making, and testing were well established and, with care, successful execution of tests could reasonably be expected. Considerably more instrumentation was also available at this time including increased use of image processing and pore pressure transducers.

Measurement of retained ground surface settlements in the two tests were very different. The settlement profile for test AM5 shows vertical displacement to be about

one third of that measured in test AM17, (Figure 4.28) near to the retaining wall although at a distance of  $2.5H$  (where  $H$ =height of excavation) behind the retaining wall settlements in the two tests were, in common with other tests on more deeply embedded walls, of the same order. In both test AM5 and test AM17 maximum displacement measured by the LVDTs was at a distance  $0.25H$  from the back of the retaining wall indicating that the pattern of displacement was similar to that seen in other tests. Significantly, magnitude of settlement, in comparison to that seen in other tests was generally much less despite the shallow wall embedment.

Heave measured during test AM5 by image processing, near to the excavation formation level, was in the order of 50% of that measured in test AM17, (Figure 4.29). Pertinently, the magnitude of the vertical displacements in these two shallow embedment tests were much less than those seen in most of the other deeper embedment tests. Furthermore, the displacements recorded at excavation formation level in test AM5 were the least of all of the tests undertaken by some considerable margin, (Figure 4.30). Horizontal movements throughout the depth of the model were also less in test AM5 than in test AM17, (Figure 4.31). The magnitude of these displacements were consistent with those seen at the retained surface and excavation formation but also towards the lower end of the range of values measured in other tests that included more deeply embedded walls and/or piles. Clearly the relatively small displacements observed in these tests, although fairly consistent when viewed in isolation, are at odds with those seen in the other tests.

#### 4.2.6 Test AM19

Test AM19 was conducted as a comparison with tests AM5 and AM17 but 10 piles were installed at excavation formation level. Sample preparation, model making and testing proceeded without problems and the displacements measured appeared reasonable in comparison with those measured in the majority of tests conducted.

The magnitude of settlements measured immediately behind the retaining wall (Figure 4.32) were between the values seen in tests AM9 and AM14 where the wall had deeper embedment but no piles and those seen in tests AM5 and AM17. At a distance of about

2.5H the displacements tended to be similar for all tests and consequently there was a relatively large variation in displacement over the retained surface in test AM19 when compared with tests AM6, AM7, AM13 and AM15, where piles had been used at the excavation formation (Figure 4.33).

At excavation formation level a fairly consistent pattern of heave was measured over the width of the excavation except very near to the retaining wall where exceptionally large values were recorded. Generally displacements were similar in magnitude to those seen in most of the other tests that had included piles, but greater than those seen in the shallow embedment wall tests without piles (Figure 4.34). Additionally, and in common with other similar tests, slightly less displacement was measured around the pile positions.

Horizontal movements (Figure 4.35) were within the range seen in tests with deeply embedded walls but without piles. Relatively large horizontal displacements were measured around the toe of the retaining wall that reduced rapidly with depth.

#### 4.3 Retaining wall displacements

The stiffness of the retaining wall was intended to be such that any deformation resulting from bending would be negligible. This was almost certainly achieved although the stiffness of the propping system influenced horizontal movements to a greater or lesser extent in all of the tests. It is therefore important that care be taken in comparing the results of the early tests with those of later tests following bleeding of the hydraulic system. Inevitably the propping system in the later tests was stiffer and resulted in smaller displacements. The use of two image processing targets fixed to the retaining wall together with LVDTs measuring horizontal displacements above the retained soil surface (Figure 4.36) was intended to enable the rotation and horizontal displacements of the wall to be quantified by independent means if assumptions about the point of rotation were made. However, problems in determining the point of rotation and the need for extrapolating the image processing data meant that good correlation between the two methods could not be achieved and the results need to be interpreted with care.

In Figure 4.37 image processing data has been extrapolated to show the horizontal displacements at the top and bottom of the retaining wall in three tests with similarly embedded walls but with varying formation stiffness. The hydraulic oil in the apparatus had been bled in the period immediately preceding the three tests considered and similar stiffness can therefore be assumed for the propping system in all tests. At the toe of the retaining wall increasing numbers of piles resulted in reduced horizontal displacements (Figure 4.37a). Test AM13 included 10 piles at the excavation formation and although the simulated excavation stage of this test was slower than most other tests conducted owing to difficulties with the drainage valve, and three times as long as test AM14, it resulted in about 50% of the displacement measured during the same operation in that test. The effect of the piles is also well pronounced in test AM15 where 5 piles were used and movement in comparison to test AM14 was reduced by about 25%.

At the retained ground surface (Figure 4.37b) the effects of the piles are initially less clear. Anticlockwise rotation resulted in the stiff wall in test AM14 moving into the retained soil as it rotated about the bottom prop. Such rotations are also apparent in test AM13 and test AM15 and are characterised by a reduction in displacement at the end of the simulated excavation stage. Overall movement of the wall was governed by displacement at the toe and similar behaviour was seen in all tests although increased overall horizontal movement occurred in test AM15 in comparison with tests AM13 and AM14. The reason for this is uncertain since the propping system was of comparable stiffness in all three tests. Despite this, relatively large displacements near to the retained surface during the simulated excavation could indicate that a lack of stiffness allowed additional movement. Prop load data for test AM15 indicates that all three props contacted and remained in contact with the retaining wall at the appropriate points throughout the excavation stage of the test which, given the excessive movement, tends to imply a problem with trapped air in the hydraulic system.

#### 4.4 Comparison of image processing and LVDT measurements of retained surface displacements.

Displacements during all tests were measured using both image processing and LVDTs (Figure 4.38). The use of two independent systems of measurement enabled greater

confidence to be placed on the accuracy of two similar sets of measurements when compared to a single set of data from either one or the other methods of recording displacements. Additionally, the use of two image processing cameras during tests AM15, AM17 and AM19 enabled the performance of the cameras and the software to be tested and an assessment of the accuracy of those measurements made. This was made possible because a substantial area of the model in the region behind the retaining wall was in the field of vision of both cameras (Figure 4.39). The main camera used for image grabbing was a monochrome CCD camera manufactured by TELI (model no.CS-3150). This camera was used in all tests and differed substantially in specification, notably focal length, from the secondary Pulnix camera (model no.TM6) used in tests AM15, AM17 and AM19. The difference in specification and significant different positioning of the cameras during these latter tests meant that comparison of the data was not straightforward.

The image processing software assigns numbers to all targets embedded in the soil surface and calculates their positions in pixel co-ordinates and subsequently in the soil plane. The positions and numbers of all control targets are specified by the user, since their positions are already known, enabling the software to calculate the camera position in an iterative manner. This means that even though it was necessary to carry out a separate analysis for the data from each camera the two sets of results could be compared by identifying individual target numbers in each set of data since both were related to the same known control target positions. This was an arduous task given the number of targets and the fact that the data from each was required to be matched manually. It was therefore only practical to carry out the exercise for a snapshot of data rather than a series of images, which would have been preferable, although the number of targets considered implies that the results can be viewed with reasonable confidence.

In view of the limited scope of the investigation it was decided to look at the overall displacement of all targets within the field of view of both cameras during the excavation stage of a random test. Experience in previous experiments had indicated that relatively small displacements would be measured during this part of the test, especially if piles were used, and would therefore provide the best means of comparison of accuracy. Displacements measured by the two cameras were plotted against each



other in Figure 4.40. From this it can be seen that there is good agreement in the data although positive horizontal displacements were measured as fairly constantly smaller values by the TELI camera. Better agreement was obtained between the vertical displacements. Apart from one or two spurious points all of the data plots fall within a range of 100 $\mu$ m. However, the majority of data fall within a band width of about 50 $\mu$ m suggesting that an accuracy of about  $\pm 25\mu$ m was achieved.

Whilst resolution appears to be extremely good, measurements of displacements in plane strain models using these techniques are known to be potentially underestimated owing to frictional effects at the Perspex window/kaolin interface. Grant (1998) found that measurements of ground surface displacements during plane strain tests on tunnels were detected by LVDTs before image processing and suggested that a stick-slip mechanism was responsible for a constant offset of about 100 $\mu$ m between the two methods of measurement. The viscosity of the lubricant used to minimise the friction effects was found to have a significant influence on the magnitude of the offset with increasing viscosity leading to progressively smaller offsets although, not surprisingly, it proved impossible to completely eliminate the offset. Grant (1998) stated that the current practice of using very high viscosity (12500cS) silicone oil prevented the clay from coming into contact with the Perspex window although the optimum method of minimising friction had yet to be confirmed. In addition to viscosity, the quantity of oil used could also be assumed to play an important part in producing good results. An extremely careful balance was necessary to ensure that sufficient oil was used to provide the necessary lubrication without being excessive as this would risk blocking of the base drain with oil seeping down under its enhanced self weight during reconsolidation on the centrifuge. This proved difficult to achieve during early tests although, with experience, the correct amount of oil could be gauged fairly easily and consistent results achieved.

A slight difference existed between the level at which image processing and LVDTs recorded displacement owing to the fact that the top row of image processing targets were embedded 5mm below the soil surface whereas the LVDTs were at the surface. Additionally, and more importantly, the top row of targets were not usually clearly

visible since swelling, during reconsolidation, tended to move the targets just above the Perspex window and therefore out of the field of view of the camera. As a consequence, the surface LVDT displacements were compared with the nearest image processing targets some 15mm below.

During the simulated excavation stage of the tests conducted image processing appeared to be more sensitive than LVDTs as far as initial movements were concerned. Figure 4.41 shows that over the first three minutes of the test no appreciable displacements were recorded by the two LVDTs nearest to the retaining wall although nearly 50 $\mu$ m settlement was recorded by image processing. However, by the time total vertical displacements reached about 150-200 $\mu$ m there was no discernible difference between the two methods of measurement although LVDTs recorded a greater magnitude for subsequent displacements. By the end of the simulated excavation stage of the test, and in common with Grant (1998), an offset in recorded settlement of about 100 $\mu$ m existed between the LVDTs and image processing (Figure 4.42). This offset was generally maintained although it increased slightly with time immediately behind the retaining wall.

The offset tends to indicate that friction effects at the window were responsible for the discrepancy in measured displacements following the simulated excavation stage of the test. However, it is uncertain why such effects were not seen during the early stages of the test as well since it would seem likely that they could be expected to be at their greatest at this stage. One possible reason for the offset is loss of lubrication at the kaolin/Perspex interface. During the reconsolidation stage of the test the polyethylene bag containing the dense fluid together with the rubber bag at excavation formation could be assumed to be effective in preventing silicone oil from being squeezed out from between the kaolin and Perspex at the formation level. Following removal of the overburden the normal stress acting around formation level could force the oil into the base of the excavation thereby enabling contact between the kaolin and Perspex and resulting in increased friction. During dismantling of models subsequent to testing, the very viscous silicone oil used to lubricate the window was often found to coat the

underside of the rubber bag at formation level thus suggesting some seepage into the excavation and the potential for local effects.

In general, good agreement was found between vertical displacements measured using LVDTs and image processing during the important simulated excavation stage of the test and comparison between the two methods of measurements gives confidence in their validity. Following the early stages of the test, an offset developed similar to that seen in previous work (Grant 1998), probably as a result of friction effects, although the accuracy with which displacements were measured at this later stage are regarded as less important to this project than the initial largely undrained response to vertical unloading caused by excavation.

#### 4.5 Pore pressures

Druck PDCR81 pore pressure transducers were placed behind the retaining wall and beneath the excavation formation (Figure 4.43). Their principal purpose was to determine the point during testing at which conditions of pore pressure equilibrium existed. During tests AM17 and AM19 three additional transducers were positioned, throughout the depth of the model, at a considerable distance from the retaining wall, as an independent check on those positioned near to the excavation. The positions of these transducers, numbered ppt8, ppt9 and ppt10, are indicated on Figure 4.43. Unfortunately, failure of at least three of the original pore pressure transducers occurred during both of these tests.

Typical pore pressure responses during the excavation stage of a test are shown in Figure 4.44, whilst typical response of the additional pore pressure transducers can be seen in Figure 4.45 which includes all of the pore pressure transducer data for test AM19. During the essentially undrained excavation stage of the tests relatively large excess pore pressures were generated as a result of unloading of the formation. Consequently, the largest changes were seen in those transducers placed immediately below the formation level whilst near to the surface pore pressure response was slight. However, despite their relatively remote position in relation to the excavation,

surprisingly marked responses were noted from the additional transducers positioned away from the excavation in tests AM17 and AM19.

Following the excavation stage of the test the excess pore pressures began to dissipate indicating significant softening associated with drainage and heave of the excavation formation. Typical pore pressure responses for this stage are shown in Figure 4.46.

The influence of piles below excavation formation level on the pore pressure response to excavation is illustrated in Figure 4.47. Two cases are considered. Firstly, the situation where the retaining wall was effectively restrained from moving laterally, i.e. tests AM10, AM11, and AM12 is shown in Figures 4.47(a) and (b). In this case there is clearly a smaller magnitude of excess pore pressure generated with increasing use of piles. The second case is where the conventional propping apparatus was used, i.e. tests AM13, AM14 and AM15 and is shown in Figures 4.47(c) and (d). The effect of piles on the generation of excess pore pressures is less clear although a greater change in pore pressure was observed in test AM14 in which no piles were used than in test AM13 where 10 piles were used. The slow response of ppt6 in test AM15 (Figure 4.47c), characterised by stepped increases in the development of excess pore pressures that occurred in between each increment of the simulated excavation, suggests that the porous stone of the transducer may have been blocked or that it had not been properly de-aired. However, the response of ppt7 in test AM15 (Figure 4.47d) indicates that some other factor, such as wall movement, may also have influenced the pore pressure response in that test. Nevertheless, in general it appears that increased use of piles led to reduced pore pressure response immediately below the excavation.

#### 4.6 Prop loads

The use of a multi propped wall with stiff props, in most of the tests, enabled the prototype excavation process to be modelled more closely than would otherwise have been possible. However, accurately determining horizontal load at various levels was not possible owing to the combination of several props and the very stiff retaining wall. Consequently, prop forces that were determined from the transducers measuring oil pressure in the hydraulic cylinders appeared to be influenced greatly by small variations

in stiffness between props. In general, the two stiffest props would carry a disproportionate amount of the total load owing to the absence of flexibility in the wall. Even where props were seen to ineffective because of air in the hydraulic system the effect on ground movement, in the short term at least, was small.

In general, but with the exception of some early tests where problems were encountered with prop performance, a pattern emerged whereby most of the horizontal load during the excavation stage of the test was taken by the most recently installed prop. A typical pattern of prop forces during the simulated excavation stage is shown in Figure 4.47 and indicates that successive prop installations generally attracted most of the load and in some tests had the effect of reducing load on the previously installed props. Typical, prop forces seen during the period following completion of the simulated excavation followed the pattern and magnitudes shown in Figure 4.48. This figure indicates that following completion of the excavation stage of the test horizontal load was generally shared between two props. During most tests load was usually shared between the props at the middle and lower levels with the top prop becoming redundant as loads developed and the test progressed.

## 4.7 Summary

The programme of tests conducted has been described. Where appropriate, analyses of data has been carried out and presented as figures that illustrate the behaviour seen during testing of the various models. Observations of significant events that may impact on the results of tests have been made.

### 4.7.1 Deep embedment walls.

In the tests on deeply embedded walls where piles were used, by and large, retained ground surface displacements were reduced in comparison to those seen in tests without piles. Furthermore, with the exception of test AM2, a clear distinction was evident between tests where piles had been used and where they had not. However, there was much less distinction, reflected in measured surface displacements, between tests that incorporated either one or two rows of piles indicating that the there may be limited

benefit from additional piles. Results of overall movements depicted as contours contradict this since they indicated a general reduction in movement throughout the model. Reductions in settlement at the retained surface were most significant close to the retaining wall but less apparent further away. At a distance of approximately  $2H$  behind the retaining wall no consistent reduction in settlement was seen. Overall, the settlement of the retained ground surface was less pronounced and was subject to less variation in the tests that included piles.

At the excavation formation heave was reduced significantly in the tests where piles were used. Marked reductions in displacement were seen around the positions of the piles leading to a more uniform distribution of heave. Near to the end wall of the strongbox and at depth displacements for all tests were similar indicating that boundary effects were influencing displacements.

#### 4.7.2 Shallow embedment walls.

Similarities exist in the results of tests AM5 and AM17 in that ground movements measured throughout the models were small. However, such behaviour is in contrast with that seen in all other tests including test AM19 where a shallow embedded wall with 10 piles was used. The results of test AM19 could be reasonably assumed to agree with those relating to comparative deep embedment walls since overall movements were of a similar order to those seen in such tests where piles were not used. Therefore generally similar displacements were generated by a test that included a shallow embedded wall, with two rows of piles at excavation formation, and two tests on more deeply embedded walls that had no piles at formation level.

### 5.1 Introduction

Use has been made of finite element analyses both prior to and after the centrifuge tests. Numerical analysis provides a powerful means for predicting the response of geotechnical structures provided that the soil model used is sufficiently sophisticated and that the user is skilled in undertaking and applying the analyses. In the context of this project numerical analyses of the centrifuge model tests was seen as a useful means of confirming any trends in the tests as well as investigating anomalies that can be difficult to quantify such as boundary effects. Additionally, such comparative analyses can provide data that may be useful in evaluating the soil model.

It has been noted in Section 2.6 that it is notoriously difficult to carry out accurate numerical analyses of complex geotechnical problems such as those associated with retaining walls at prototype scale. There are numerous reasons for this which include significant areas of uncertainty such as details of stress history, three dimensional effects, ground water level and variations in overall stiffness caused by buried structures and services as well as structures above ground level. It is therefore attractive to have in the physical problem conditions of plane strain, combined with largely known and controlled boundary conditions, such as exist in the centrifuge models, to enable close comparison with numerical analyses of the same problem. Good numerical predictions should be expected since there is very close comparison with the actual physical model boundary conditions.

The series of analyses that were conducted before the main series of centrifuge tests were merely intended to provide an indication of the soil behaviour and magnitude of displacements that might be expected in a model without piles. These preliminary analyses therefore sought to establish a suitable geometry and stress history for the model whilst subsequent and more detailed analyses (Kopsalidou 2000) were intended to model more accurately both an excavation without piles and the ground response to the likely stiffening effects of piles.

However, with the limitations of the use of numerical analyses in mind the purpose of the second series of analyses was largely to supplement the centrifuge test results. Consequently, there was not an expectation that there would be an especially close correlation of displacement profiles particularly where analyses included the use of piles. It was also felt that, despite the poor predictions that might result from finite element analyses, the results may still provide a useful means of comparison that, owing to the inherent complications and uncertainty involved, could not be made easily between simplified small scale model tests and field data.

Two separate series of analyses were carried out in which a total of eleven separate analyses were produced and the important aspects of these are reported. The program used for all analyses was SSCRISP (Stallebrass 1992) a modified version of the CRISP, CRItical State Program, (Britto and Gunn, 1987) an incremental finite element program developed to carry out geotechnical analysis using the Critical State framework for soil behaviour. The 3-Surface Kinematic Hardening (3-SKH) model (Stallebrass, 1990), described in Chapter 2, has been incorporated into the program to enable modelling of the behaviour of overconsolidated soils with a non-linear soil model which is elasto-plastic at overconsolidated states. The model has been validated against tests on reconstituted clays and has been used to model a series of centrifuge tests (Stallebrass and Taylor, 1997). Further details of the program are given by Ingram (2000) and the soil parameters used in the analyses are as given by Stallebrass and Taylor, (1997) and are also included in Table 5.1. Using output from the finite element analyses, and based on the stress history modelled, a value of  $s_u=86.4\text{kPa}$  has been determined for the soil at excavation formation level immediately prior to commencement of the excavation.

## 5.2 Details of preliminary finite element analyses to assist in determining a suitable stress history for the centrifuge model tests

At the time that the first analyses were conducted the primary purpose of the exercise was to give some indication of a reasonable starting point for the centrifuge testing. The predictions were intended to assist in the selection of an appropriate preconsolidation pressure (in the consolidometer) that would satisfy the requirement to achieve a reasonable magnitude of measurable ground movement in the model whilst



still providing an essentially stiff overconsolidated sample. The subsequent and more detailed analyses were therefore not a particular consideration at this juncture although some of the data from the preliminary analyses proved useful in determining how improvements in the later predictions could be made.

The first stage in preparing for the analysis was to produce a rather simple mesh but with sufficient concentration of nodes at critical positions to enable a reasonable estimate of ground displacements. All soil elements were included in the primary mesh, Figure 5.1, and then appropriate elements removed, in stages, as the analysis proceeded to simulate the stress history of the sample and the excavation. In the process of these additional elements were introduced at prop positions, Figure 5.2, to generate the final mesh.

In using the sophisticated 3-SKH soil model, which was specially developed to predict effects of recent stress history, it becomes necessary to reproduce in the analyses as much detail as possible of the sample preparation phase. The kinematic surfaces of the model should then be correctly aligned at all parts of the mesh when the imposed stress changes associated with the excavation process are modelled. However, the need to model the changes in effective stress at all times becomes difficult when trying to replicate the conditions imposed by the centrifuge at 100g. This is because SSCRISP is unable to apply gravitational accelerations to pore water and, consequently, there is a need to specify the 100g pore pressure distribution at the start of the analysis. In order to enable the correct effective stress history of the sample to be modelled at 1g followed by testing at 100g it is necessary to manipulate the in situ gravity level such that, during the first stage of the analysis, the induced stresses caused by the self weight of the soil balance the increase in pore water pressures with depth, (Grant, 1998). When this procedure is implemented the resulting effective stress profile at the commencement of the analysis, prior to consolidation during the period of generating stress history in the mesh, is determined by the surcharge only. The key stages of the procedure, and how they affect the effective stress in the sample, are depicted in Figure 5.3. The insitu stresses in the sample were set up such that  $K_0 = 1 - \sin\phi'$ .

Commencement (Stage 1) of the analysis was with the soil under a preconsolidation pressure of 500kPa in the consolidometer. This was followed by the swelling stage (Stage 2) in which the vertical effective stress,  $\sigma'_{vmax}$ , resulting from the preconsolidation pressure of 500kPa was reduced to  $\sigma'_v = 250\text{kPa}$ . Stages 1 and 2 were both carried out as fully drained analyses. The in-situ gravity level required for all stages of the analysis, prior to modelling the effects of the centrifuge, was dictated by the acceleration and density of the soil in relation to water and for 100g, with saturated density of kaolin= $17.44 \text{ kN/m}^3$ , the required gravity level,

$$N = \frac{\gamma_w \times 100}{\gamma_s} \quad 5.1$$

$$N = \frac{9.81 \times 100}{17.44} = 56.25g. \quad 5.2$$

Stage 3 was the removal of the remainder of the surcharge loading and substitution of the wall elements into the mesh. The in situ stress changes associated with embedded wall installation were discussed in Chapter 2 and the importance of such stress changes and associated displacements should not, in general, be overlooked. This is because significant ground movements are known to be associated with wall installation and would therefore be certain to influence the overall magnitude of movements. However, the intention of the preliminary analyses was to establish the likely lower bounds for displacement thus making the use of a 'wished in place' wall justifiable. The soil elements in the area of the excavation were also removed in Stage 3 and replaced with stresses that were equal in magnitude to the total stresses resulting at the excavation formation level and also that behind the retaining wall with gravity maintained at 56.25g.

One important difference between physical and numerical modelling is in the control over the stress history of the soil. This can be specified and modelled with confidence in the finite element analyses although in the centrifuge tests the dissipation of excess pore pressure during model making is not easily controlled or quantified with great accuracy. In the centrifuge tests significant dissipation of suction that was generated upon removal from the consolidation press was found to have occurred. This was apparent from the pore pressure transducers both before and following spin up of the

centrifuge and is a problem that is probably exacerbated by a long period of model preparation. The implication of lower than expected pore pressures are changes in the direction of the stress path over an increased depth at the base of the model in relation to that which would occur if the suction had been maintained. This could result in a stiffer response at formation level and lead to reduction in overall displacements in comparison to the finite element analyses.

In Stage 4 gravity was increased to 100g to simulate the effect of the centrifuge and the support pressures were increased accordingly.

Stage 5 was the removal of the stresses applied in Stage 4 and their replacement with props. This stage, being of short duration, was carried out assuming undrained conditions.

Three subsequent analyses were carried out with preconsolidation pressures of 300kPa, 400kPa and 750kPa followed by swelling to 250kPa in an attempt to confirm that the results of the first analysis were reasonable but also to gain an indication of the likely effects of such variations. However the results were difficult to interpret owing to conflicting information gained from the 300kPa analysis. Surprisingly, this particular analysis suggested that displacements for such a preconsolidation pressure would be of a similar magnitude as those for a preconsolidation pressure of 750kPa as shown in Figure 5.4 in which displacements at the excavation formation level for each of the analyses are presented. A possible reason for the reduced movement in the 300kPa run was that the in situ  $K_0$  would be lower and could therefore lead to smaller movements in comparison to the other analyses.

The results of the preliminary analyses were difficult to interpret with confidence although the range of displacements predicted demonstrated that measurable movements could be expected and were therefore useful in deciding upon parameters for the centrifuge model tests. It was concluded that a preconsolidation pressure of 500kPa should be used for the tests since a maximum displacement at excavation formation level of the order of 1mm, which is well within the measuring capabilities of the image analysis, was predicted (Figure 5.4).

Comparison of the predicted excavation formation displacements with those measured using image processing in test AM9 and test AM14, in which no piles were installed, are shown in Figure 5.5. Whilst the overall order of magnitude of displacement is similar, although somewhat underpredicted by finite element analyses, the profile is very different implying that the numerical predictions may be improved with the use of a finer mesh near to the wall.

### 5.3 Observations and results of a series of finite element analyses of the centrifuge model tests.

A further series of numerical analyses using SSCRISP were carried out in an attempt to model the centrifuge tests (Kopsalidou 2000). This work formed part of an MSc project based on some of the centrifuge tests and the opportunity is taken here to compare the results of the numerical and physical modelling. A new and more detailed mesh was produced for the analyses since, amongst other things, it was felt that the fairly coarse mesh used in the preliminary analyses could have been a significant contributing factor to the inaccurate predictions of displacement profiles. Near to the retaining wall large shear strains could be expected which can cause problems at such an interface and a concentration of finer elements in this area could help to provide more accurate results. The new mesh also provided flexibility that enabled the piles at excavation formation level to be modelled as well as variations of the retaining wall embedment depth. In essence, however, the manner in which the analyses were carried out was very similar to the preliminary analyses and the various stages in the sequence of events modelled are shown in Figure 5.6.

Seven separate analyses were carried out based on centrifuge tests AM9 and AM14 which themselves were modelled in two separate analyses. The remaining five analyses, also based on tests AM9 and AM14, were then used to explore the effect of changes in a variety of parameters. The details of all analyses are summarised in Table 5.2. Centrifuge tests AM9 and AM14 were nominally the same although the prop stiffness was known to vary between the two tests owing to problems discussed in Chapter 4. Additionally, differences in the exact timings of the various excavation

stages of the simulated excavation sequence of the tests were identified and subsequently replicated in the analyses (Figure 5.7).

In general six significantly different analyses were undertaken that sought to determine the effects of the duration of simulated excavation, wall embedment depth, prop stiffness and the use of piles to reduce ground movements. Pertinent results of these analyses, RUN 1, RUN 2, RUN 3, RUN 5, RUN 6 and RUN 7, are discussed. The remaining analysis, RUN 4, was carried out to confirm that some quite large differences in the period of reconsolidation on the centrifuge prior to the simulated excavation stage of the tests could be expected to have only a small influence on the overall results. Since this was found to be the case the results of this analysis, which varied only slightly from the datum analyses on which it was based, are not discussed.

#### 5.3.1 Datum analyses on a deep embedded wall in which the duration of the simulated excavation was varied.

For the tests on the deeply embedded wall two basic analyses were carried out that were intended to duplicate the results of the respective centrifuge model tests. These were RUN 1 (centrifuge test AM9) and RUN 3 (centrifuge test AM14). Importantly, these also established a datum against which other analyses, RUN 6 and RUN 7 where piles were modelled, could be compared.

Whilst variations in the duration of events within the excavation sequence are evident from Figure 5.7 the overall duration of the two tests was similar and, at the end of excavation, the heave displacements shown by the analyses were very similar (Figure 5.8). Slightly increased heave near to the retaining wall is seen in RUN 1 in which the formation support pressure,  $\sigma_v$ , was removed slightly earlier than in RUN 3. Additionally, the settlement profiles at the retained ground surface were of a similar pattern and magnitude and, consequently, the differences in excavation sequence in the centrifuge tests are assumed to have only a minor influence on overall movements.

When compared with the results of centrifuge tests AM9 and AM14 the finite element analysis predictions of formation displacement were encouraging since the overall magnitude of movement was reproduced with good accuracy (Figure 5.9). The patterns of movement were however very different, the centrifuge tests having almost certainly been influenced by boundary effects on the end wall of the strong box. Against the retaining wall at formation level large heave movements were seen in the centrifuge tests whereas virtually no movement was predicted by the FEA. The lack of heave movement against the toe of the retaining wall was found to be a feature of all FEA predictions although at distances as close as 10-15mm from the face of the wall predicted values of heave were about half of the measured values. Therefore despite the problems of fixity at the wall/soil interface overall predictions of movement were not substantially affected.

Comparison of retained surface settlements in Figure 5.9 indicate that finite element analyses predict displacement to occur over a much greater distance behind the wall. With the finite element analyses there is much less variation in magnitude of displacements over the length of the settlement trough and, owing to the fact that the soil elements were fixed to the wall elements, significant displacements, seen immediately behind the wall in the centrifuge tests, were not predicted. Indeed, a small amount of heave was predicted next to the wall at the retained ground surface leading to the conclusion that, in particular, the behaviour in this region was not well predicted by finite element analysis.

### 5.3.2 A shallow embedded wall.

A shallow embedded wall was modelled in RUN 2 and used the excavation sequence and timings recorded in centrifuge test AM9. This means that a direct comparison may be drawn between RUN 1 and RUN 2 to determine the effects of wall embedment (Figure 5.10). Surprisingly small differences exist between the formation displacements predicted by the two analyses with only marginally greater heave displacements seen over the width of the excavation for the shallow embedded wall.

A comparison may also be made between analysis RUN 2 and centrifuge tests AM5 and AM17 in which shallow embedded walls were used. The duration of the simulated excavation stages of these tests is shown in Figure 5.11. At a glance, the excavation stage for test AM5 appears considerably longer than that for tests AM9 and AM17. However, in test AM5 there was a delay in commencing draining of the dense fluid following installation of the top prop. As a result, the overall excavation duration, i.e. the period over which  $\sigma_v$  and  $\sigma_h$  were reduced, was similar to that in tests AM9 and AM17.

Comparison of the finite element analysis predictions with the measurements of formation displacement from the centrifuge tests AM5 and AM17 are disappointing with maximum displacement in the finite element analysis predictions being about 3 times those observed in the centrifuge tests (Figure 5.10). Although, friction at the end wall of the strongbox could be assumed to account for some of the discrepancy the difference is probably exacerbated owing to the unusually small displacements seen in the shallow embedded wall centrifuge tests.

At the retained ground surface (Figure 5.12) the settlement predicted by FEA and that seen in the centrifuge tests differed in a similar way to the more deeply embedded walls shown in Figure 5.9. In general, the FEA predicted movements of a greater magnitude over a larger area and consequently the rapid reduction in settlement seen beyond a distance of 60mm behind the retaining wall in centrifuge test AM17 was not a feature of the results of the FEA. Maximum displacements in the centrifuge tests occurred at about  $0.5H$  behind the retaining wall whilst those in the FEA occurred at three times this distance.

### 5.3.3 The effect of prop stiffness.

The difficulties in maintaining a stiff propping system during some of the early centrifuge tests undoubtedly resulted in increased displacements in comparison to those conducted after test AM9. Unfortunately the prop stiffness during test AM9 and those conducted previously cannot be accurately known but, when considered in the context

of the results of other comparable centrifuge tests, the displacements measured in the early tests are not especially excessive. However, the effects of an arbitrarily decreased prop stiffness were investigated in analysis RUN 5 in which prop stiffness was reduced by a factor of 1000 in relation to that used for the other analyses.

Determining the stiffness of the propping system in the analyses in a manner that could be compared with the centrifuge tests was carried out by two simple analyses in which single three noded elements of identical geometry and stiffness to those used in the analyses were subjected to incremental loading up to 100N. Two of the nodes were fixed during loading such that displacement of the third node could be determined and from this a spring stiffness, comparable to that obtained from tests on the centrifuge model apparatus could be calculated. Results of the analyses showed that the stiffness of the propping arrangement used in most of the retaining wall analyses was  $19.5 \times 10^6 \text{ N/m}$  whilst for the soft props, in RUN 5, the stiffness was  $19.5 \times 10^3 \text{ N/m}$  (Figure 5.13). These values can be compared with  $1.75 \times 10^6 \text{ N/m}$  for the prop stiffness of the centrifuge apparatus (from test AM13 onwards),  $30 \times 10^6 \text{ N/m}$  for a typical propped excavation in London Clay (Simpson 2001) and a value of  $280 \times 10^6 \text{ N/m}$  for numerical analyses carried out by Powrie and Li (1991). Further comparison with the assumed range of  $100\text{-}300 \times 10^6 \text{ N/m}$  for the excavation at the site of the former Knightsbridge Crown Court (Geotechnical Consulting Group, 1998) indicates that the stiffness of the centrifuge apparatus was reasonably close to the stiff propping used in the analyses but less stiff than that used in practice.

Noticeable increases in heave at excavation formation level resulted from the decreased prop stiffness shown in Figure 5.14 when compared with the results of RUN 1. Whilst heave increased in magnitude by approximately 25% with reduced prop stiffness, vertical displacements behind the retaining wall increased, on average, by the substantially greater margin of about 75% (Figure 5.15). The much larger retained ground surface movements were associated with wall movements that were double those predicted by RUN 1 (Figure 5.13).

Clearly, large variations in prop stiffness such as those modelled have a significant influence on settlement behind the retaining wall and it seems that in analysis RUN 5, in



which a fairly extreme condition was modelled, the magnitude and distribution of displacements was affected greatly by the very low prop stiffness rather than vertical unloading of the excavation formation. Unlike the other analyses carried out in this series, the greatest increase in displacement in comparison to RUN 1 was horizontally at the retaining wall rather than vertically at the excavation formation.

When the results of the analyses are compared with those of the centrifuge tests it is apparent that prop stiffness may not have a very significant influence on the magnitude of movement unless it is reduced substantially such that overall displacements are governed by wall displacement rather than heave at excavation formation level. In most of the finite element analyses, for example, the prop stiffness modelled was at least ten times that of the centrifuge tests whilst the overall magnitude of predicted displacement was similar to measured movements.

#### 5.3.4 The effect of piles on vertical displacements at excavation formation level and the retained ground surface with a deeply embedded wall.

The results of the material tests conducted on piles that had been incorporated in the centrifuge model for test AM13 (see Section 3.8 and Figure 3.21) suggested that an appropriate value of Young's Modulus for use in the finite element analyses was  $E=800\text{MPa}$  whilst Poisson's ratio of  $\nu=0.3$  was assumed. Plane strain modelling of the piles used at excavation formation presented a particular problem that could only be overcome by simplification in the numerical analyses in RUN 6 and RUN 7. The piles used in the plane strain centrifuge model were discrete elements within the soil. Therefore, whilst they provided a general stiffening effect to the ground below excavation formation level they did not constitute a plane strain element per se. Such an arrangement was required to be represented in a more simple form for the numerical analyses. The plane strain nature of the analyses meant that an equivalent 'embedded wall' was substituted for the piles to provide a similar stiffening effect. The requirement to provide an equivalent stiffness whilst maintaining an identical embedment depth to the piles modelled in the centrifuge tests meant that this equivalent wall was considerably more slender than the individual piles that it represented.

However, the stress changes associated with the installation of a such a wall would of course be very different to the piles used in the centrifuge tests. An alternative, and equally valid, approach to that used would have been to maintain the width of the piles whilst proportionately reducing the pile material stiffness.

Substitution of an embedded wall for the individual piles, whilst not ideal, is regarded as a necessary compromise and is considered a normal approach for modelling such effects in plane strain analyses. For this reason a similar simplification to that used in the analyses of the centrifuge model tests was used in the plane strain finite element analyses carried out prior to construction of the deep basement at the site of the former Knightsbridge Crown Court (Geotechnical Consulting Group, 1998) details of which were given in Section 2.9.

Comparison of the heave displacements at excavation formation level are shown in Figure 5.16. The large reductions in heave near to the retaining wall, that were seen in the centrifuge model tests, were not repeated in the finite element analyses. In areas local to the positions in which piles were modelled in the FEA, significant reductions in the magnitude of heave displacements are evident although in areas near to and distant from the retaining wall the effect of piles appears to be relatively insignificant. Unlike the centrifuge model results, the distinction is more clear between the use of one and two rows of piles although when considered in the context of the overall displacement profile it appears from these results that there may not be any particular benefit in the use of two rows of piles.

These results are reflected at the retained ground surface where, in common with the other previous finite element analyses, settlement profiles bore little resemblance to the respective centrifuge test results especially near to the retaining wall (Figure 5.17). Not surprisingly therefore, given the results of RUN 1, vertical displacements against the retaining wall were not a feature of any of the subsequent FEA. This appears to have led to large under prediction of settlement in the area immediately behind the retaining wall and, conversely, far field movements were significantly over predicted since the analyses once again implied larger displacements that extended over a much greater area than seen in the centrifuge model tests. However it is noted that successive

reductions in settlement were predicted by increased use of piles in the finite element analyses although the predicted magnitude of reduction was much less significant than that measured in the centrifuge model tests. Overall, the shape of the settlement trough in all analyses was consistent and the magnitude of reduction of settlement differed from the centrifuge tests by a factor of approximately 2.

#### 5.3.5 Horizontal and retaining wall displacements.

In Figure 5.18 a comparison of finite element analysis RUN 1 predictions of horizontal displacements behind the retaining wall is made with those measured in centrifuge tests AM9 and AM14. Whilst this analysis may have benefitted from the simplifications associated with the omission of piles at excavation formation level the magnitude of the displacements is in good agreement with those measured in the model tests although the profile is less accurate. In the centrifuge tests most displacement occurred at the level of the excavation formation whilst in the analysis it was concentrated at the retaining wall toe. Immediately behind the retaining wall the predicted profile suggests displacements that are significantly smaller than those measured in the two centrifuge tests whereas horizontal displacements beneath the wall are substantially overpredicted. However, it is likely that boundary effects at the base of the strongbox contributed to a reduction in deep-seated horizontal displacements in the centrifuge tests.

A further comparison that is useful in determining the reasons for the generally large differences in measured and predicted displacements is made in Figure 5.19 which shows contours of horizontal displacement for both centrifuge test AM14 and the analysis RUN 1. This figure confirms that the overall magnitude of displacement at the boundaries of the excavation was well represented in the analysis but that relatively large differences in actual and predicted displacements elsewhere in the model led to significant errors in prediction of distribution of displacements at formation level and at the retained ground surface. The contours of displacement in Figure 5.19 demonstrate that most horizontal movement was concentrated in a fairly small area immediately behind the retaining wall in the centrifuge test whilst a smooth variation over the entire plane strain section was predicted in RUN 1. The consequence of the contrasting patterns of displacement is to over predict movement remote from the excavation.

Horizontal displacements of soil behind the retaining wall were measured using image processing in the centrifuge tests. Additionally, direct measurements of horizontal wall displacements were made using LVDTs (Figure 3.47) and image processing. The data from both the image processing targets that were fixed to the wall and the LVDTs required extrapolation to determine the displacements and rotation of the retaining wall. There was no redundancy with the horizontal LVDT system and any errors in transducer output had a significant effect on interpreted wall movement. This led to obvious inaccuracies and consequent difficulties with confident interpretation of data. The array of image processing targets embedded in the soil immediately behind the retaining wall, however, were found to provide a reliable and consistent means of measuring soil displacement. Whilst a direct comparison between wall displacements predicted by FEA and horizontal soil movements measured using image processing in the centrifuge tests would be inappropriate in assessing the validity of the predicted wall deformations it is nonetheless useful when considering the relative magnitude of displacements.

The lack of horizontal movement against the retaining wall at the retained soil surface shown throughout the other results of the finite element analyses, and depicted in Figure 5.20, is consistent with the FEA generally. The magnitude of horizontal displacements clearly decreased with increasing numbers of piles, in both the FEA predictions and the centrifuge model tests. However, the FEA significantly underpredicted the effects of the piles on these displacements.

Only slight reductions in predictions of horizontal displacement resulted from the introduction of piles in RUN 6 and RUN 7. Furthermore, the maximum retaining wall displacement reduced by only approximately 25% with the use of two rows of piles whilst, in contrast, reductions in horizontal displacement of up to approximately 60% accompanied the introduction of piles in the centrifuge model tests.

Relatively large variations in the magnitude of rotation of the retaining wall between finite element analysis RUN 1 and centrifuge test AM14 are shown in Figure 5.21. The results of the analyses could differ from the centrifuge tests but, equally, the need for extensive extrapolation of image processing and LVDT data could imply inaccurate

assessment of wall displacement in the centrifuge tests. Since a fairly close correlation has been seen to exist between the magnitude of measured and predicted displacements behind the retaining wall it would seem reasonable to assume that there should be an equally close correlation between the measured and predicted wall movements. If such an assumption was correct it would further confirm the difficulty of confident interpretation of the retaining wall movement data from the centrifuge tests and would imply that the interpretation of the data thus far may be misleading.

#### 5.4 Discussion.

The use of piles at the excavation formation could be expected to influence ground movements locally but, with knowledge of the mechanisms of movement around a deep excavation, a more global influence could also be reasonably expected. The FEA predictions of displacement at the excavation formation level, however, showed an essentially local response around the piles positions whilst at relatively small distances away the effect was minimal. Under-predictions of vertical displacement near to the retaining wall on both the excavation and retained side of the wall were a significant feature of the results and underline the difficulties inherent in conducting such analyses, even for the relatively simple condition without piles.

The anomalous over-prediction of far field settlements behind the retaining wall were probably contributed to by boundary effects at the end wall of the strong box in the centrifuge tests and continuity between the soil and wall elements in the finite element analyses. These were also compounded by high in situ stresses behind the retaining wall at ground surface. Nonetheless, as with the excavation formation displacements, the general settlement profiles differed fundamentally near to the retaining wall.

Comparison of the excavation formation displacements predicted by the relatively simple preliminary analysis, the more detailed analysis and the centrifuge test are made in Figure 5.22. Large variations are apparent in the finite element analyses predictions of magnitude of displacement but the profiles of displacement are essentially similar. Despite the large differences seen in the results of the analyses the predictions of both

are substantially different to the behaviour seen in the centrifuge test to such an extent that neither analysis could be said to give more accurate predictions than the other.

Near to the excavation end wall of the strongbox there is a strong likelihood that boundary effects influenced the displacements in the centrifuge tests since a greater, rather than a lesser magnitude of heave could be expected on this line of symmetry. At the excavation formation level the finite element analyses predictions of displacement were a reasonable representation of the centrifuge tests away from the retaining wall. Clearly, without accurate predictions of displacement at this point, i.e. the point of unloading, the displacements elsewhere would not be expected to be predicted accurately.

The difficulty in establishing a realistic value for the centrifuge apparatus prop stiffness may have been a source of error in the finite element predictions. Nevertheless, the fact that the magnitude of overall horizontal displacement was well represented at depth tends to indicate that problems were more acute elsewhere. For instance, the areas immediately adjacent to the wall and pile elements seem also to be areas of the most significant error when compared to the centrifuge test results. Clearly, obstacles exist when accurately modelling complicated problem such as this and errors local to the wall and piles could easily influence the pattern of movements even though the overall stiffness was correct thereby enabling the magnitude of displacements to be fairly well predicted.

## 5.5 Summary.

Comparison has been made between two series of finite element analyses in an attempt to model aspects of the behaviour seen in the centrifuge tests. The first series of analyses whilst using a sophisticated soil model were of a fairly rudimentary nature. The subsequent analyses (Kopsalidou 2000) sought to model more closely the nuances of some of the individual centrifuge tests and, in so doing, attempted to predict similar displacements to those measured.

The overall magnitude of predicted vertical displacements was in general agreement with those seen in the centrifuge tests although the influence of piles at excavation formation level was underestimated. Larger displacements at the retained ground surface were predicted than those measured in the centrifuge model tests and these extended over a significantly greater distance behind the retaining wall. The distribution of displacements were not well represented in the finite element analyses and areas of the most significant difference were around wall and pile elements implying that these elements may have made a significant contribution to the relatively poor predictions.

In contrast with predictions of vertical displacement the magnitude of horizontal displacement was well represented by finite element analyses. Furthermore, the analyses were useful in confirming the limitations of the instrumentation used to measure retaining wall displacements in the centrifuge model tests.

The fact that there were inconsistencies when comparing the results of the finite element analyses with the centrifuge tests prevents the drawing of clear conclusions. Whilst the piles had a significant effect on the magnitude of horizontal and vertical ground movement in the centrifuge tests the finite element analyses suggested a much reduced influence. This is because the analyses predicted large reductions in excavation formation displacement but only in a small area concentrated around the piles and with minimal effects elsewhere.

Further analyses would be useful in exploring the influence of prop stiffness and wall embedment further and an alternative approach to modelling the effects of piles, such as the 'equivalent material stiffness' method suggested by Ou et al (1996), may provide a more representative distribution of displacement at the retained ground surface. However, such an exercise would be time consuming and was not considered essential for confirming the behaviour seen in the centrifuge tests. Furthermore, when a similar approach was used in a series of preliminary finite element analyses for the deep excavation at the site of the former Knightsbridge Crown Court the predicted reduction in displacement was marginal.

In conclusion it appears that a relatively complicated geotechnical problem is difficult to model accurately, even with a sophisticated soil model. The more detailed series of analyses carried out by Kopsalidou (2000) subsequent to the centrifuge tests, whilst able to model more closely the detail of individual tests, failed to achieve significantly better predictions. Interface effects between soil and wall elements and high in situ horizontal stresses at ground level seem likely to be an important factor in explaining the differences between the centrifuge tests and finite element analyses. Such effects may be difficult to overcome and, given the degree of complexity of the problem and the limitations of the analyses, it seems likely that a significant amount of additional research would be required to investigate the discrepancies and enable the improvements in prediction necessary to adequately represent the behaviour seen in the centrifuge tests. Nevertheless it is important to note that, although complex stress paths were imposed, very small movements seen in the centrifuge tests were predicted with good accuracy. Furthermore, the trends in the analyses indicate that the general behaviour is well represented by the finite element analyses.



### 6.1 Introduction

The purpose of this chapter is to draw together the significant findings from the series of centrifuge tests undertaken and to provide an explanation of the behaviour seen. In order to enable the results to be of maximum use they are, where possible, presented within the context of other sources of data relating to the specific problem of establishing and quantifying trends or reducing ground movements near to deep excavations.

Since the use of piles to provide enhanced base stiffness is a relatively novel concept its use in practice has, thus far, been very limited. However some numerical and field monitoring data of an excavation, in which the process modelled was implemented, were available and other relevant and comparable data from field monitoring of deep excavations in general have been useful in assessing the effects of the technique.

The purpose of installing piles beneath the formation level of an area to be excavated is to provide a stiffening effect to the area of soil that will be subjected to large changes in vertical stress during the undrained vertical unloading associated with the excavation process. Nevertheless, in order to quantify the stiffening effect it is necessary to know the initial stiffness of the soil. Determining the stiffness of even the relatively homogeneous mass of soil used in the centrifuge model is not straightforward and the problem becomes even more complicated with the introduction of piles at excavation formation level. This means that, whilst it would be advantageous to view the problem in terms of relative stiffness, such an approach is inappropriate owing to the level of complexity, limited test data and insufficient knowledge of material parameters.

However, if a relationship exists in the model tests between the displacements resulting from excavations in which the formation was not stiffened and those in which piles were used then this could be used to indicate how similar measures used in the same situation at prototype scale could influence displacements. It therefore follows that in

determining the relative stiffening effects between the model and the prototype the influence of piles should be viewed in terms of an overall effect in the model and then an estimate made of their likely effect in the prototype.

## 6.2 The development of heave during the simulated excavation

### 6.2.1 Soil behaviour on unloading

Whilst displacements at the retained ground surface were measured with LVDTs and comparison made with image processing data the measurement of displacement at excavation formation level was made using image processing alone. The reliance on image processing data for measurement of formation displacements brings into question the accuracy of the assessment of the soil response to unloading since the true magnitude of displacement may be affected by frictional effects, particularly near to the end wall of the strongbox where two boundaries exist in close proximity to the image processing targets. However, a close correlation was found to exist between LVDT and image processing data at the retained ground surface (discussed in Section 4.4) which tends to suggest that frictional effects are not very significant over the range of displacements with which this project is concerned. The displacements measured at formation level by image processing during the simulated excavation can therefore be considered to be a reasonable representation of the soil response with perhaps some influence from boundary effects at the end wall of the strongbox.

The excavation formation is subjected to large reductions in vertical stress during the simulated excavation in the centrifuge tests. This is characterised by the generation of significant negative excess pore pressure in the soil immediately beneath the excavation; the magnitude of change in pore pressure decreases with increasing distance from the unloaded surface. Typical pore pressure responses during the simulated excavation stage of test AM13 were shown in Figure 4.44 and are reproduced in Figure 6.1.

In Figure 6.2 image processing data has been used to show the development of heave in a datum test (AM14) during the simulation of excavation when the total stress,  $\sigma_v$ , was reduced. It would have been preferable to use data from test AM13 to enable better comparison between Figures 6.1 and 6.2 but this was not possible owing to failure of some of the pore pressure transducers in test AM14 whilst the excavation formation displacement in test AM13 was influenced by the use of piles. During the unloading caused by excavation there is an initially small, possibly elastic, response resulting in heave displacement at formation level. This increases steadily as  $\sigma_v$  is gradually reduced by decreasing air pressure acting at excavation formation level. Quite a large variation in displacement over the width of the excavation is evident by the time the simulated excavation is complete with the greatest movement occurring near to the retaining wall. The magnitude of heave in this area was probably influenced by displacement of the toe of the retaining wall towards the excavation whereas near to the end wall of the strongbox reduced displacement at this relatively early stage might have resulted from boundary effects. However, it is clear from other data, presented in this chapter, that friction against the end wall was not a significant contributing factor to the magnitude of displacements after some consolidation had taken place following the simulated excavation.

The image processing targets, placed 5mm below the excavation formation level, show a range of displacements in Figure 6.2 that are within the maximum and minimum values plotted on Figure 6.3. This shows the general response to vertical unloading in which the maximum heave was near but not immediately adjacent to the retaining wall and the minimum heave was near to the end wall of the strong box. Displacement measured during the first two stages of excavation constituted only 25% or less of the total movement generated at the completion of the simulated excavation whilst a significant increase in the rate of displacement accompanied the final stage of unloading. This is because, during the early stages of excavation the soil strength is mobilised and the soil immediately below the excavation largely resists the heave. However, as the excavation progresses and approaches the final stage, plastic straining begins and spreads through the soil mass immediately below the excavation. A state of passive failure is reached when  $s_u$  is mobilised over the embedded depth of the wall.

After excavation is complete and with increasing time, further plastic straining at greater depths below formation level leads to mobilisation of soil strength over an enlarged perimeter of soil around the base of the excavation. This contributes to overall stability beneath the excavation and results in a reduction in the rate of movement. However, heave at the excavation formation continues as water, supplied from the base drain, seeps towards the excavation resulting in further plastic straining associated with softening. The behaviour described is shown in Figure 6.4 in which contours of vertical displacement at three stages (end of excavation, 15 minutes and 30 minutes after excavation completed) of a typical test (AM14) are shown depicting the soil response due to and after excavation. Very small movements are seen to have resulted from excavation but after 15 minutes there is a spread of movement throughout the soil beneath the excavation and behind the retaining wall. After a further 15 minutes there is only significant additional movement in the soil immediately below the formation.

#### 6.2.2 Test results from deeply embedded walls

In Figure 6.5a-c the vertical arrays of image processing targets beneath the excavation formation level have been used to show the magnitude and spread of vertical displacement with depth for three tests that were geometrically similar but had different numbers of heave reducing piles. Thus the effective stiffness of the formation varied between the tests. At the simulated excavation stage of the tests frictional effects at the end wall of the strongbox differed substantially between test AM14, in which no piles were used, and tests AM13 and AM15, which respectively had 2 and 1 row of piles. In test AM14 friction at the end wall of the strongbox clearly played a part in reducing heave displacements as shown by the black line representing the magnitude of displacements against this boundary. In tests AM13 and AM15 larger displacements were observed near the end wall of the strongbox, especially in the region of soil near to the excavated surface. However the differences in absolute movement are not very large and it is likely that any friction effects were small.

In all tests the green line, representing the array of targets immediately adjacent to the toe of the retaining wall, show a sharp upward displacement that was localised in the area above the toe. Beneath this the retaining wall surcharge pressure prevented

significant displacement. The effect of the wall surcharge diminished with increasing distance from the wall in test AM14 (Figure 6.5a) and as a consequence displacements progressively increased towards the centre of the excavation. As depth below excavation formation level increased the magnitude of heave decreased such that at a depth approximately equal to the excavation depth (H) heave was negligible although this could also have been influenced by the close proximity of the base of the model.

Conversely, the displacement of the piled formations of tests AM13 and AM15 are most appropriately described as block movement. This is characterised on the graphs (Figures 6.5b and c) by substantially reduced variation in the measured displacements when compared with test AM14 and minimal variation in magnitude over depth, especially in the zone between the toe of the retaining wall and the base of the piles. The remarkably consistent distribution of displacements across the width of the excavation indicate that the piles have a significant influence on displacements over the entire formation area despite their relatively discrete nature.

Nevertheless, it appears that displacements above the toe of the retaining wall in test AM13, and to a lesser extent in test AM15, show a tendency to develop at an increased rate compared with those at depth. A significant change in average variation of vertical movement with depth occurs at about 35mm below formation level and marks an increase in magnitude of displacement. This suggests that the undrained shear strength,  $s_u$ , is becoming fully mobilised. Also, the simulated excavation stage of test AM13 was more than twice the duration of tests AM14 and AM15 (Figure 6.6) and relatively greater softening could have occurred in this test. With this in mind, the degree of reduction in displacements seen in test AM13 is especially pertinent as the substantially greater duration of the test implies that the provision of piles over a wider area of the formation may have additional benefits.

In Figure 6.7a-c image processing has been used to measure vertical displacements in tests AM13, AM14 and AM15 20 minutes after completion of the respective simulated excavations. Some consolidation had obviously occurred during this period and displacements, in all three tests, are shown to have increased substantially with time. In test AM14 (no piles), frictional effects at the end wall of the strongbox were still

noticeable but, despite this, the maximum heave measured was still of a similar magnitude to test AM15 (Figure 6.7b) in which friction was clearly of much less significance. In both tests AM13 and AM15 the maximum displacement was measured at the end wall of the strongbox implying negligible boundary effects.

The distorting effects of endwall friction on the results of test AM14 obscure the true maximum heave displacement although, with reference to Figure 6.7, it seems likely that this would be in excess of 1.8mm. A strong trend has therefore emerged whereby the use of piles leads to a reduction in displacement and that increased use of piles leads to further reductions in displacement. This is confirmed in Figure 6.7c where the results of test AM13 show that, even substantially after the completion of the simulated excavation, block movement of the soil near to the piles was maintained and heave reduced.

For ease of comparison the data in Figures 6.5 and 6.7 are all replotted at the same scale in Figure 6.8. The stiffening effects of the piles are, not surprisingly, progressive although this is not especially apparent from the displacements seen at the end of the simulated excavation (Figure 6.8a-c). In contrast, 20 minutes later, the beneficial influence of 10 piles is clear (Figure 6.8f) although displacements local to the row of piles in test AM15 (Figure 6.8e) are also reduced in relation to test AM14 (Figure 6.8d). Increasing time diminishes the effectiveness of the piles as well as the area over which they influence heave displacements and so the use of two rows of piles, such as in test AM13, has obvious potential benefits over the single row in test AM15.

Each row of piles in tests AM13 and AM15 was located midway between two arrays of image processing targets. Therefore, in order to provide a simplified representation of the vertical displacement at the pile positions and enable comparison with the general formation displacement, the average displacement of the two arrays of image processing targets, that were approximately coincident with the opposing extreme fibres of each row of piles, have been used. The displacements are presented in Figure 6.9a-b in which displacements at the end of the simulated excavation (Figure 6.9a) and 20 minutes later (Figure 6.9b) are shown.

Upon completion of the excavation the displacements near to both rows of piles in both tests were remarkably similar despite the considerable additional duration of the excavation phase in test AM13. Displacement varies at a relatively constant rate beneath an area about 25mm below the excavation formation level whilst, in common with the general pattern of behaviour, there is evidence of heave of a slightly increased magnitude immediately below formation level. After some consolidation (Figure 6.9b) displacements along the line of piles near to the retaining wall in tests AM13 and AM15 remained very consistent although the magnitude of displacement had doubled. The depth of the zone of softening near to the excavation formation level is significantly greater than in Figure 6.9a although the maximum heave at the pile positions is still considerably less than that occurring elsewhere along the excavated surface, especially near to the end wall of the strongbox, with the exception of the area influenced by the wall surcharge as shown in (Figure 6.8d-f).

### 6.2.3 Test results from shallow embedded walls

In tests AM17 and AM19 the retaining wall embedment depth was reduced to 25mm compared with 40mm for most tests. A datum test, AM17, in which no piles were used at the excavation formation can therefore be compared with test AM19, in which 10 piles were used, and also with the more deeply embedded wall tests discussed in Section 6.2.2. In Figure 6.10a-b graphs showing the heave below excavation formation level in the two tests are presented. In both tests the retaining wall surcharge tended to have a reducing influence on heave near to the retaining wall, in a similar way to that seen for the more deeply embedded walls.

It would be reasonable to expect greater displacements to be generated in tests involving retaining walls of reduced embedment. In test AM17, however, the magnitude of vertical displacements suggested that overall stiffness was more similar to that seen for a piled formation and deep embedment wall (Figure 6.11 a-c). This is because at the end of the simulated excavation stage of test AM19 displacements were of a similar magnitude to those measured in tests AM13 and AM15 in which both deeply embedded walls and piles were used. The displacements measured in test AM17, therefore, appear to be difficult to comprehend owing to significant

inconsistencies when viewed in the context of the displacements measured in the tests using deeply embedded walls.

Conversely, a similar comparison, at the end of the simulated excavation, between test AM19 and the more deeply embedded wall tests (Figure 6.12a-c) suggests that the displacements, where piles were used, were of a reasonable and consistent magnitude. The slightly wider range of values in the displacement data implies that in test AM19 the soil beneath excavation formation level did not achieve such well defined block behaviour as that seen in tests AM13 and AM15. This could be reasonably expected given the potential for greater movement attributable to the relatively small retaining wall embedment depth. Additionally, displacements in the area very near to the retaining wall, and immediately below excavation formation level, were of a much greater magnitude than seen elsewhere although these rapidly reverted to values that were consistent with the general trend at a fairly shallow depth. Overall, the displacements seen in test AM19 appear to correlate well with the tests on the deeply embedded walls whilst the results of the datum test appear exceptional and probably misleading. However, if the piles effectively extend the wall embedment depth then the influence of wall embedment would become less noticeable when piles were used.

In view of the absence of correlation between the displacements at the end of the simulated excavation in tests AM17 and AM19 it is perhaps surprising that, after a period of consolidation following excavation, the same trends seen in the deeply embedded walls become a feature of the shallow wall tests. When comparison is made between the tests, in Figure 6.13a-b, block movement in test AM19 is apparent, although not as clearly defined as with the deep embedment wall tests, whereas a strong similarity exists between the pattern of displacements in test AM17 and those seen in test AM14 (Figure 6.6a). The magnitude of maximum displacements, however, are similar although the behaviour of the soil over the depth of the piles beneath the excavation formation is subtly different since most of the arrays of image processing targets especially away from the retaining wall and end wall of the strong box in Figure 6.13b indicate the soil moving as a block. This behaviour became more apparent following a period of consolidation, as shown in the comparison of displacements in Figure 6.14a-d.



It is necessary to view the displacements after a considerable period of consolidation following the unloading caused by excavation before the influence of the piles can be appreciated in terms of reduced displacement at excavation formation level. In Figure 6.15 image processing data has been used to depict the comparative displacements near to the excavation formation level 60 minutes after completion of the simulated excavation in tests AM17 and AM19. The influence of the piles at this point is clear since a marked depression in the heave profile associated with test AM19 coincides with the pile positions although the magnitude of maximum heave of 2.5mm suggests very large strains around the base of the excavation consistent with considerable volume changes. Only after significant consolidation resulting in swelling and softening of the excavation formation were the benefits of the piles in the shallow wall embedment tests realised.

It is apparent that, after considerable time following the simulated excavation, the behaviour seen in test AM17 shows consistency with the other tests from which reliable data have been gathered but it seems that the sample was itself somewhat stiffer prior to the unloading stage of the test. There are a number of possible reasons for this although an error in sample preparation seems most probable. At the time that the test was undertaken the test procedure was well established and consistent results were expected. Some problems were encountered with the consolidation press but it was thought that the sample was not affected. However, in view of the duration over which the sample was prepared, entailing long periods such as weekends, when the equipment was not checked, it is possible that the sample could have been subjected to excess pressure and that this had gone unnoticed.

## 6.3 Settlement at the retained ground surface

### 6.3.1 Introduction

At the retained ground surface settlements are influenced by both the unloading at formation level and also any flexibility that exists in the wall and propping system. In most of the tests undertaken the propping was less stiff than had been intended leading to increased settlement. However, some wall movement is beneficial since this tended

to amplify the effects of stiffening the excavation formation thereby demonstrating that the use of piles could mitigate against a lack of stiffness in the propping system.

Several of the propped wall tests, including the datum test in which no piles were used, were repeated owing to doubts over their adequacy to provide representative and reliable data. Of these the conventionally propped deep embedment wall tests that are considered most reliable, owing to the superior performance of the apparatus, are tests AM13, AM14 and AM15. Additionally, these tests benefitted from increased use of instrumentation, and also increased image processing for test AM15. Despite the fact that a number of the tests were repeated the displacements measured during later tests showed a remarkable consistency with earlier but comparable tests that were, owing to problems in testing, less successful. i.e. tests AM7, AM9 and AM6 respectively.

### 6.3.2 Test results

In Figure 6.16 comparison is made between the retained ground surface settlements at the end of the simulated excavation stage attributable to solely horizontal movement of the retaining wall. This is possible because horizontal wall movement was virtually eliminated in tests AM10, AM11 and AM12 (Figure 6.17) owing to the use of the modified apparatus shown in Figure 4.1 which allowed the displacements resulting from heave to be assessed separately. Therefore, if the displacements measured in tests AM10, AM11 and AM12 are subtracted from those measured in tests AM14, AM13 and AM15 respectively (as has been done to produce Figure 6.16) then an approximation of settlement from retaining wall movement alone can be made. The comparison is not perfect since the time taken to achieve unloading in tests AM10, AM11 and AM12 was only about 2 minutes whereas the same stage was reached after between 7 and 18 minutes in the conventional tests. However, the intention is merely to demonstrate that, in the main series of tests, a significant proportion of the retained ground surface settlement resulted from horizontal wall movement. Consequently, prop stiffness plays an important part in controlling ground movement behind the retaining wall.

From Figure 6.16 it is clear that most of the displacement generated in the tests resulted from wall movement but that the introduction of piles to the excavation formation reduced these displacements as well as those resulting directly from the vertical unloading caused by excavation. This suggests that the piles provide a general stiffening of the area around the excavation and that this in turn has the effect of reducing settlements at ground surface. This means that the piles work in two ways since they are seen to stiffen the formation against lateral movement at the toe of the retaining wall and they have also been shown to provide a certain amount of tensile restraint to the soil beneath the excavation formation level.

Substantially more settlement near to the retaining wall was observed in test AM14 in which no piles were installed at formation level and successive reductions in displacement accompanied the introduction of one and two rows of piles. Reductions in maximum settlement of approximately 40% and 55% are seen near to the retaining wall with one and two rows of piles, respectively, but this effect reduces fairly sharply at greater distances from the excavation.

The manner in which settlement behind the retaining wall is reduced is significant since the greatest reduction in magnitude of displacement tends to coincide with the position of maximum displacement for an unstiffened formation, i.e. test AM14. In all tests this has consistently occurred at a distance of  $0.5H$  behind the retaining wall.

Such localised reductions in the settlement trough have obvious potential for avoiding the notoriously damaging angular distortions associated with differential settlement. Further away from the retaining wall, at distances beyond about  $2H$ , it appears that the use of piles did not affect the magnitude of settlement to any discernible extent. However, displacements had in any case reduced substantially in this area suggesting the influence of boundary effects since measurable displacements are generally accepted to affect an area behind the retaining wall of up to  $4H$ .

It is important that these displacements are not viewed in isolation from other parameters that may distort or unduly influence the apparent behaviour. The effects of duration of the simulated excavation process is a particularly important factor owing to

the influence of the scaling laws on time related processes. Figure 6.6 shows that the simulated excavation in test AM13 was considerably longer than for tests AM14 and AM15. This was because the dense fluid drainage pipe was restricted owing to overtightening at a union.

Clearly, a test of a longer duration could be expected to result in larger displacements than the same test in which the unloading caused by the excavation process was completed more quickly. This means that the magnitude of displacements measured in test AM13 are conservative, in comparison to tests AM14 and AM15, and would certainly have been further reduced had the simulated excavation been carried out over a shorter duration. Since 10 piles were used in test AM13 the reduction in settlement is significant and implies that the stiffening effects of additional piles are important.

## 6.4 Prop loads and horizontal displacements

### 6.4.1 Introduction

The principal purpose of this project was to focus on the soil behaviour around the base of the excavation and to see how this may influence the displacements behind the retaining wall at ground level. Information gained from monitoring prop loads would as a consequence be regarded as peripheral. However, the test results indicate trends at the excavation formation level that influence prop loads and their inclusion within this section is therefore important.

Prop loads are inextricably linked to prop stiffness and it is therefore impossible to separate the two. It has also been demonstrated, in Section 6.3, that prop stiffness plays an important part in controlling ground movements behind the retaining wall. The method of propping used in the majority of the tests, whilst appearing relatively stiff during test preparation, failed to meet expectations and led to much larger vertical displacements behind the retaining wall than would be expected in a comparable prototype. Clearly, the magnitude of horizontal displacements would, as a consequence, also be greater than could be reasonably expected at prototype scale but the influence of the piles in reducing these movements is nonetheless clear.

#### 6.4.2 Test results

In Figure 6.18 the gradual reduction in fluid pressure providing support to the retaining wall during a typical test (AM15) is depicted by a dotted line. The ordinate is the sum of the total prop load acting during the excavation sequence and the total fluid pressure normalised by the total fluid pressure prior to excavation commencing. Immediately before the top prop was installed the total prop load was zero, no fluid had been drained and the expression reduces to unity. Therefore unity on the ordinate represents the total fluid pressure acting on the retaining wall during the period of reconsolidation prior to the simulated excavation. Installation of the top prop prior to draining any fluid increased the value on the ordinate to about 1.5. However, as the fluid drained during the first stage of the excavation the prop load remained fairly constant and by the end of this stage the normalised support pressure from props and fluid was slightly less than unity. This means that the total lateral support was fractionally less than that provided throughout the period of reconsolidation. The two subsequent levels of prop installation however restored and increased the support pressure to a value equal to about twice the original fluid pressure upon completion of the excavation. Thereafter the total prop load continued to rise as excess pore pressures behind the retaining wall dissipated. The development of support pressure suggests that the propping system was, for the greater part of the excavation sequence, subjected to forces in excess of the of the fluid pressure used to support the retaining wall during reconsolidation. Therefore, contrary to the assessment of the overall performance of the apparatus the graph implies a stiff propping system.

It is possible that small amounts of air trapped in the hydraulic system could lead to a soft initial prop response, as the air was compressed, followed by a very stiff and relatively unyielding support. Such behaviour would not necessarily be inconsistent with the results of the apparatus tests reported in Chapter 4.

Whether there was initially a lack of stiffness in the propping system or not the props certainly permitted noticeable horizontal wall displacement. This means that the toe of the retaining wall could be expected to rely on the soil below excavation formation level to generate a certain amount of passive resistance the magnitude of which was

determined by the effectiveness of the propping. Mobilisation of passive resistance would obviously vary inversely with increasing prop stiffness. However, the ability to provide such support reduces with time following the simulated excavation especially as the imposed groundwater regime subjected the soil around the base of the excavation to quite high pore pressures. Any softening would clearly reduce the maximum available passive resistance.

Nonetheless the stiffening influence of piles is apparent from image processing data of horizontal displacements behind the retaining wall (Figure 6.19) at the completion of the simulated excavation. The stiffness of the propping system was known to be comparable in the three tests considered suggesting that the use of one row of piles led to approximately 50% reduction in horizontal movement whereas two rows of piles reduced the displacement to about 30% of that measured in the formation without piles. Such reductions, although quite large, correlate well with those seen for settlement behind the retaining wall (Figure 6.16).

The strong influence of piles on horizontal displacement would be expected to be reflected, to some extent, in the measured prop forces since similar total horizontal forces could be expected in all tests. In order to provide an indication of this the development of prop loads during the simulated excavation stage of tests AM13, AM14 and AM15 is shown in Figure 6.20. It should be noted that the total prop loads beyond the excavation stage in tests AM13 and AM14 are not known owing to one or more of the oil pressure transducers becoming out of range at this time. This is because significantly greater prop forces than had previously been experienced were recorded, following bleeding of the hydraulic system, requiring the amplification of output from the transducers to be reduced. This was carried out prior to test AM15 and permitted the hydraulic oil pressure in all props, during and subsequent to vertical unloading, to be logged correctly. These data are presented in Figure 6.21 and indicate that, following excavation, the total prop force increased steadily as excess pore pressures generated in the vicinity of the retaining wall and excavation formation dissipated.

The reduction in total prop force with the introduction of successive rows of piles is clear, even from the limited amount of data relating to the period of simulated

excavation in test AM13, AM14 and AM15. With one row of piles the total prop force was reduced by about 30% and further reduction is indicated in test AM13 in which an additional row of piles was installed. Owing to the excessive duration of the simulated excavation stage of test AM13 it is likely that the magnitude of prop force is over estimated in relation to tests AM14 and AM15 although the trend of reducing prop loads with increasing use of piles at excavation formation level is nonetheless evident.

#### 6.5 Consideration of the test results within the context of the expectations of existing frameworks

Complications are encountered when attempting to categorise the behaviour of the centrifuge model tests in terms of the Peck (1969) ideas of magnitude and distribution of ground movements that could be expected around excavations. This is because the definition of parameters used to bring together a rather limited amount of good quality monitoring information was necessarily rather vague and restricted in order to establish reasonable guidelines that covered a wide range of ground conditions and support stiffness.

The potentially low stiffness of the propping system in tests AM13, AM14 and AM15 means that comparison of the settlement data within the Peck (1969) framework should be made with care although it is more reasonable to present data relating to tests AM10, AM11 and AM12 within this context (Figure 6.22). (In common with most published data, settlement,  $d$ , and the distance from the retaining wall,  $x$ , are normalised with respect to the excavation depth,  $H$  to enable the data to be presented non-dimensionally).

Tests AM10, AM11 and AM12 had a near rigid lateral support system and were conducted principally to establish that stiffening of the excavation formation by the introduction of piles would influence the retained surface settlements and sought to achieve this without undue influence of retaining wall movements. The normalised settlements in Figure 6.22 show small reductions in settlement with increased use of piles near to the retaining wall although beyond a distance behind the retaining wall of  $2H$  the piles appear to have no influence.

The normalised settlements for all three tests falls into zone 1 which, in the first instance, would seem unreasonable given that the clay used in the centrifuge tests was fairly soft. The modified apparatus used in these tests means that support to the model retaining wall could be considered very stiff. This was reflected in image processing measurements of horizontal displacements in the soil immediately behind the retaining wall which, at less than 0.2mm in all three tests (Figure 6.17), was negligible and at prototype scale (20mm) would suggest an extremely stiff propping system. Consequently, almost all of the settlement behind the retaining wall can be assumed to be a result of heave at the excavation formation. Based on Peck's (1969) suggestions it could therefore be reasonable to expect the normalised settlement profile to fall within the zone 1 region, since there were no significant wall installation effects.

Normalised settlements within the context of the suggested expected settlements caused by excavation in stiff clay (Carder 1995), are shown in Figure 6.23. The data fall within the range suggested as upper bounds for low and high stiffness props which seems reasonable since although the props were very stiff the soil used in the model was relatively soft. Carder (1995) suggests the presence of measurable settlements over an area up to four times the excavation depth behind the retaining wall which the centrifuge tests cannot confirm owing to the proximity of the end wall of the strongbox. Even with extrapolation of the settlement trough it is difficult to confirm broad agreement. The rather large positive displacement at a distance of 3H in test AM11 is an exception which is probably spurious.

For the simplified tests AM10, AM11 and AM12 (i.e. with effectively very stiff propping) the displacements fell reasonably within the bounds suggested by Peck (1969) and Carder (1995) although they were closer to the more extensive field monitoring data used by Carder (1995). Other data from the centrifuge tests are therefore presented within this framework since it is also considered more applicable. Increasing use of piles at excavation formation level showed a clear reduction in settlement behind the retaining wall. Reductions in maximum displacement, in the area immediately behind the wall, resulting from the use of piles were in the region of 30-40% depending on the number of piles used.



In Figure 6.24 the results of the three conventional propped wall tests AM13, AM14 and AM15 are presented within the framework of expected displacements owing to excavation in stiff clay, (Carder 1995). Settlements for all of the centrifuge tests are considerably greater than could be expected for a typical excavation in stiff clay using a low stiffness support. However, the differences are not considered unreasonable given the comparative stiffness of the clays used in the centrifuge model and those encountered in the field.

## 6.6 Consideration of the test results with field monitoring data and associated numerical analyses predictions

In Figure 6.25 the normalised retained ground surface settlements measured in tests AM13, AM14 and AM15 are compared with those from finite element analyses predictions (Geotechnical Consulting Group, 1998) and monitoring data from the site of the former Knightsbridge Crown Court. The site and the centrifuge model possess some elements that are geometrically similarly proportioned, as shown in Figure 6.26, although the depth of the excavation differs significantly. The finite element analysis predicted a reduction in maximum displacement resulting from the use of piles of about 25% to 30% whilst the actual maximum measured displacement was, in turn, about 75% of that predicted. The finite element predictions were therefore fairly accurate although somewhat conservative.

In the centrifuge tests much greater reductions, of between 40% and 55%, were seen with the use of piles. This seems reasonable owing to the much greater soil stiffness in the field compared to the model and the use of piles might therefore have a relatively greater effect. However it should also be noted that there is a significantly greater reduction in vertical stress at formation level associated with the additional depth of excavation at Knightsbridge Crown Court. This could be expected to contribute to potentially increased displacements from both wall and formation movements. However, the finite element analyses predictions of the model behaviour (Kopsalidou 2000) predicted reductions in displacement when using piles that were less than those seen. In modelling the prototype at Knightsbridge Crown Court, Geotechnical Consulting Group, (1998) also predicted reductions in displacement resulting from the

use of piles but of a greater magnitude. This suggests that the respective finite element analyses do not predict similar influence of piles.

Whilst the overall magnitude of displacements in the centrifuge tests and field appear to be reasonably well predicted by both sets of finite element analyses accurately modelling the effects of the piles is much more difficult and there is a lack of consistency suggested by the results of the two sets of analyses undertaken. This means that establishing correlations between the centrifuge tests and finite element predictions of the field problem is difficult but also not entirely unexpected owing to the complexity of the problem. Quantifying the overall stiffening effect of the piles cannot therefore be readily achieved using the results of the finite element analyses considered in this project although the generally good consistency achieved in the results of the centrifuge tests may permit such an estimate to be made.

## 6.7 Summary

The model testing has succeeded in its intended aim to enable a clear view of the model behaviour to be formed. This has been achieved by the comparison of high quality data acquired from a series of tests in which small variations in key parameters were made. This approach has enabled the influence of piles as a means of stiffening the ground beneath a deep excavation to be assessed.

The results of the centrifuge tests, including anomalies, have been compared and discussed and reasons for the behaviour seen have been explained and justified. The quality of the data used has been assessed and, in particular, differences in the testing procedure that could influence or unduly distort the test results have been considered. Shortcomings of the test procedure and apparatus have been highlighted especially where this has resulted in limited or incomplete test data that has prevented conclusive interpretation.

Whilst the performance of the apparatus did not always meet expectations as far as stiffness of the propping system is concerned it provided sufficient consistency to enable the series of tests to confirm that piles can be used as a means of reducing

ground movement around deep excavations. In the tests undertaken it was found that most of the movement behind the retaining wall was caused by insufficient stiffness in the propping system rather than vertical unloading at the base of the excavation. However this does not detract from the test results and has emphasised the importance of formation stiffness in resisting all movements. The piles have been found to work in two ways that combine to reduce both vertical displacements at the retained ground surface and horizontal displacements behind the retaining wall resulting from flexibility in the propping system.

The piles appear to work in tension over their embedded length to reduce heave at the base of the excavation when it is subjected to vertical unloading caused by removal of the overburden during excavation. This means that the soil over the depth of the piled zone tends to behave as a block. In addition the piles provide a general stiffening effect to the soil in the passive zone thereby reducing horizontal wall movement and also reducing prop loads.

The reduction in heave at formation level, with the use of piles, has been found to correlate well with a similarly reduced magnitude of settlement at the retained ground surface as well as horizontal displacement behind the retaining wall over the period considered. The use of an additional row of piles enhances the stiffening effects seen with a single row of piles although the further benefit accruing is not of the same magnitude. However, after a period of consolidation following the simulated excavation, the block behaviour in the soil below excavation formation level was better maintained when more piles were used. This means that the required degree of stiffening of the excavation formation at prototype scale is likely to be governed in part by the duration of the activities surrounding the excavation and the speed with which the formation can be reloaded by the new construction.

### 7.1 Introduction

The work described was conducted to investigate the influence of heave reducing piles in reducing vertical and horizontal ground movements around deep excavations. In this chapter the experimental approach is summarised and conclusions drawn. The implications and relevance of the conclusions are considered and recommendations for further work are made.

### 7.2 Experimental procedure

Apparatus was designed and manufactured and a total of nineteen plane strain model tests carried out in the geotechnical centrifuge at City University. The tests enabled a 12m deep top down excavation process to be modelled in which the stiffening effects of cast in situ piles at excavation formation level were observed. The apparatus consisted of a series of hydraulic props that were jacked into position against a retaining wall at the same time as support, that was designed to mimic the vertical and horizontal stress provided by unexcavated soil, was removed.

Comparison was made between datum tests, in which the excavation formation level was not stiffened, and two further sets of tests in which the density of piles placed in the excavation formation was varied. In a few tests the effect of reducing the retaining wall embedment depth was also modelled. The models were made from overconsolidated samples of Speswhite kaolin prepared from slurry at 1g in a consolidation press. Support to the vertical and horizontal excavation surfaces, prior to simulating the excavation process, was provided by the use of a dense fluid contained within a polyethylene bag against an embedded retaining wall and compressed air contained within a latex membrane at the excavation formation level. When an acceleration of 100g was reached, models were left to achieve conditions of effective stress equilibrium prior to conducting the simulated excavation.

Pore pressures were monitored with miniature pore pressure transducers whilst displacements of the retaining wall and retained ground surface were measured using LVDTs. In addition, images obtained from either one or two CCD cameras mounted on the centrifuge swing were processed using specialist software to determine the magnitude and spread of displacements at the excavation formation level as well as sub surface movements elsewhere in the model.

A preliminary series of four finite element analyses was conducted to determine the magnitude of displacements that may be expected in the centrifuge tests where piles were not used. These were conducted using the CRISP finite element program in which the 3-Surface Kinematic Hardening (3-SKH) model, an elasto-plastic soil model developed at City University, had been implemented. This model enables the important behaviour of the soil, including the effects of recent stress history and variation of stiffness dependent on strain, to be reproduced. The purpose of the analyses was to provide a basis for determining a suitable stress history for the centrifuge model and was carried out at model scale.

Consideration and interpretation of data resulting from a further set of finite element analyses, produced by a more detailed parametric study involving accurate modelling of the events of some specific centrifuge tests, has also been carried out. This has helped to confirm and clarify the essential behaviour seen in the centrifuge tests.

An extensive review of literature concerning ground movements around excavations has been carried out as part of this project. The mechanisms of movement are well understood although there are conflicting views on the influence of embedded wall installation. A great deal of the literature has been produced following monitoring of movements during construction and this has been used to compile charts that are widely used to make predictions of the likely magnitude of displacements near to excavations in a range of ground conditions. Predictions of ground movement, for all but the most complex of excavations, are therefore made with reference to previous experience of similar work. This means that the many variables that may affect the magnitude of displacements cannot be properly quantified.

### 7.3 Conclusions

This project has focussed on one of a number of causes of ground movements associated with deep excavations and has explored the influence of a novel method of placing piles in an excavation formation that has been used to reduce displacements. The combined use of physical model testing and numerical analysis has provided clear insight into the effects of stiffening the ground below excavation formation level and comparison with field monitoring data has confirmed the beneficial influence of the technique.

The behaviour seen in the centrifuge tests has been remarkably consistent and allows a number of statements to be made concerning the effects of cast in situ piles used to enhance the stiffness of the ground below excavation formation level in propped excavations.

The maximum settlement behind the retaining wall occurs at a distance of  $0.5H$ , where  $H$  is the depth of excavation, and significant displacements are apparent over the full length of retained soil, up to  $3H$  behind the retaining wall. The influence of piles on settlement is limited to a distance of about  $2H$ .

Magnitudes of displacement are highly dependent upon the current depth of excavation with much increased movements accompanying the deepest levels of excavation. Only 25% or less of overall displacements were seen to occur as a result of the first two stages of excavation whilst the remaining 75% of displacement was associated with the last 40% of excavation. The proportions of movement associated with each stage of excavation were not influenced by the introduction of piles at excavation formation level.

When the retaining wall was virtually prevented from moving horizontally during any stage of excavation settlement behind the wall was reduced substantially in relation to the propped excavations modelled. However, despite the small magnitude of movement generated by such stiff support the introduction of a row of piles at a distance of three pile diameters from the face of the retaining wall led to a reduction in maximum vertical

displacement behind the retaining wall of about 25%. The maximum displacement was reduced by about 40% with the introduction of an additional row of piles at a distance of six pile diameters from the retaining wall. Horizontal displacements behind the retaining wall were also influenced with reductions of about 25% and 50% for one and two rows of piles respectively.

When the propping system was less stiff the effect of one and two rows of piles was to reduce settlements behind the retaining wall by about 40% and 55% respectively whilst horizontal displacements were reduced by 50% and 70% respectively. The piles therefore had a strong influence on the magnitude of both vertical and horizontal movements but showed consistently more influence on horizontal movements.

Time has been shown to play an important part in the development and magnitude of displacements in relation to the formation stiffness. Over the relatively short periods of time taken to complete the excavation process the additional benefit accruing from the use of two rows of piles when compared to one row was not very significant. However, with increasing time associated with excess pore pressure dissipation near to the excavation formation, additional piles were shown to be more effective in controlling ground movements.

The introduction of piles at excavation formation level created a general stiffening effect that reduced horizontal movement at the toe of the retaining wall and led to reductions in overall prop load. At the end of excavation total prop loads were reduced by about 30% when one row of piles was installed at excavation formation level and about 40% for two rows of piles.

The piles provided restraint against heave movements at the excavation formation and therefore also acted in tension. The soil mass around the piles tended to behave as a block and displacement with increasing depth below excavation formation level was fairly constant over the entire width of the excavation. This behaviour was observed for excavations in which both one and two rows of piles were used despite the relatively discrete nature of the elements. With increasing time after completion of the excavation

the block behaviour became less well defined although the effect was better maintained when the greater number of piles were used.

Finite element analyses of the centrifuge models also predicted reductions in displacement when piles were modelled at excavation formation level. Increasing use of piles resulted in progressive reductions in settlement behind the retaining wall. However, only 10% reduction in settlement was predicted due to stiffening the excavation formation. Finite element analysis predictions of horizontal displacement at the toe of the retaining wall also showed progressive reductions with a maximum effect of about 25% for two rows of piles.

In Figure 7.1 the magnitude of reduction in settlement at the retained ground surface resulting from the use of piles is shown schematically. A similar graph in Figure 7.2 depicts the influence of piles on horizontal displacements. The value of displacement used in normalising the abscissa of the graphs is that given by the maximum vertical and horizontal displacement measured in one particular test (test AM14). Maximum displacements from other tests, in which piles were used in conjunction with a propped wall (tests AM13 and AM15) or where the retaining wall was effectively prevented from moving laterally (tests AM10 AM11 and AM12), have then been used to establish the other data points enabling trend lines to be drawn. These figures summarise the results of the experimental work. Figures 7.1 and 7.2 show that piles at excavation formation level have a greater influence on horizontal than vertical displacements and are most effective in reducing ground movement when used in conjunction with a low stiffness support system. As lateral restraint to the retaining wall is increased the effect of the piles reduces slightly owing to the generally stiffer system. However, even for a very stiff support system maximum reductions in movements are about 40% and 50% for vertical and horizontal movements respectively. When prop stiffness is low the maximum reductions are increased to 55% and 70% for vertical and horizontal movements respectively.



#### 7.4 Limitations and implications of the results.

The main limitation of the experimental work is that it was carried out on relatively soft soil samples. This means that the influence that could be expected when using the technique to stiffen the formation of an excavation in stiff clay would be exaggerated in the centrifuge model. Nonetheless, the effects of a soft soil sample could be considered to be offset to some extent by the use of lightweight and relatively flexible model piles. The influence of other variables (for example existing buried structures and services), which may also act to reduce ground movements in the field, were not present in the tests. This means that for stiffer soils at prototype scale the datum against which the influence of piles should be compared is reduced in comparison to the datum for the centrifuge tests. The very large magnitude of reduction in ground movement achieved in the tests however suggest that the technique could be an extremely effective means of reducing both vertical and horizontal ground movements as well as allowing possibilities for reducing prop stiffness where the control of ground movements is considered less critical.

Where existing basements are incorporated into new developments the effect of existing foundations, both deep and shallow, during unloading associated with demolition is ignored. This often leads to time consuming and costly phased working whereby only partial unloading of the formation level is permitted prior to reloading from the new structure. Such restrictions are especially relevant when buried structures, such as tunnels, exist in close proximity to the excavation. The influence of existing piles in such cases could be considered and may allow a less restricted approach.

In general there is a reluctance to provide piled foundations for new structures when deep excavation is involved owing to the fact that large stress reductions caused by excavation will provide an adequate bearing capacity for a raft foundation. However, the alternative approach of including piles should be considered when the control of ground movements is considered a critical issue.

The use of piles at excavation formation level has been shown to be beneficial in reducing ground movements although the circumstances in which their use is

considered is important. In general, piles near to the retaining wall have been found to provide substantial reductions in both vertical and horizontal ground movement and increasing the intensity of piles, by providing an additional row towards the centre of the excavation, has a small additional benefit in the short term (i.e. largely undrained conditions). However, if an excavation is to be left open for an extended period prior to reloading from construction such that there is time for dissipation of pore pressures then additional piles have an important influence on maintaining the block behaviour of the ground below excavation formation level that results in reduced displacements.

## 7.5 Recommendations for further research

The tests undertaken in this project have been limited by the few parameters that have been varied. Further work should therefore be undertaken to determine the influence of varying the depth of the piles and their positions within the base of the excavation as well as their layout. The possibilities of controlling ground movements to within reasonable limits, whilst reducing prop stiffness owing to enhanced excavation formation stiffness, should be investigated. Such an approach could significantly influence the cost and time required to complete an excavation especially if it permitted a reduction in the number of levels of temporary propping required.

The use of piles in conjunction with reduced embedment retaining walls should be investigated further since this could provide significant savings in terms of design load on retaining walls and consequent reduction in construction cost.

The influence of shallow foundations that are often present in existing basements that are to be redeveloped should be explored. Whilst the deep stiffening associated with the block behaviour induced by piles would not seem so likely the lateral stiffening effects may be considerable.

Continued monitoring of ground movement around deep excavations combined and correlated with model testing and numerical analyses will provide much needed additional data to enable predictions of displacement to be made with more confidence.

## REFERENCES

Al-Tabbaa, A, 1987. Permeability and stress-strain response of speswhite kaolin, PhD Thesis, University of Cambridge.

Al-Tabbaa A, Wood, DM, 1989. An experimentally based 'bubble' model for clay. Proc. Third Int. Conf. on Numerical Methods in Geomechanics, pp91-99.

Anderson WF, Yong KY, Sulaiman JI, 1985. Shaft adhesion on bored piles and cast in-situ piles. Proceedings of the 11<sup>th</sup> International Conference on Soil Mechanics and Foundation Engineering, San Francisco, 1333-1336.

Atkinson JH, 1993. An introduction to the mechanics of soils and foundations. McGraw-Hill Book Company Europe, pp 98, 164-167.

Atkinson JH, Richardson D, Stallebrass SE, 1990. Effect of recent stress history on the stiffness of overconsolidated soil. Geotechnique 40, No. 4, 531-540

Bolton MD, Powrie W, 1987. The collapse of diaphragm walls retaining clay. Geotechnique 37, No. 3, 335-353.

Bolton MD, Powrie W, 1988. Behaviour of diaphragm walls in clay prior to collapse. Geotechnique 38, No. 2, 167-189.

Bolton MD, Powrie W, Symons IF, 1990a The design of in situ walls retaining overconsolidated clay: Part I Short term behaviour, Ground Engineering, 23, No.1, 34-40.

Bolton MD, Powrie W, Symons IF, 1990b. The design of stiff in situ walls retaining overconsolidated clay: Part II, Long term behaviour, Ground Engineering, 23, No.2, 22-28.

Britto AM, Gunn MJ, 1987. Critical state soil mechanics via finite elements. Ellis Horwood, Chichester.

Brooker, EW, Ireland, HO, 1965. Earth pressure at rest related to stress history. Canadian Geotechnical Journal, Vol II, No 1.

Burford D, 1988. Heave of tunnels beneath the Shell Centre, London, 1959-1986, Geotechnique 38, No 1, 135-137.

Burland JB, Simpson B, St John HD, 1979. Movements around excavations in London Clay, Proceedings 7<sup>th</sup> European Conference on Soil Mechanics, Brighton, 1, pp 13-30.

Carder DR, 1995. Ground movements caused by different embedded wall construction techniques, TRL Report No. 172, Transport Research Laboratory, Berkshire.

Carder DR, Bennett SN, 1996. The effectiveness of berms and raked props as temporary support to retaining walls, Transport Research Laboratory, Berkshire, pp 13-14.

Clough W, O'Rourke TD, 1990. Construction induced movements of in situ walls. Proceedings of design and performance of earth retaining structures, Ithaca, NY, ASCE GSP 25, 430-470.

Cole KW, Burland JB, 1972. Observation of retaining wall movements associated with a large excavation, Proceedings of 5<sup>th</sup> European Conference on Soil Mechanics and Foundation Engineering, Madrid.

Cooling, LF, 1948. Settlement analysis of Waterloo Bridge. Proceedings of the 2<sup>nd</sup> International Conference on Soil Mechanics and Foundation Engineering, Rotterdam 2 pp 130-134.

Craig WH, Yildirim S, (1976). Modelling excavations and excavation processes. Proceedings of the 6<sup>th</sup> European Conference on Soil Mechanics and Foundation Engineering, Vol 1, pp 33-36.

Craig, WH, 1995. Geotechnical Centrifuges: Past, Present and Future. Geotechnical Centrifuge Technology, Ed. RN Taylor, Blackie Academic and Professional, Glasgow.

Davis A, Auger D, 1979. La butee des sables: essais en vraie grandeur. Annales de l'institut technique du batiment et des travaux publics serie SF/166 pp 69-92, September.

Fernie R, 1998. Private communication.

Fernie, R, St John, HD, Potts, DM, 1991. Design and performance of a 24m deep basement in London Clay resisting the effects of long term rise in groundwater, Proceedings of 10<sup>th</sup> European Conference on Soil Mechanics and Foundation Engineering.

Fuglsang, LD, Ovesen, NK, 1988. The theory of modelling to centrifuge studies, centrifuges in soil mechanics, Craig, James and Schofield, Eds. Balkema, Rotterdam.

Geotechnical Consulting Group, 1998. Knightsbridge Crown Court redevelopment for Harrods Limited. Appendix B: Finite Element Analysis Report, for Kvaerner Cementation Foundations.

Grant, RJ, 1998. Movement around a tunnel in two-layer ground. PhD Thesis, City University.

Gourvenec, SM, Powrie, W, 1999. Three-dimensional finite-element analysis of diaphragm wall installation, Geotechnique 49, No.6, 801-823.

Higgins KG, Potts DM, Symons IF, 1989. Comparison of predicted and measured performance of the retaining walls of the Bell Common Tunnel, TRRL Contractor Report 124.

Ingram, PJ, 2000. The application of numerical models to natural stiff clays. PhD Thesis, City University.

Jardine RJ, Potts DM, Fourie AB and Burland JB, 1986. Studies of the influence of non-linear stress-strain characteristics of soil structure interaction. *Geotechnique*, 36, 3 pp 377-396.

Kimura T, Takemura J, Hiro-oka A, Okamura M, Park J, 1994. Excavation in soft clay using an in-flight excavator, *Centrifuge 94*, Leung, Lee and Tan (eds) Balkema, Rotterdam.

Kopsalidou K, 2000. A numerical investigation of ground movements around multi-propped deep excavations. MSc Dissertation, City University.

Loh CK, Tan TS, Lee FH, 1998. Three-dimensional excavation tests, *Centrifuge 98*, Kimura, Kusakabe, Takemura (eds), Balkema, Rotterdam.

Mair RJ, 1979. Centrifugal modelling of tunnel construction in soft clay, PhD Thesis, University of Cambridge.

Mayne PW and Kulhawy FH, 1982.  $K_0$  – OCR relationships in soil, *Proc ASCE J.Geotech Eng Div Vol 108 (GT6)*, June.

Nash DFT, Lings ML, Ng CWW. Observed heave and swelling beneath a deep excavation in Gault Clay, *Geotechnical aspects of construction in soft ground*, Mair and Taylor (eds) Balkema, Rotterdam.

Ng, CWW, Yan, RWM (1999). Three-dimensional modelling of a diaphragm wall construction sequence, *Geotechnique* 49, No.6, 825-834.

Ohishi K, Katagiri M, Saitoh K, Azuma K, 1999. Deformation behaviour and heaving analysis of deep excavation, International Society for Soil Mechanics and Foundation Engineering: Underground Construction in Soft Ground, Tokyo.

O'Rourke TD, 1981. Ground movements caused by excavations, Journal of the Geotechnical Engineering Division of the Proceedings of ASCE, Vol. 107, No. 79, pp 1159-1178.

Ou C-Y, Liao J-T, Cheng W-L, 2000. Building response and ground movements induced by a deep excavation, Geotechnique 50, No.3, 209-220.

Ou C-Y, Wu T-S, Hsieh H-S, 1996. Analysis of deep excavation with column type of ground improvement I soft clay, Journal of Geotechnical Engineering, Vol.122, No.9, September, pp709-716, ASCE

Padfield CJ, Mair RJ, 1984. Design of retaining walls embedded in stiff clays, CIRIA Report 104, CIRIA, London.

Pantelidou H, 1994. Changes in soil stiffness associated with diaphragm walling, PhD Thesis, University of London.

Peck RB, 1969. Deep excavations and tunnelling in soft ground, Proceedings of 7<sup>th</sup> ICSMFE, Mexico, pp 259-290.

Phillips R, 1995. Geotechnical centrifuge technology, Blackie Academic & Professional, Taylor , R N (Ed) Glasgow, pp 34-59.

Potts DM, Fourie AB, 1984. The behaviour of a propped retaining wall: Results of a numerical experiment, Geotechnique, 34, No. 3, 383-404.

Potts DM, Fourie AB, 1986. A numerical study of the effects of wall deformation on earth pressures. Int. J. Numer. Analyt. Meth. In Geomech. 10, pp383-405.

Powrie W, 1986. The behaviour of diaphragm walls in clay, PhD Thesis, University of Cambridge.

Powrie W, 1995. Geotechnical centrifuge technology, Blackie Academic & Professional, Taylor, R N (Ed) Glasgow, pp 61-92.

Powrie W, Kantartzi C, 1992. Installation effects of diaphragm walls in clay. ICE Retaining Structures Conference, Cambridge.

Powrie W, Kantartzi C, 1996. Ground response during diaphragm wall installation in clay: centrifuge model tests, *Geotechnique* 46, No. 4, 725-739.

Powrie W, Li ESF, 1991. Finite element analyses of an in situ wall propped at formation level, *Geotechnique* 41, No. 4, 499-514.

Powrie W, Pantelidou H, Stallebrass SE, 1998. Soil stiffness in stress paths relevant to diaphragm walls in clay, *Geotechnique* 48, No. 4, 483-494.

Powrie W, Richards DJ, Kantartzi C, 1994. Modelling diaphragm wall installation and excavation processes, *Centrifuge 94*, Leung, Lee and Tan (Eds) Balkema, Rotterdam.

Raison CA, 1988. Queen Elizabeth II Conference Centre, Discussion, Burland JB, Kalra JC, *Proc. Instn Civ. Engrs*, Part 1, 84, Feb, 95-124

Rampello S, Stallebrass S E, Viggiani GMB, 1998. Panel Report: Ground movements associated with excavations in stiff clays: current prediction capability. Conference on hard soils and soft rocks, Naples, Italy.

Richards DJ, Powrie W, 1998. Centrifuge model tests on doubly propped embedded retaining walls in overconsolidated kaolin clay, *Geotechnique* 48, No.6, 833-846.

Richards DJ, Powrie W, Page JRT, 1998. Proceedings ICE Geotechnical Engineering, 131, July, pp 163-170.



Schofield AN, 1980. Cambridge geotechnical centrifuge operations, *Geotechnique* 30, No. 3, 227-268.

Schofield AN, Taylor RN, 1988. Development of standard geotechnical centrifuge operations. *Centrifuge 88*, Ed Corté, Balkema, Rotterdam.

Schofield AN, Wroth CP, 1968. *Critical state soil mechanics*. London, McGraw-Hill.

Skempton AW, 1961. Horizontal stresses in an overconsolidated Eocene clay. *Proceedings of the 5<sup>th</sup> International Conference on Soil Mechanics and Foundation Engineering*, Paris, France, Vol I, 352-357.

Sills GC, Burland JB, Czechowski MK, 1977. *Proceedings of the 9<sup>th</sup> International Conference on Soil Mechanics and Foundation Engineering*, Tokyo, Vol II, 147-154.

Simpson B, 1992. Retaining structures: displacement and design, *Geotechnique* 42, No.4, 541-576

Simpson S, 1998. Private Communication.

Simpson S, 2001. Private Communication.

Stallebrass, SE, 1990. Modelling the effect of recent stress history on the deformation of overconsolidated soils, PhD thesis, City University.

Stallebrass SE, Taylor RN, (1997). The development and evaluation of a constitutive model for the prediction of ground movements in overconsolidated clay, *Geotechnique* 47, No2, 235-253.

Stewart DI, 1989. Ground water effects on in-situ walls in stiff clay, PhD Thesis, University of Cambridge.

St John HD, 1975. Field and theoretical studies of the behaviour of ground around deep excavations in London Clay, PhD Thesis, University of Cambridge.

St John HD, Potts DM, Jardine RJ, Higgins KG, 1993. Prediction and performance of ground response due to construction of a deep basement at 60 Victoria Embankment, Predictive Soil Mechanics, Thomas Telford.

Symons IF, Carder DR, 1993. Stress changes in stiff clay caused by the installation of embedded retaining walls, ICE Retaining Structures Conference, Cambridge.

Taylor RN, 1995. Centrifuges in modelling: Principles and scale effects. Geotechnical centrifuge technology, Blackie Academic & Professional, Taylor , RN (Ed) Glasgow, pp 19-33.

Taylor RN, 1995. Buried structures and underground excavations, Geotechnical centrifuge technology, Blackie Academic & Professional, Taylor , RN (Ed) Glasgow, pp 93-115.

Taylor, RN, Grant, RJ, Robson. S, Kuwano, J, 1998. An image analysis system for determining plane and 3-D displacements in soil models. Centrifuge 98, Kimura, Kusakabe and Takemura (Eds), Balkema, Rotterdam.

Tedd P, Chard BM, Charles JA, Symons IF, 1984. Behaviour of a propped, embedded retaining wall in stiff clay at Bell Common tunnel, Geotechnique 34, No. 4, pp 513-532.

Twine D, Roscoe H, 1997. Prop loads: guidance on design, CIRIA Funders Report FR/CP/48.

Viggiani G, 1992. Small strain stiffness of fine grained soil. PhD thesis, City University, London.

Watson GVR, Carder DR, 1994. Comparison of measured and computed performance of a propped, bored pile retaining wall at Walthamstow, Proc of ICE, Geotechnical Engineering, 107, July, pp 127-133.

Whittle AJ, Hashash, YMA, 1992. Analysis of the behaviour of propped diaphragm walls in a deep clay deposit, ICE Retaining Structures Conference, Cambridge.

Wood LA, Perrin AJ, 1984. Observations of a strutted diaphragm wall in London clay: a preliminary assessment, Geotechnique 34, No.4, 563-579.

Woods RI, Clayton CRI, 1992. The application of the CRISP finite element program to practical retaining wall problems, ICE Retaining Structures Conference, Cambridge.

Xie KH, Zhang DJ, Wang X, 1999. FEM analysis of excavation with soils improved in its passive zone, International Society for Soil Mechanics and Foundation Engineering: Underground Construction in Soft Ground, Tokyo.

Analysis no.	Type	No of rows heave of Piles	Length of piles (m)	Prop Stiffness (MN/m/mm)	Comments	Vertical displacement (mm)	Horizontal displacement (mm)
Run 1	Plane strain	2	24 (both rows)	100	Narrow section of site Datum analysis	16.3	21.4
Run 2	Plane strain	2	24,14 (no of shorter piles doubled)	100	Shorter piles used near to centre of excavation	16.4	21.5
Run 3	Plane strain	2	As run 2	100 (300 at B5 and B6)		13.7	18.5
Run 4	Plane strain	4	24 (all rows)	100 (No prop at B0, 300 at B5 and B6)	Wide section of site	15.6	20.3
Run 5	Plane strain	4	24 (all rows)	100 (10 at B0, 300 at B5 and B6)		15.3	19.3
Run 6	Axi-symmetric	4 (pile rings)	24 (all rows)	100 (10 at B0, 300 at B5 and B6)	As run 5 but hoop stiffness reduced by factor of 1000	6.4	8.4
Run 7	Axi-symmetric	4 (pile rings)	24 (all rows)	100 (10 at B0, 300 at B5 and B6)	As run 5 but loading in E-W direction instead of N-S	6.4	8.4
Run 8	Axi-symmetric	4 (pile rings)	24 (all rows)	100 (10 at B0, 300 at B5 and B6)	As run 5 but pile stiffness reduced from E=11Gpa to E=8GPa	15.5	19.4

Table 2.1

Summary of finite element analyses carried out prior to construction of a deep basement at the site of the former Knightsbridge Crown Court including predictions of maximum vertical and horizontal displacements.

Quantity	Prototype wall	Model wall
length	1	1/N
self weight stress	1	1 at N gravities
stress x area	1	1/N <sup>2</sup>
strain	1	1
curvature	1	N
Young's modulus (E)	1	1
The following are expressed per	metre length	1/N metre length
moment of inertia (I)	1	1/N <sup>4</sup>
intensity of load	1	1/N
shear force	1	1/N <sup>2</sup>
bending moment	1	1/N <sup>3</sup>

Table 3.1      Scale factors for centrifuge tests on model diaphragm walls.  
(after Powrie 1986).

	Propping arrangement		
	Wall “fixed” in position horizontally	Wall propped at 3 levels	
Wall embedment depth	40mm	40mm	25mm
Pile layout	Test reference		
0 piles	AM10	AM1*, AM2, AM9, AM14	AM3*, AM4*, AM5, AM16*, AM17
5 piles	AM12	AM6, AM15	
10 piles	AM11	AM7, AM13	AM18*, AM19
15 piles		AM8*	

\* Denotes tests that were abandoned prior to simulated excavation stage of test.

Table 4.1 Details of tests conducted.

Test reference	Test date	Wall embedment depth	Visible area for image processing	Type of support to retaining wall	No. of rows of piles	Comments
AM1	16/12/98	40mm	partial view of excavation formation	hydraulic props	0	Failed owing to leak of dense fluid upon spin up. Test continued to check apparatus. Apparatus OK but drainage of dense fluid was rapid. Very limited field of vision for image processing. Heave of soil at excavation formation level caused clash with tapered plate at base of apparatus. Instrumentation : 2 No. PPTs and 7 No. LVDTs at retained soil surface).
AM2	2/3/99	40mm	formation + 160mm behind retaining wall	hydraulic props	0	Datum test using modified apparatus to avoid contact of soil at formation level with apparatus. Smaller bore drainage pipe led to better control of support pressure reduction. Quite a successful test but with limited instrumentation (2 No. PPTs and 7 No. LVDTs at retained soil surface).
AM3	15/3/99	25mm	formation + 160mm behind retaining wall	hydraulic props	0	Test aborted owing to leak on spin up. No data available.
AM4	27/4/99	25mm	formation + 160mm behind retaining wall	hydraulic props	0	Test aborted. Drain valve failed to open. No data available.
AM5	20/5/99	25mm	formation + 160mm behind retaining wall	hydraulic props	0	Successful test following change of bag owing to leak but test delayed. New drain valve with actuation using rotary solenoid. Two image processing targets fixed to retaining wall. Model left on bench over night following initial failure of polyethylen bag. Excavation formation and trench required re-trimming in order to place the apparatus. Instrumentation : 4 No. PPTs and 7 No. LVDTs at retained soil surface).
AM6	18/6/99	40mm	formation + 160mm behind retaining wall	hydraulic props	5	First use of cast in situ piles. Successful test but a sudden loss of air pressure immediately before the test resulted in premature unloading of the excavation formation. Drainage valve slow to open.
AM7	9/7/99	40mm	formation + 160mm behind retaining wall	hydraulic props	10	Successful test but piles proved to be defective because of an unexpected chemical reaction caused by pre-mixing the 'Fastcast' resin components with the aluminium trihydrate filler.
AM8	28/7/99	40mm	formation + 160mm behind retaining wall	hydraulic props	15	Test aborted owing to leak prior to spin up. No data available.

Table 4.2 Details of tests conducted showing development of experimental technique and with comments on performance of apparatus.

Test reference	Test date	Wall embedment depth	Visible area for image processing	Type of support to retaining wall	No. of rows of piles	Comments
AM9	27/9/99	40mm	formation + 200mm behind retaining wall	hydraulic props	0	Test delayed. Drain valve failed to open at first attempt. Prop load failed to develop in bottom prop. Suspect air trapped in hydraulic system. Instrumentation: 7 No. PPTs and 7 No. LVDTs at retained soil surface).
AM10	22/9/99	40mm	formation + 200mm behind retaining wall	fixed wall	0	Simplified test with retaining wall effectively prevented from moving horizontally. Rubber bag burst on spin up owing to inadequate support. Centrifuge stopped immediately and bag replaced although one image processing target attached to the retaining wall was lost. Excavation partially filled with water.
AM11	14/10/99	40mm	formation + 200mm behind retaining wall	fixed wall	10	Clay near surface failed to come into contact with window. Two additional LVDTs used to measure horizontal displacement of retaining wall. Excavation partially filled with water.
AM12	3/11/99	40mm	formation + 200mm behind retaining wall	fixed wall	5	Rubber bag burst 30 minutes after spin up. Centrifuge stopped and bag replaced. Excavation partially filled with water.
AM13	23/11/99	40mm	formation + 200mm behind retaining wall	hydraulic props	10	Problem with consolidometer leading to loss of pressure owing to load cell failure. Control using ram pressure transducer. A successful test with very good response from PPTs. Apparatus performed well with increased prop loads compared with tests prior to test AM10. Very slow to drain dense fluid owing to overtightening of a union.
AM14	14/12/99	40mm	formation + 200mm behind retaining wall	hydraulic props	0	Very successful datum test.
AM15	28/1/00	40mm	entire model	hydraulic props	5	Successful test. Repeat of AM6. Two cameras used for image processing allowing the entire plane strain model to be viewed.
AM16	23/2/00	25mm	entire model	hydraulic props	0	Test aborted. Leak of dense fluid upon spin up.
AM17	13/3/00	25mm	entire model	hydraulic props	0	Successful test. 3 additional PPTs positioned distant from the retaining wall. However some PPTs failed owing to a problem with the junction box on the centrifuge.
AM18	7/4/00	25mm	entire model	hydraulic props	10	Stop centrifuge to replace slip rings after 24 hours of consolidation. Image processing computer crashed during test. Test aborted.
AM19	11/5/00	25mm	entire model	hydraulic props	10	Successful test. Loss of about 20kPa of fluid pressure led to test slightly early for pore pressure equilibrium.

Table 4.2 (contd.) Details of tests conducted showing development of experimental technique and with comments on performance of apparatus.



Application	Prop stiffness (N/m)
Centrifuge model prior to test AM13	Not known,(< $1.75 \times 10^6$ )
Centrifuge model after test AM13	$1.75 \times 10^6$
Numerical analyses of centrifuge model tests (Kopsalidou 2000).	$19.5 \times 10^3$ - $19.5 \times 10^6$
Typical excavation in London Clay	$30 \times 10^6$
Site of the former Knightsbridge Crown Court, (Geotechnical Consulting Group, 1998)	$100$ - $300 \times 10^6$

Table 4.3 Comparison of spring stiffness of props in centrifuge tests with numerical analyses and excavations in London Clay.

Parameter	Value
M-stress ratio at critical state ( $q'/p'$ )	0.89
$\lambda$ -gradient of normal compression line in $v:\ln p'$ space	0.073
$\kappa$ -average gradient of unload-reload line in $v:\ln p'$ space	0.005
$\Gamma$ -specific volume on the critical state line when $p'=1\text{ kPa}$	2.994
A-coefficient of $p'$ in relationship for $G'_{\max}$	1964
T-ratio of size of history surface to bounding surface for 3-SKH model	0.25
S-ratio of size of yield surface to bounding surface for the 3-SKH model	0.08
$\psi$ -exponent in the hardening modulus for the 3-SKH model	2.5
m-exponent of $R_0$ in relationship for $G'_{\max}$	0.2
n-exponent of $p'$ in relationship for $G'_{\max}$	0.65
$\gamma_s$ -unit weight of soil (kaolin)	17.44kN/m <sup>3</sup>
$\gamma_w$ -unit weight of water	9.81kN/m <sup>3</sup>

N.B. The shear modulus is given by

$$\frac{G'_{\max}}{p'_r} = A \left( \frac{p'}{p'_r} \right)^n R_0^m \quad (\text{Viggiani, 1992})$$

in which  $p'_r$  = reference pressure (1kPa)

Table 5.1 Details of values assigned to soil parameters used in numerical analyses.

Analysis	Centrifuge test modelled	Pre-excavation details	General test details
RUN 1	AM9	1 day of consolidation	40mm wall embedment
RUN 2	AM9 but with wall embedment decreased	1 day of consolidation	25mm wall embedment
RUN 3	AM14	1 day of consolidation	40mm wall embedment
RUN 4	AM9	12 days of consolidation	40mm wall embedment
RUN 5	AM9 but with reduced prop stiffness	1 day of consolidation	40mm wall embedment soft props
RUN 6	AM9 but with 5 piles	1 day of consolidation	40mm wall embedment 5 piles
RUN 7	AM9 but with 10 piles	1 day of consolidation	40mm wall embedment 10 piles

Table 5.2 Details of numerical analyses of centrifuge model tests carried out by Kopsalidou (2000) The results of these analyses were compared with a set of preliminary finite element analyses and the centrifuge test results.

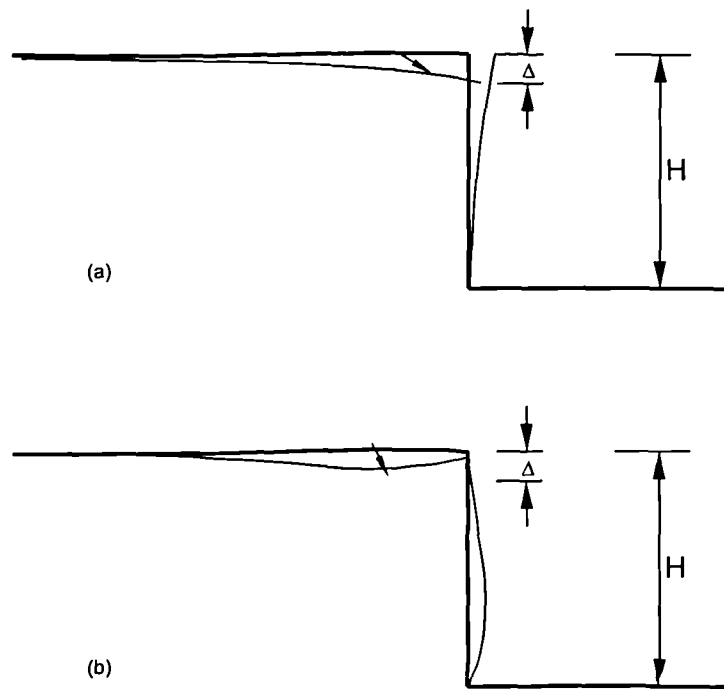


Figure 2.1 Typical patterns of displacement behind retaining walls (Burland et al, 1979).

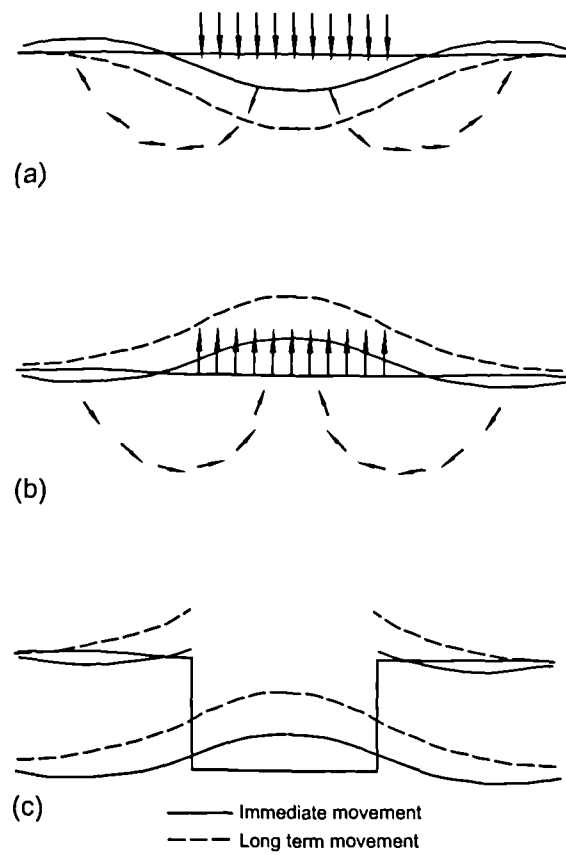


Figure 2.2 Soil response to unloading caused by excavation (Burland et al, 1979).

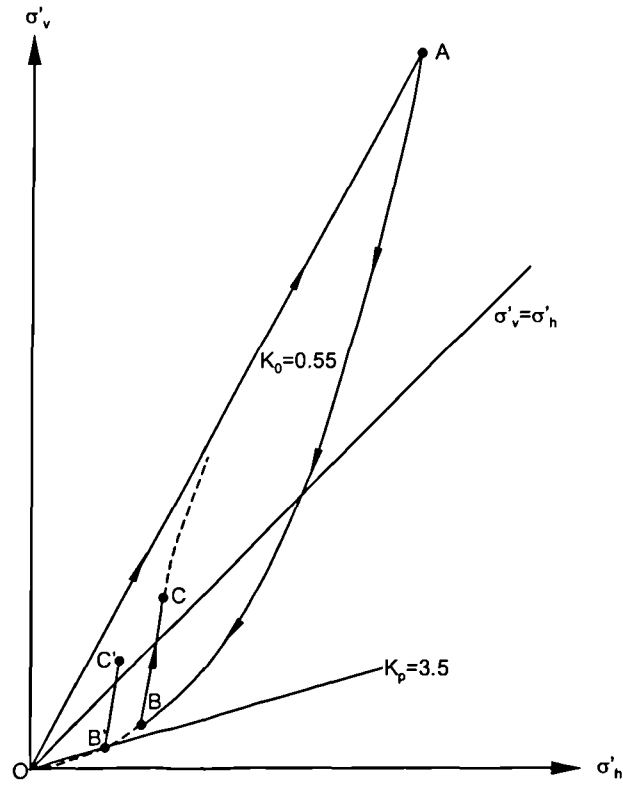


Figure 2.3 Influence of stress history on  $K_0$  (Burland et al, 1979).

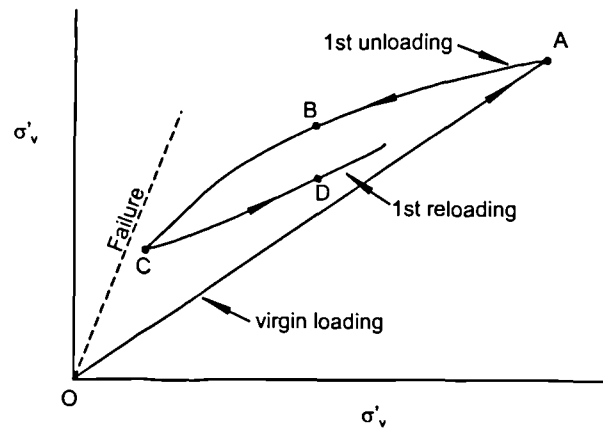


Figure 2.4 Influence of stress history on  $K_0$  (Mayne and Kulhawy, 1982).

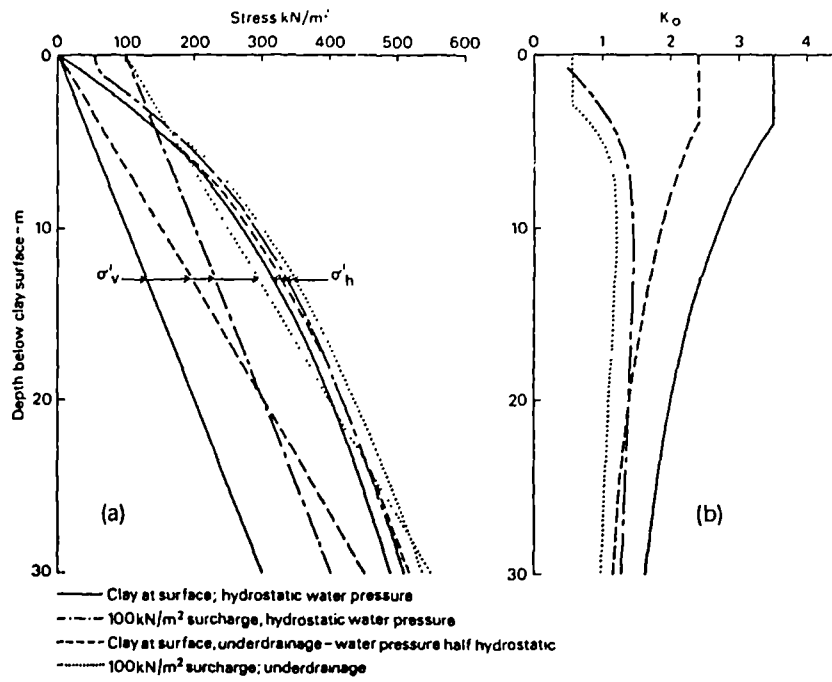


Figure 2.5 Influence of stress history on  $K_0$  and  $\sigma'_h$  in heavily overconsolidated clay (Burland et al, 1979).

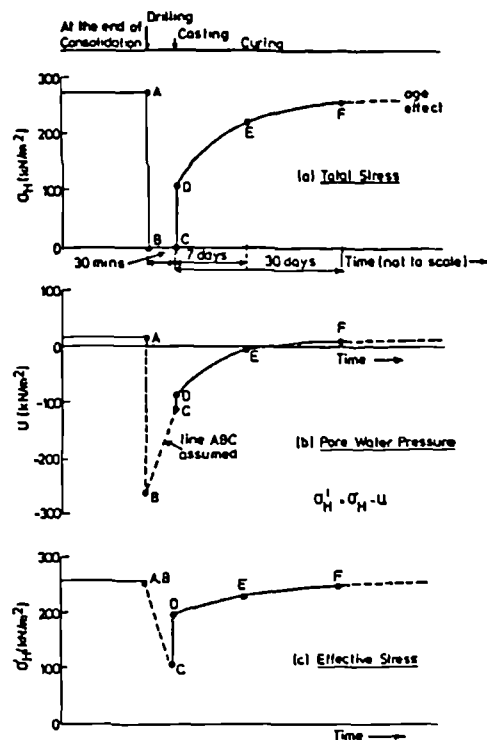


Figure 2.6 Stress changes with time caused by bored pile installation (Anderson et al, 1985).

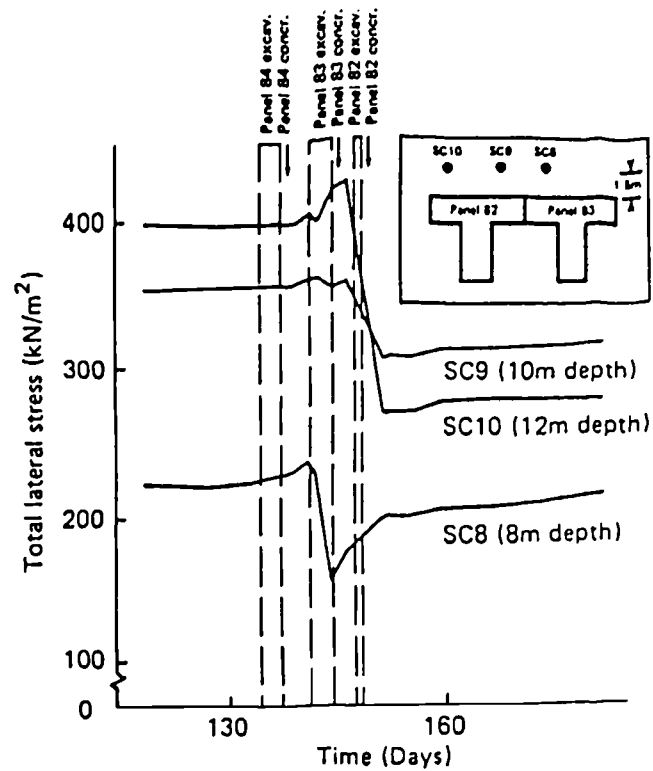


Figure 2.7 Stress changes during diaphragm wall installation (Symons and Carder, 1993).

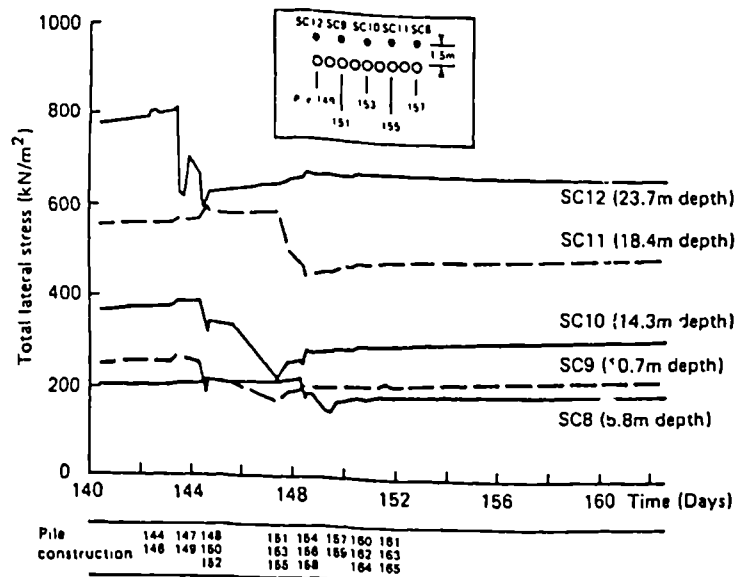


Figure 2.8 Stress changes during bored pile wall installation (Symons and Carder, 1993).

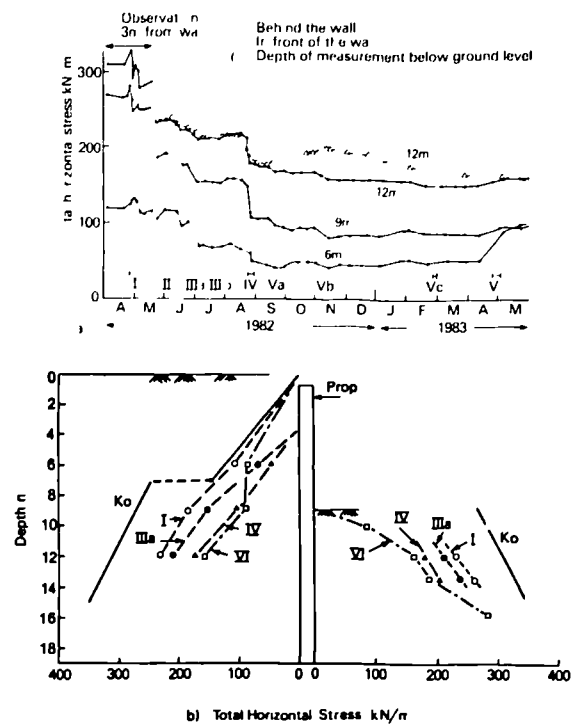


Figure 2.9 a) Change in total horizontal stress with time  
b) Distribution of the total horizontal stress in the soil 0.6m from the diaphragm at various stages of excavation wall at Bell Common (Tedd et al, 1984).

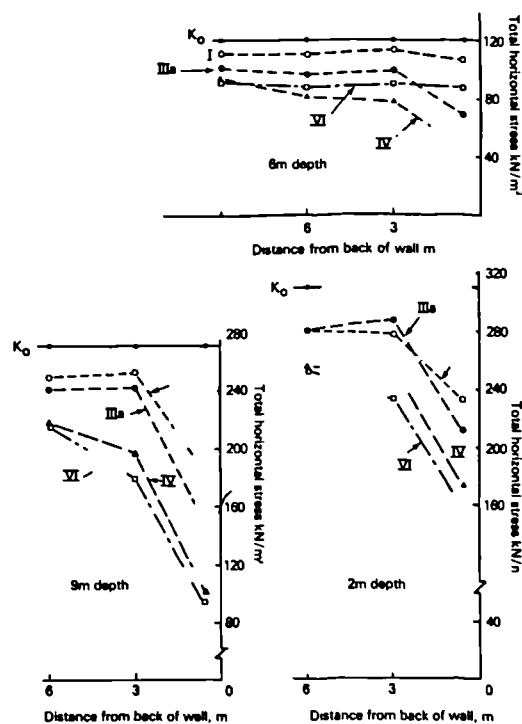


Figure 2.10 Distribution of the total horizontal stress in the soil with distance from back of the wall (Tedd et al, 1984).

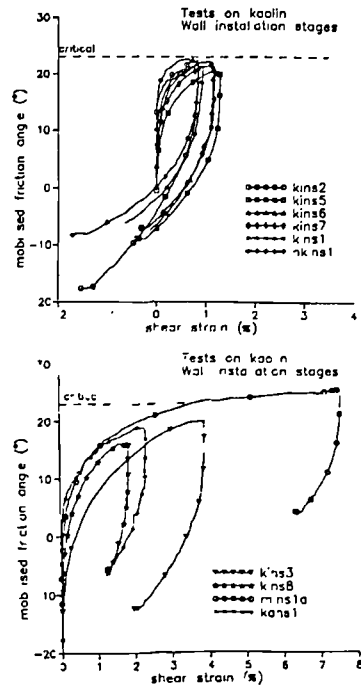


Figure 2.11 Mobilised friction angle  $\phi'_{mob}$  against shear strain  $\epsilon_s$ , during trench excavation and concreting (a) Tests with low in-situ  $K_0$  and (b) Tests with high in-situ  $K_0$  (Pantelidou, 1994).

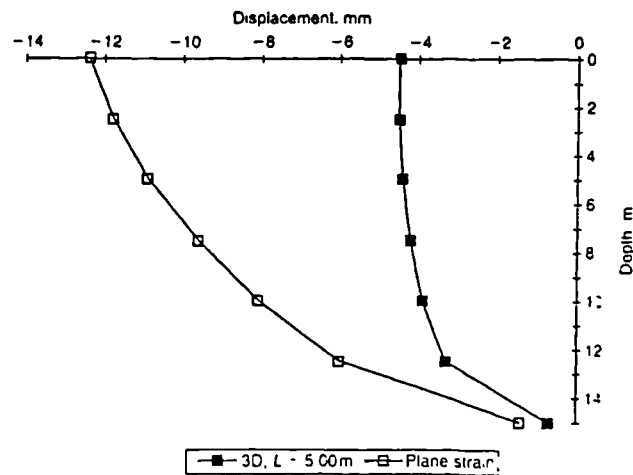


Figure 2.12 Horizontal displacements along the wall/soil interface following completion of the wall: comparison between plane strain and 3D analysis with 5m panels (Gourvenec and Powrie, 1999).



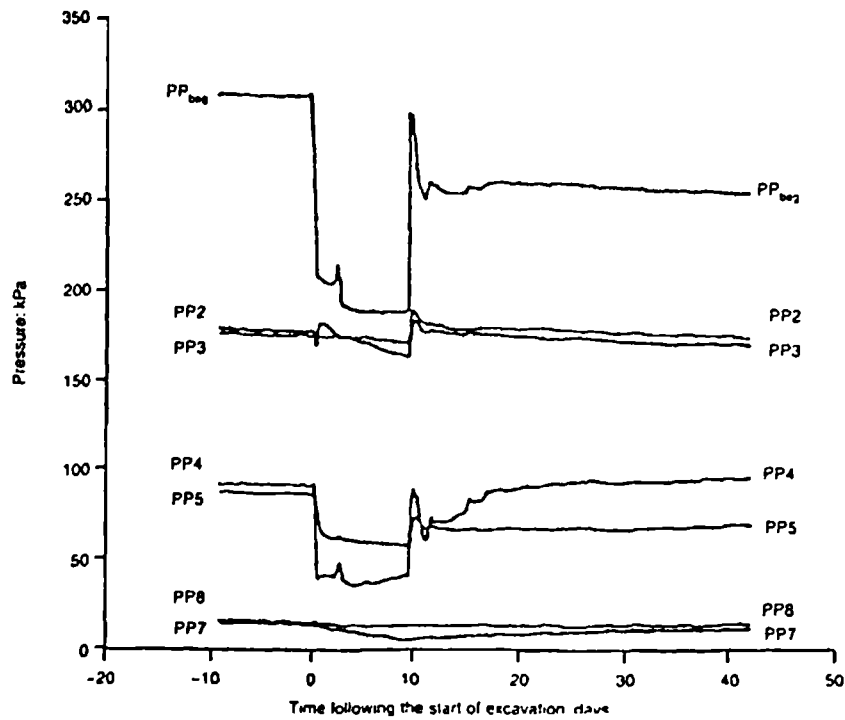


Figure 2.13 Changes in pore water pressure during excavation under bentonite slurry and concreting: plain strain trench with full height groundwater level (Powrie and Kantartzi, 1996).

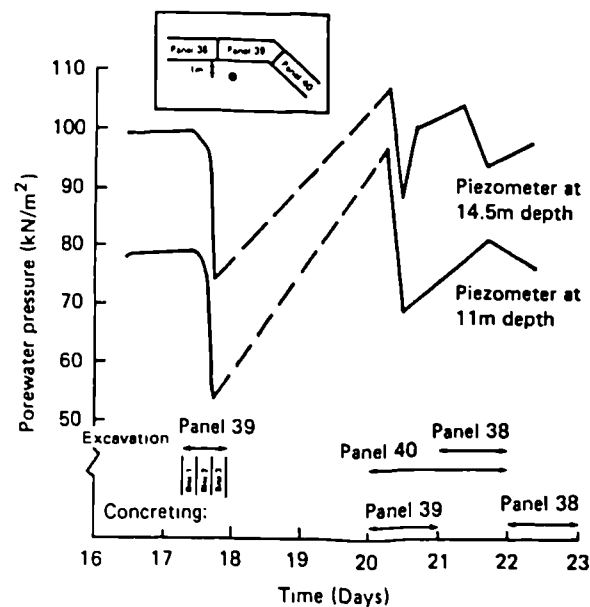
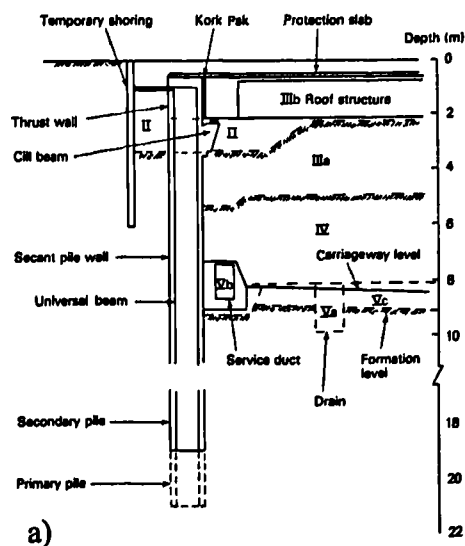


Figure 2.14 Influence of retaining wall installation on pore pressure (Symons and Carder, 1993).



Stage	Description	Period
I	Construction of the secant pile wall	26/4/82-6/5/82
II	Excavation for construction of cill beam and thrust wall	24/5/82-11/6/82
IIIa	Excavation to 5 m	1/7/82-3/7/82
IIIb	Construction of the roof structure	8/7/82-11/8/82
IV	Excavation to 8 m	23/8/82-31/8/82
V	Minor excavations within tunnel	
a	Excavation for drain	21/9/82-23/9/82
b	Excavation for construction of service duct	9/11/82-11/11/82
c	Excavation to formation level	28/2/83
VI	Installation of drain and backfilling behind thrust wall	28/4/83-5/5/83

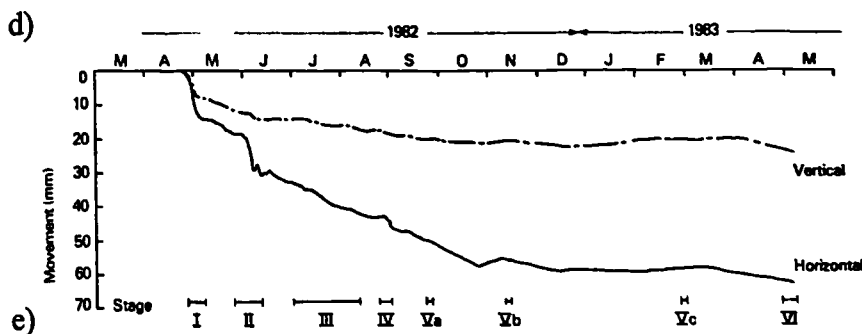
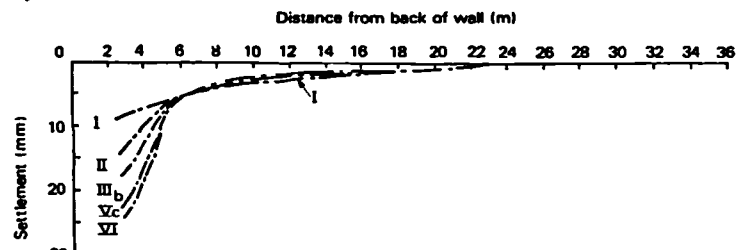
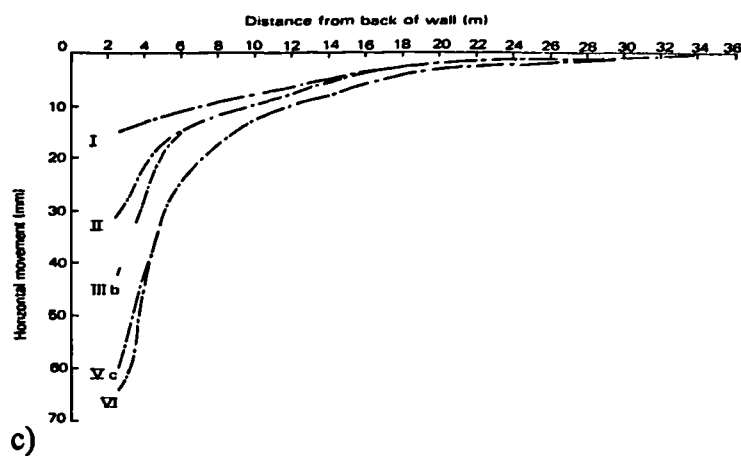
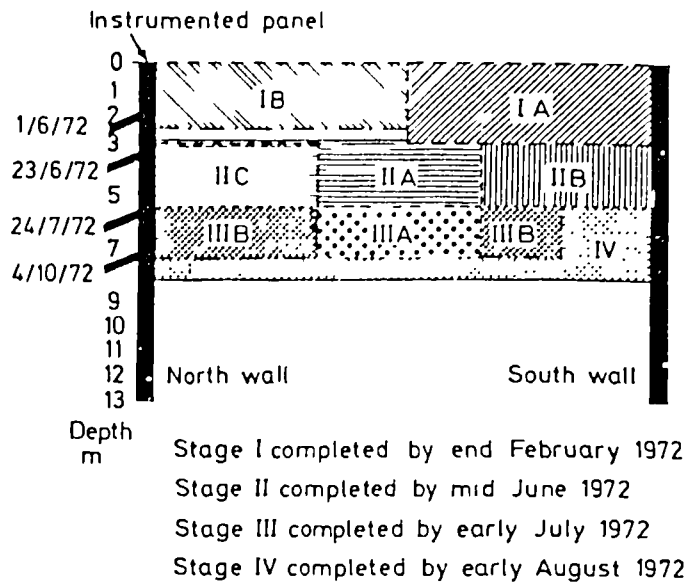
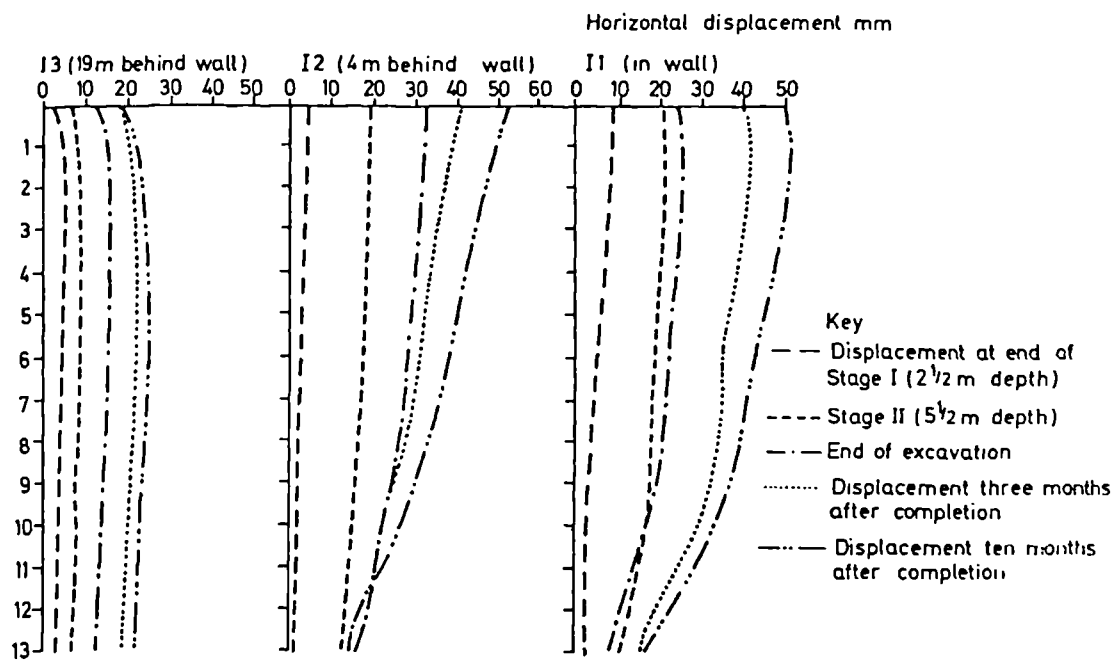


Figure 2.15 Magnitude, distribution and development of surface movement behind the wall (Tedd et al, 1984):

- a) Section through the retaining wall
- b) Stages of construction
- c) Horizontal movement towards excavation
- d) Vertical movement
- e) Movement recorded at surface station 2-6 m from back of wall



a)



b)

Figure 2.16 (a) Progress of excavation  
(b) Horizontal movements of wall and ground at Neasden  
(Sills et al, 1977).

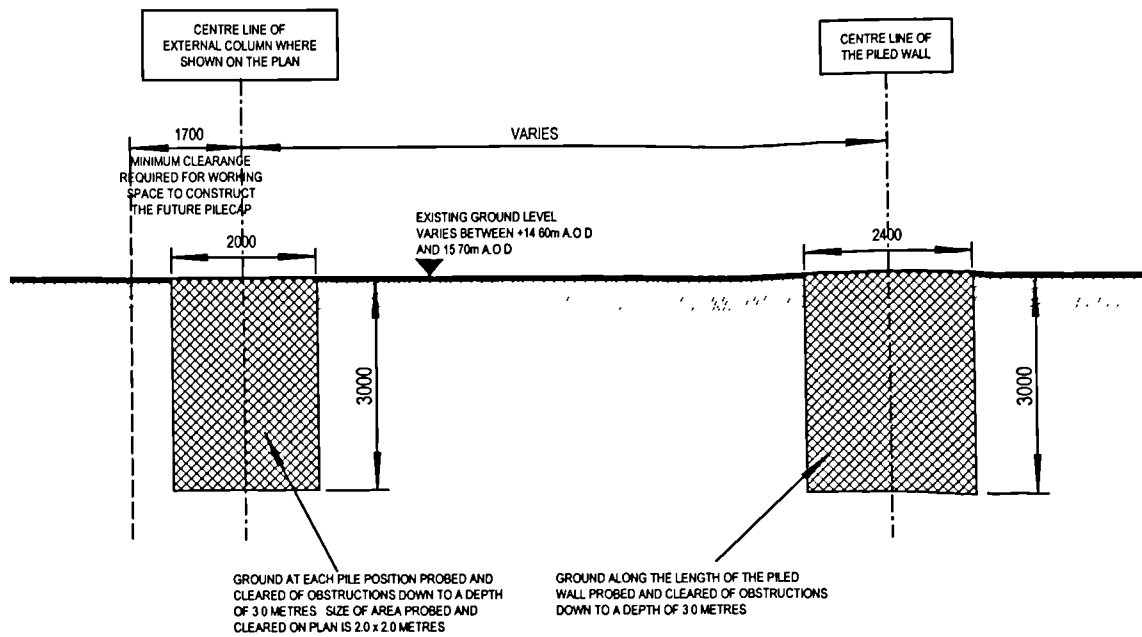


Figure 2.17 Typical pile probe operation carried out prior to piling

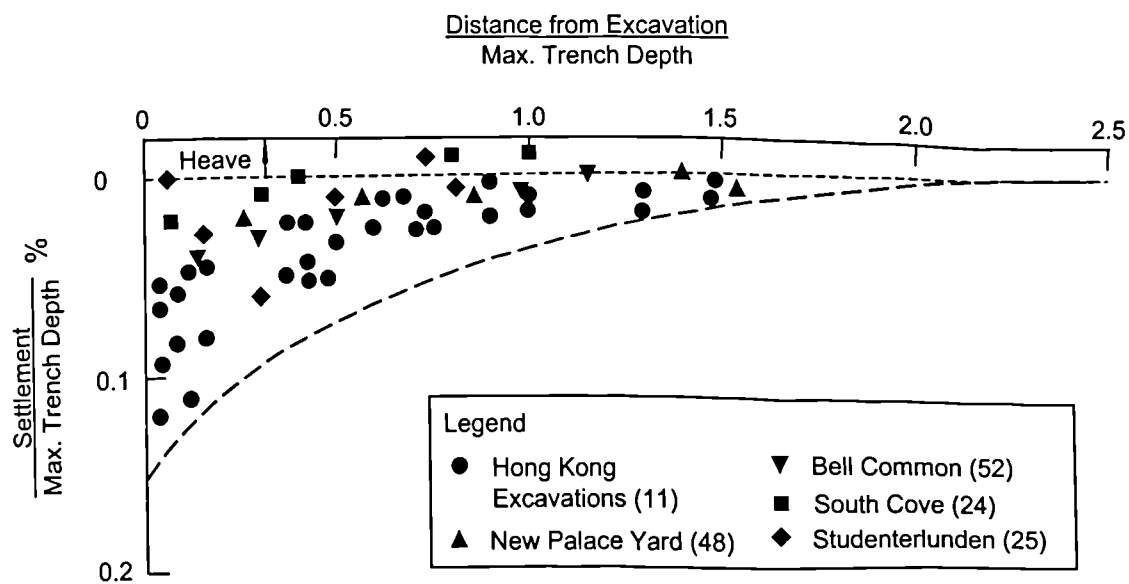


Figure 2.18 Measured settlements caused by the installation of concrete diaphragm walls (Rampello et al, 1998 after Clough and O'Rourke, 1990).

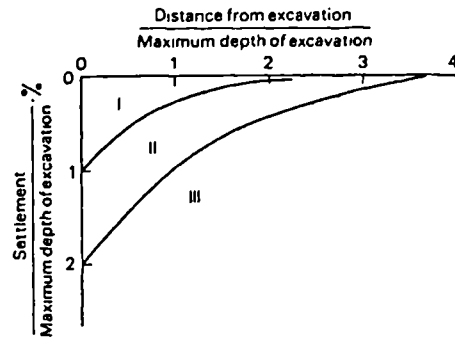


Figure 2.19 Magnitude of settlement expected next to braced excavations (Burland et al, 1979 after Peck, 1969).

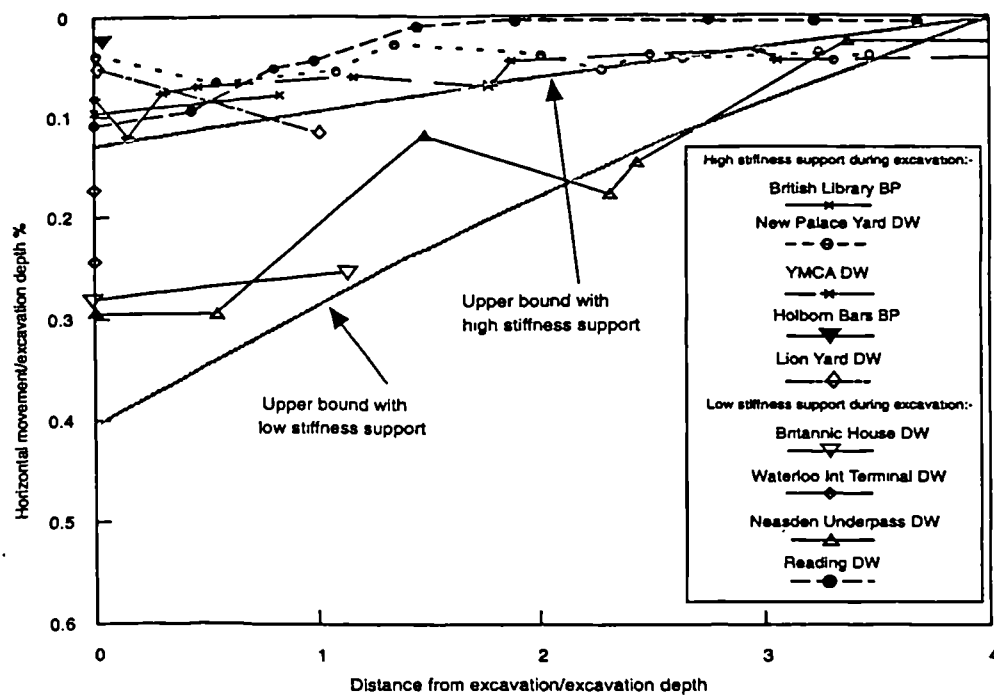


Figure 2.20 Horizontal surface movement caused by excavation in front of wall (stiff clay) (Carder, 1995).

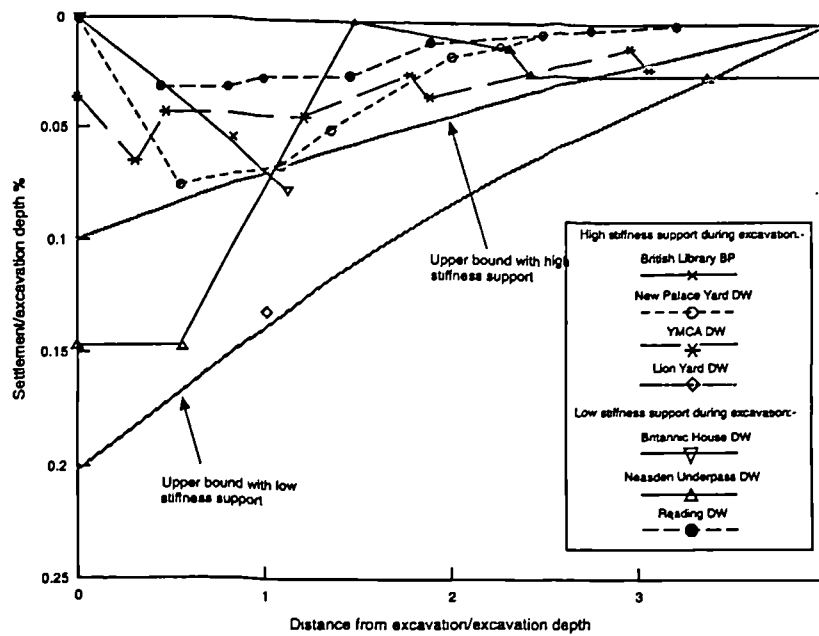


Figure 2.21 Surface settlement caused by excavation in front of wall (stiff clay) (Carder, 1995).

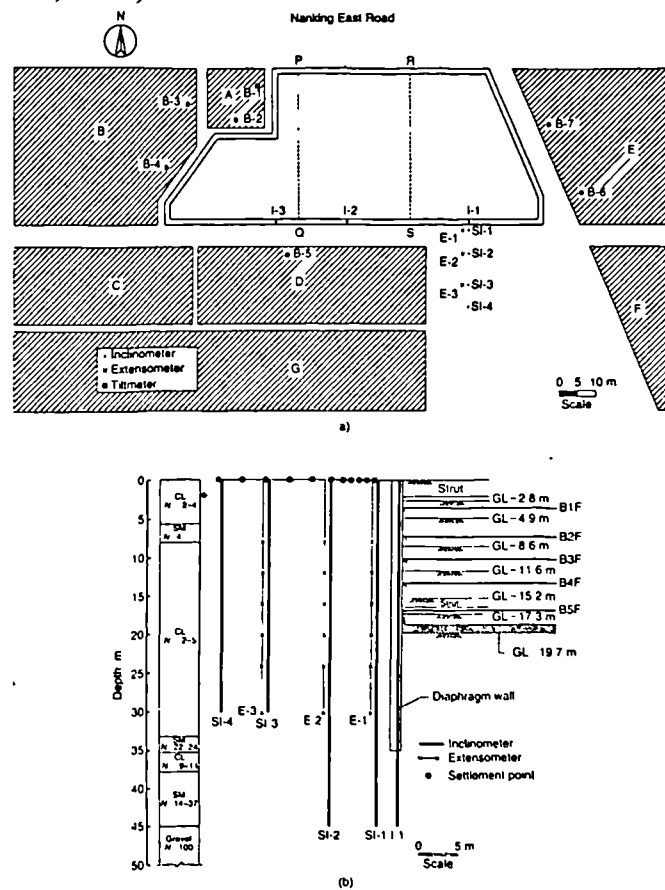
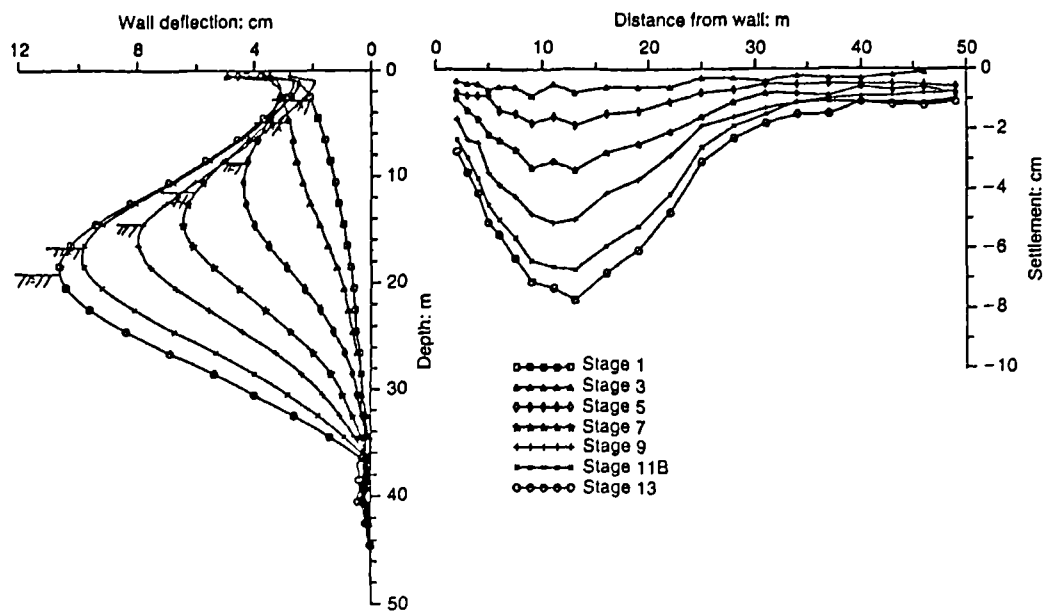


Figure 2.22 a)and b) Details of a 19.7m deep top down excavation in Taipei (Ou et al, 2000).



a)

Stage No.	Construction day	Construction activities
1	156-162	Excavated to elevation -2.80 m
2	164-169	Installed section H300 × 300 × 10 × 15 at first prop level (elevation -2.0 m), preload = 784.8 kN per prop
3	181-188	Excavated to elevation -4.9 m
4A	217	Cast floor slab (B1F) at elevation -3.5 m
4B	222-328	Demolished first level of prop and cast ground level of slab
5	233-255	Excavated to elevation -8.6 m
7	318-337	Excavated to elevation -11.8 m
9	363-378	Excavated to elevation -15.2 m
11A	419-423	Excavated to elevation -17.3 m (centre strip)
12A	425-429	Installed H400 × 400 × 13 × 21 sections at second prop level (elevation -16.5 m), preload = 1177 kN per prop (centre strip)
11B	430-436	Excavated to elevation -17.3m (side strips)
12B	437-444	Installed H400 × 400 × 13 × 21 sections at second prop level (elevation -16.5 m), preload = 1177 kN per prop (side strips)
13	445-460	Excavated to elevation -19.7 m
15	506-520	Cast floor slab (B5F) at elevation -17.1 m
16	528	Demolished second level of prop

b)

Figure 2.23 a) Observed wall deflections and ground surface settlements in the main observation section  
b) Conditions of construction between stages 4B and 5 (Ou et al, 2000).

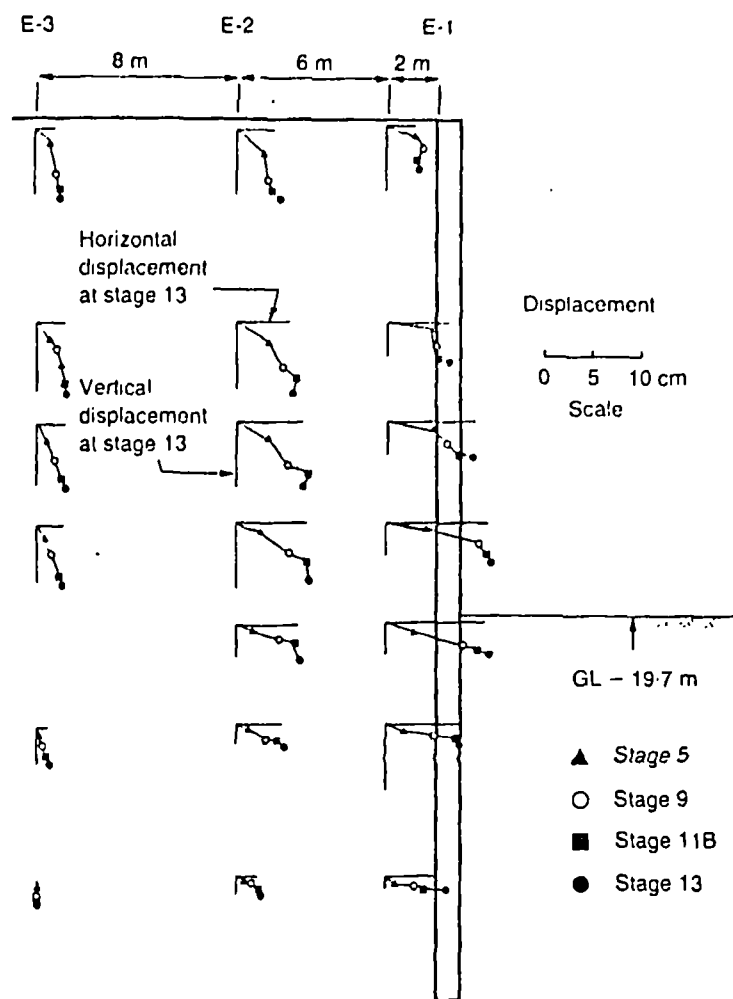


Figure 2.24 Vectors of the soil movements from stages 5 to stage 13 (see figure 23b) (Ou et al, 2000).



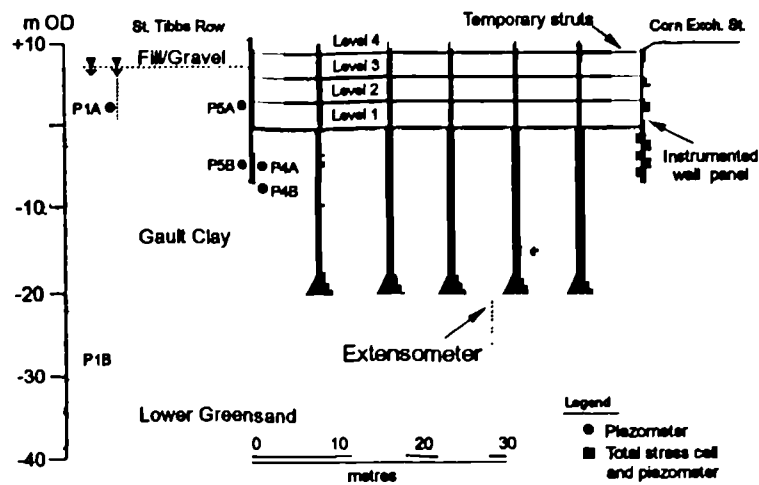
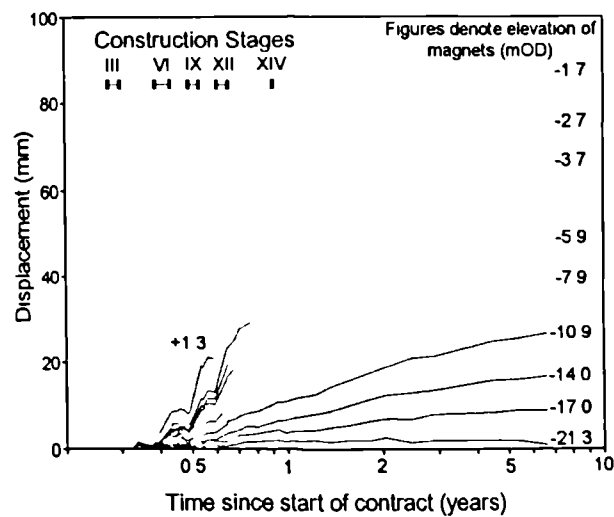


Figure 2.25 Cross section through 3 storey top down excavation (Nash et al, 1996).

	Construction operation	Period
I	Construction of diaphragm wall	18/4 - 3/6/89
II	Construction of bored piles	6/6 - 17/7/89
III	Reduced level dig to level 4	11/7 - 20/7/89
IV	Casting of level 4 slab	25/7 - 14/8/89
V	Installation of level 4 props	18/8 - 12/9/89
VI	Excavation to level 3	21/8 - 6/9/89
VII	Casting of level 3 slab	12/9 - 3/10/89
VIII	Installation of level 3 props	26/9 - 29/9/89
IX	Excavation to level 2	28/9 - 13/10/89
X	Casting of level 2 slab	18/10 - 3 11/89
XI	Installation of level 2 props	23/10 - 2/11 89
XII	Excavation to level 1	9/11-28 11 89
XIII	Casting of level 1 slab	21/12 -30 1 90
XIV	Removal of all props	26/2 - 27 2 90

a)



b)

Figure 2.26 a) Main stages of construction  
b) Movements vs time (Nash et al, 1996).

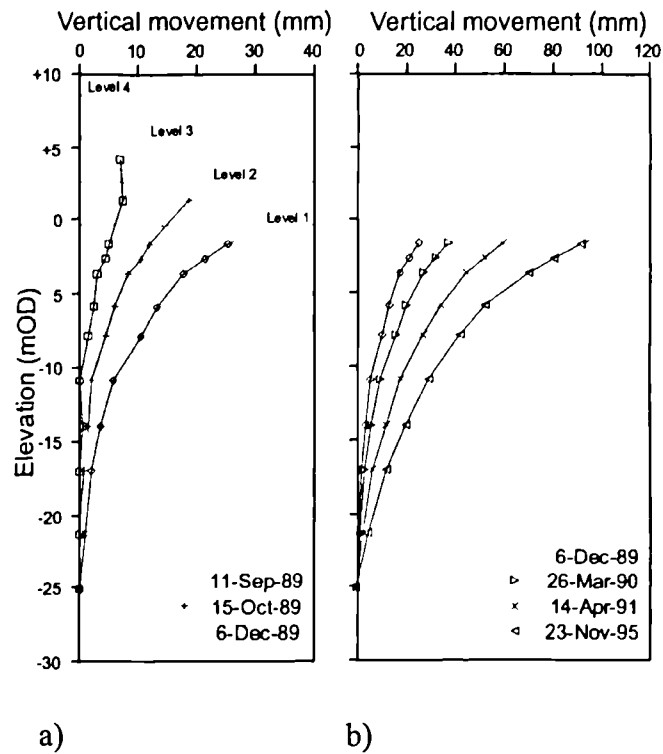


Figure 2.27 Heave beneath an excavation  
a) During excavation  
b) Following completion of excavation (Nash et al, 1996).

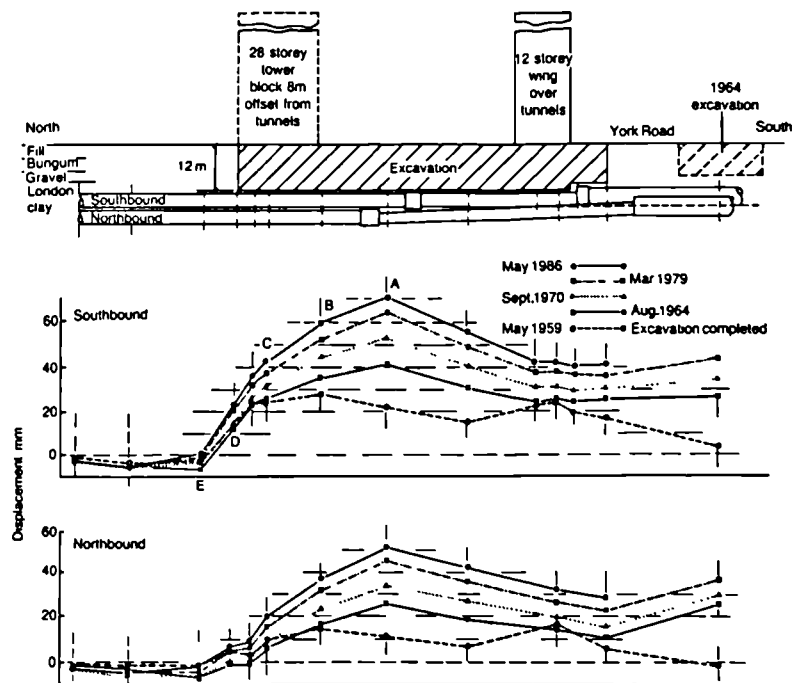


Figure 2.28 Section through the excavation at the Shell Centre on the South Bank showing displacements of the tunnel crowns (Burford, 1988).

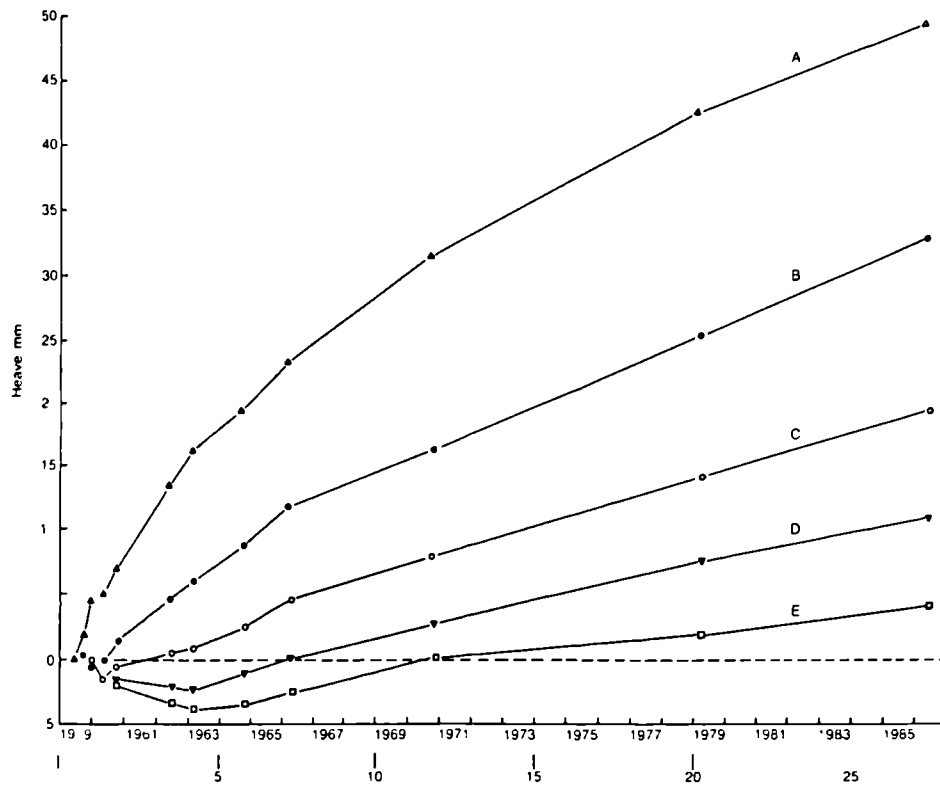


Figure 2.29 Long term uplift of selected points in the crown of the southbound tunnel beneath the Shell Centre.(Burford, 1988).

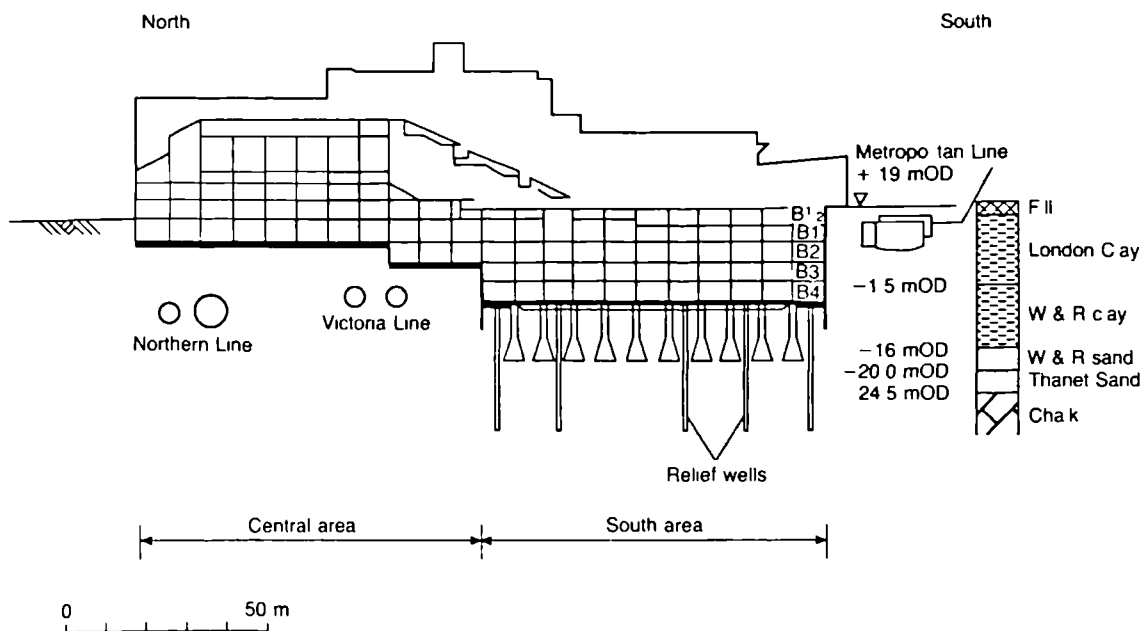


Figure 2.30 North-South section through British Library (Simpson, 1992).

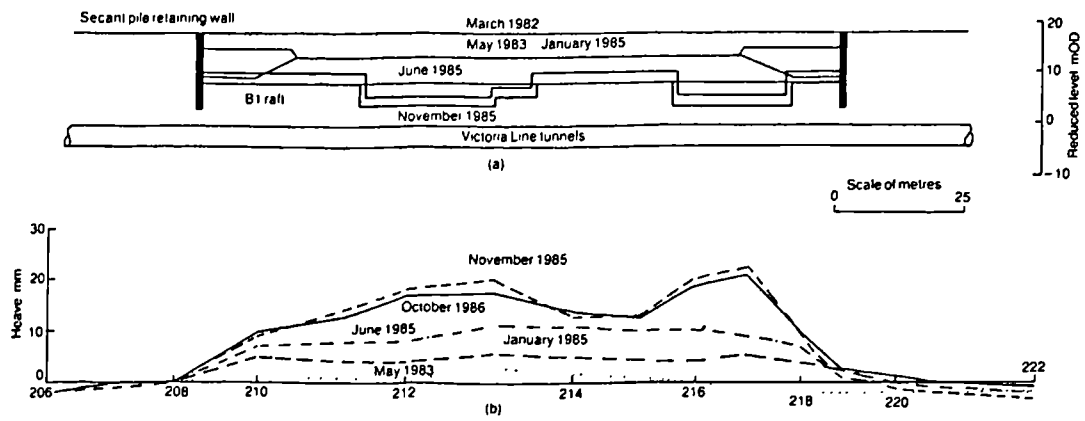


Figure 2.31 Tunnel movements at British Library  
a) East-west section  
b) Heave profile along line of tunnel  
(Raison, 1988).

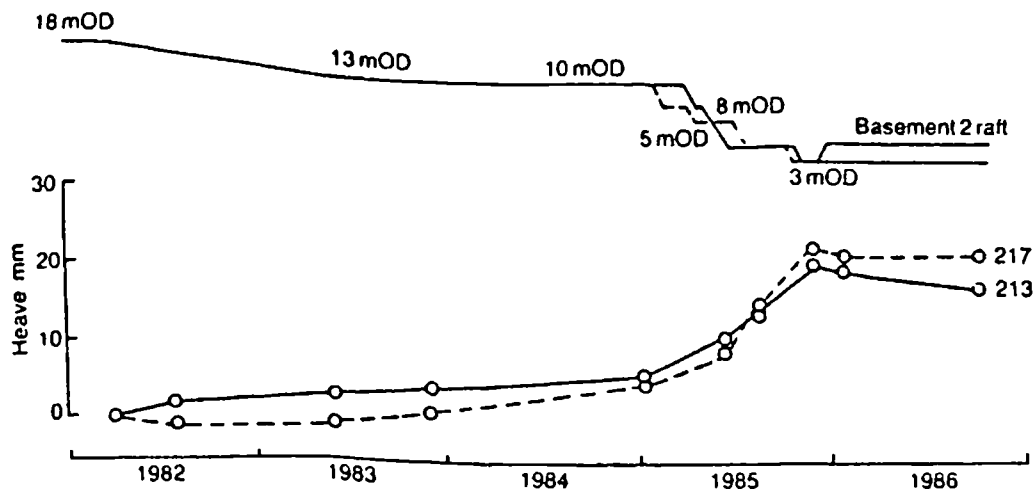


Figure 2.32 Rate of heave in tunnel at the site of British Library (Raison, 1988).

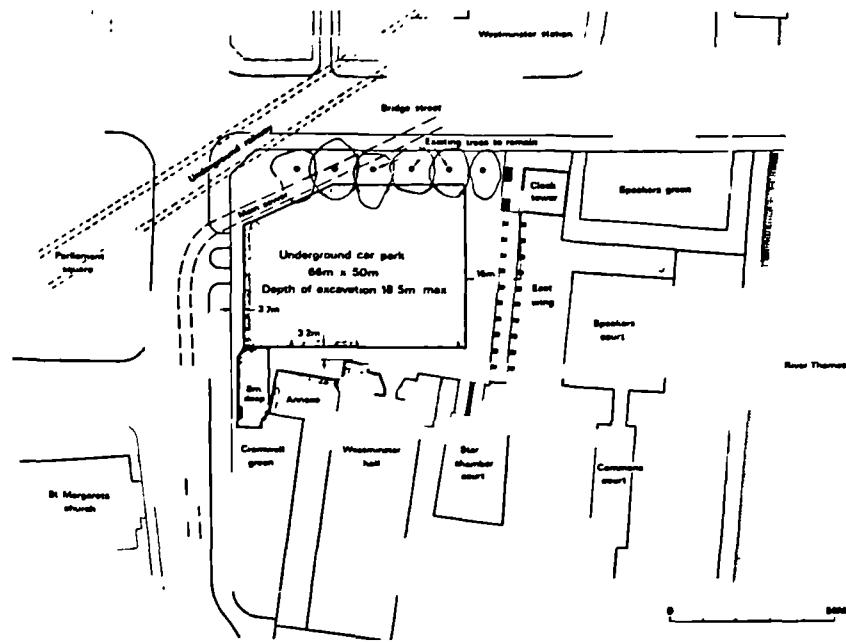


Figure 2.33 Palace of Westminster: location plan (Burland et al, 1979).

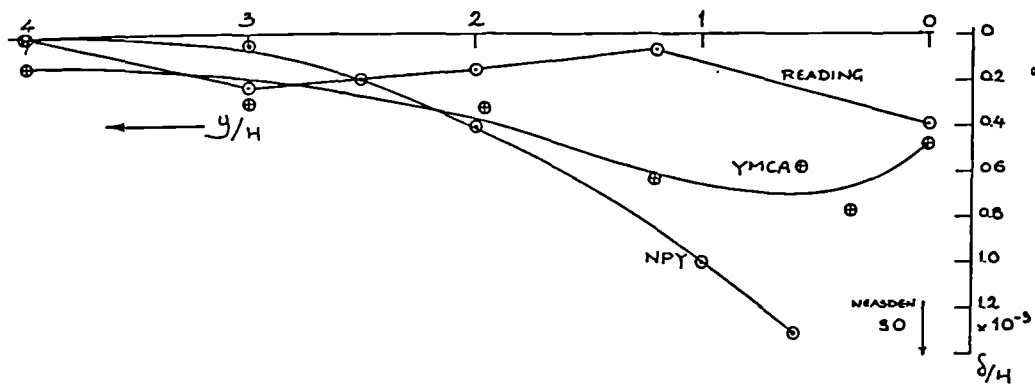


Figure 2.34 Summary of observed settlements (St John, 1985).

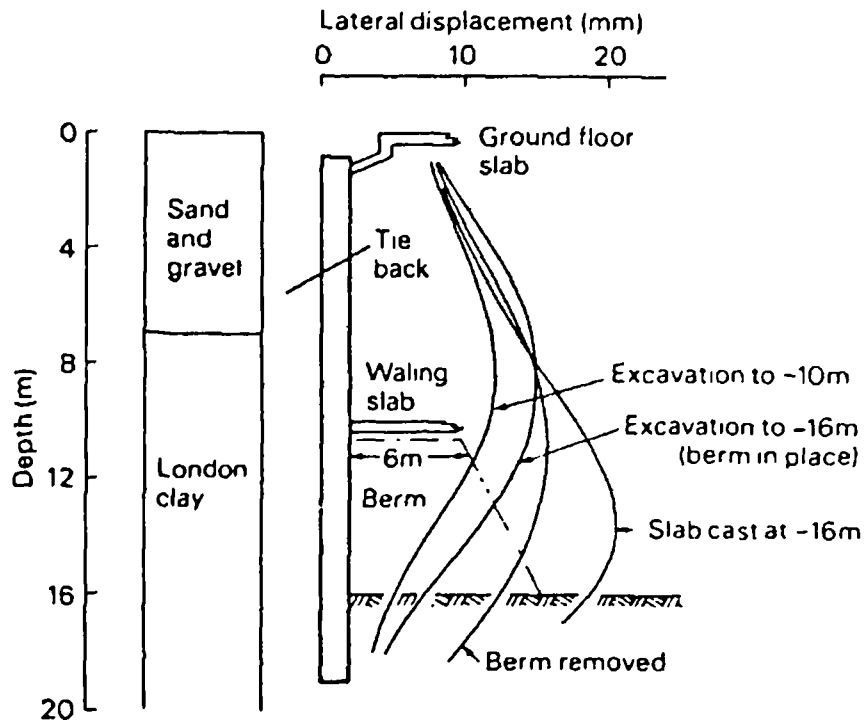


Figure 2.35 Central YMCA: Influence of perimeter berm on wall movement (Burland et al, 1979).

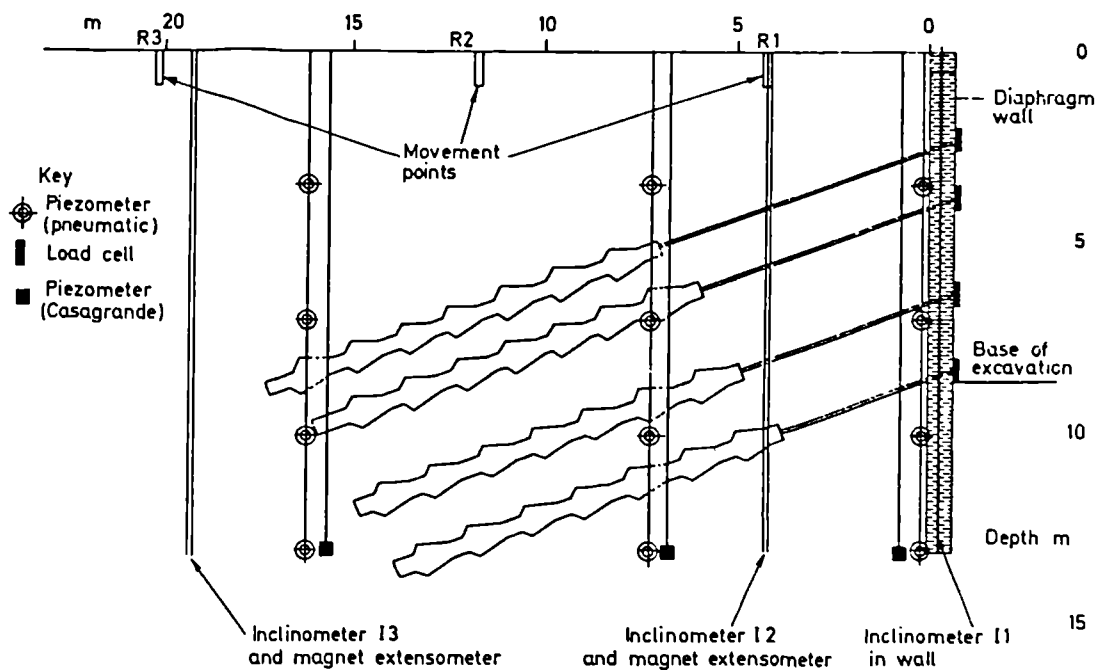


Figure 2.36 Strong ground anchored excavation at Neasden (Sills et al, 1977).

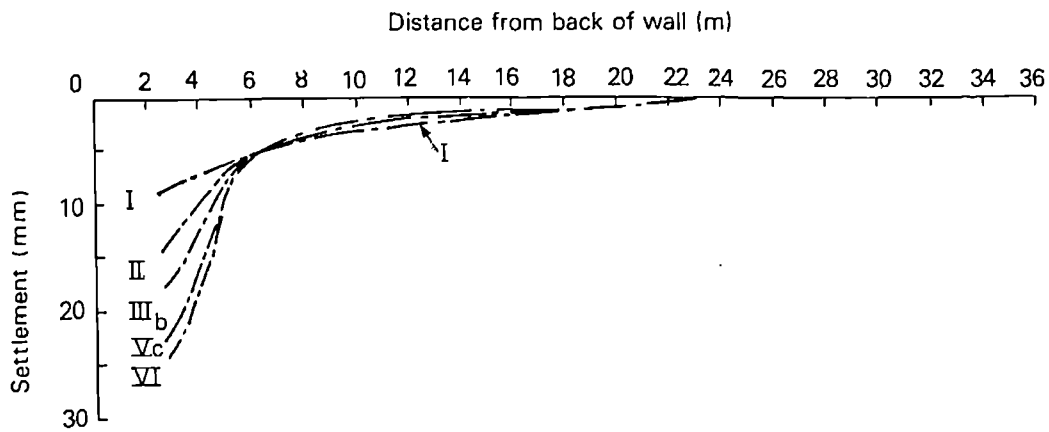


Figure 2.37 Magnitude of settlement behind the retaining wall at Bell Common (Tedd et al, 1984).

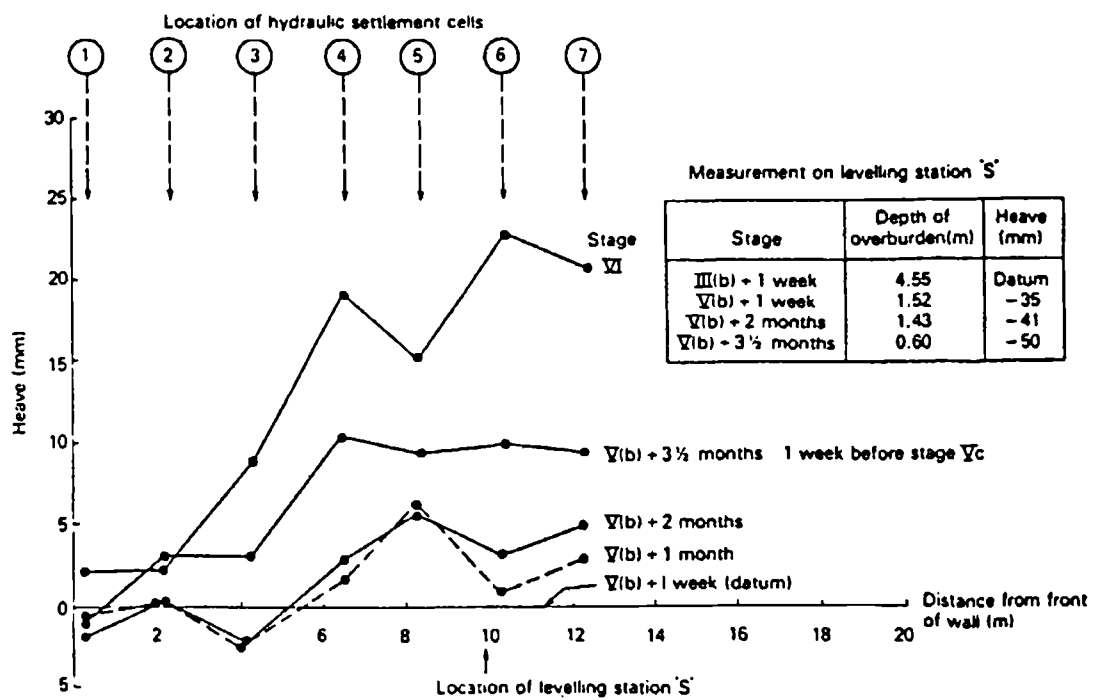


Figure 2.38 Measurement of near surface vertical displacements in front of the retaining wall at Bell Common (Tedd et al, 1984).

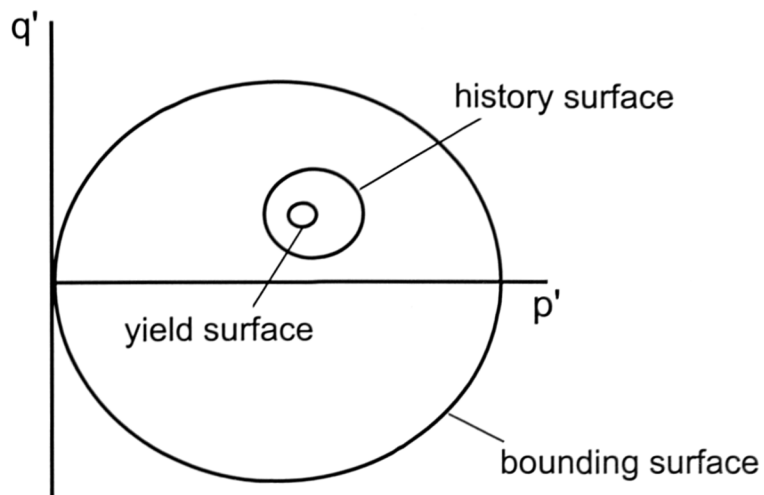


Figure 2.39 Sketch of the 3-SKH model in triaxial stress space (Stallebrass and Taylor, 1997).

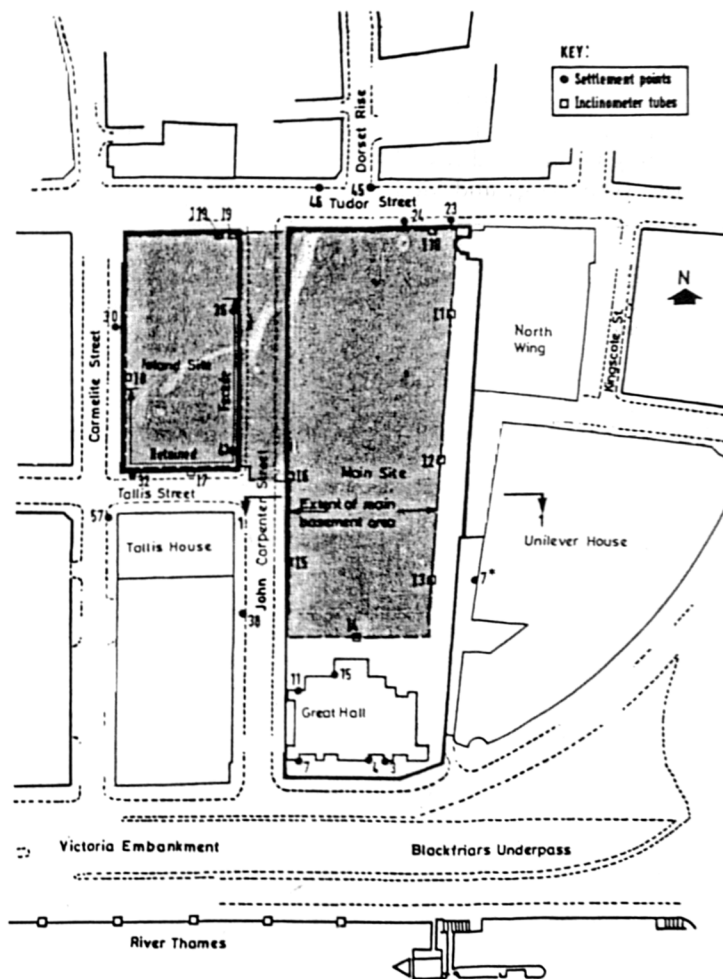


Figure 2.40 Plan on site at 60 Victoria Embankment (St John et al, 1993).



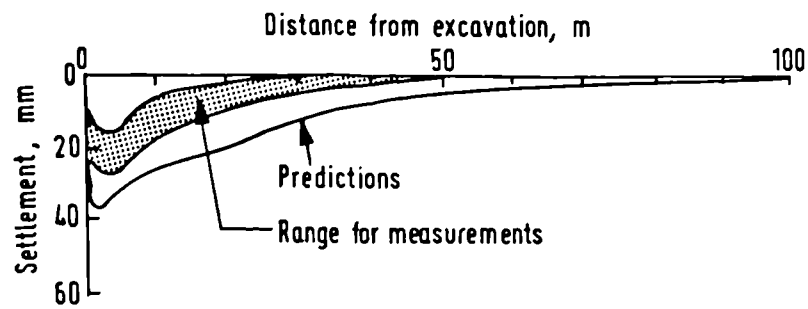


Figure 2.41 Settlements versus distance from excavation (St John et al, 1993).

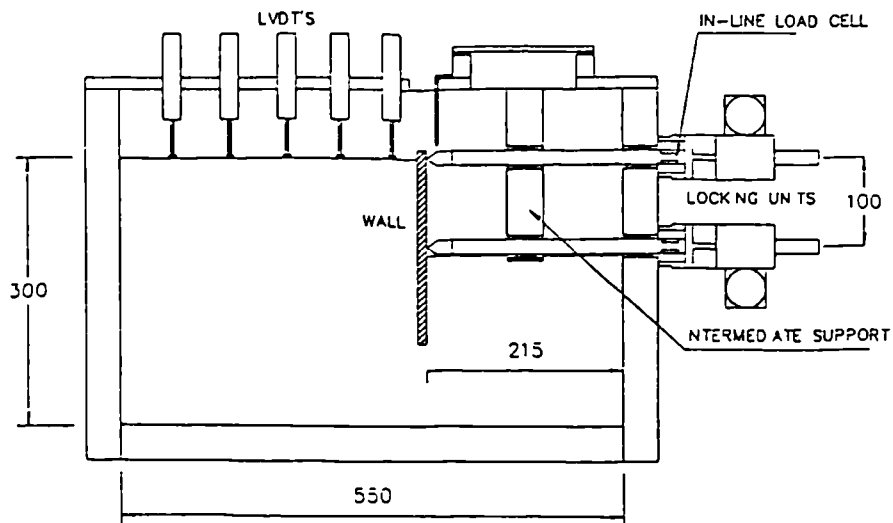


Figure 2.42 Cross section through multi-propped retaining wall centrifuge model (Powrie et al, 1994).

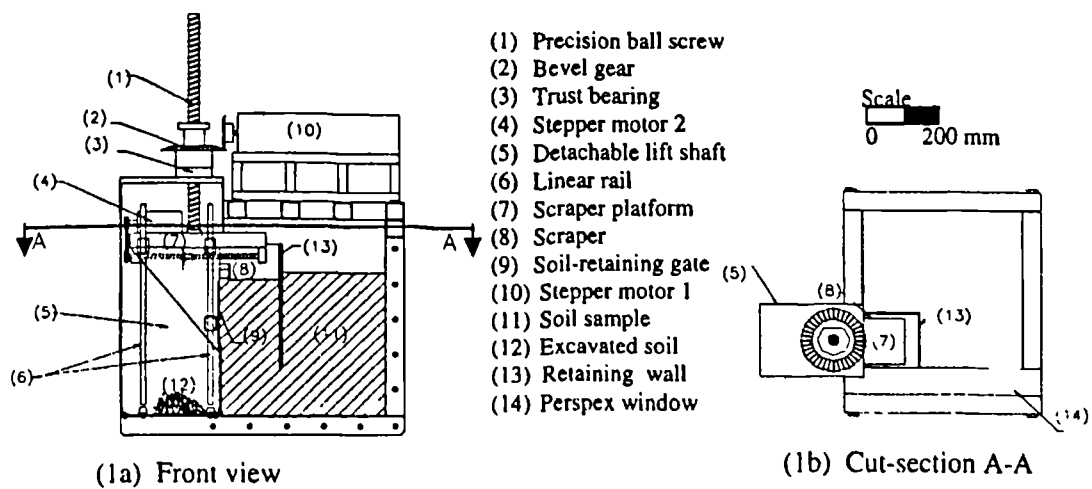


Figure 2.43 Schematic diagram of the 3D in-flight excavator (Loh et al, 1998).

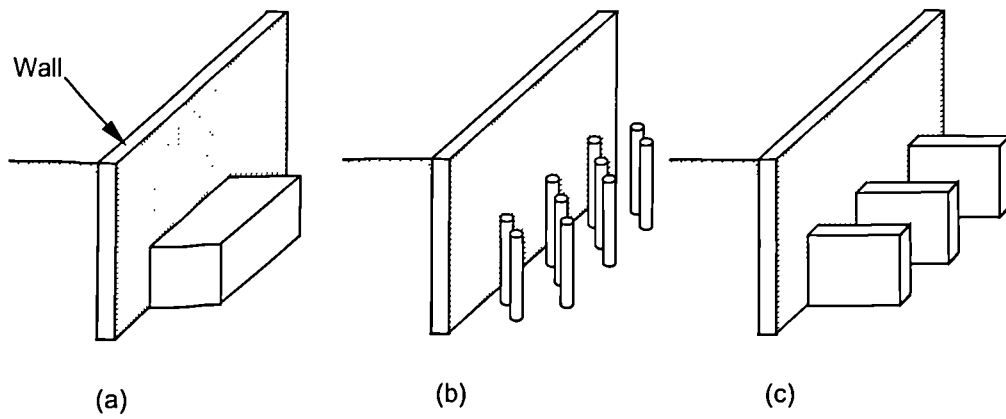


Figure 2.44 Typical patterns of treated soil mass used in excavation  
a) block type  
b) column type  
c) wall type  
(Ou et al, 1996).

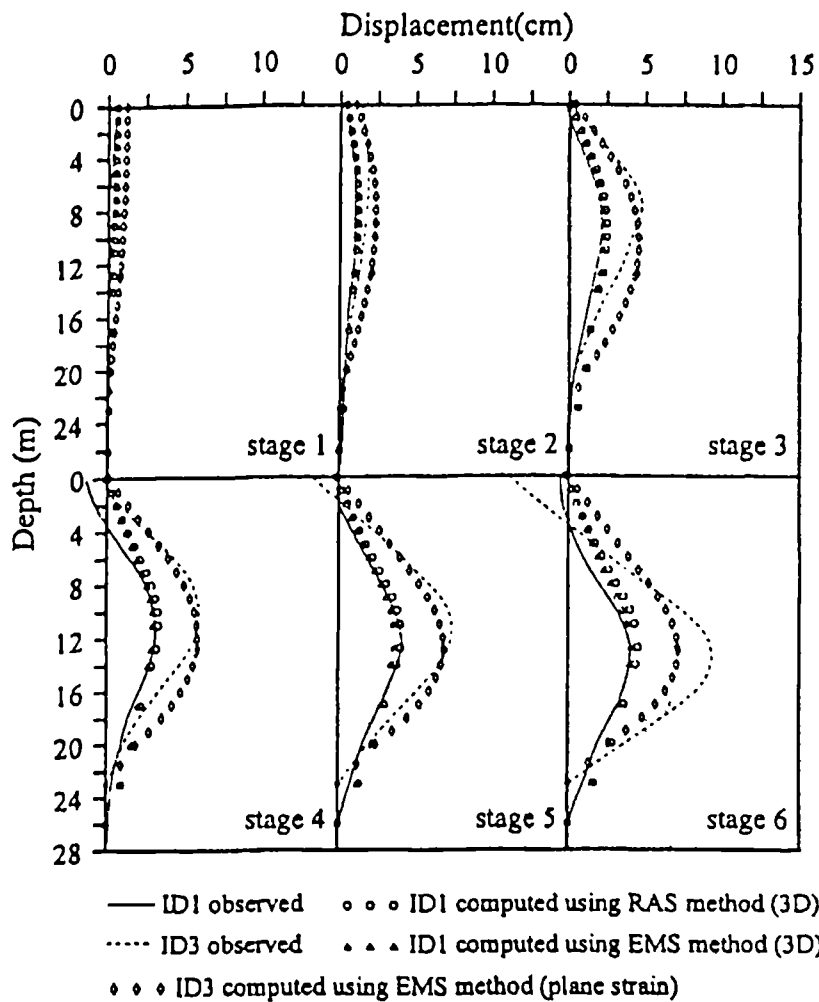


Figure 2.45 Comparison of measured wall deflections and computed wall deflections from both RAS and EMS methods (Ou et al, 1996).

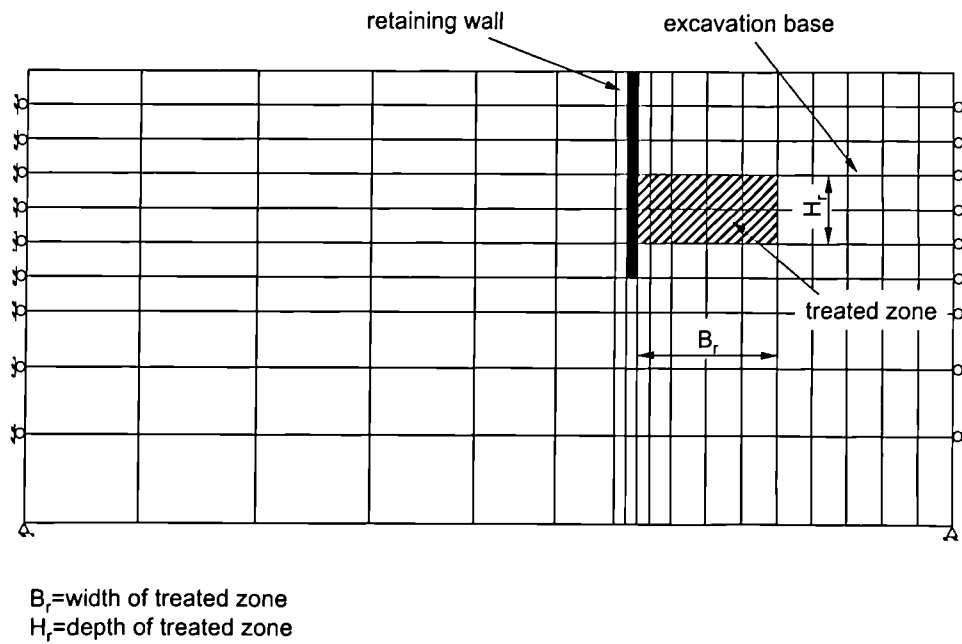


Figure 2.46 Finite element mesh for analysis showing treated zone (Xie et al, 1999)

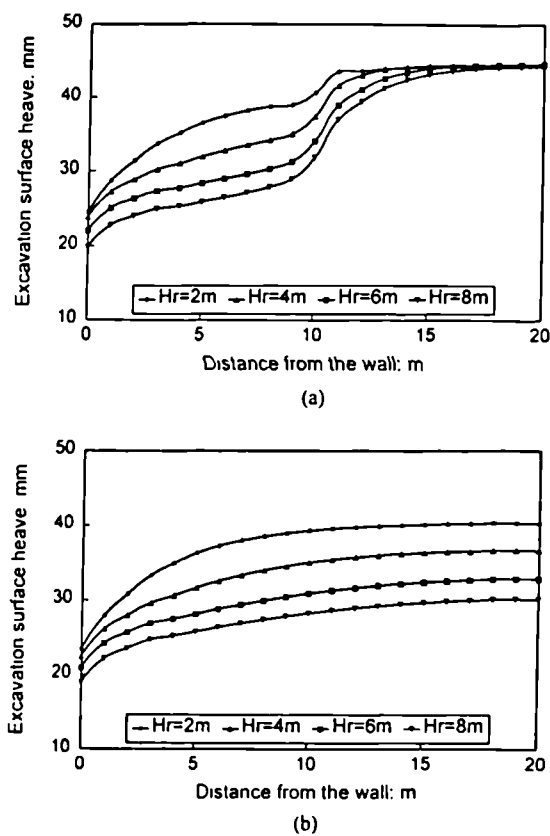


Figure 2.47 Variation, at various treated depths ( $H_r$ ), of excavation base heave with increase in distance from wall ( $B_r$ ) for the treated widths:  
a)  $B_r=10\text{m}$   
b)  $B_r=20\text{m}$   
(See Figure 2.46 for key to notation) (Xie et al, 1999).

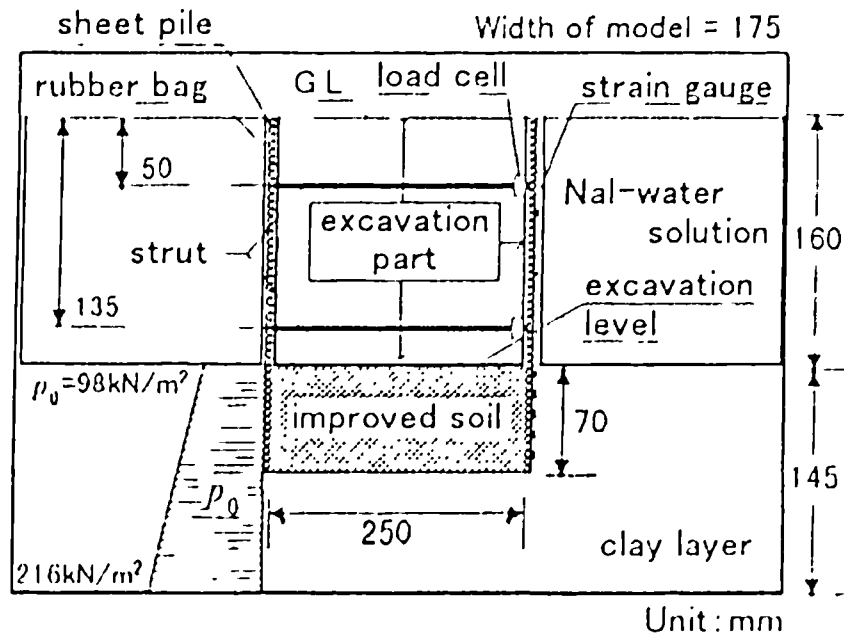


Figure 2.48 Layout of centrifuge modelling test (Ohishi et al, 1999).

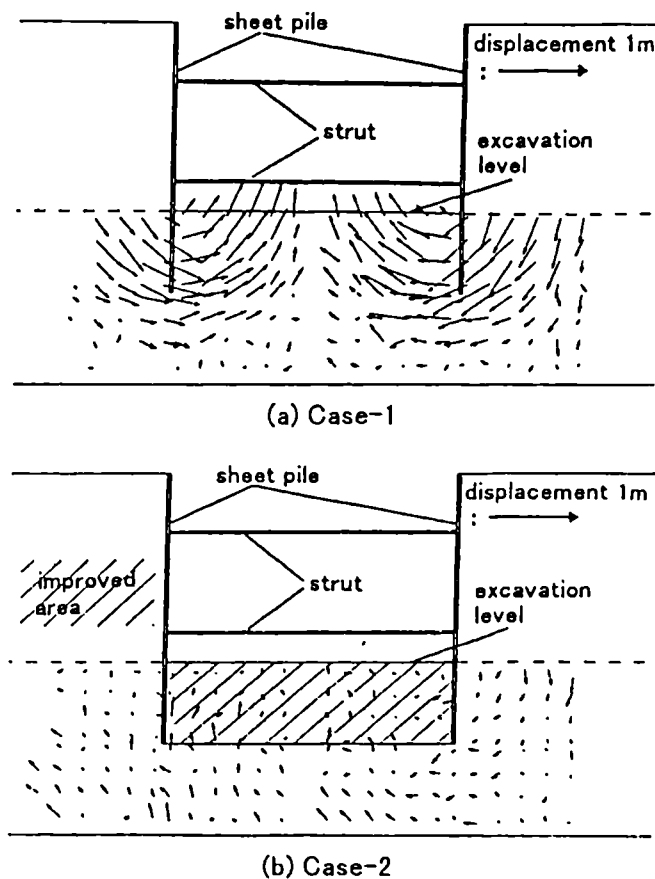


Figure 2.49 Ground displacements at the end of excavation showing comparison between unimproved (Case 1) and improved (Case 2) soil (Ohishi et al, 1999).

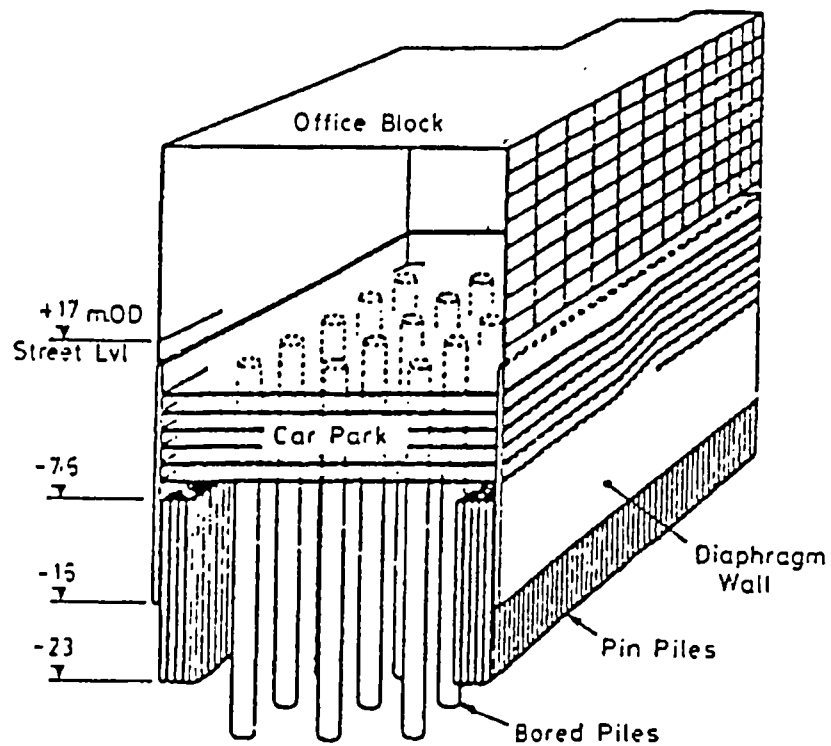


Figure 2.50 General geometry of excavation at Aldersgate Street, London (Fernie et al, 1991).

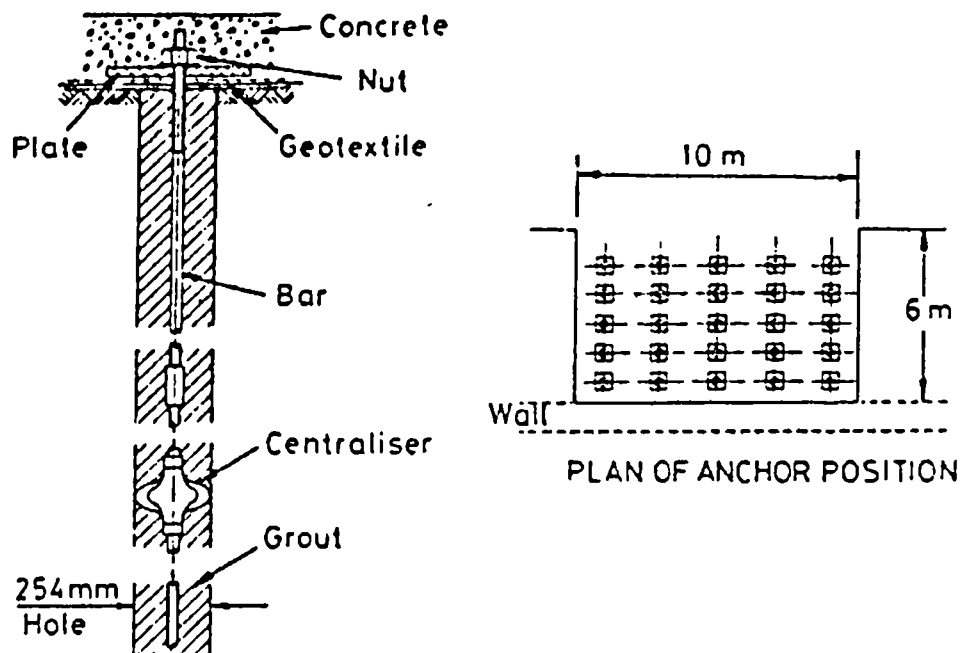


Figure 2.51 Detail of typical pin pile (Fernie et al, 1991).

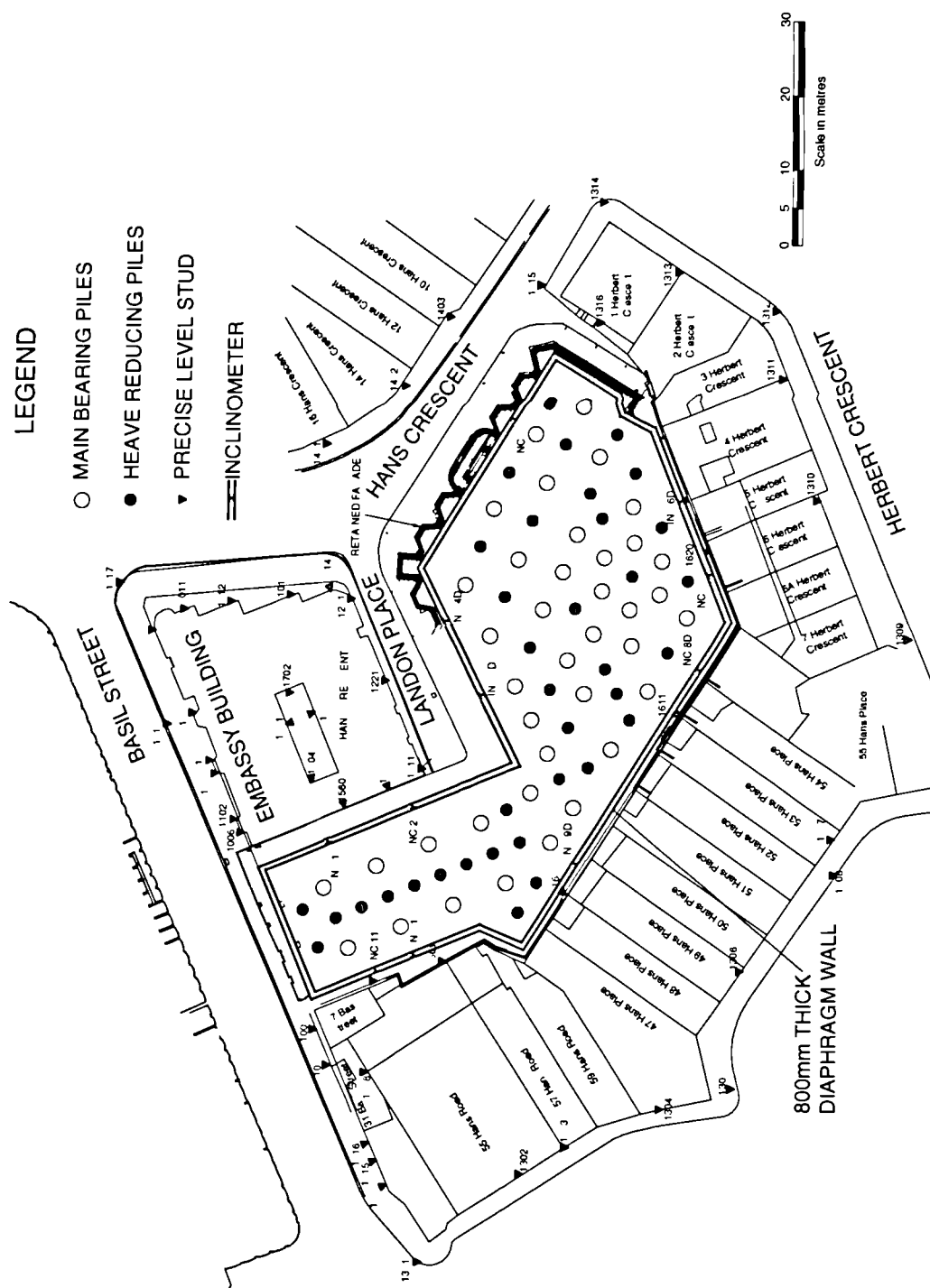


Figure 2.52 Site of the former Knightsbridge Crown Court showing the outline of the diaphragm wall and the pile layout. Also shown are positions of inclinometers and precise levelling studs that formed part of the monitoring during construction

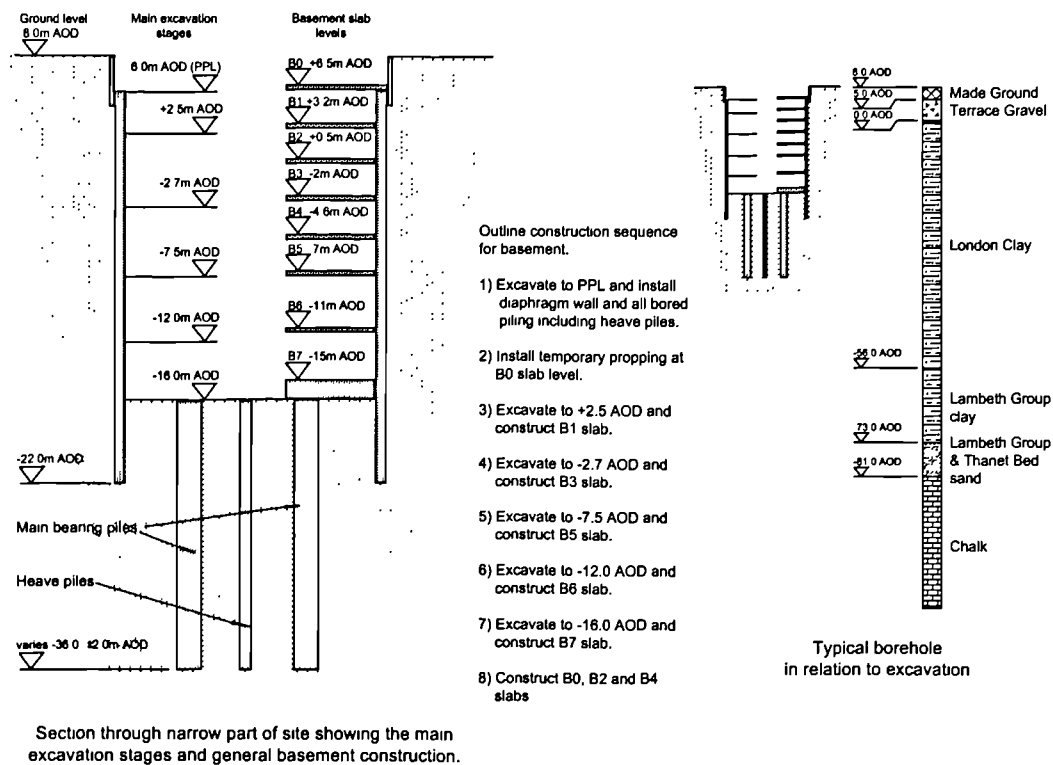


Figure 2.53 Typical section through the top down basement construction at the site of the former Knightsbridge Crown Court showing the general construction sequence and a typical borehole.

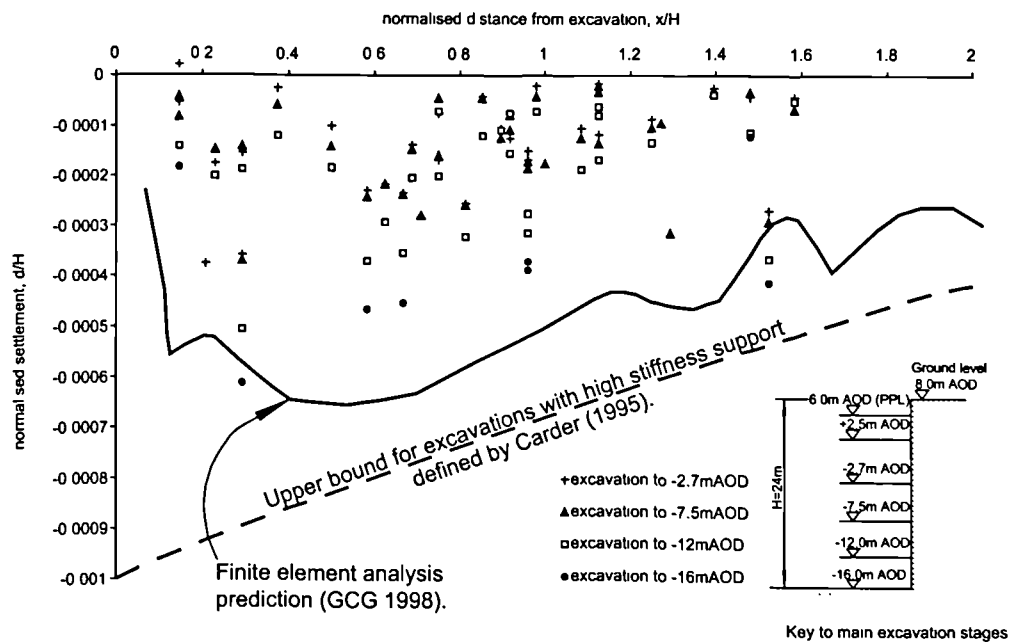


Figure 2.54 Normalised settlement around the top down excavation at the former Knightsbridge Crown Court site at completion of basement excavation. Included are the finite element analysis prediction, site monitoring data and an upper bound for expected settlements suggested by monitoring data from similar excavations.

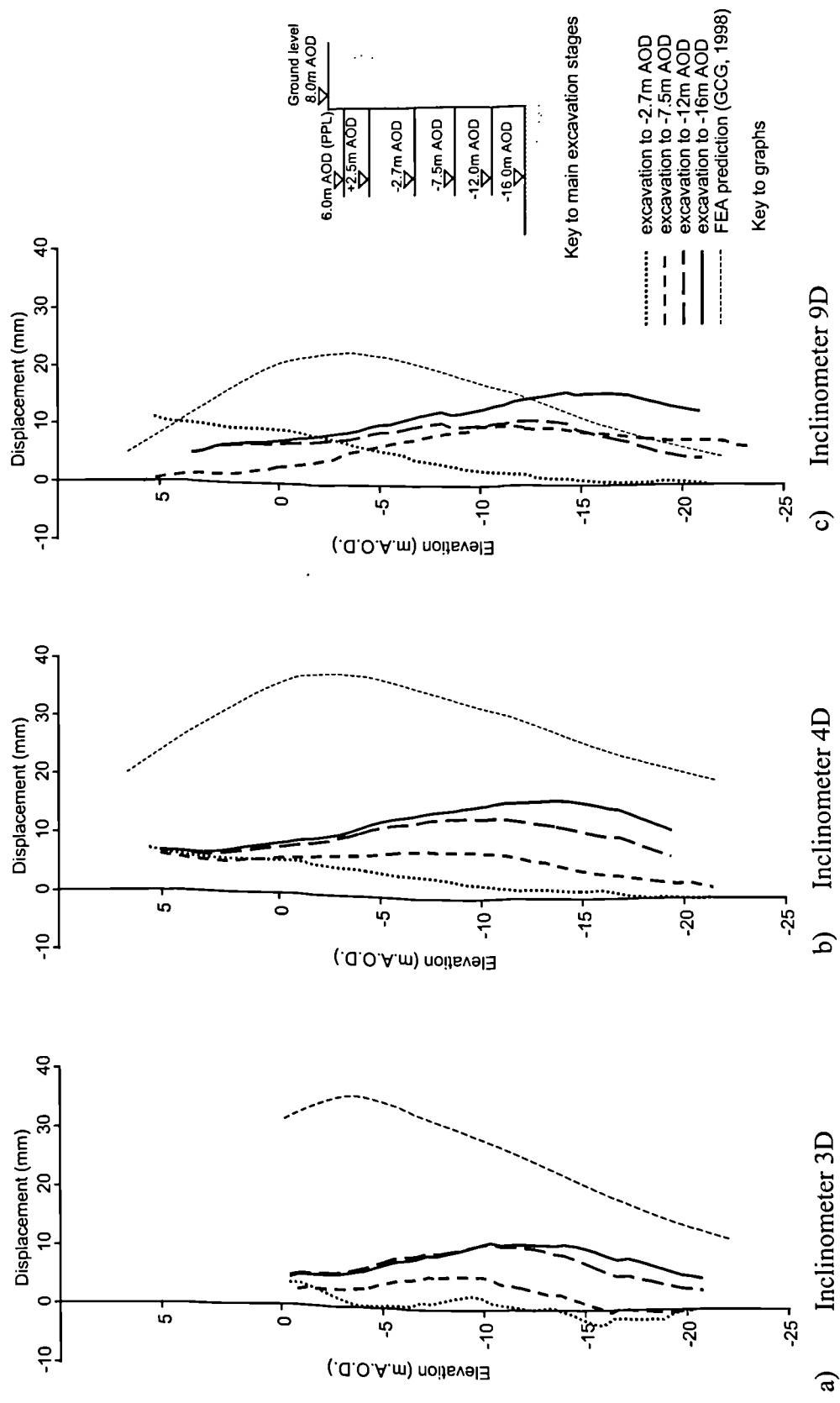


Figure 2.55 Horizontal displacements of the retaining wall at the site of the former Knightsbridge Crown Court measured using inclinometers at key stages during the excavation.



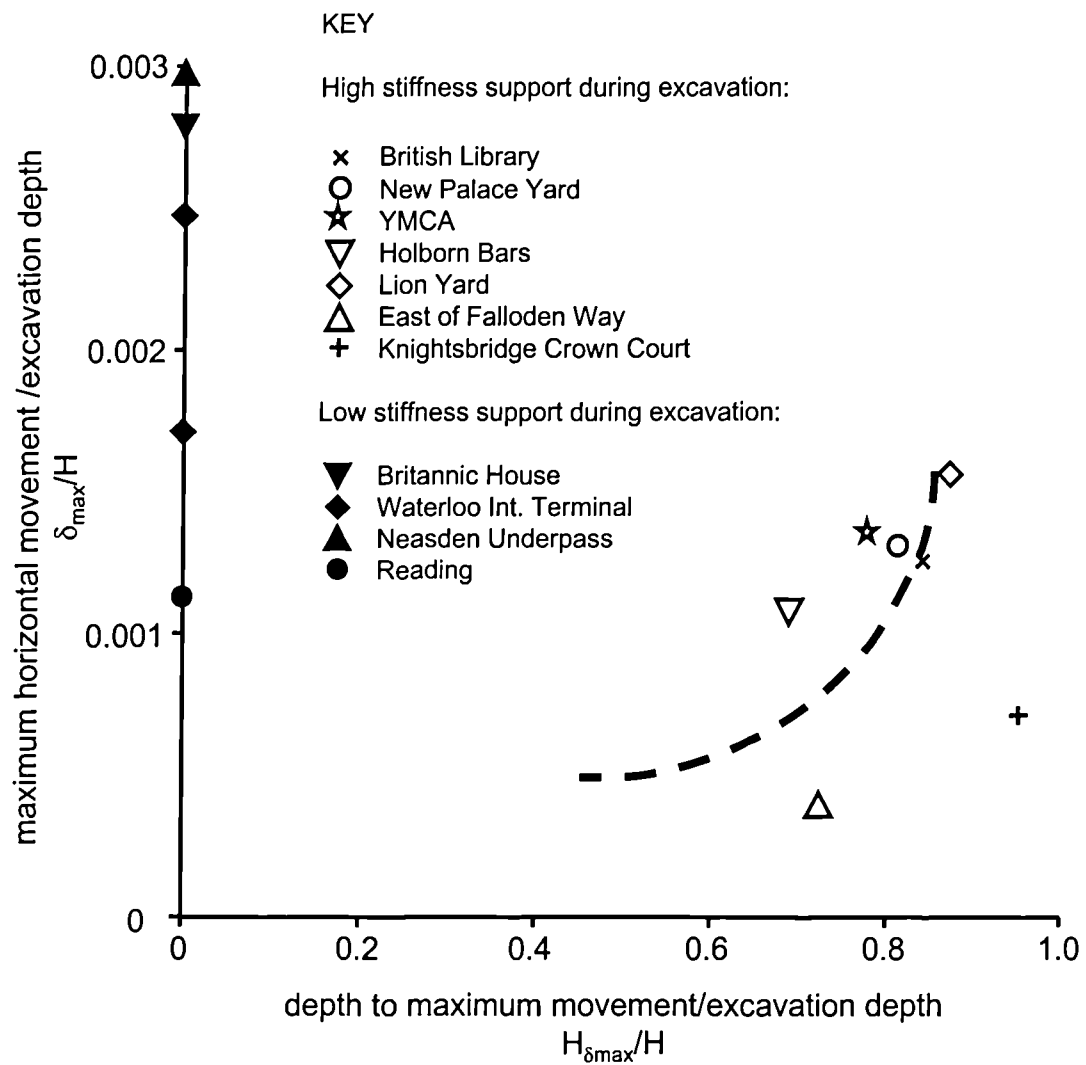


Figure 2.56 Comparison of horizontal wall movements at the site of the former Knightsbridge Crown Court with field measurements of other excavations in stiff clay. (after Carder, 1995).

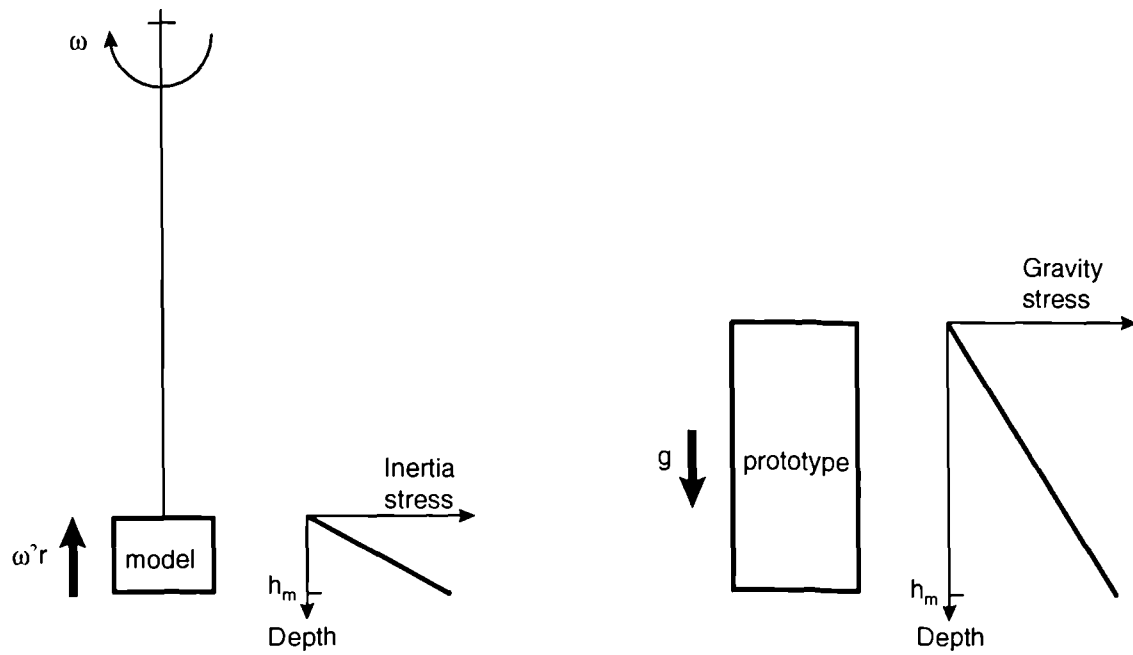


Figure 3.1 Inertial stresses in a centrifuge model compared with gravitational stresses in a corresponding prototype (after Taylor 1995)

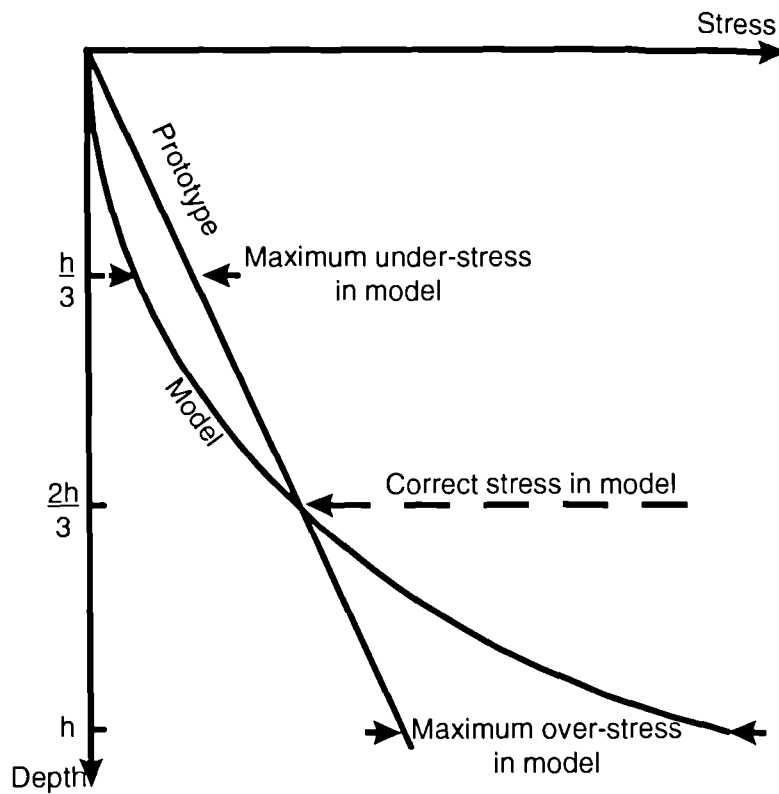


Figure 3.2 Stress variation with depth in centrifuge model compared with a corresponding prototype (after Taylor 1995)

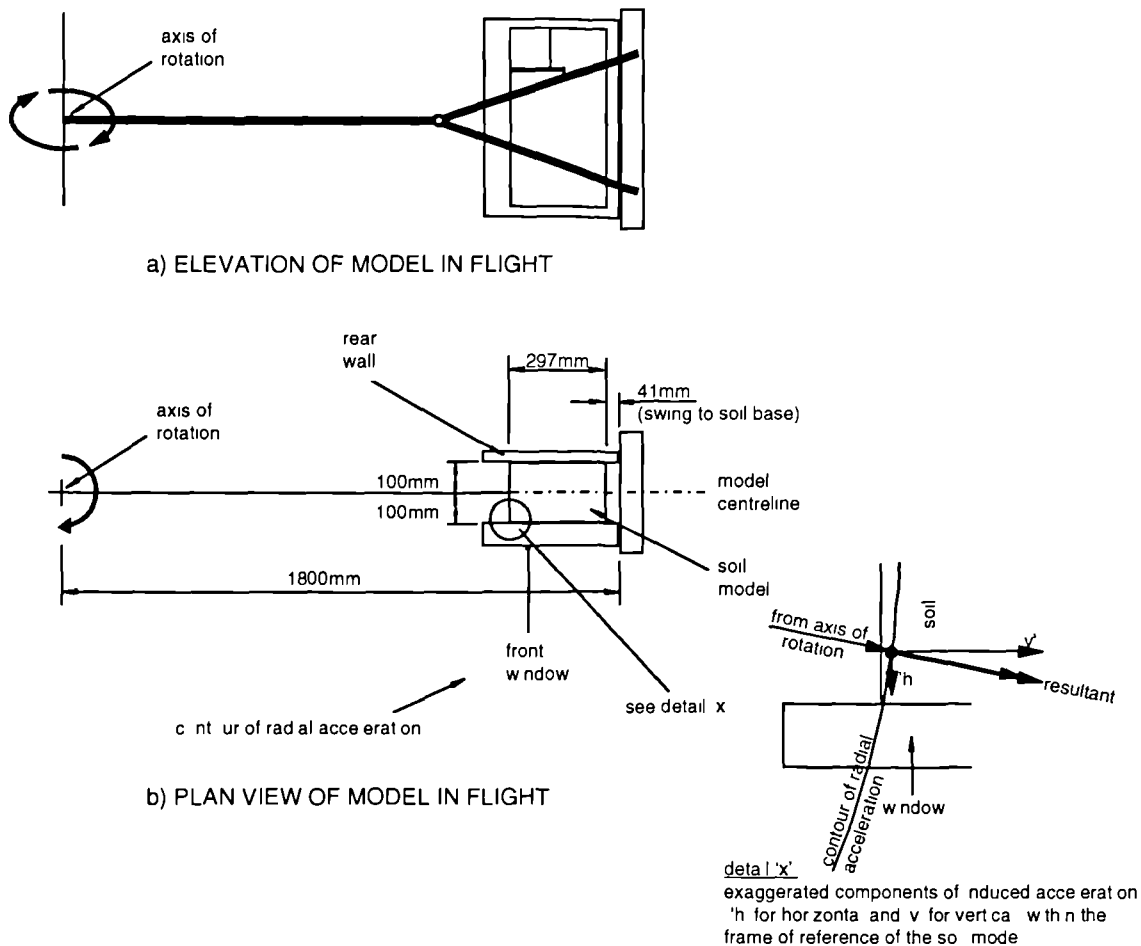


Figure 3.3 Geometry of a typical model on the Acutronic 661 geotechnical centrifuge at City University, London showing a) elevation of model in flight; b) components of induced acceleration (after Grant 1998)

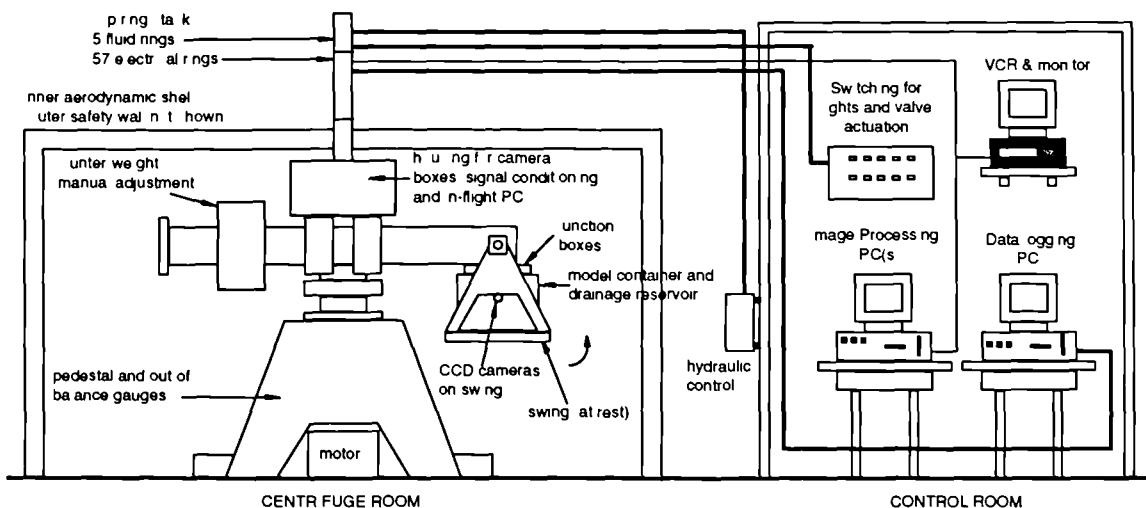


Figure 3.4 Schematic diagram of the Acutronic 661 geotechnical testing facility at City University, London - capacity 40g.tonnes, radius 1.8m to swing base in flight (after Grant 1998)

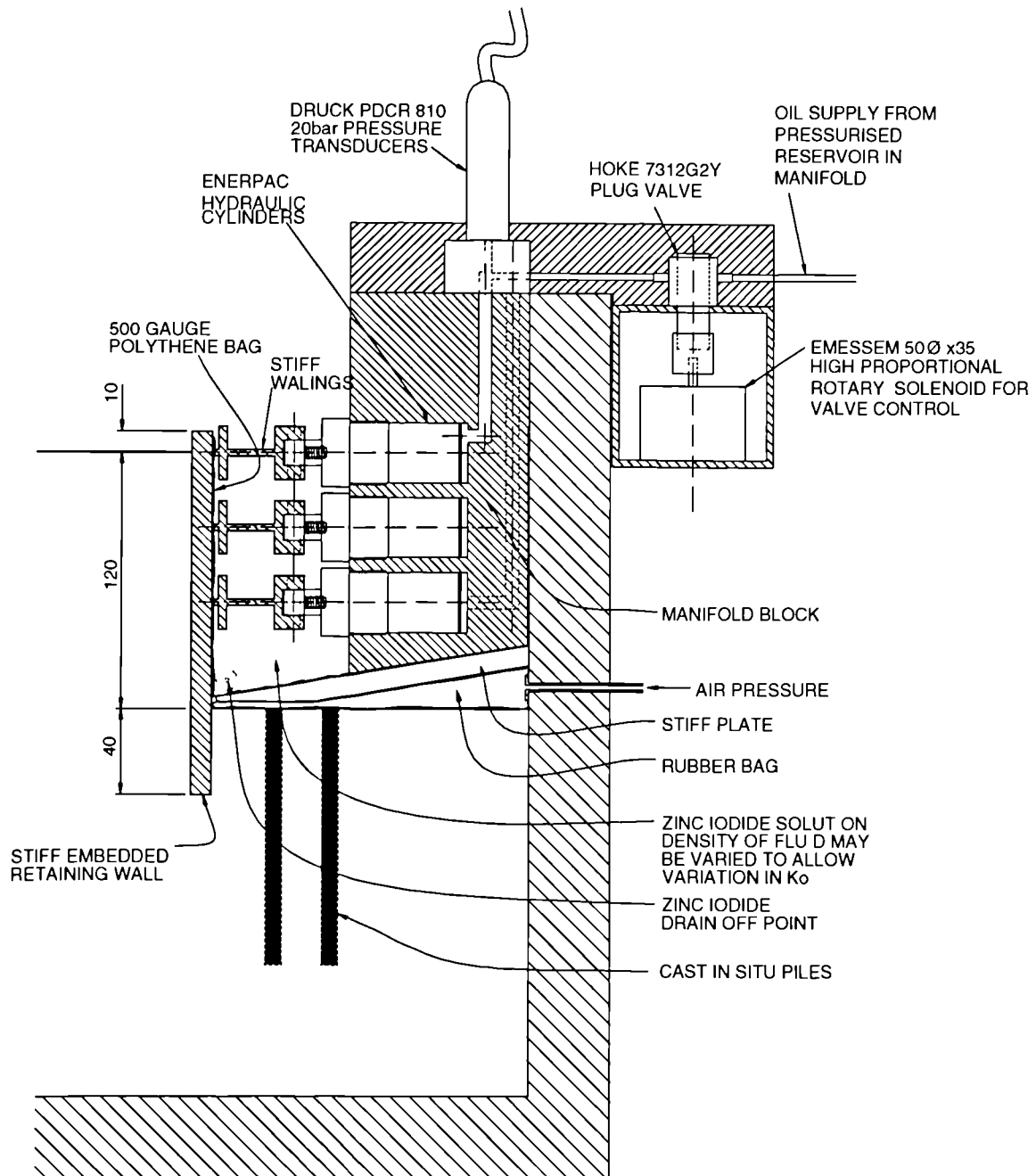


Figure 3.5 General arrangement of main apparatus prior to modification after test AM1.

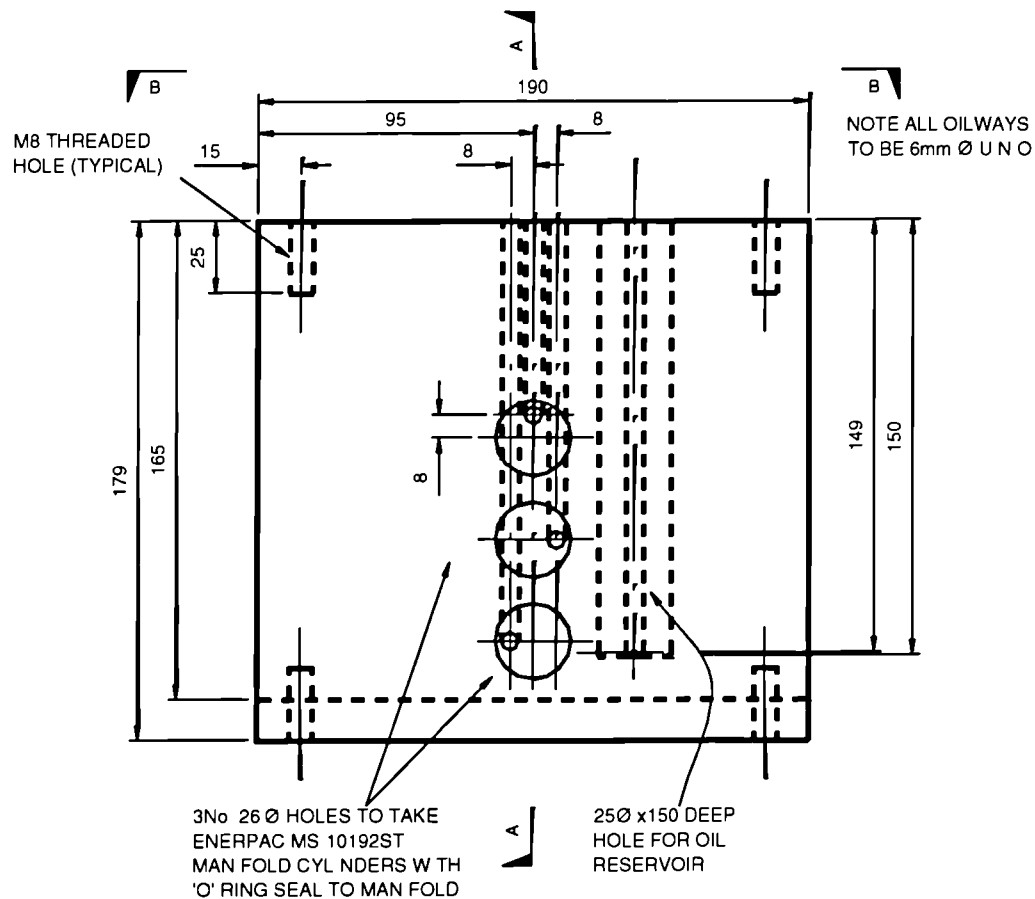


Figure 3.6 Elevation on manifold unit showing location of hydraulic cylinders, oil reservoir and oilways (See Figures 3.7 and 3.8 for section A-A and section B-B).

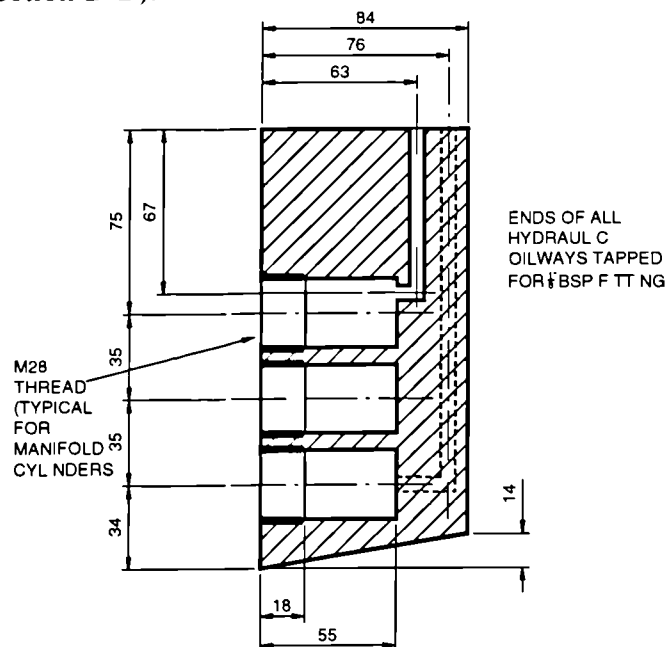


Figure 3.7 Section A-A through manifold unit showing hydraulic oilways. For location see Figure 3.6.

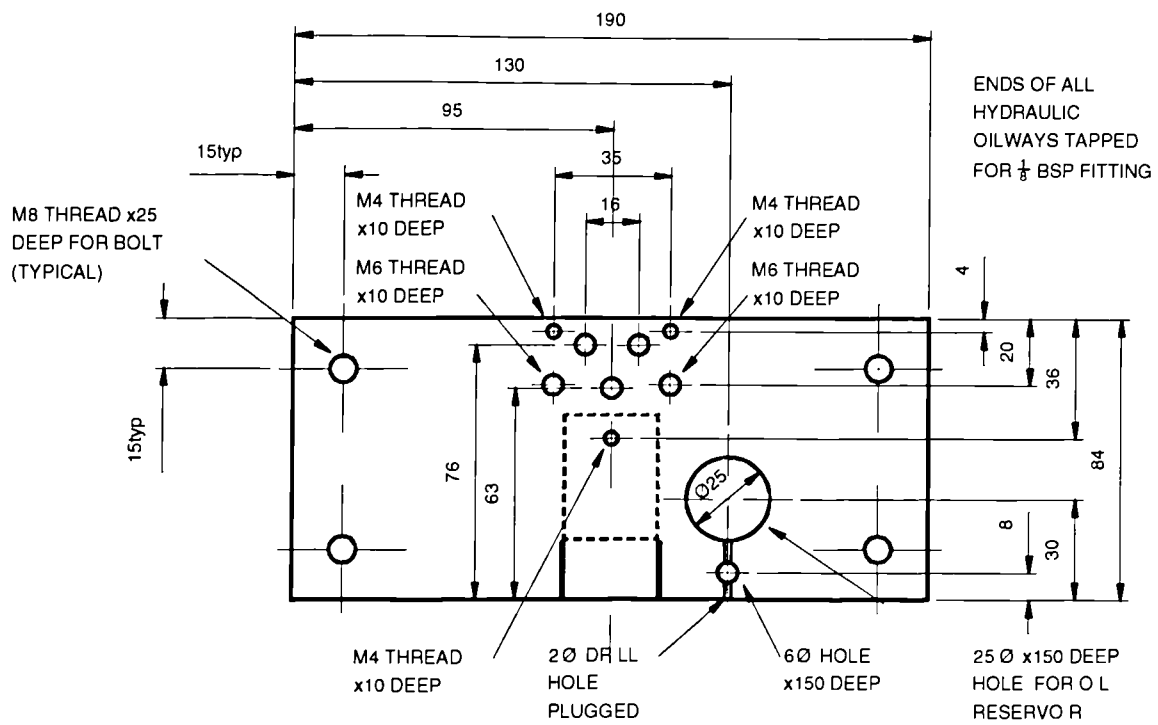


Figure 3.8 Plan B-B on manifold unit showing position of hydraulic oil reservoir and oilways for hydraulic cylinders. For location see Figure 3.6.

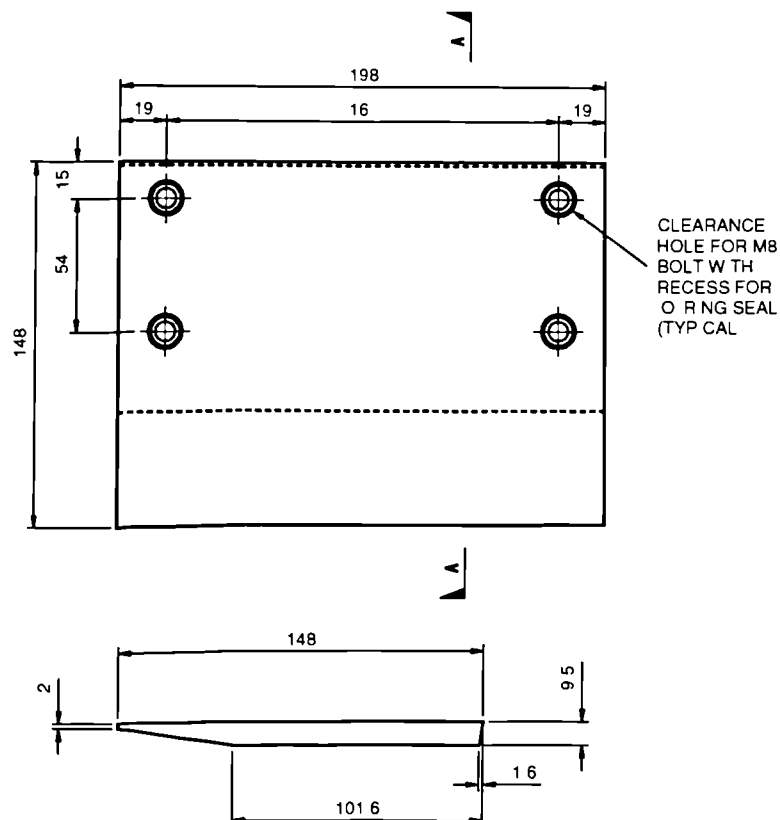


Figure 3.9 Plan and section through tapered aluminium plate used to separate the membranes containing compressed air and dense fluid



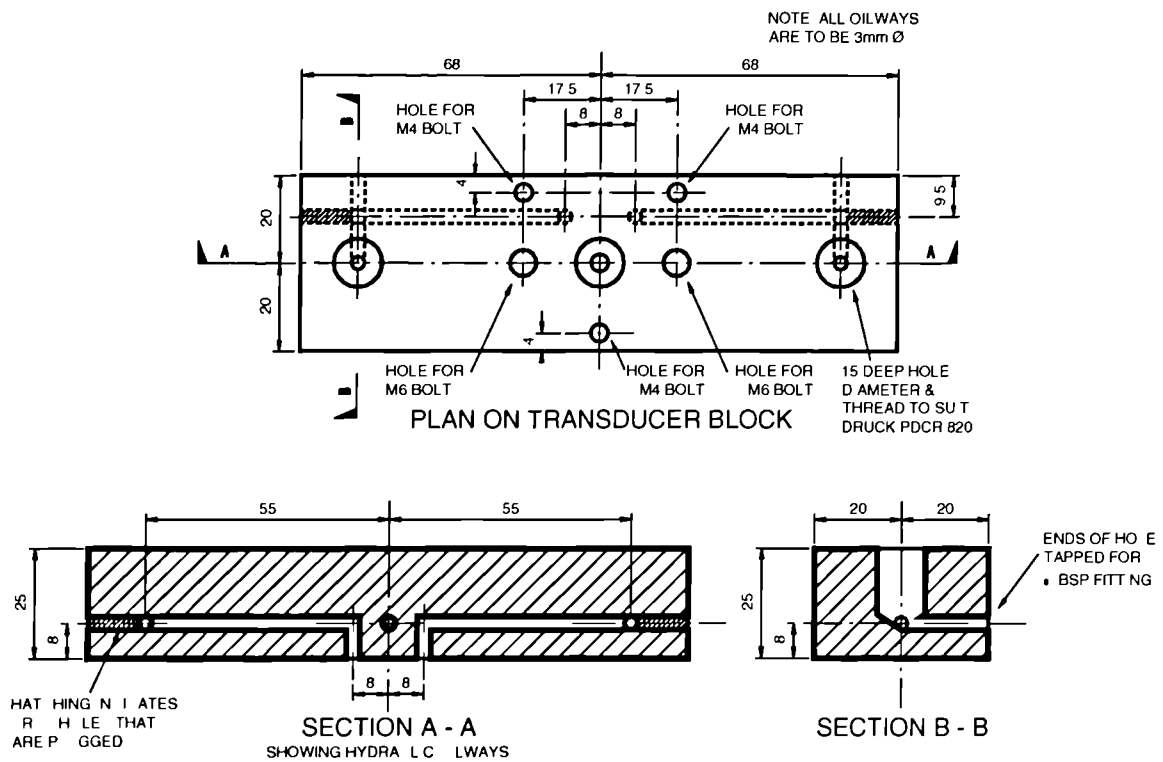


Figure 3.12 Details of transducer block bolted to top of manifold apparatus to enable measurement of oil pressure in hydraulic cylinders

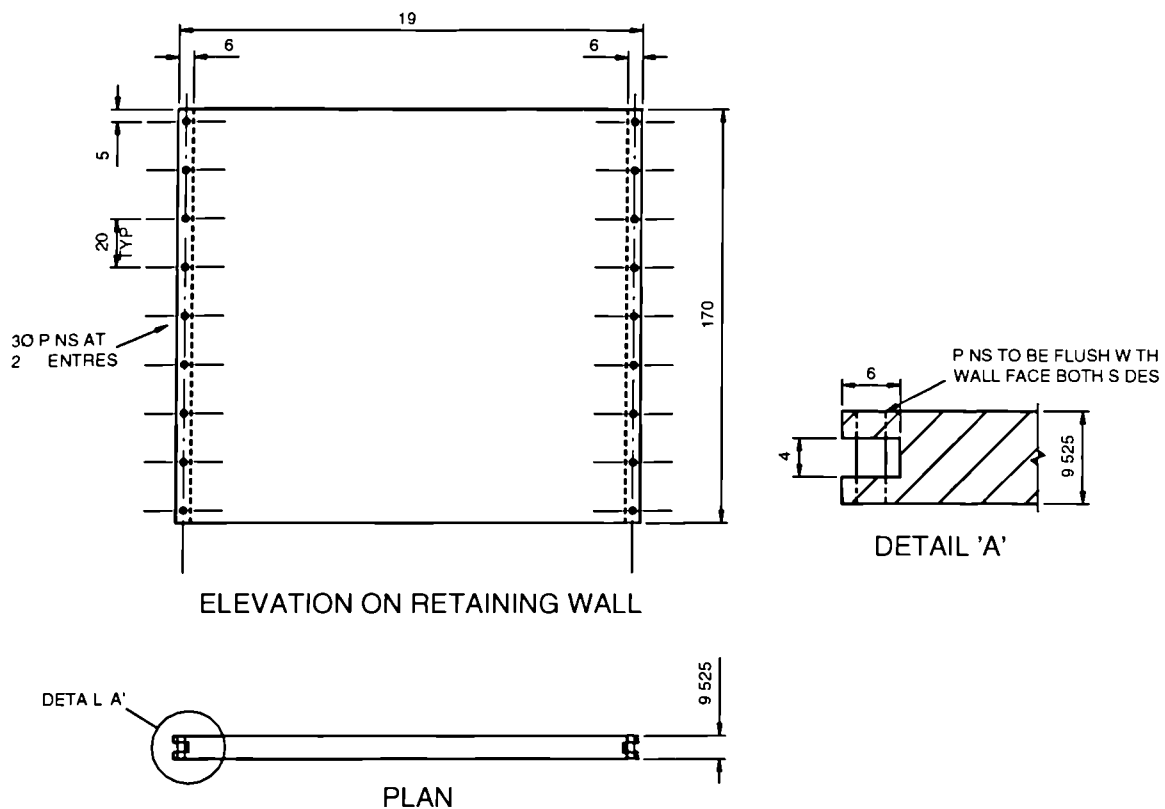


Figure 3.13 Details of model retaining wall and method of securing cast silicone rubber seals into rebates





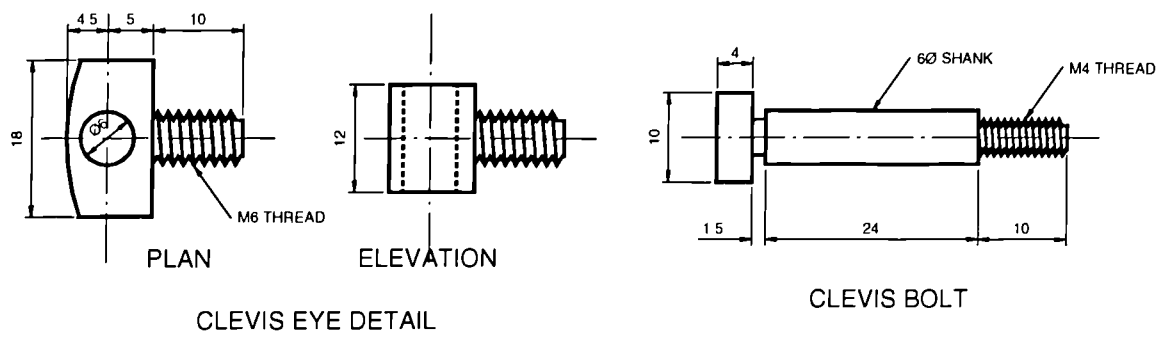


Figure 3.16 Detail of clevis eye and pin used to connect waling to hydraulic piston

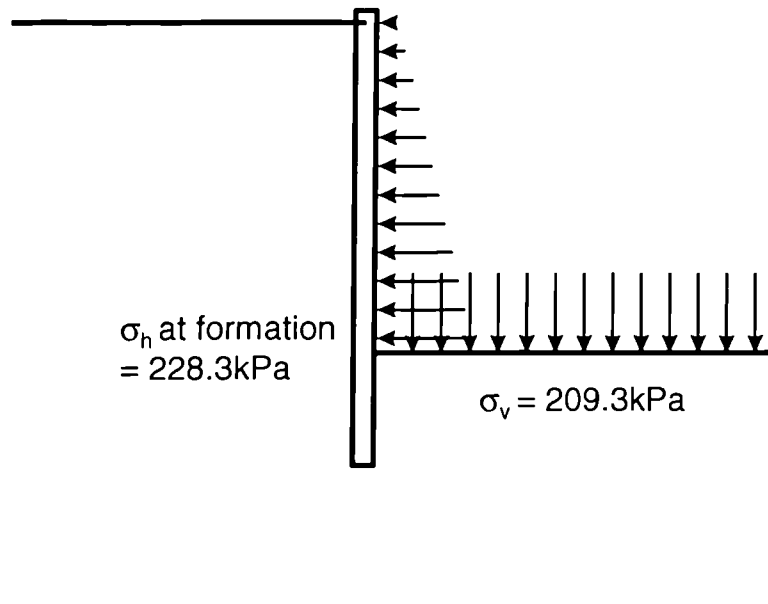


Figure 3.17 Imposed horizontal and vertical total stresses acting within excavation during consolidation on the centrifuge

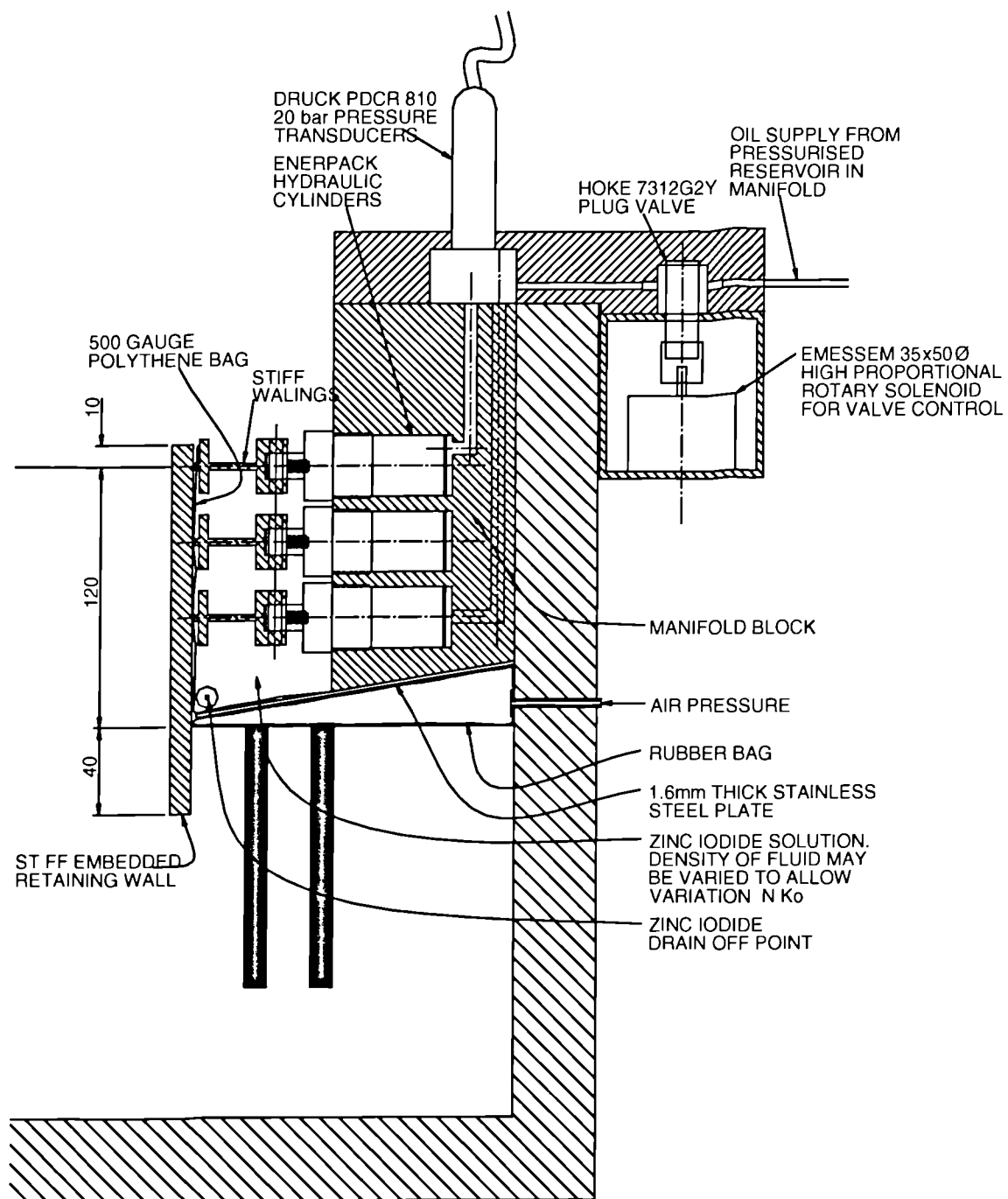


Figure 3.18 General arrangement of main apparatus following modification after test AM1.

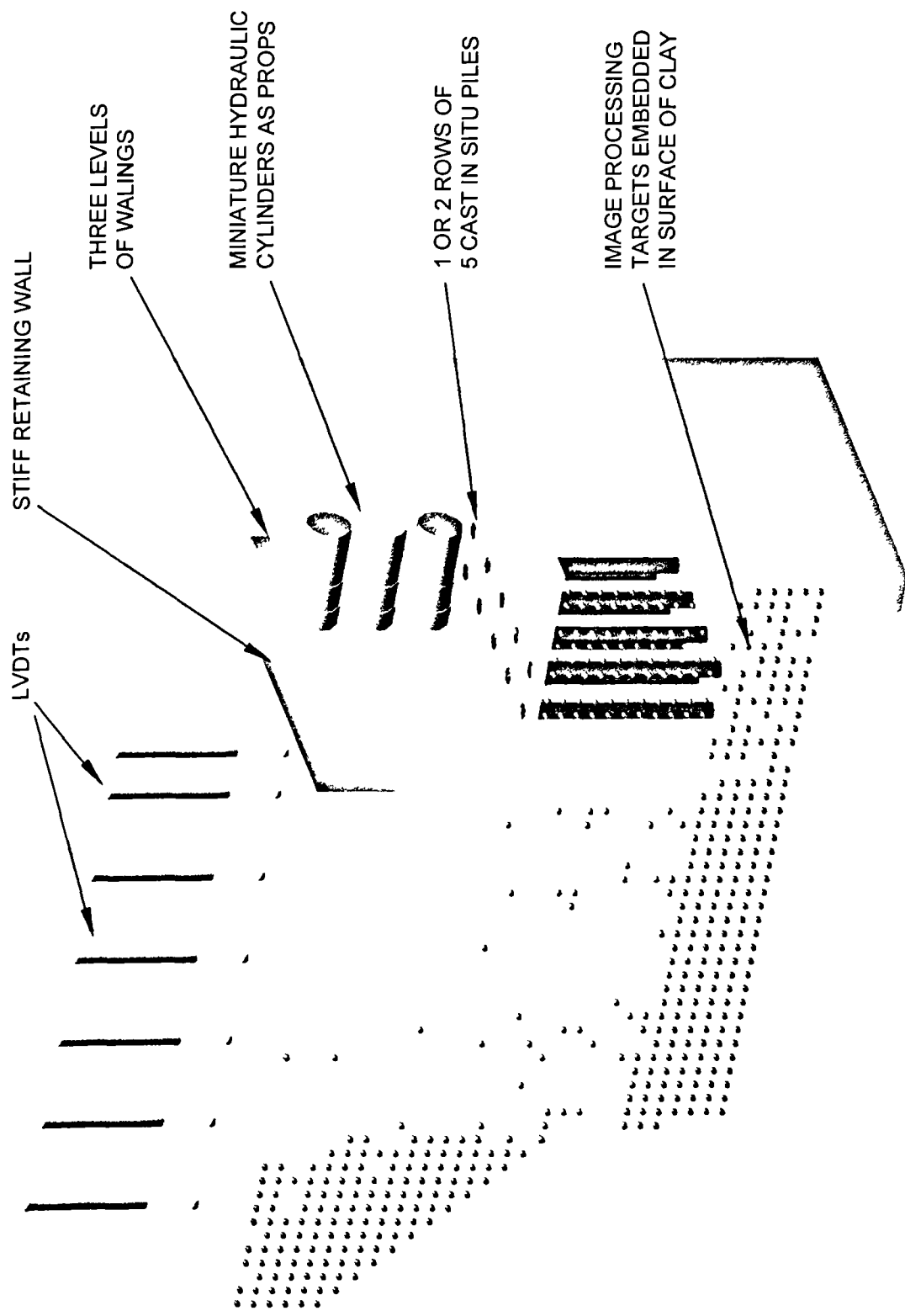


Figure 3.19 General view of the model showing key components of the apparatus

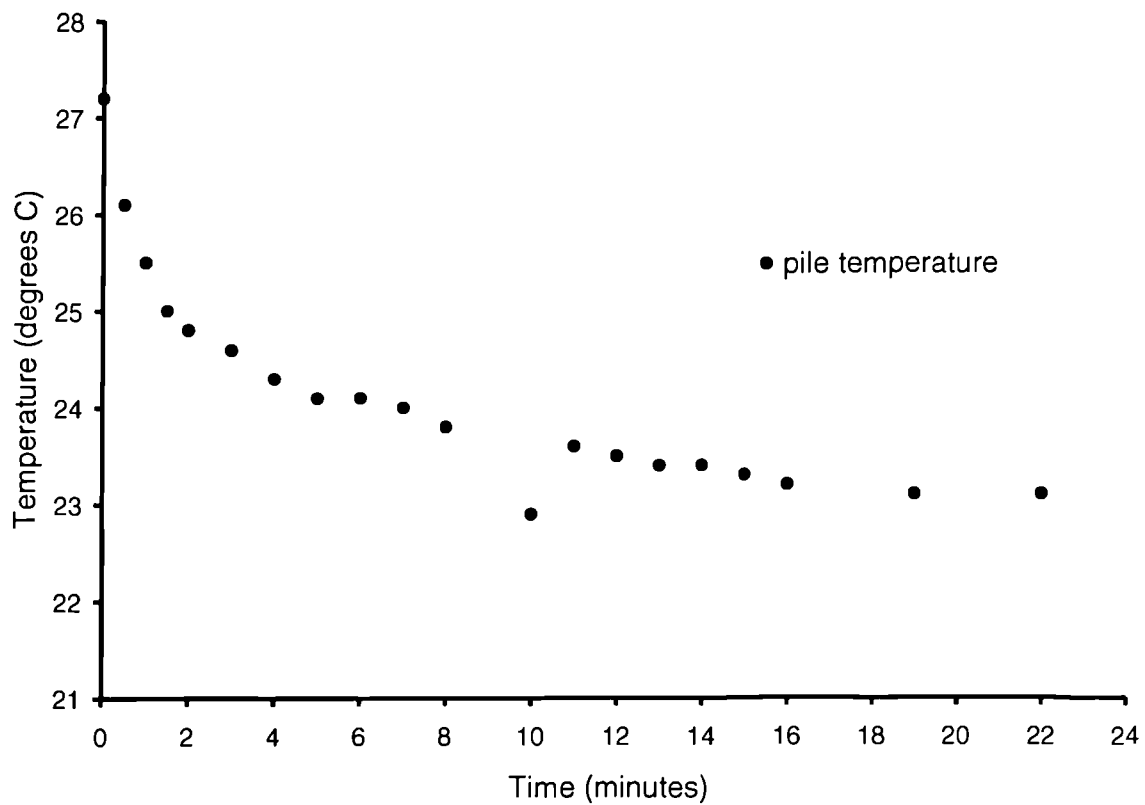


Figure 3.20 Curing exotherm measured during trial pile casting in kaolin using Sika Biresin G27 polyurethane 'fastcast' resin

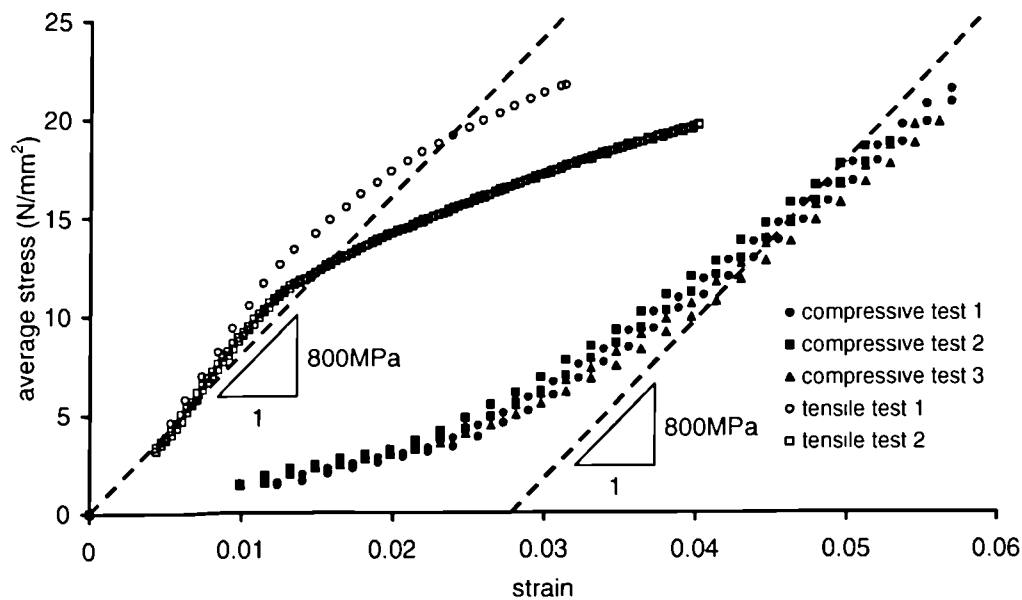


Figure 3.21 Comparison of tensile and compressive tests on piles used in test AM13 and made from Sika Biresin G27 mixed 50:50 w/w with aluminium trihydrate (ON) filler. Samples for tensile tests were 49mm long x 8mm  $\phi$  and samples for compression tests were 10mm high x 11.8mm  $\phi$ .

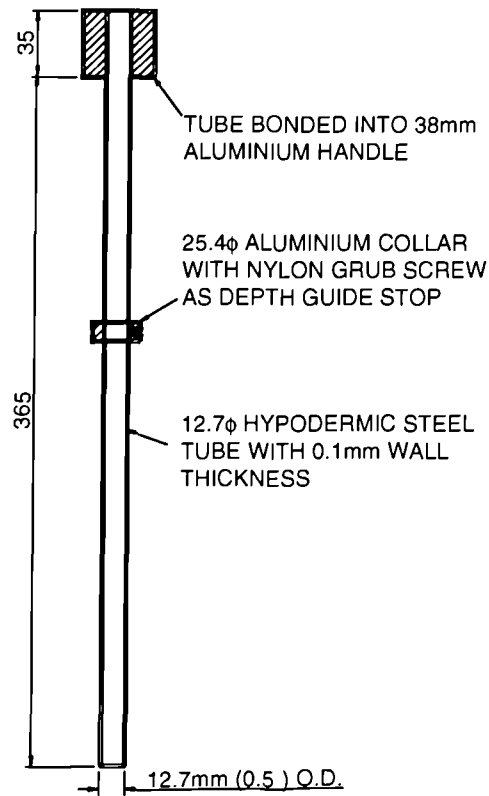


Figure 3.22 Detail of tool used for forming model pile bores

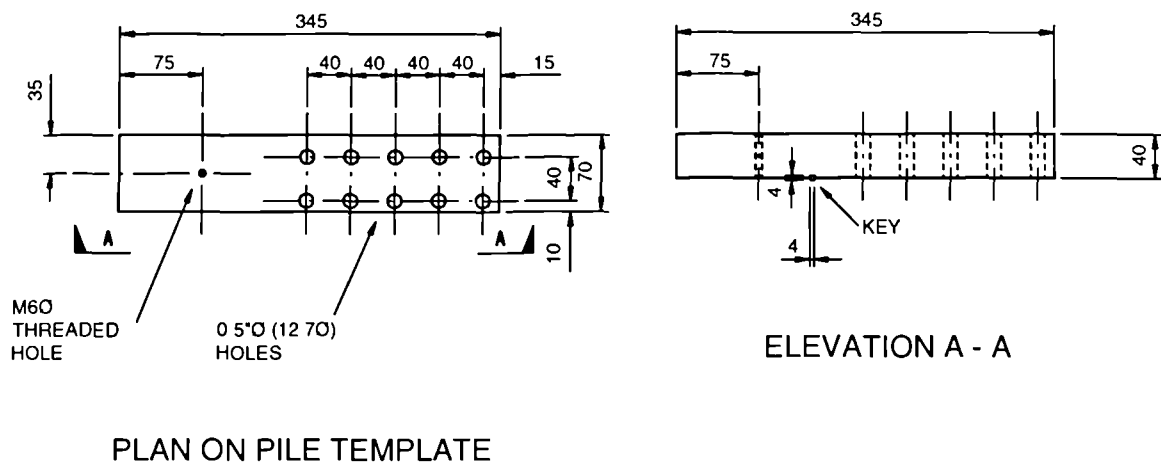


Figure 3.23 Detail of template used to position and bore piles

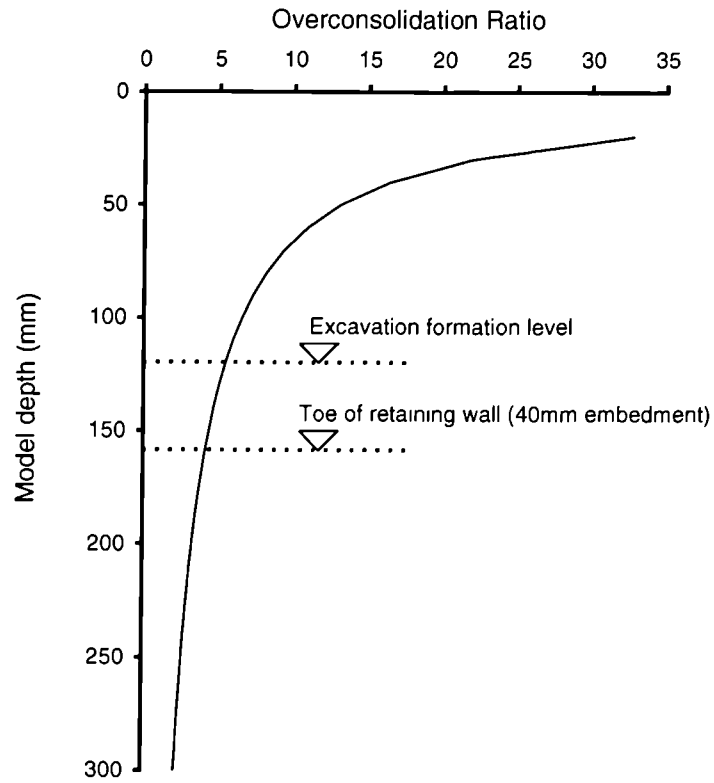


Figure 3.24 Variation of overconsolidation ratio with depth in model

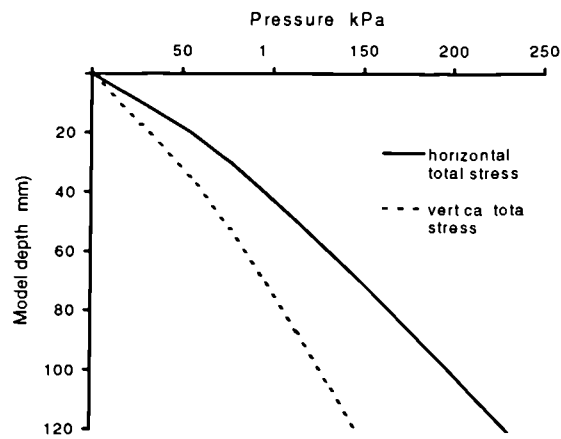


Figure 3.25 Theoretical vertical and horizontal total stress distribution over depth of excavation

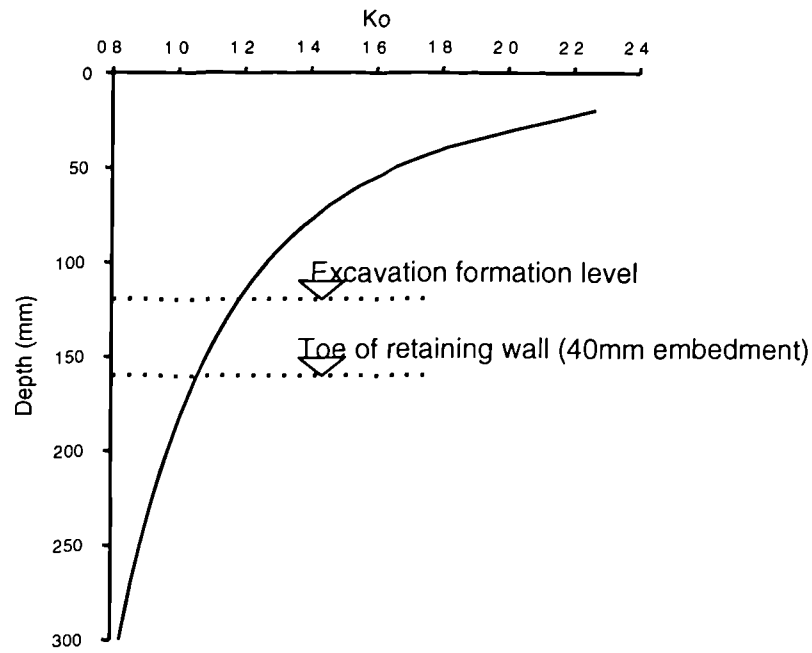


Figure 3.26 Variation of  $K_0$  with depth over depth of model

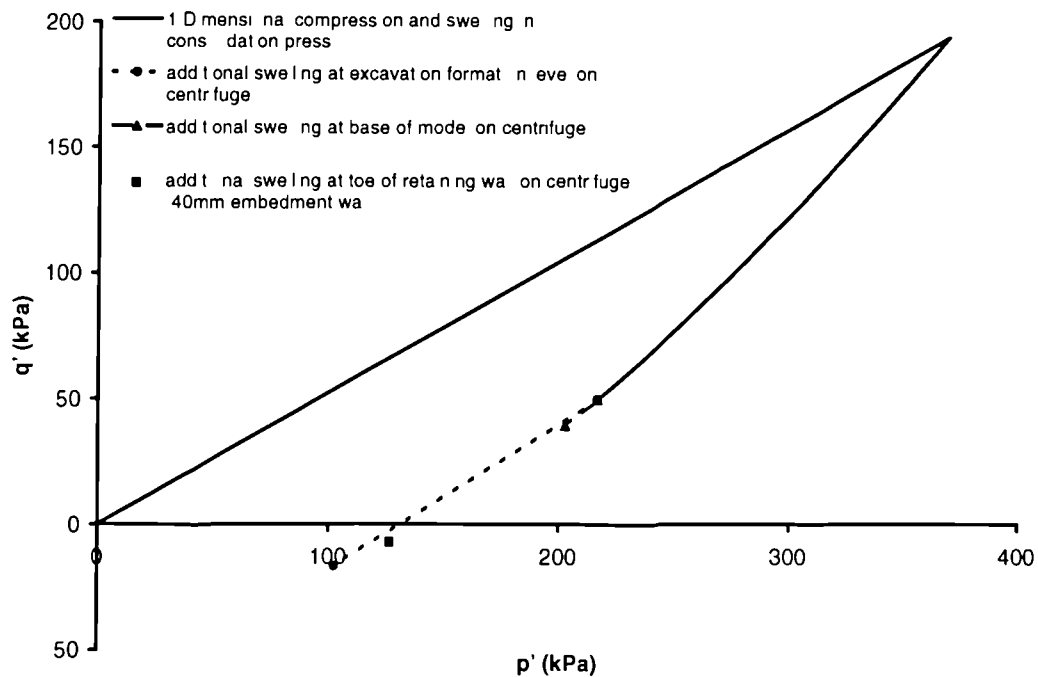


Figure 3.27 Stress history of a typical model following one dimensional compression and swelling in consolidation press and additional swelling during consolidation on the centrifuge prior to the simulated excavation stage of test





Figure 3.28 Consolidation press used for sample preparation prior to model making

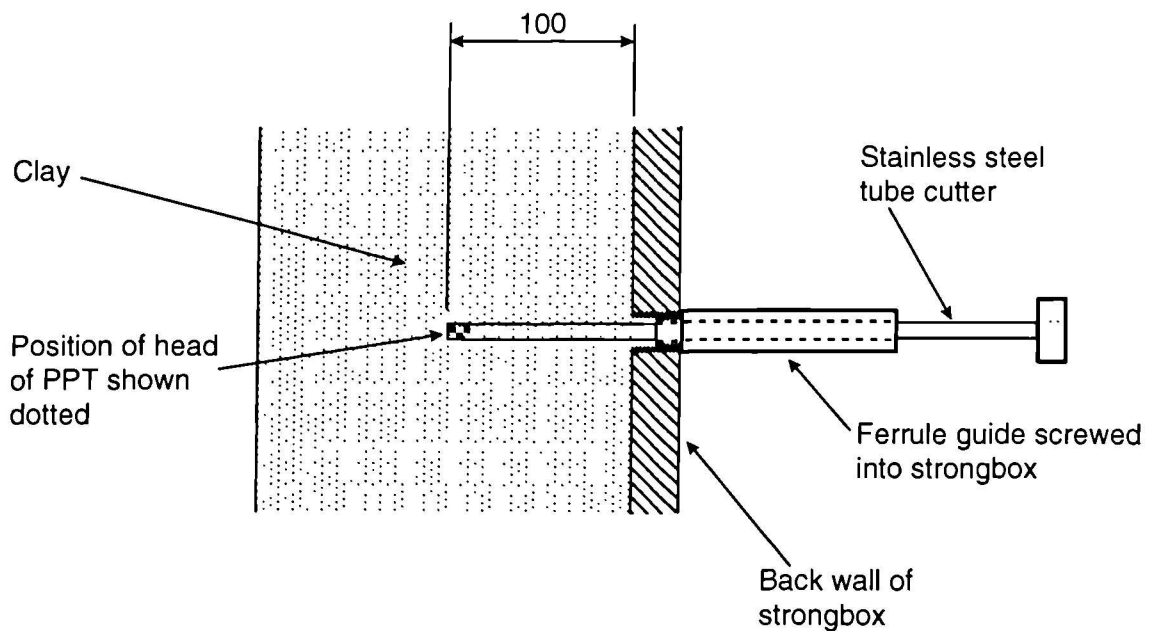


Figure 3.29 Method of ensuring correct positioning of pore pressure transducers within model



Figure 3.30 A typical soil sample immediately after removal from the consolidation press. Excess water pump grease that accumulated on the front surface was carefully scraped off to enable good contrast for image processing



Figure 3.31 Top surface of the sample was trimmed to the approximate level using a 50mm diameter brass tube cutter



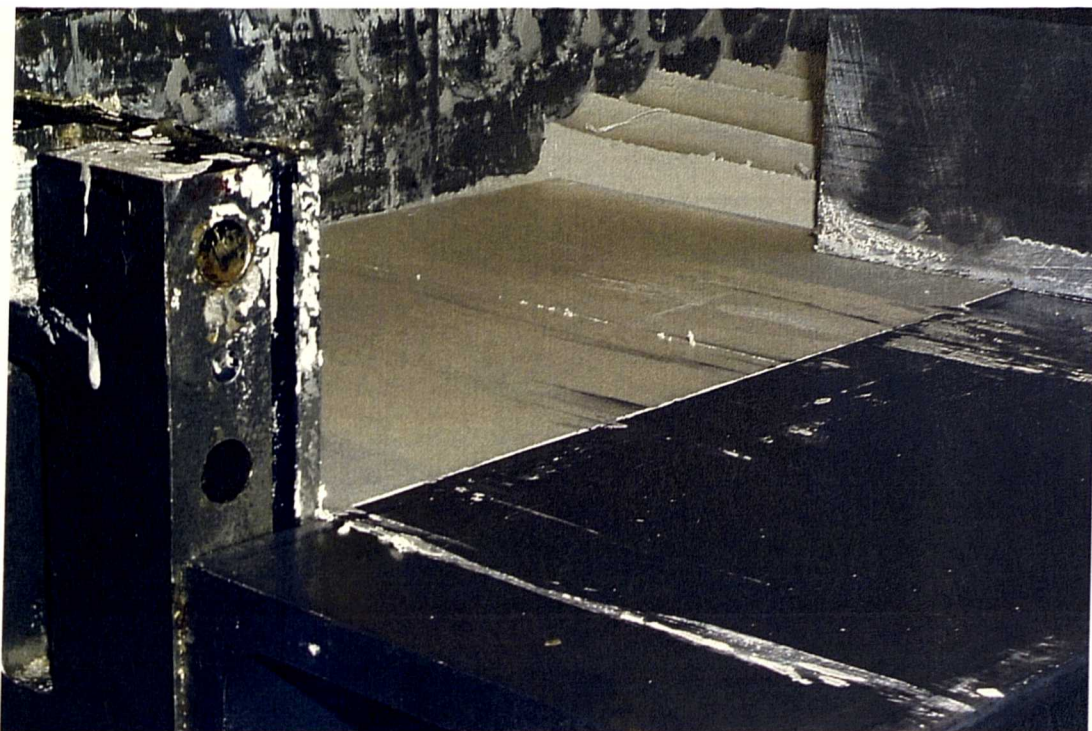


Figure 3.32 Final trimming to level was carried out using an extruded aluminium box section guided with a 150mm wide shelf angle bolted to the strongbox



Figure 3.33 Clay ramp behind position of retaining wall to prevent loss of liquid paraffin into the excavation during consolidation on the centrifuge





Figure 3.34 Jig used for forming excavation and trench for embedded wall

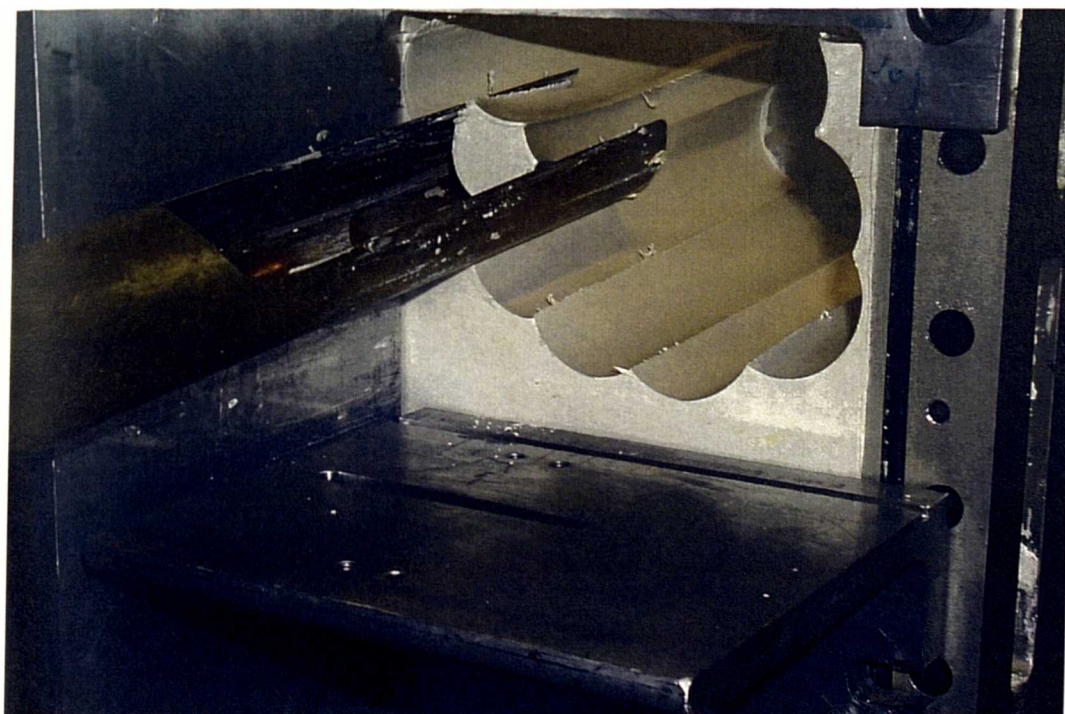


Figure 3.35 Initial removal of soil for excavation



Figure 3.36 Trimming of excavation using aluminium box section cutter

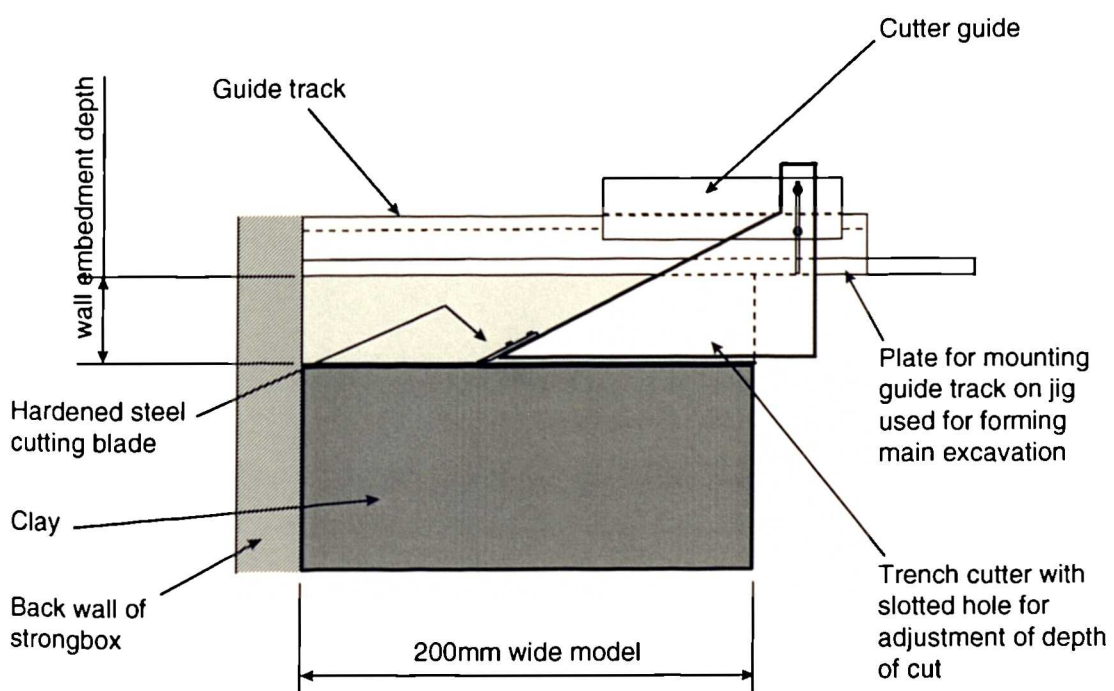


Figure 3.37 Method of cutting trench below excavation formation level for embedded wall



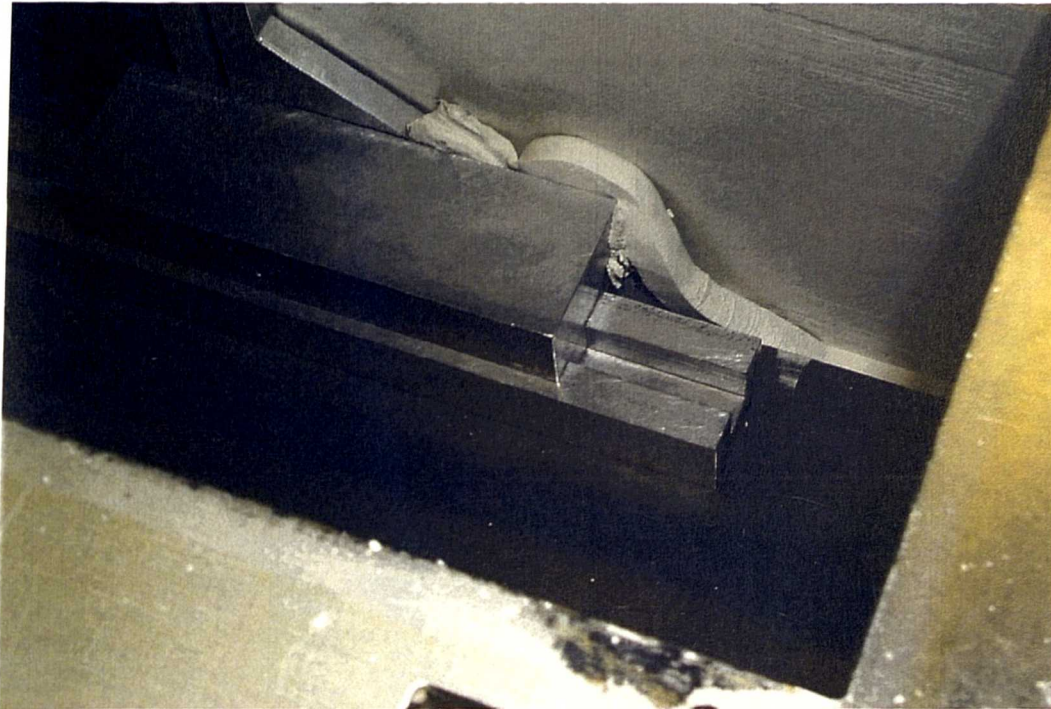


Figure 3.38 Track guided cutting tool in use. Approximately 5mm of clay was removed in each pass of the cutter

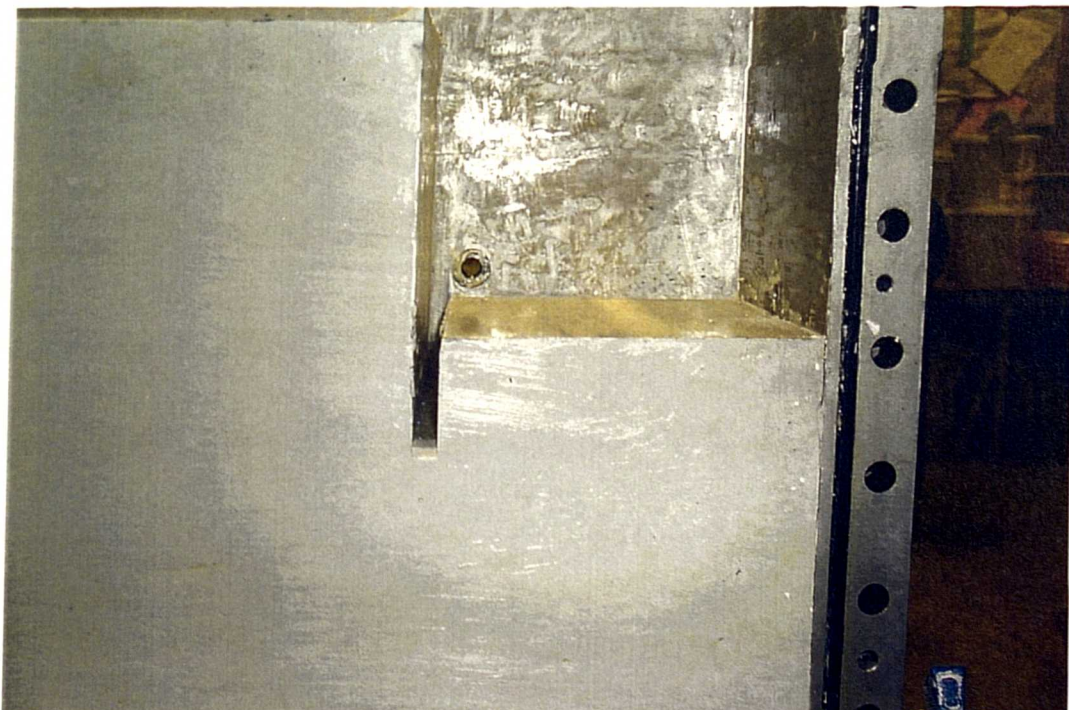


Figure 3.39 Completed excavation and trench

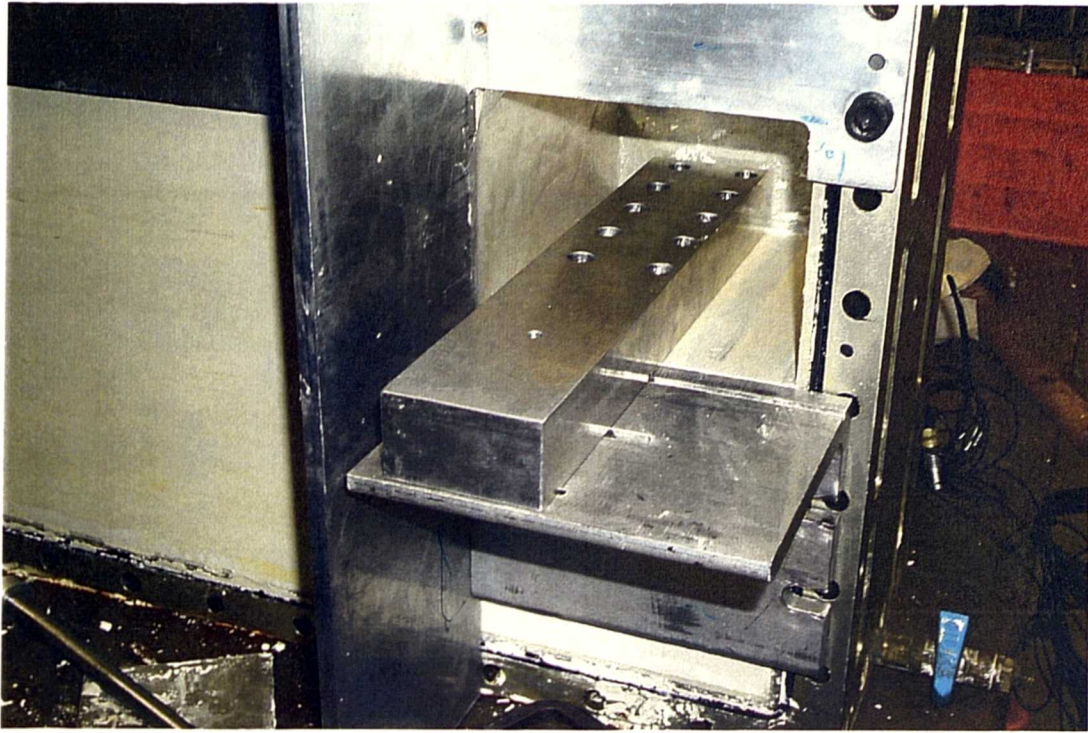


Figure 3.40 Pile cutting template bolted into position on excavation jig

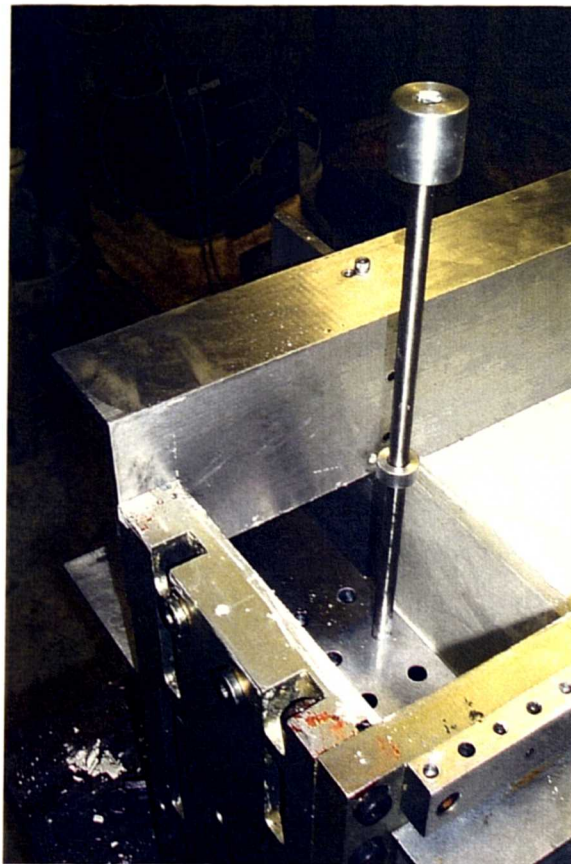


Figure 3.41 Forming pile bores using stainless steel tube cutter



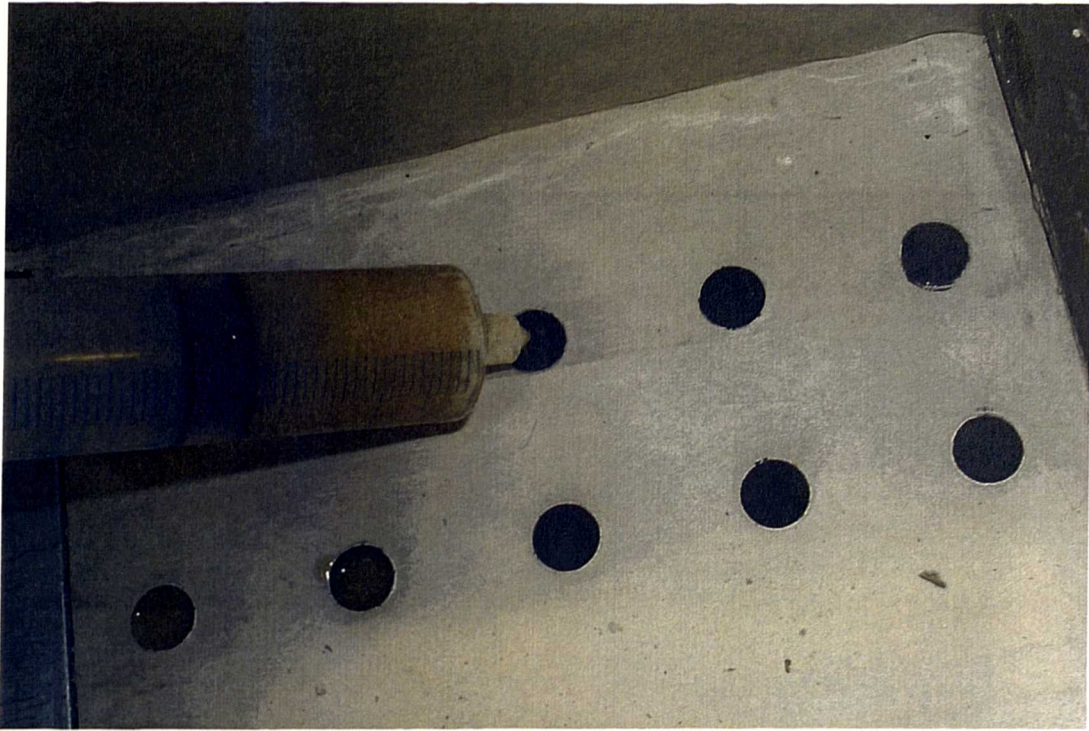


Figure 3.42 Dispensing polyurethane 'fastcast' resin into pile bores



Figure 3.43 Installing prop module apparatus into the strongbox



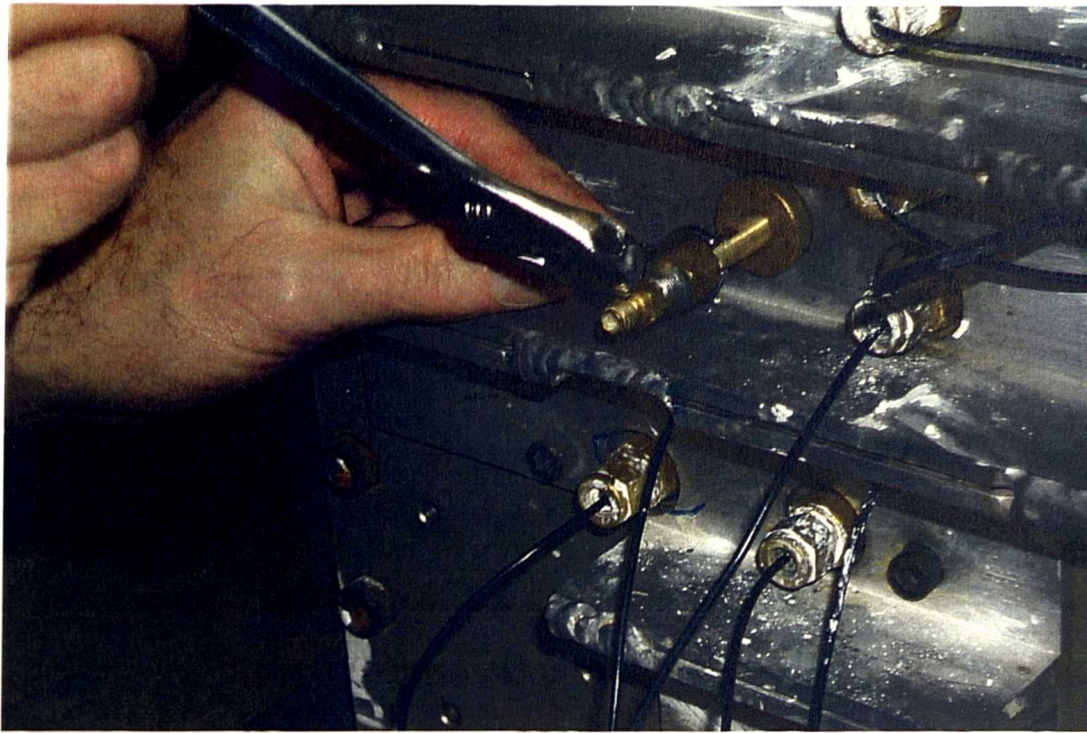


Figure 3.44 Tightening the drainage fitting into the backwall of the strongbox. Great care was necessary to avoid damage to the polyethylene bag

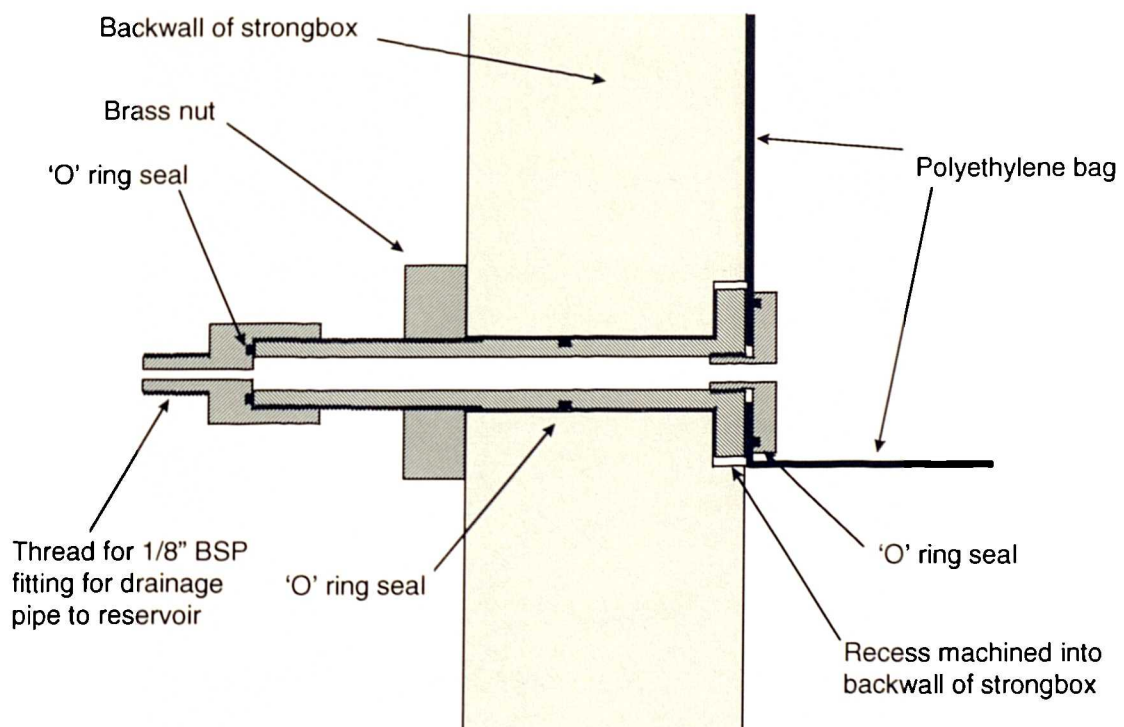


Figure 3.45 Detail of drainage fitting for polyethylene bag at base of excavation



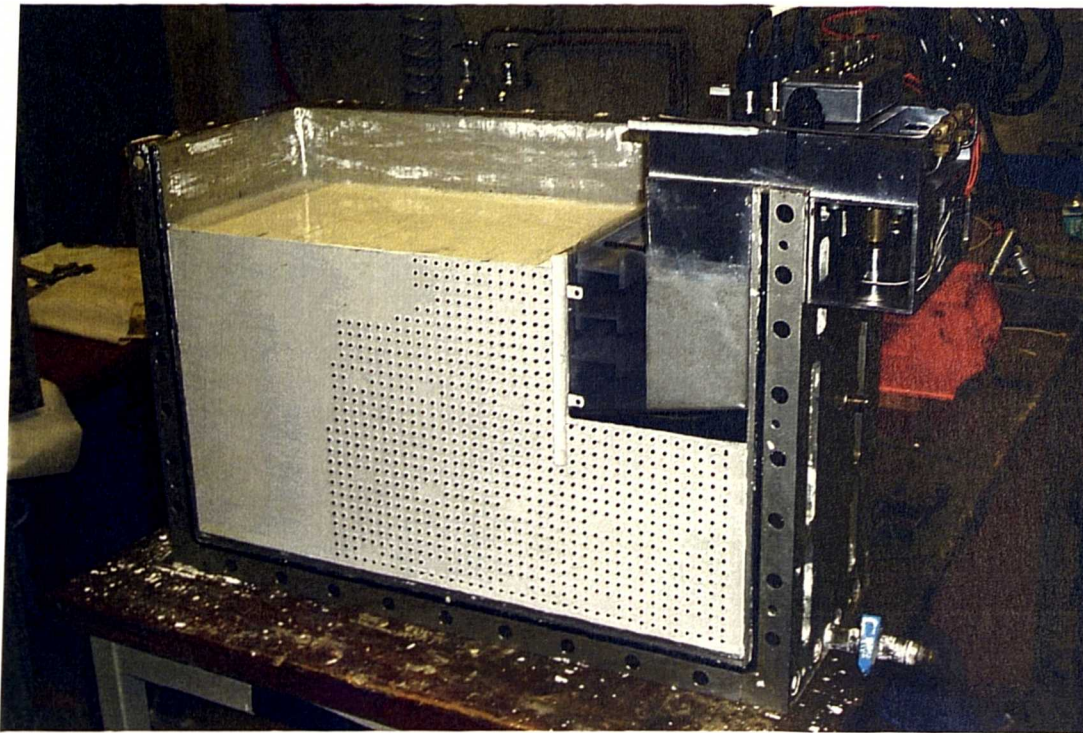


Figure 3.46 A completed model with image processing targets for single camera image grabbing

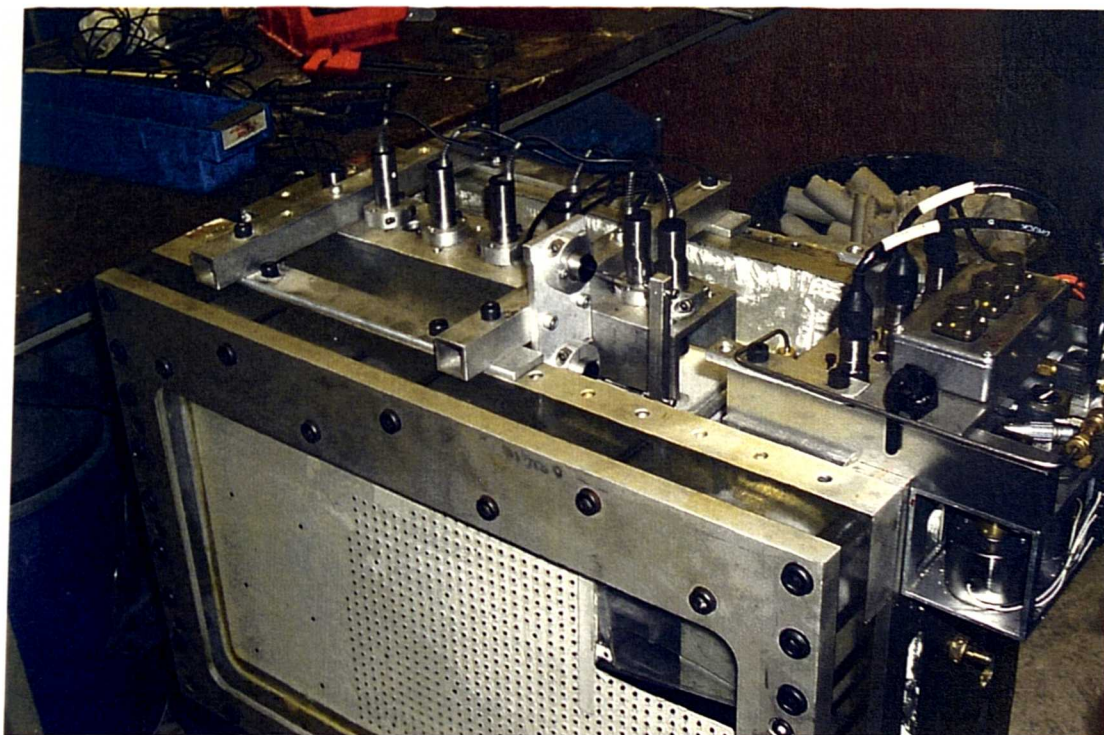


Figure 3.47 LVDTs for measurement of retained surface displacement and wall rotation

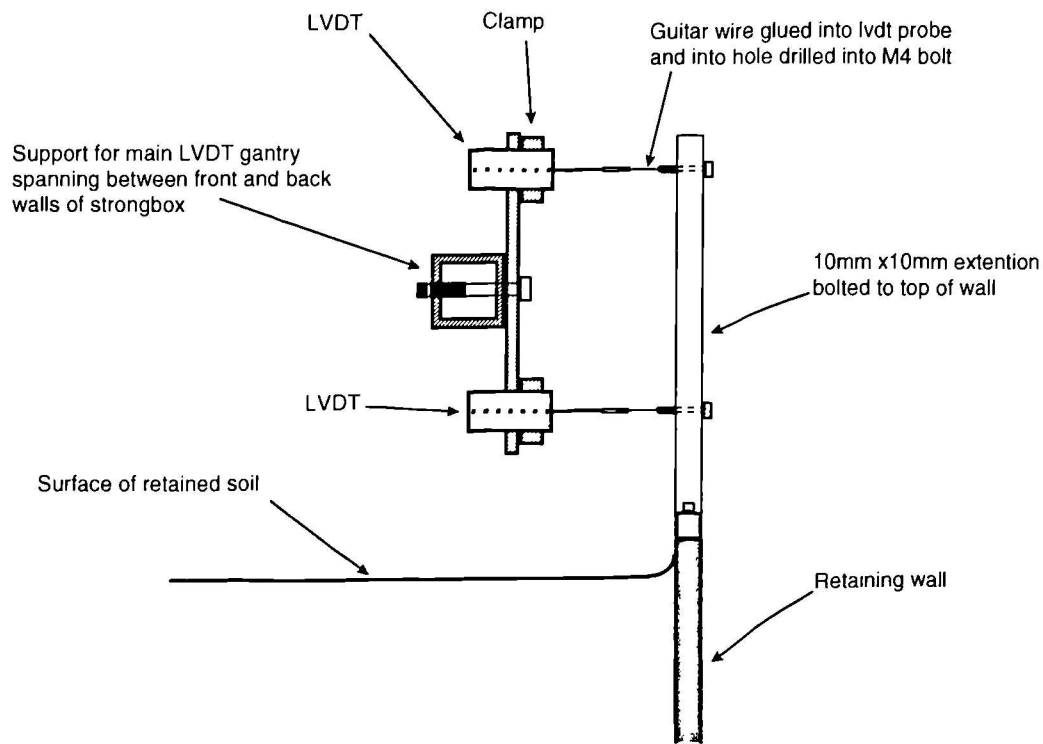


Figure 3.48 Method of positioning LVDTs to enable wall measurement of wall rotation

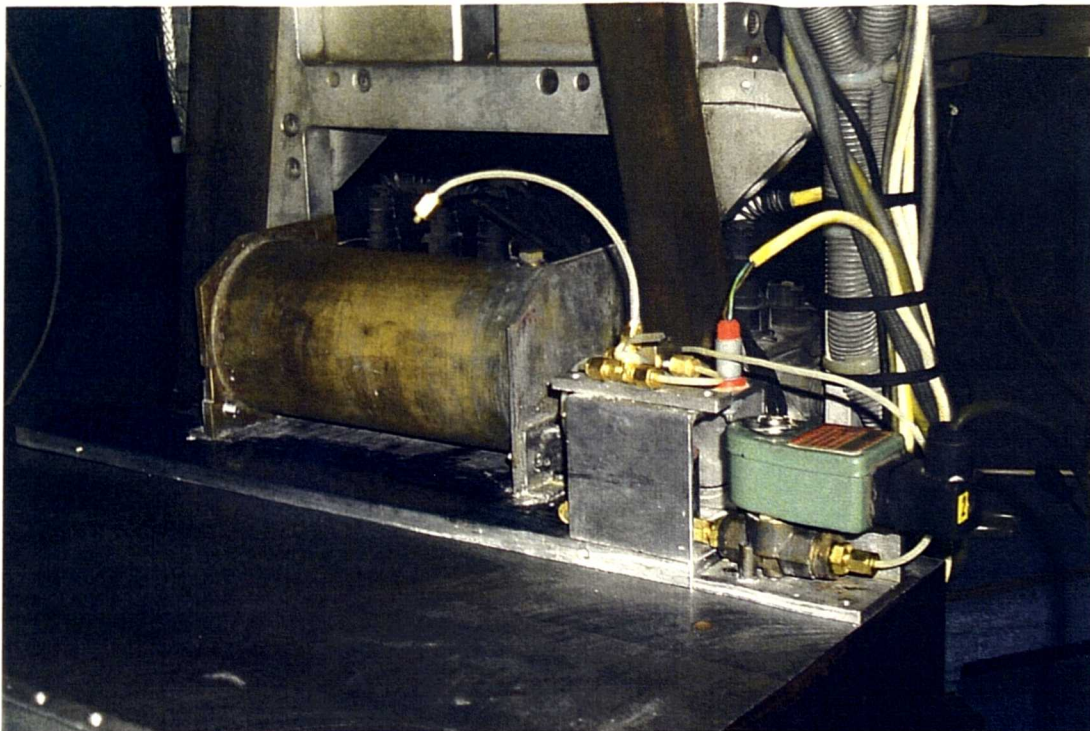


Figure 3.49 Drainage reservoir for storage of zinc iodide solution together with two valves, connected in parallel, to control drainage. Unreliability led to the use of two valves in an attempt to increase the likelihood of successful testing



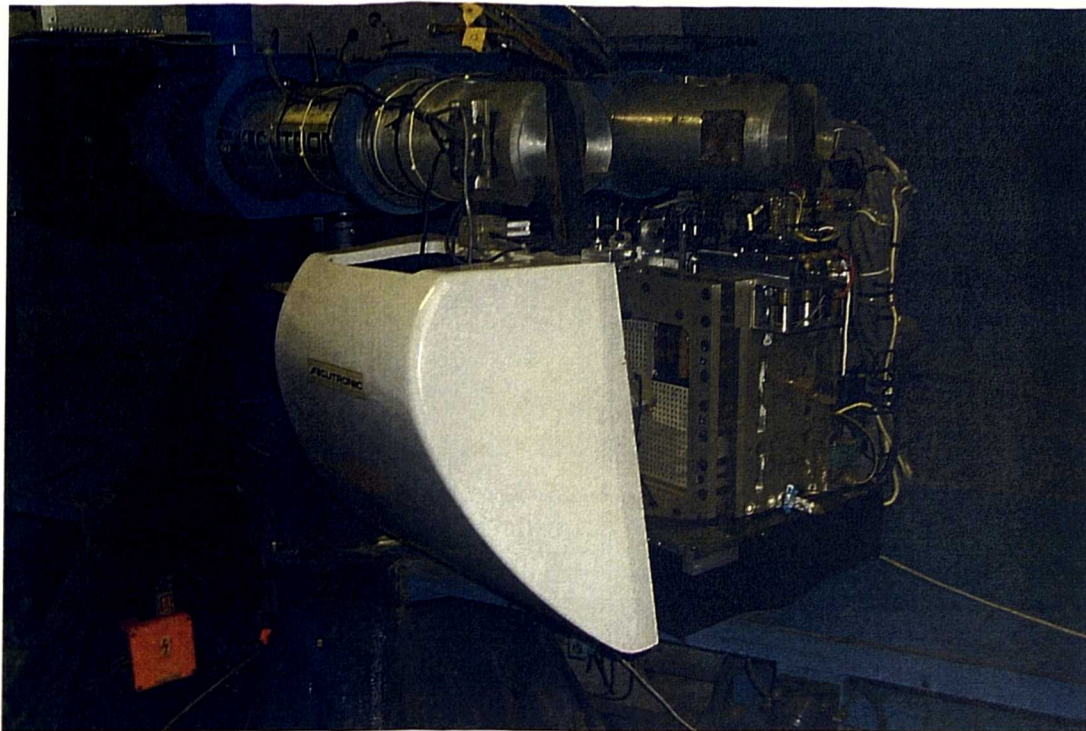


Figure 3.50 Model on centrifuge swing and ready for spin up

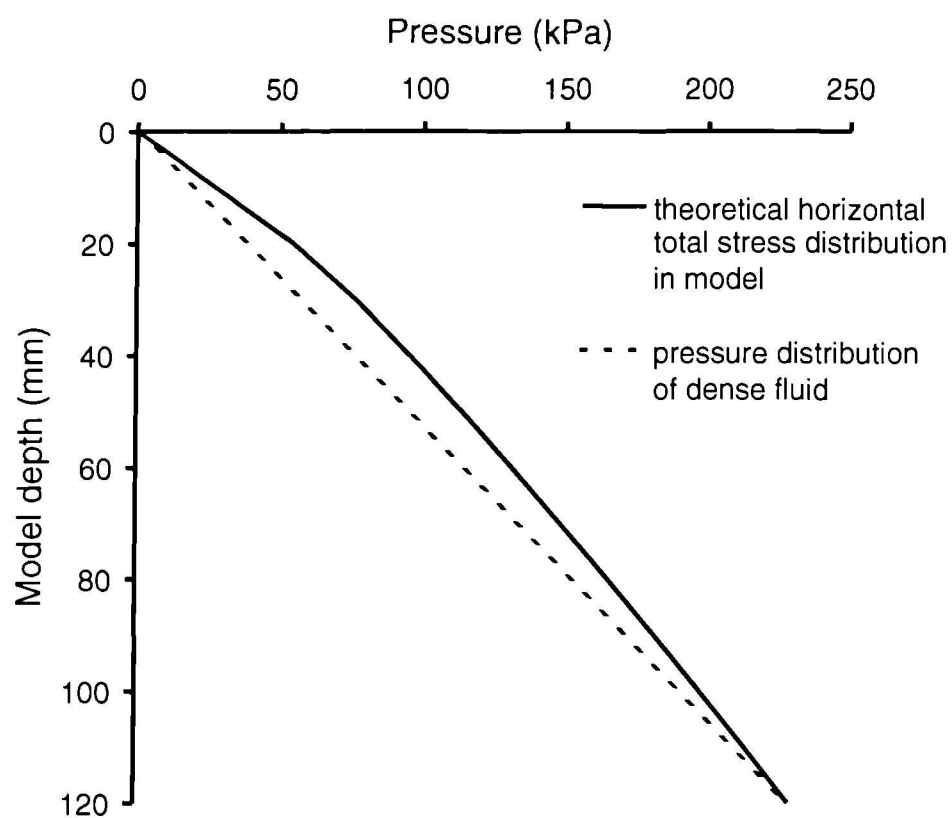


Figure 3.51 Non linear distribution of total horizontal stress over depth of excavation and comparison between theoretical and imposed total horizontal stress distribution over depth of excavation

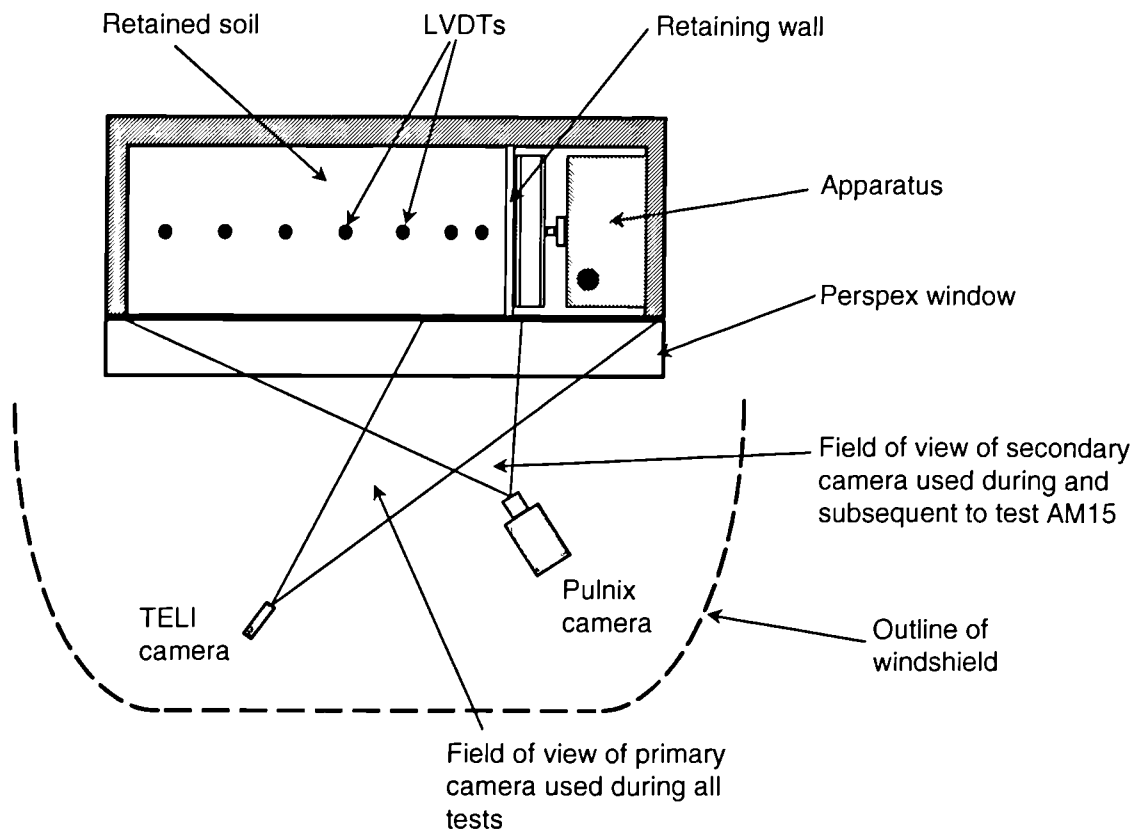


Figure 3.52 Positioning of cameras used for image processing.

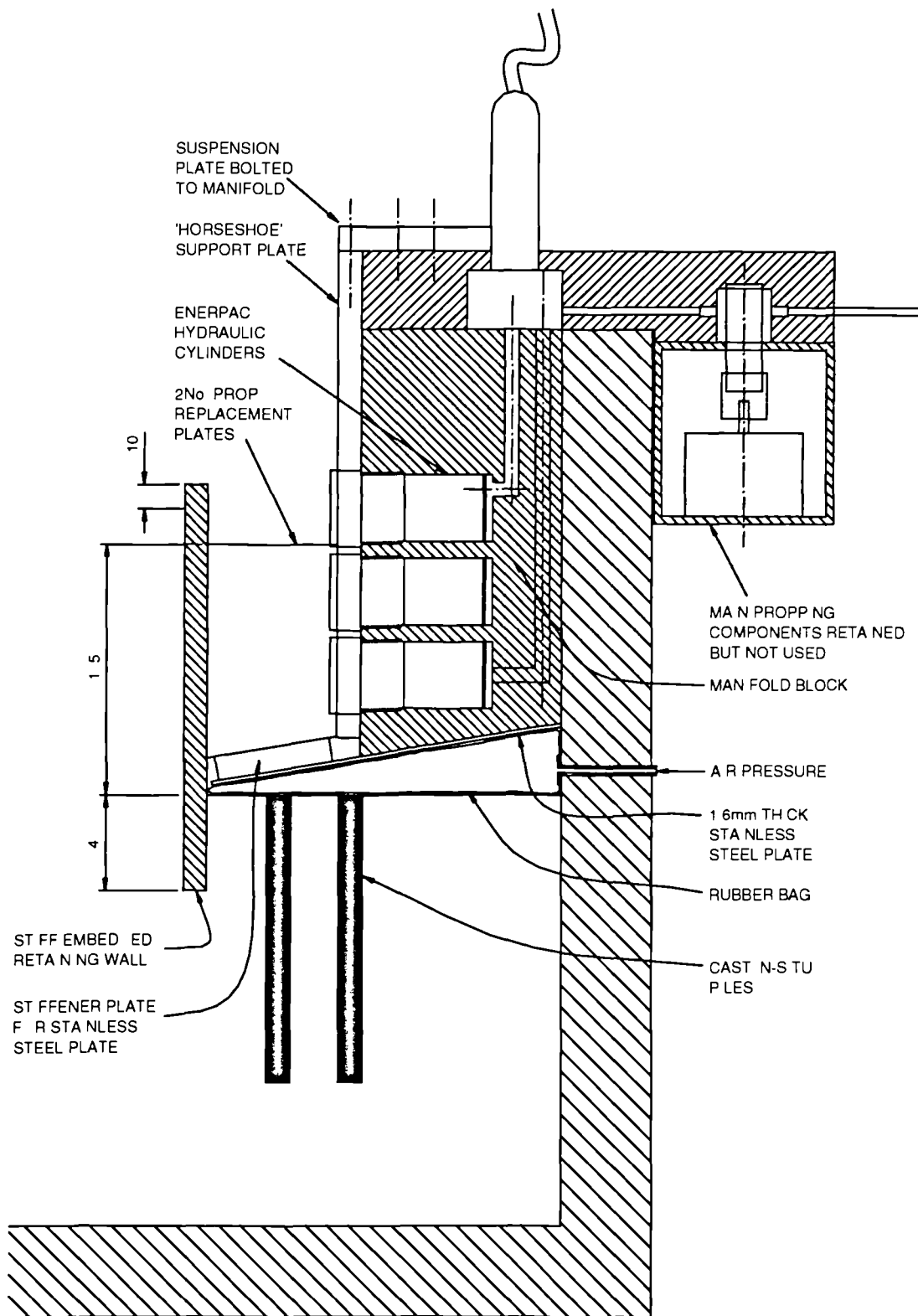


Figure 4.1 General details of the modified apparatus used to ensure negligible horizontal wall movement in test AM10, AM11 and AM12.

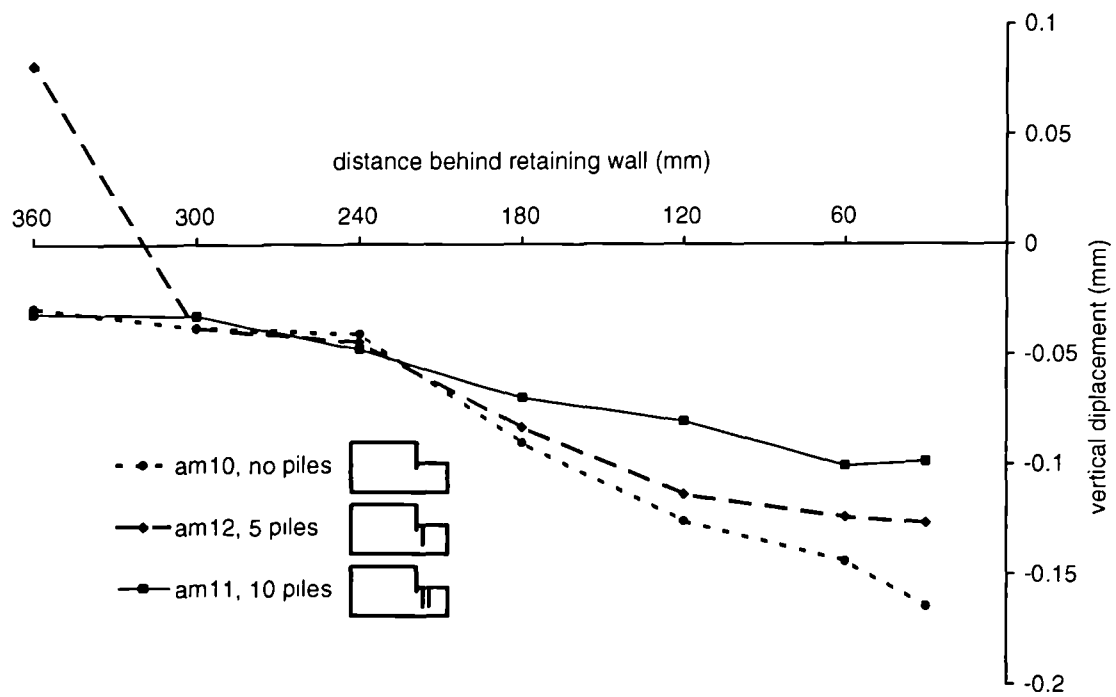


Figure 4.2 Settlement profile behind wall on completion of excavation during tests using 'fixed' wall

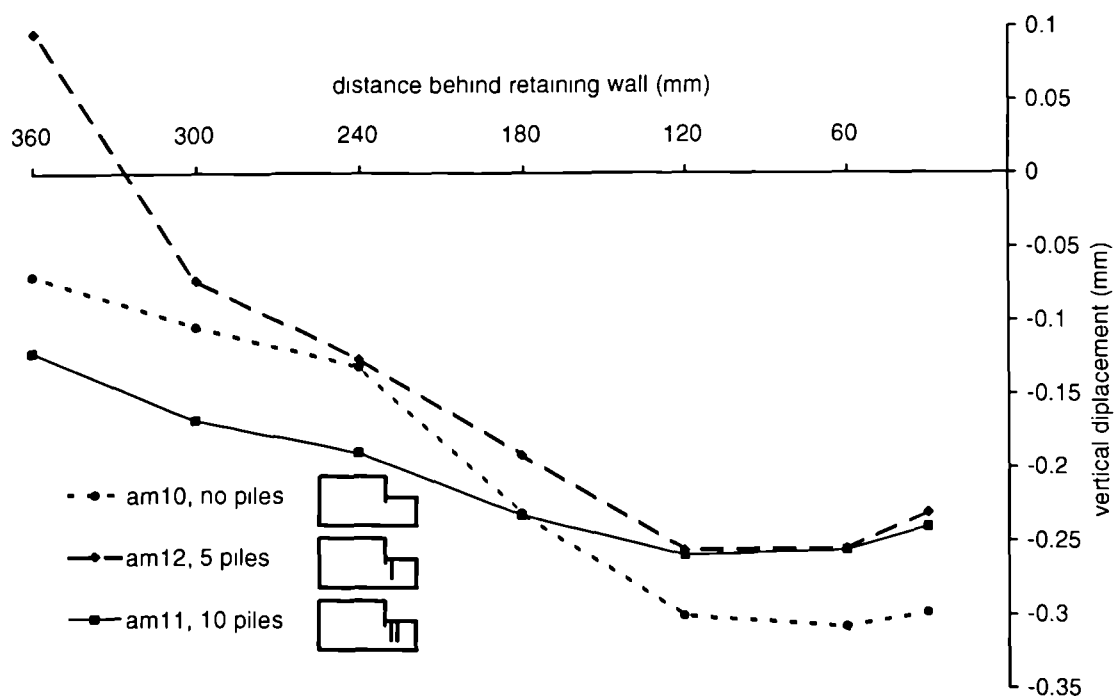


Figure 4.3 Settlement profile behind wall 60 minutes after completion of excavation during tests using 'fixed' wall

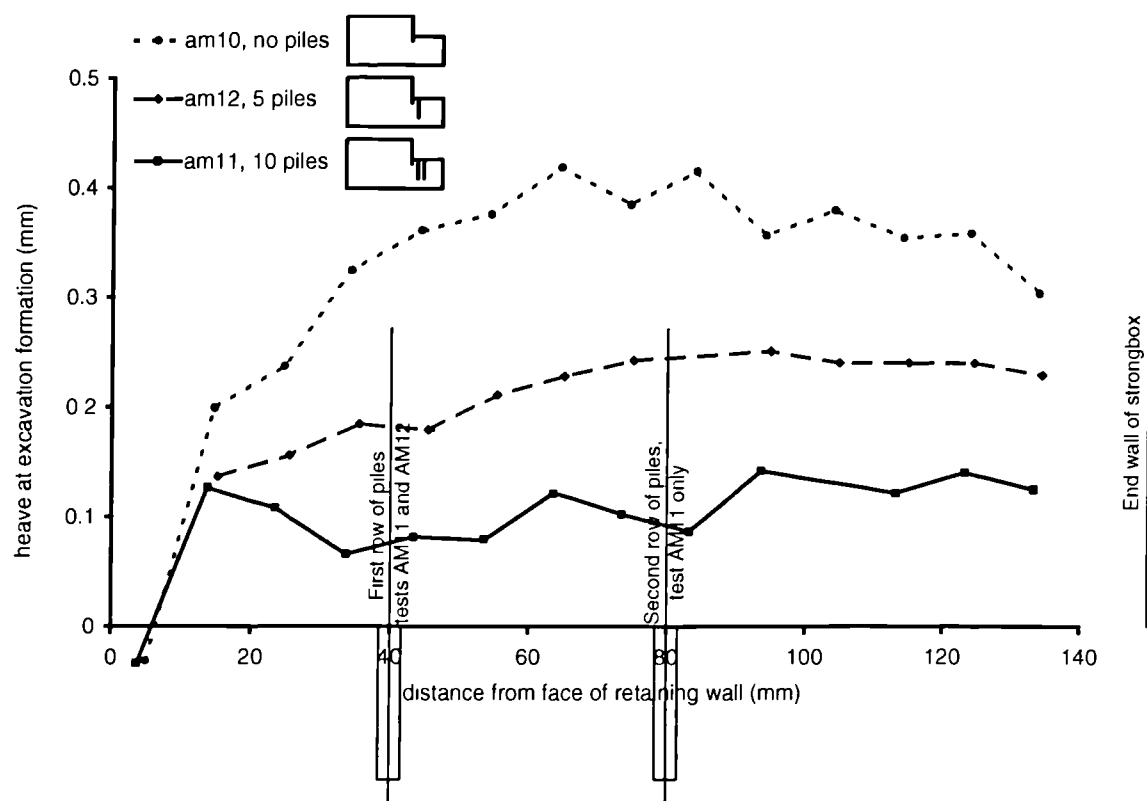


Figure 4.4 Formation displacements, measured using image processing, at end of excavation during tests using 'fixed wall'

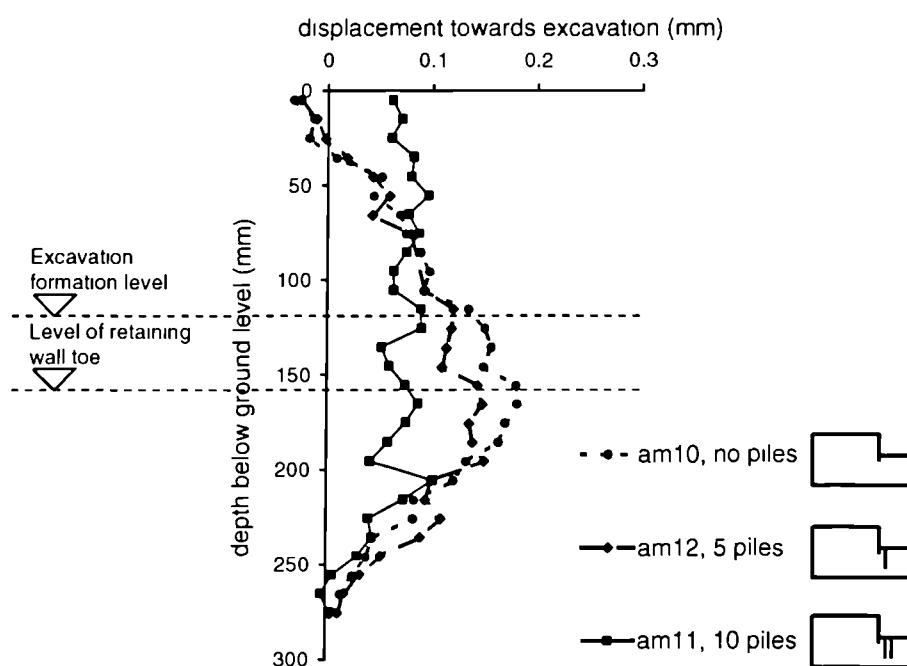


Figure 4.5 Horizontal displacements, measured immediately behind and below the retaining wall using image processing, at end of excavation during tests using 'fixed wall'



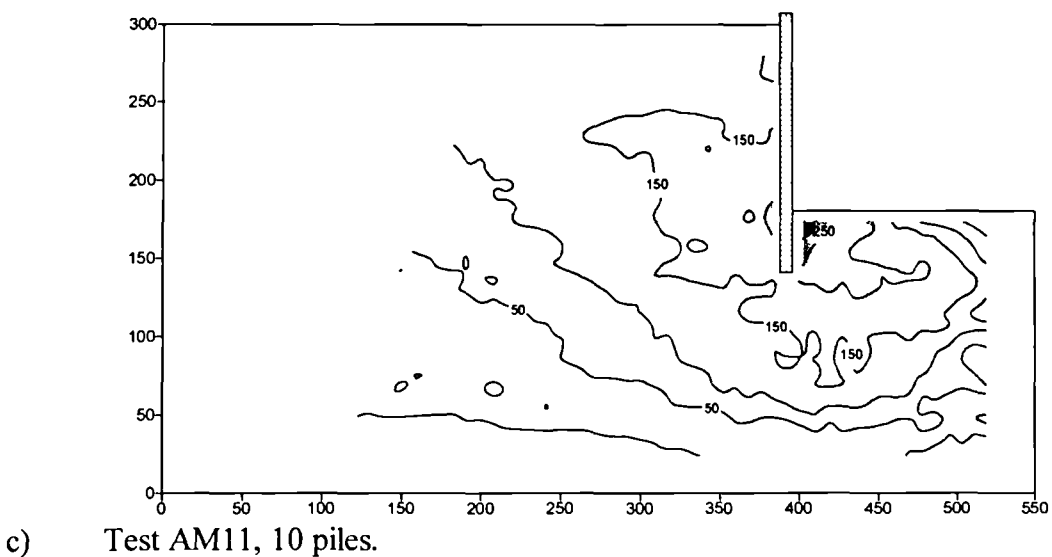
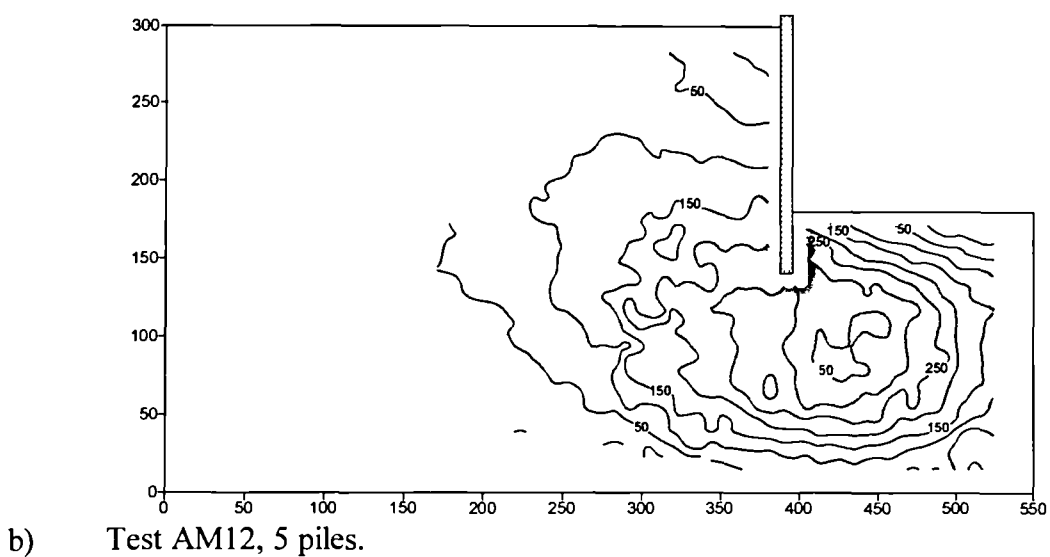
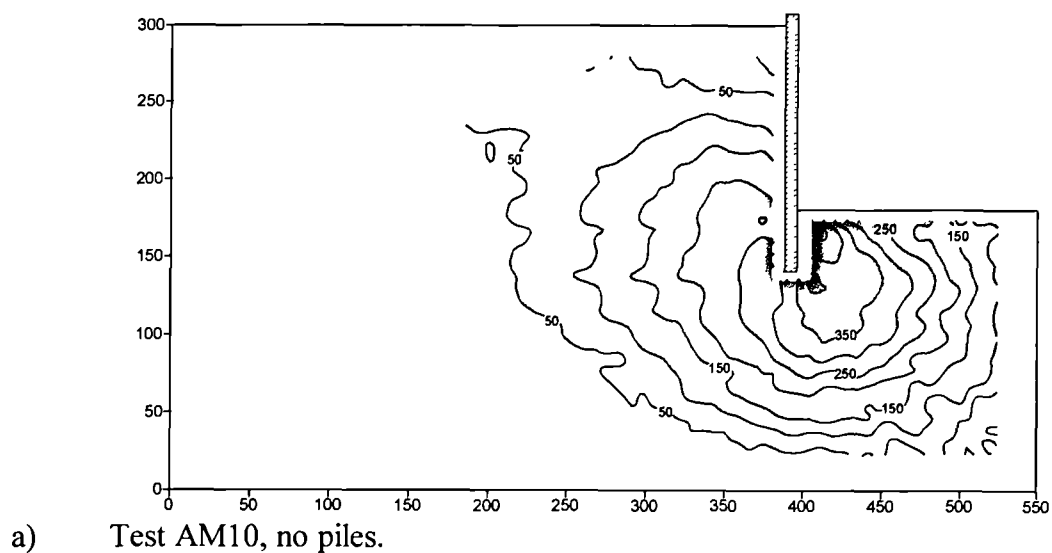


Figure 4.6 Contours of horizontal movement, 30 minutes after completion of simulated excavation. (Displacements in  $\mu\text{m}$ )

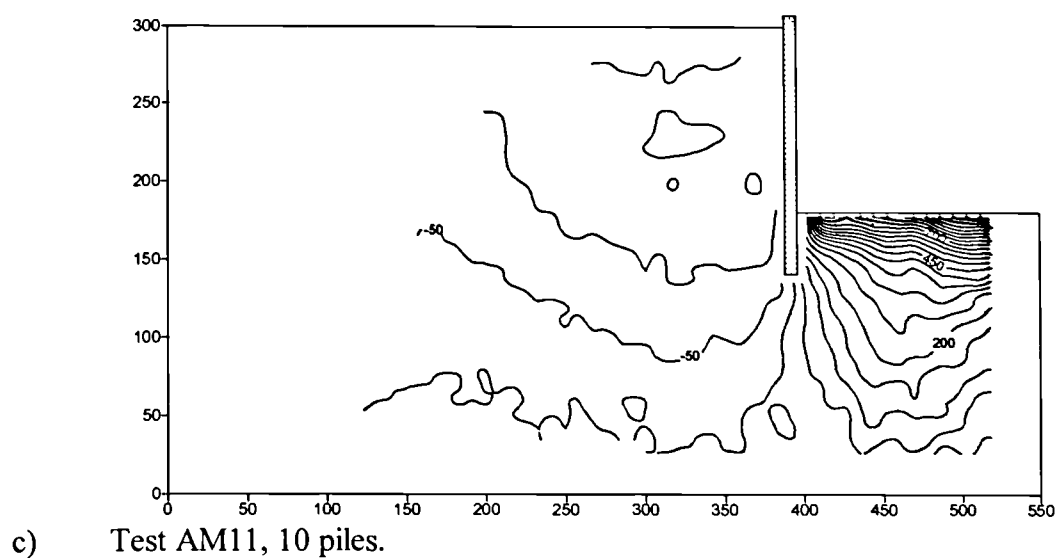
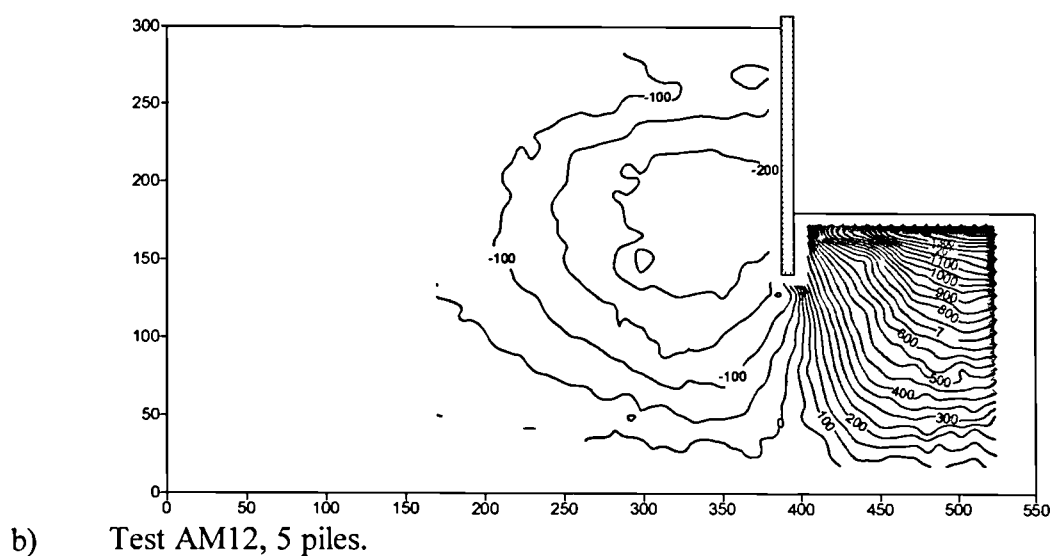
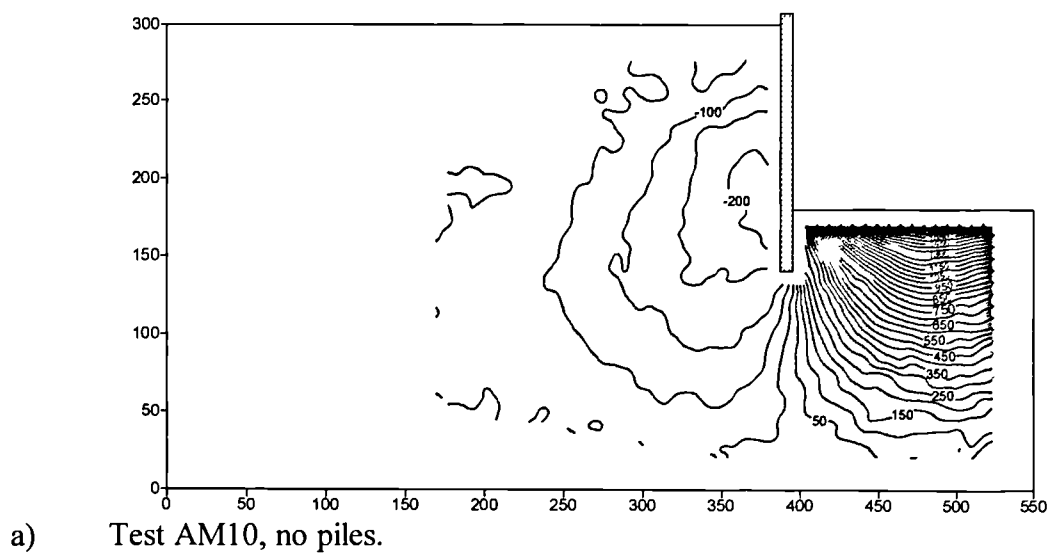


Figure 4.7 Contours of vertical movement, 30 minutes after completion of simulated excavation. (Displacements in  $\mu\text{m}$ )

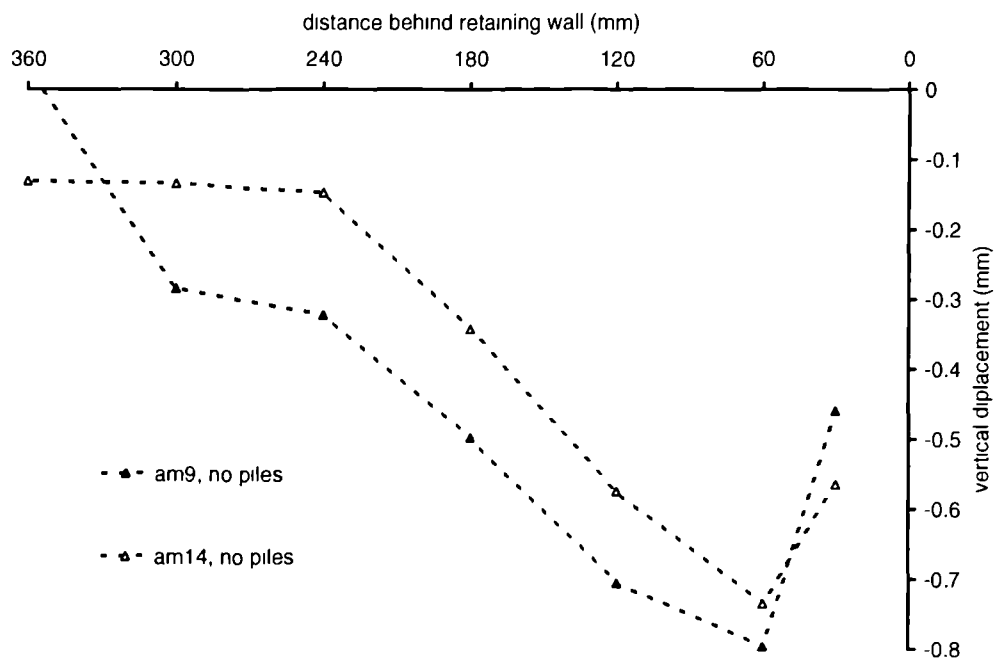


Figure 4.8 Settlement behind retaining wall at completion of simulated excavation for tests AM9 and AM14

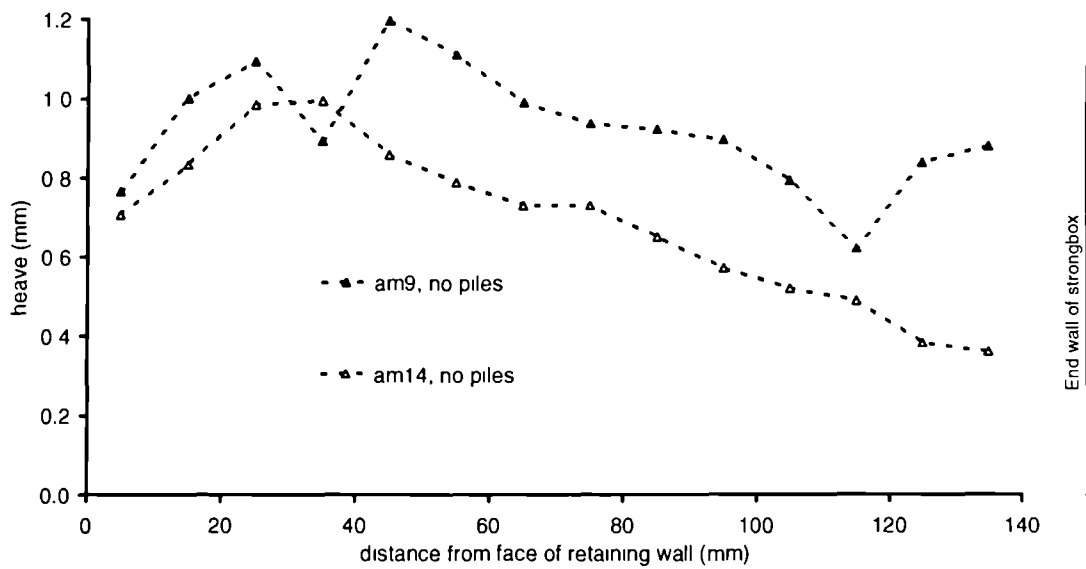


Figure 4.9 Formation displacements measured using image processing at end of simulated excavation for tests AM9 and AM14

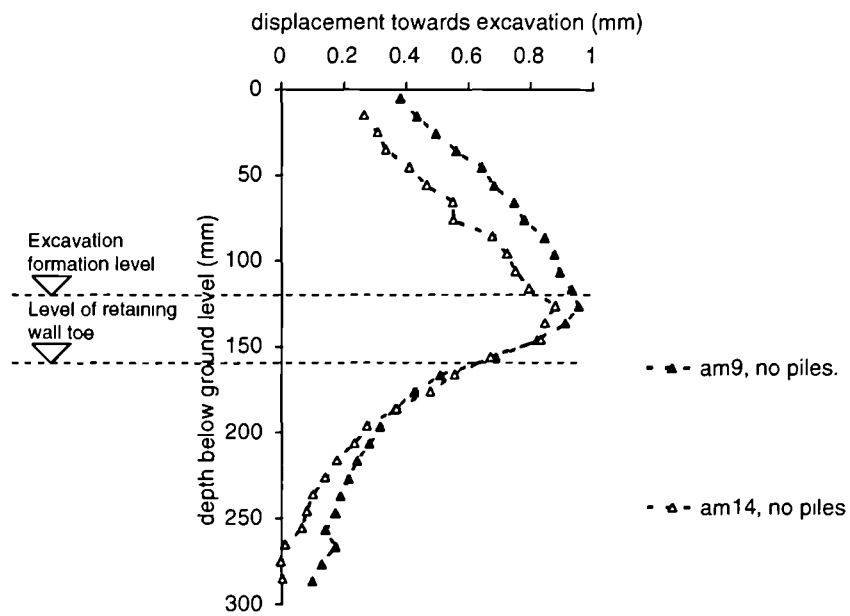
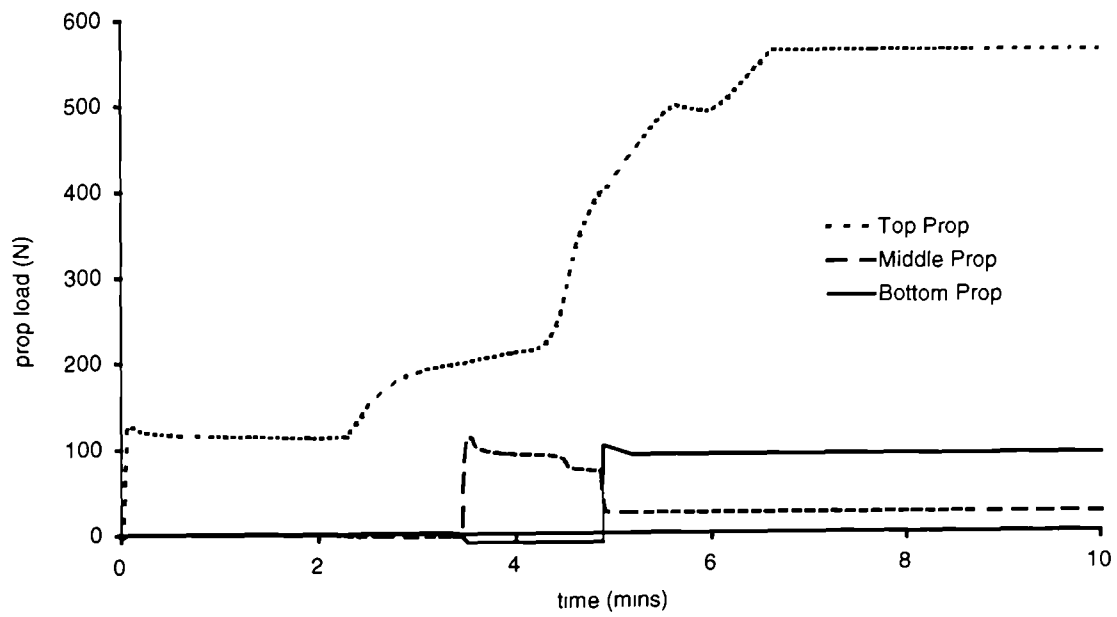
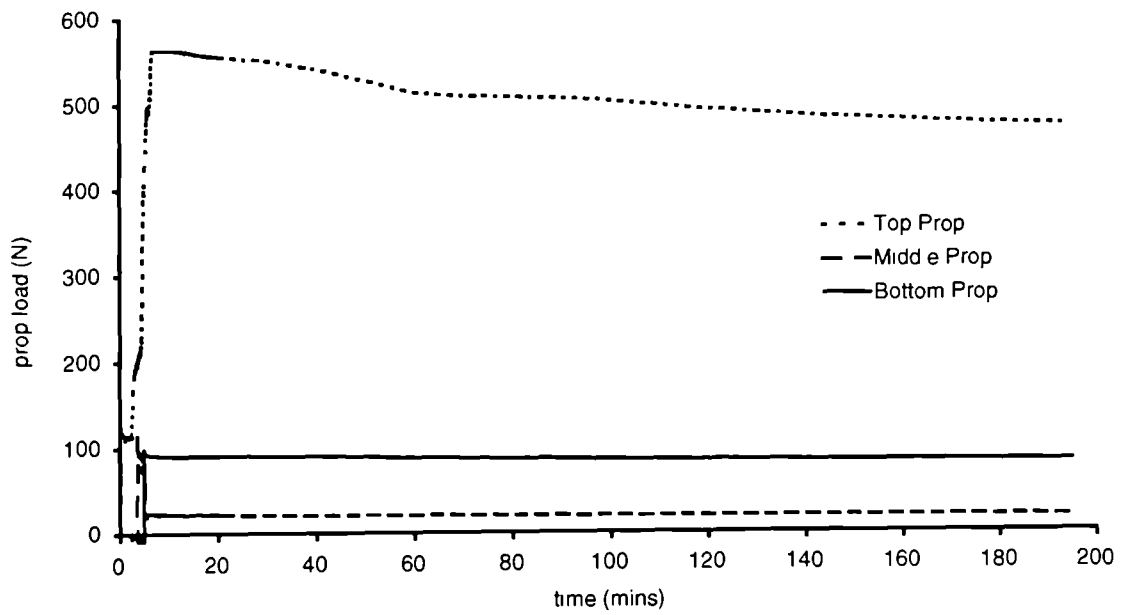


Figure 4.10 Horizontal displacements, measured immediately behind and below the retaining wall using image processing, at end of simulated excavation for tests AM9 and AM14



a) Prop loads measured during simulated excavation stage.



b) Prop loads measured during and subsequent to simulated excavation.

Figure 4.11 Prop loads measured during and after simulated excavation stage of test AM9

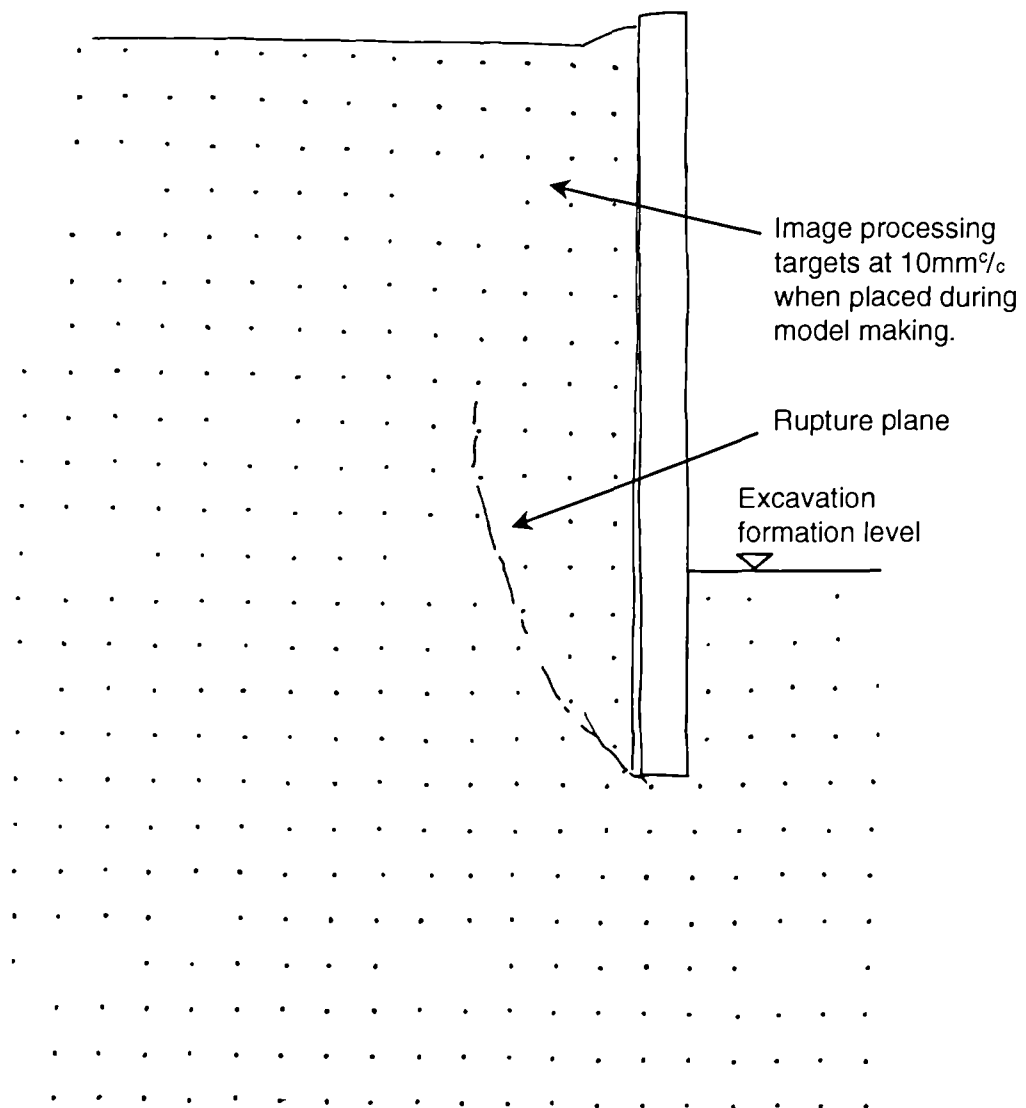


Figure 4.12 Rupture line behind retaining wall at end of test AM9 sketched following removal of the model from the centrifuge swing.

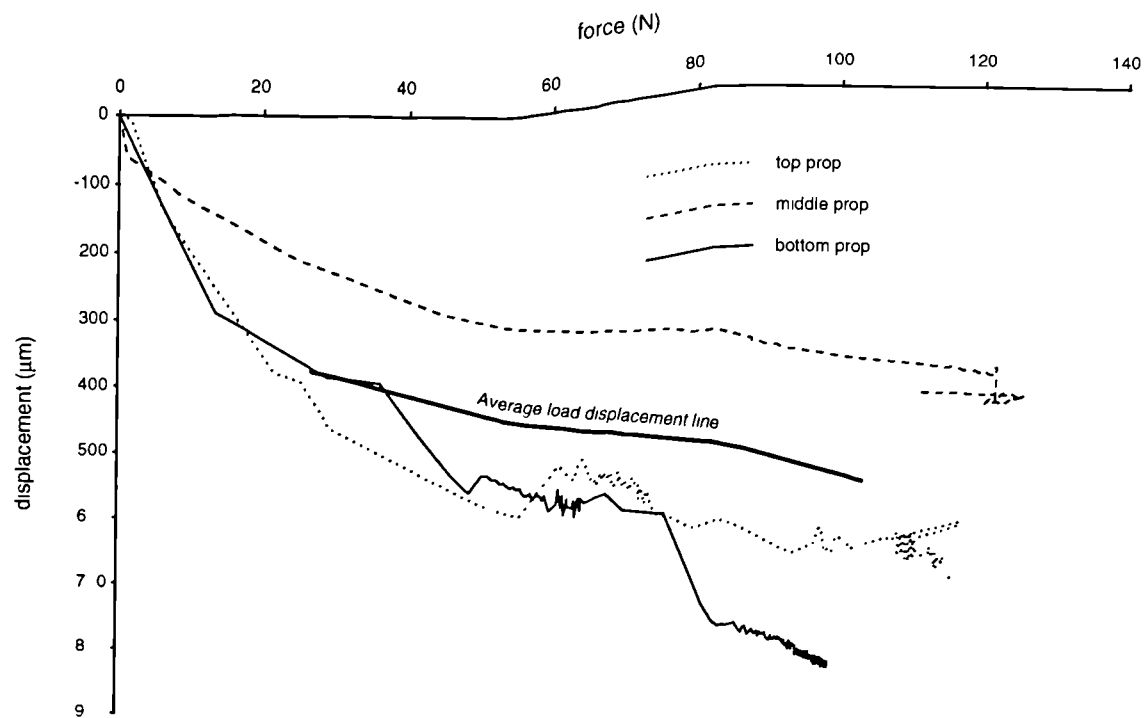


Figure 4.13 Graph of displacement of hydraulic cylinder pistons with increasing load in apparatus test.

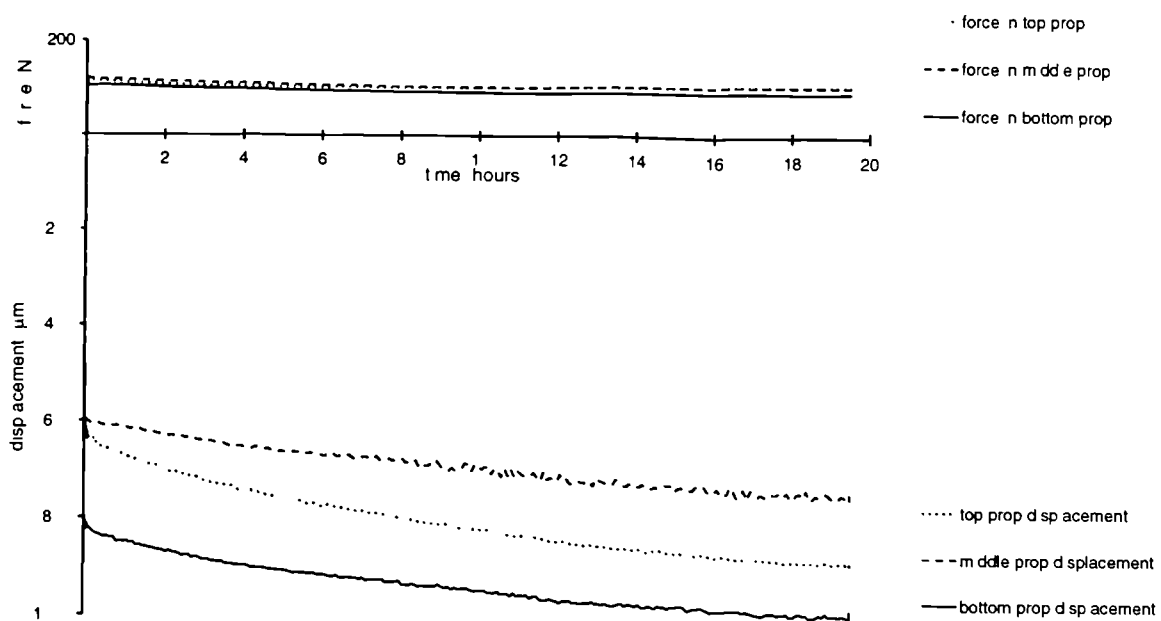
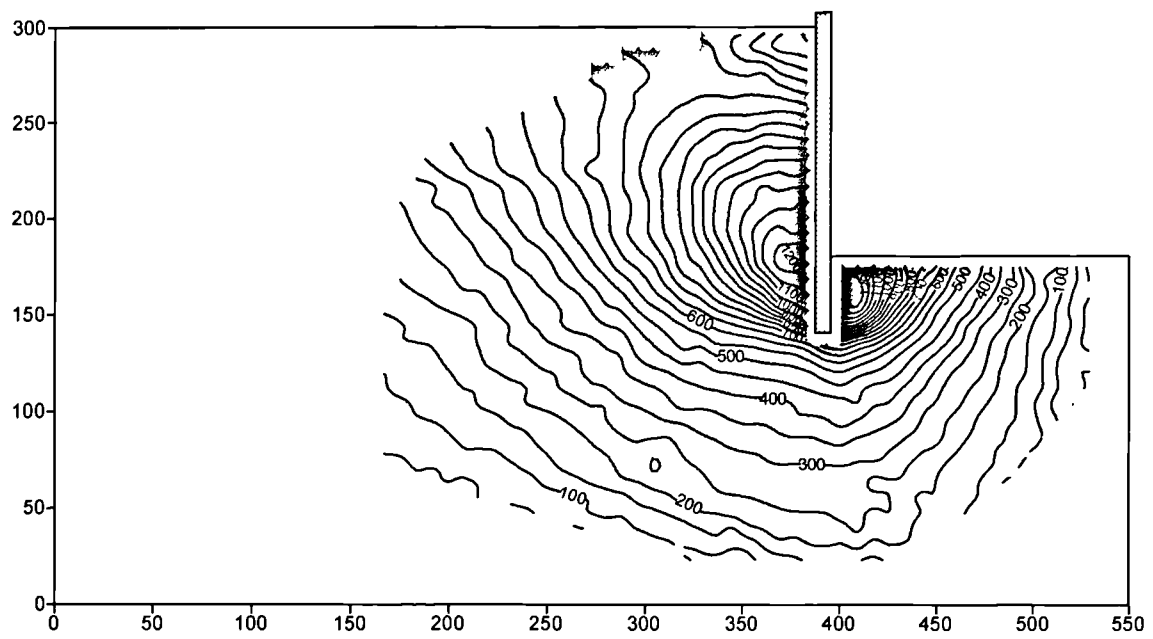
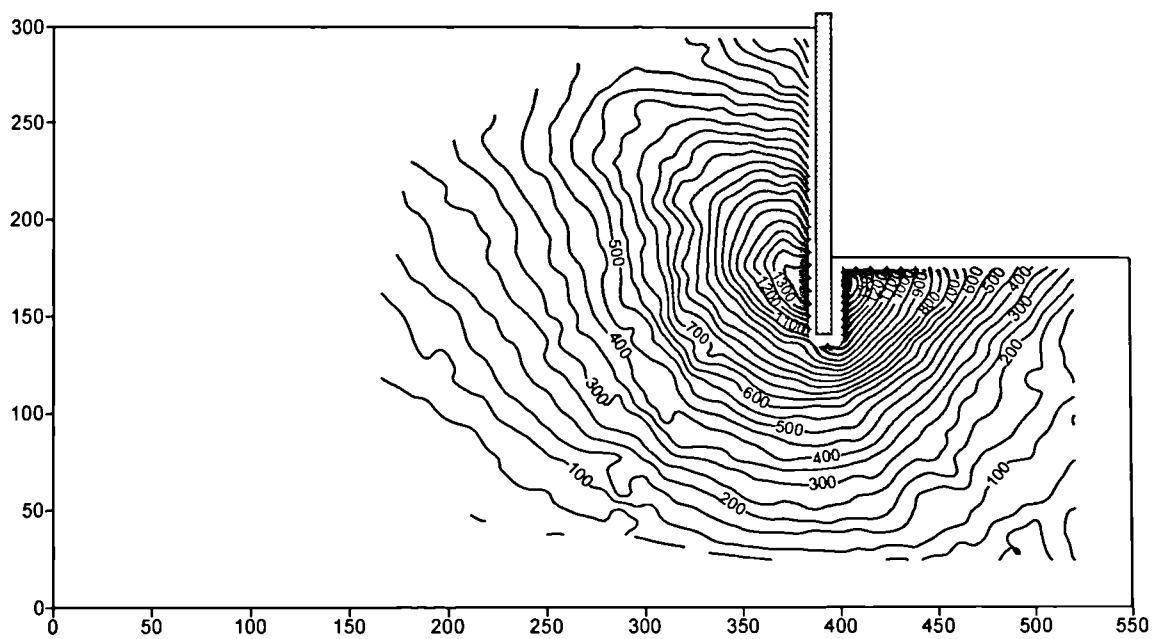


Figure 4.14 Graph of displacement of hydraulic cylinder pistons with time under constant load (also shown) in apparatus check.



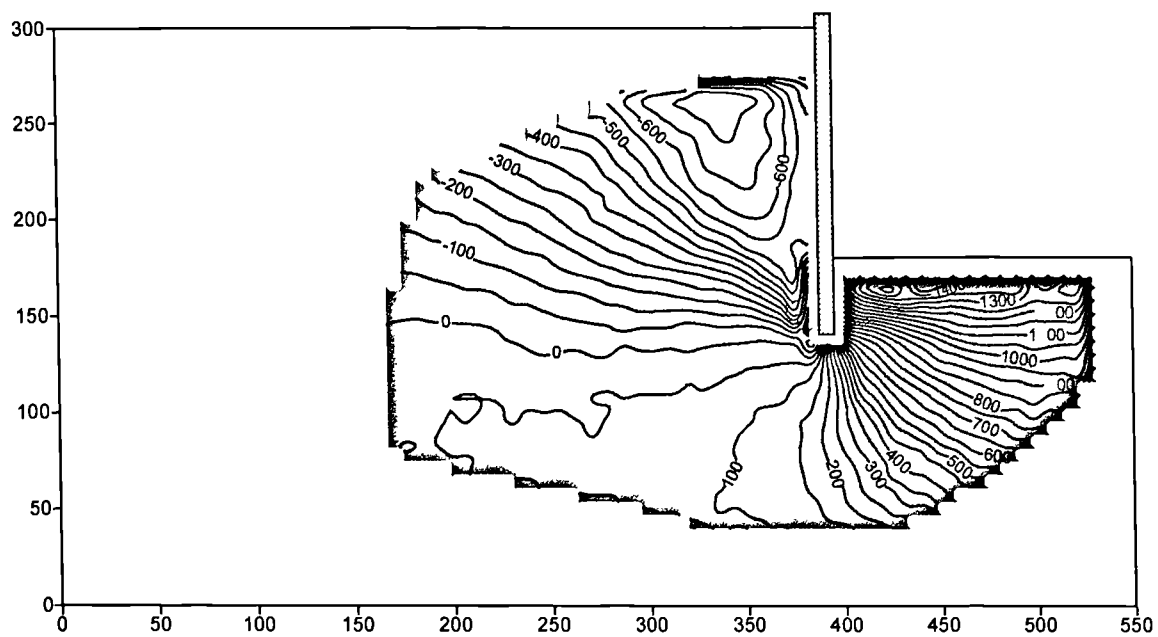
a) Test AM9, no piles.



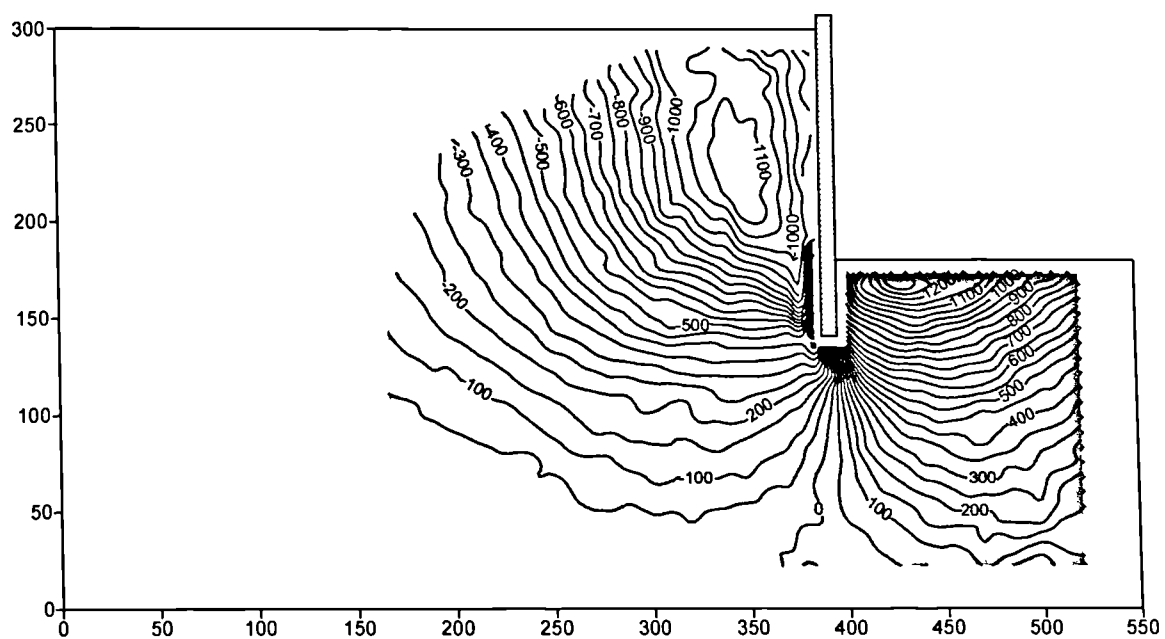
b) Test AM14, no piles.

Figure 4.15 Contours of horizontal movement after 15 minutes.  
(Displacements in  $\mu\text{m}$ ).





a) Test AM9, no piles.



b) Test AM14, no piles.

Figure 4.16 Contours of vertical movement after 15 minutes.  
(Displacements in  $\mu\text{m}$ ).

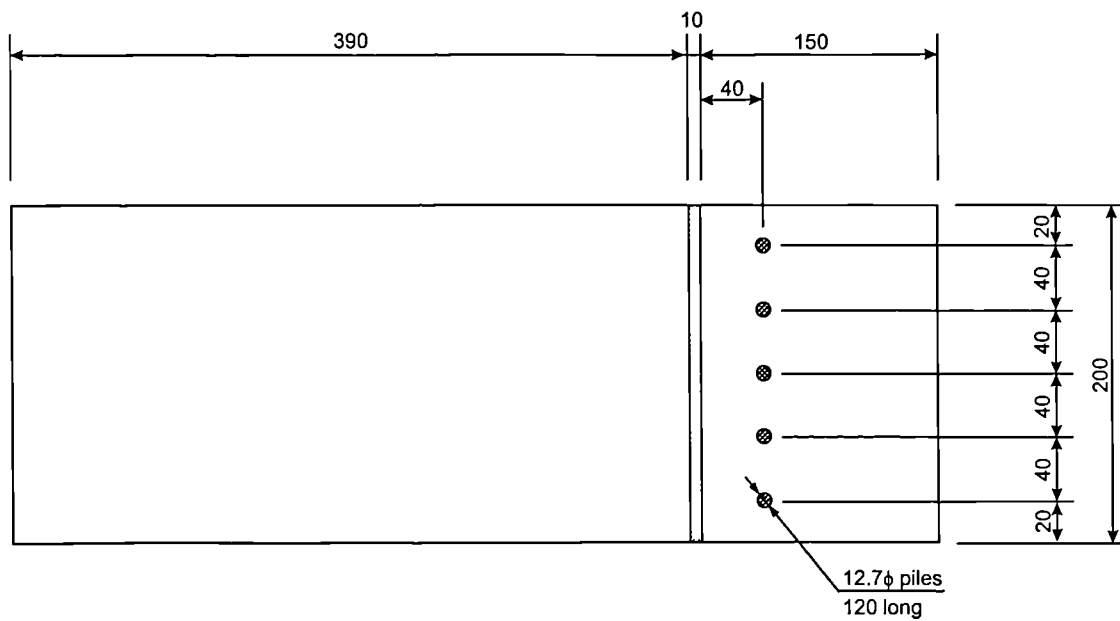


Figure 4.17 Layout of piles in tests AM6 and AM15

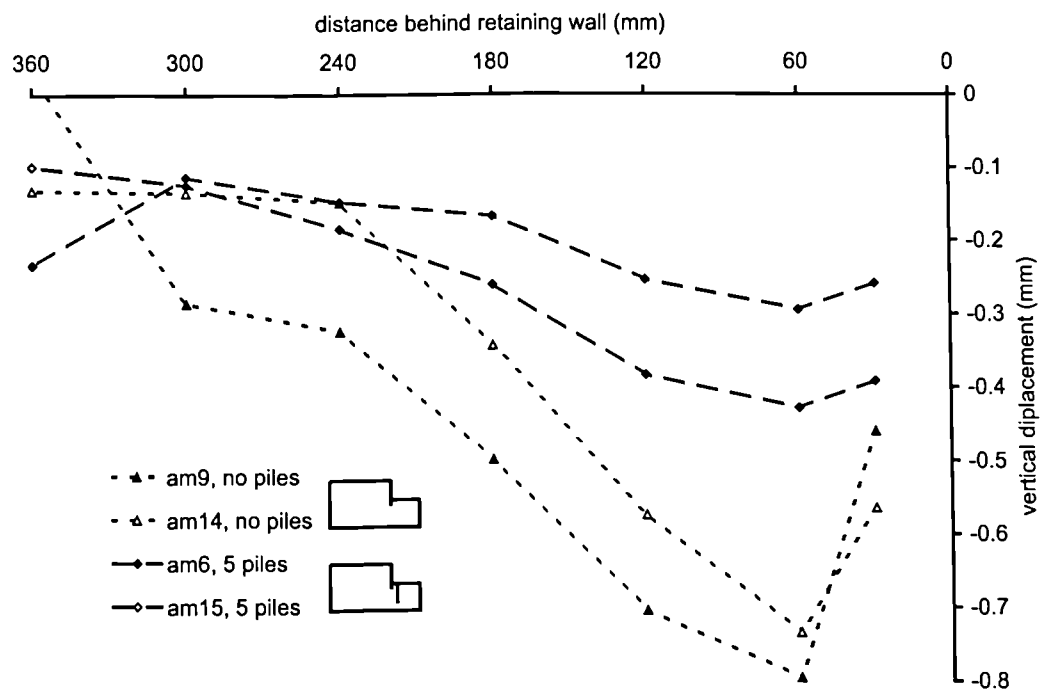


Figure 4.18 Comparison of settlement behind retaining wall at completion of simulated excavation between tests AM6 and 15 and AM9 and 14

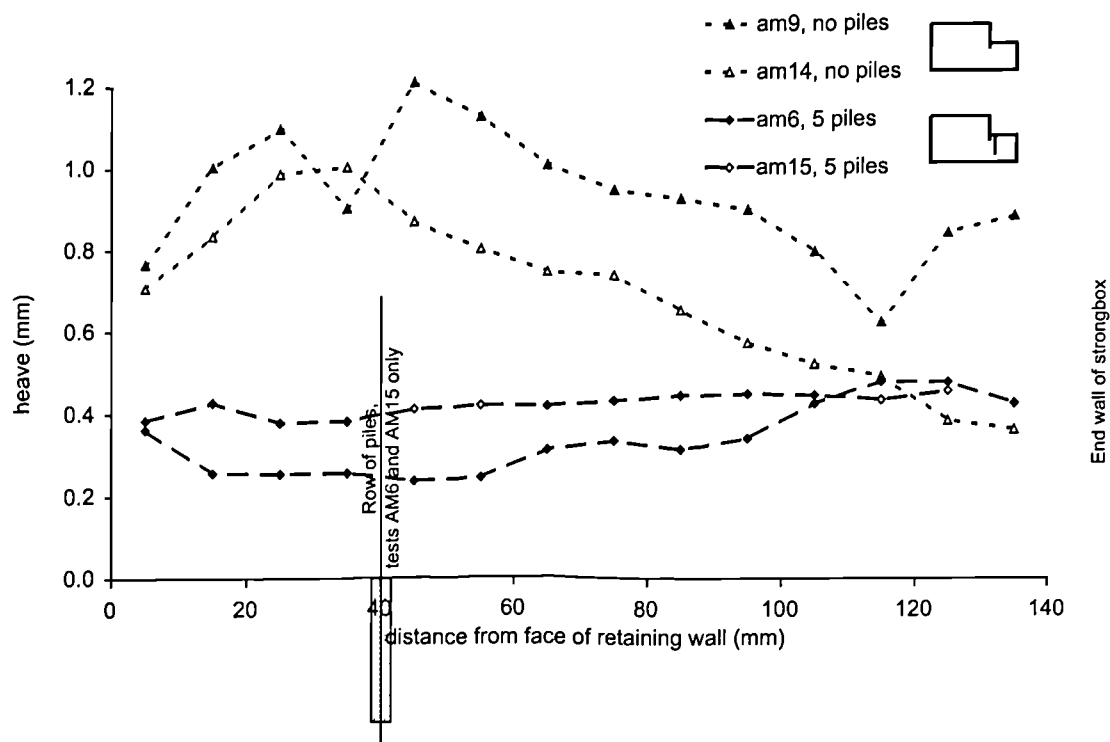


Figure 4.19 Comparison of excavation formation displacements measured using image processing at end of simulated excavation between tests AM6 and 15 and AM9 and 14

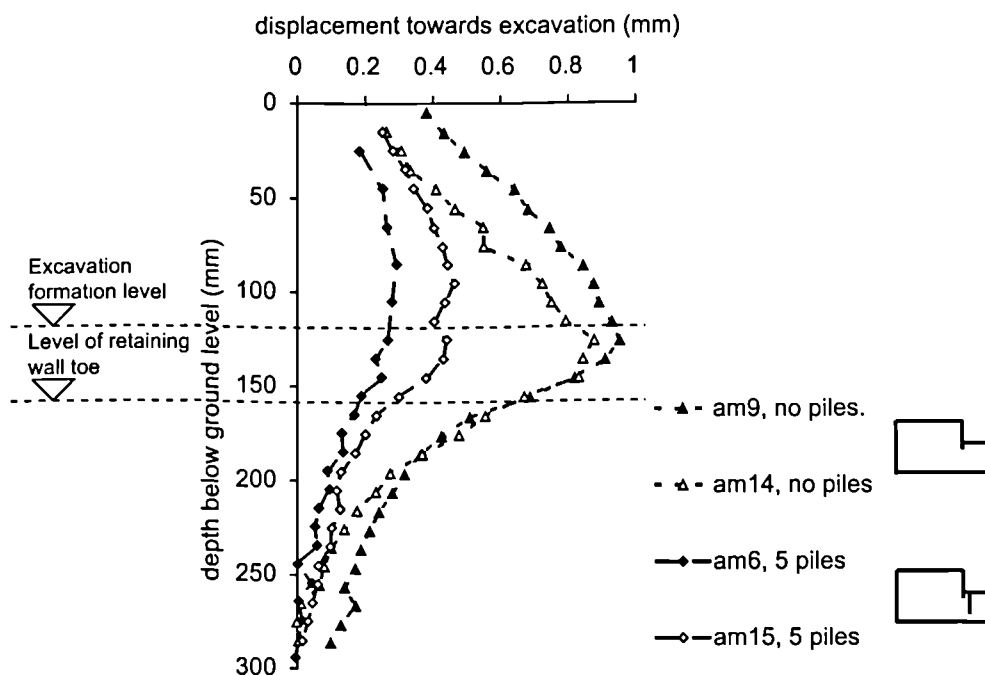


Figure 4.20 Comparison between horizontal displacements, measured immediately behind and below the retaining wall using image processing, at end of simulated excavation for tests AM9 and 14 and tests AM6 and 15.

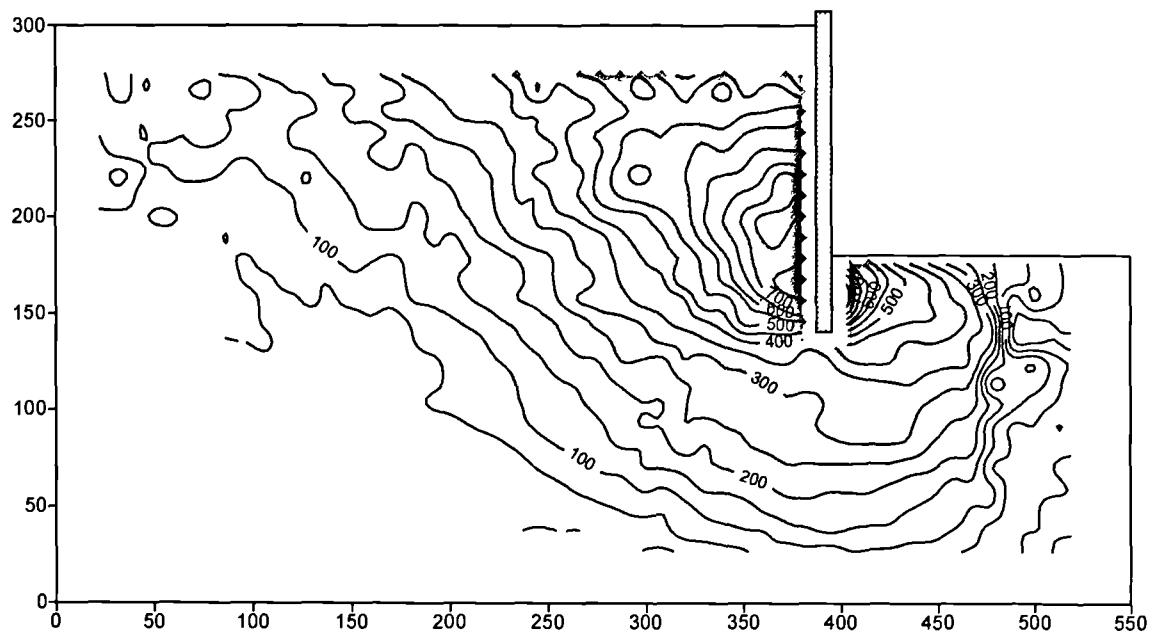


Figure 4.21 Test AM15-contours of horizontal movement after 15 minutes  
Displacements in  $\mu\text{m}$

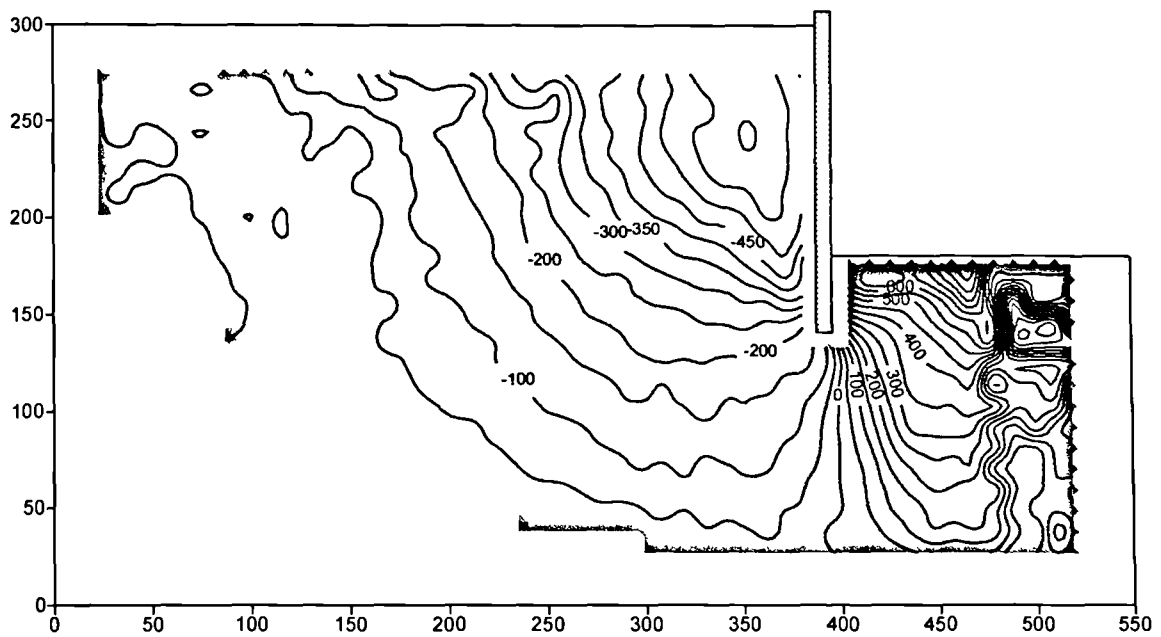


Figure 4.22 Test AM15-contours of vertical movement after 15 minutes  
Displacements in  $\mu\text{m}$ .

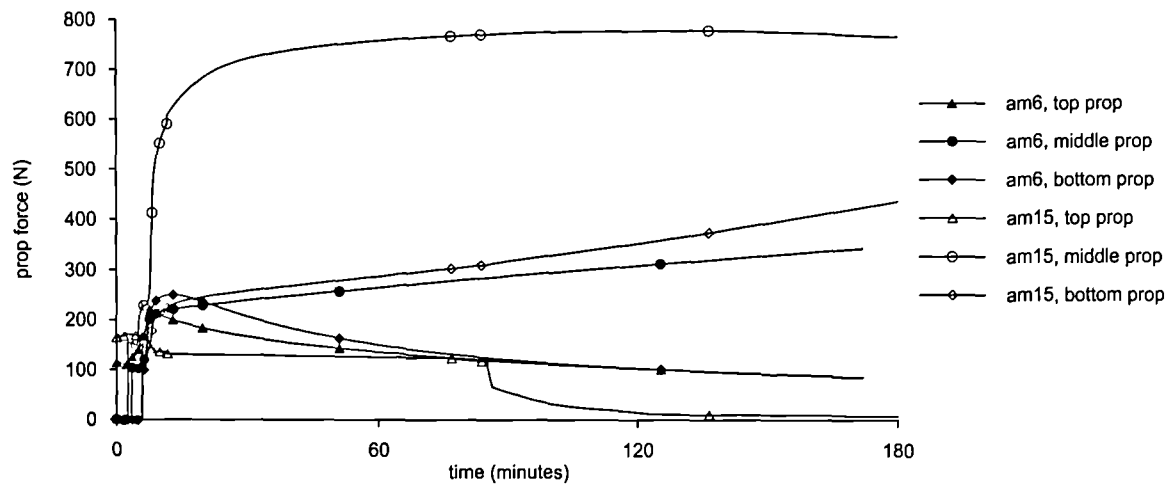


Figure 4.23 Prop loads, determined from oil pressure transducers, during and after the simulated excavation stages of tests AM6 and AM15

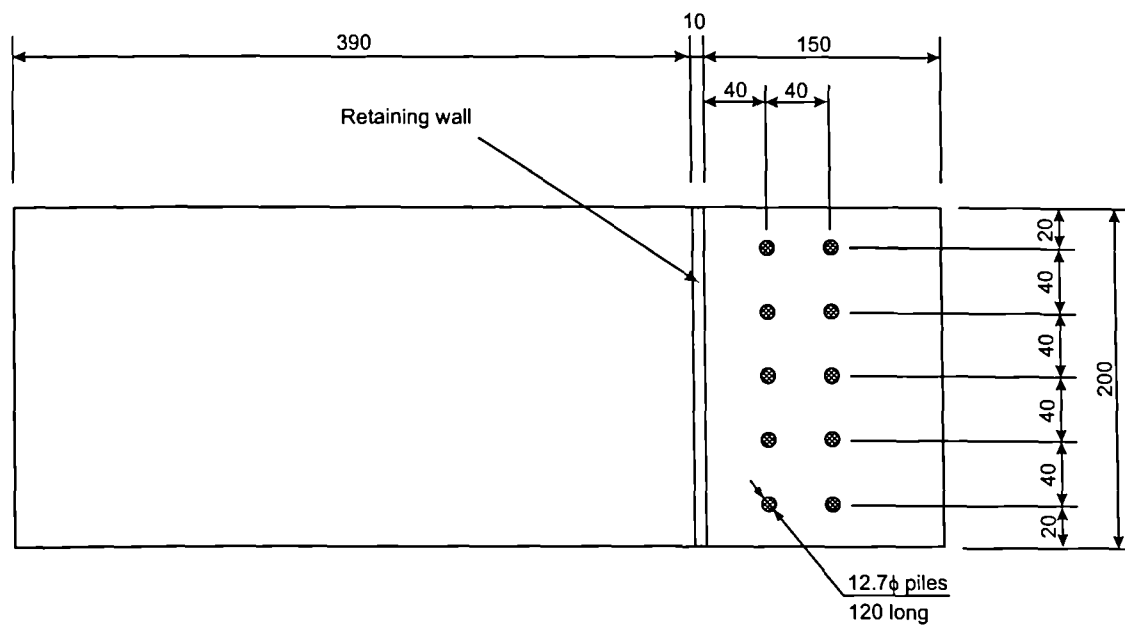


Figure 4.24 Layout of piles in tests AM7 and AM13

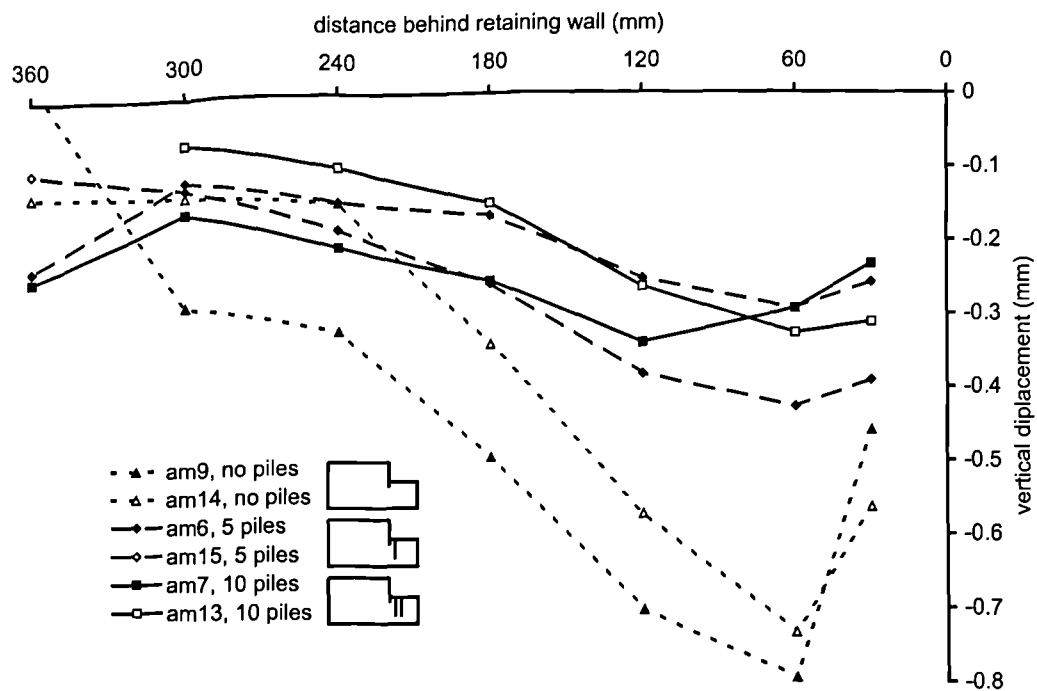


Figure 4.25 Comparison of settlement behind retaining wall at completion of simulated excavation for tests with and without piles at excavation formation

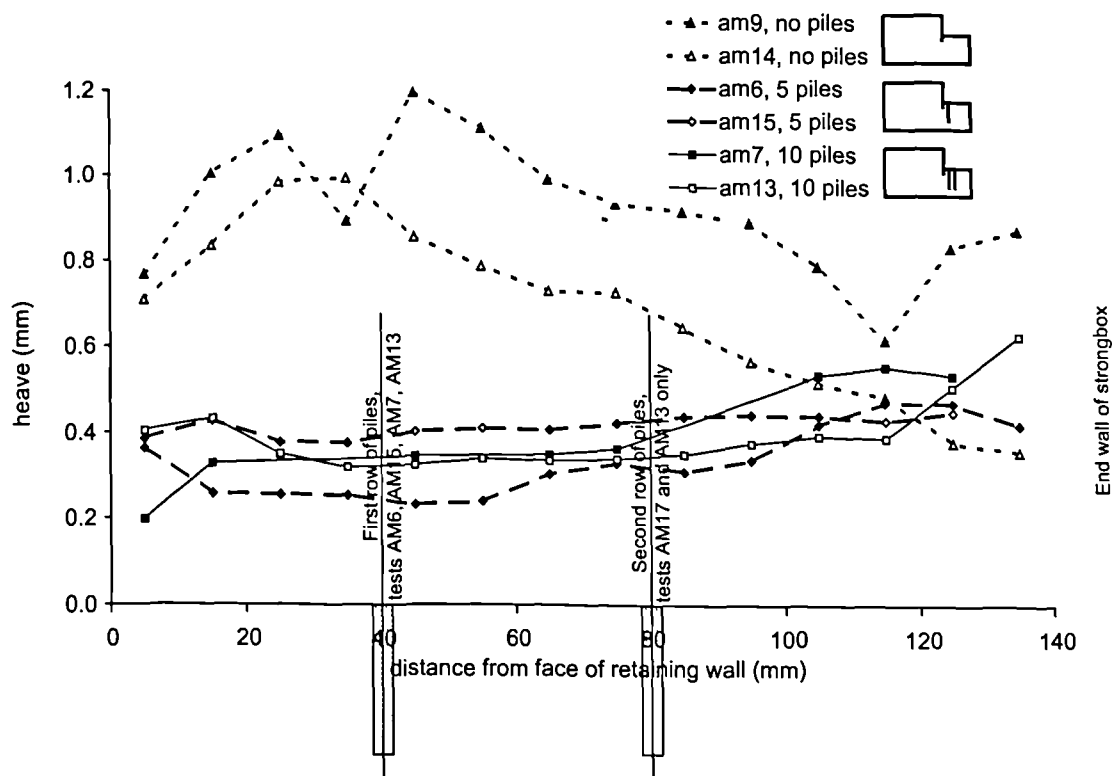


Figure 4.26 Comparison of excavation formation displacements measured using image processing at end of simulated excavation for tests with and without piles at excavation formation

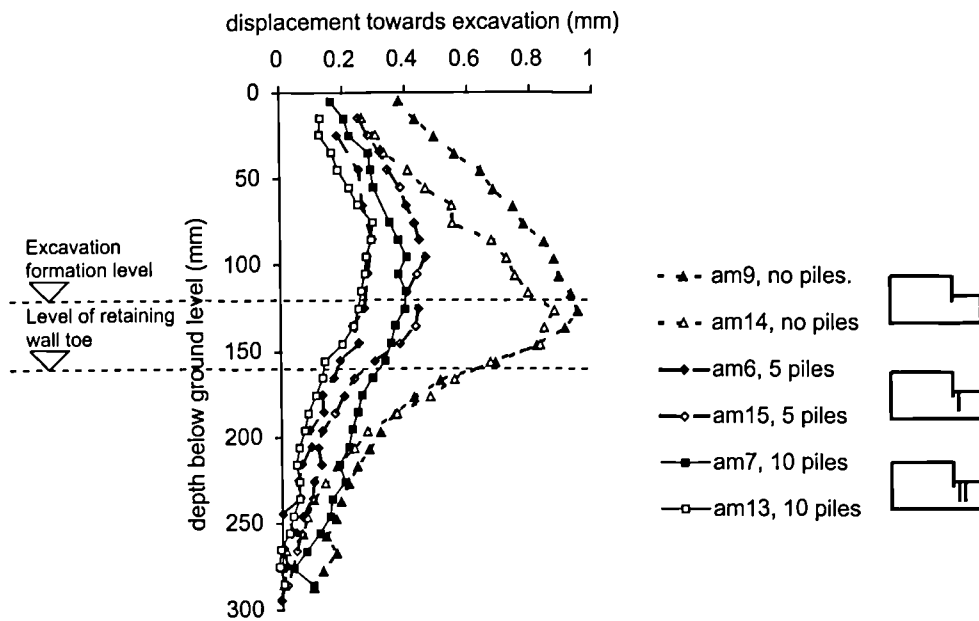


Figure 4.27 Comparison of horizontal displacements immediately behind and beneath the retaining wall measured using image processing at end of simulated excavation for tests with and without piles at excavation formation

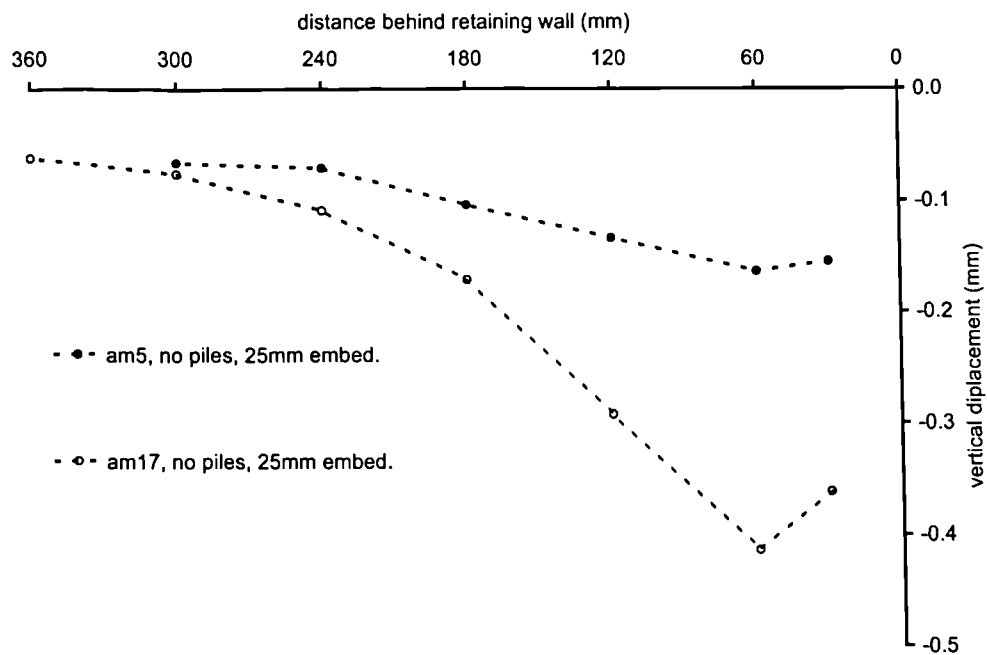


Figure 4.28 Comparison of settlement behind retaining wall at completion of simulated excavation between tests AM5 and AM17

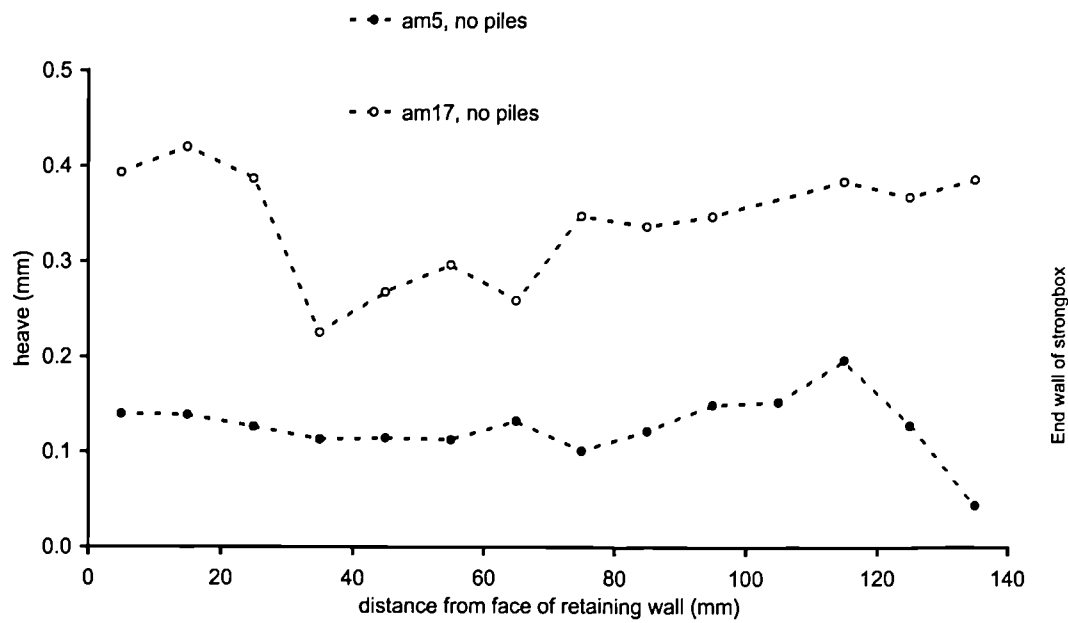


Figure 4.29 Heave measured using image processing at end of simulated excavation for tests AM5 and AM17

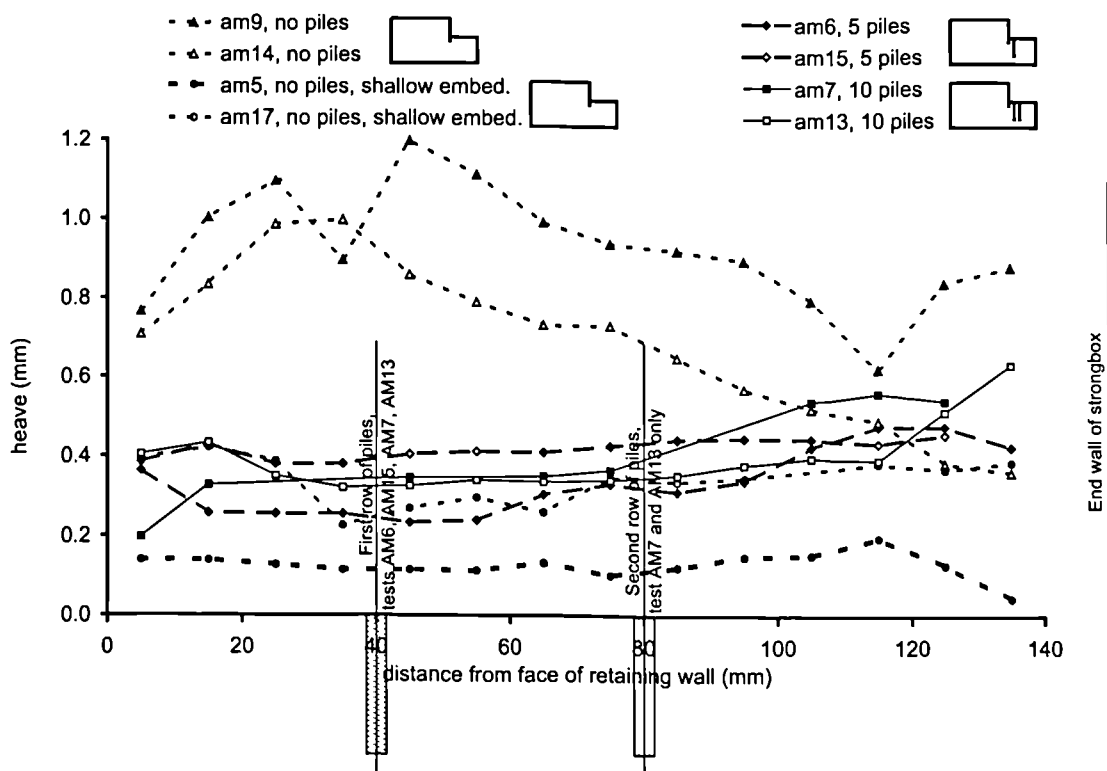


Figure 4.30 Formation displacements measured using image processing at end of simulated excavation for test AM5 in comparison with measurements for other tests



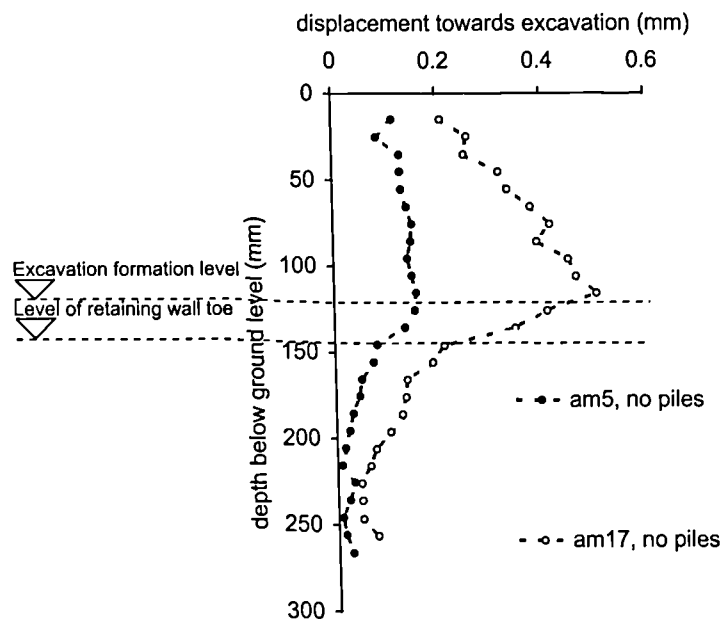


Figure 4.31 Horizontal displacements measured immediately behind and beneath the retaining wall in tests AM5 and AM17

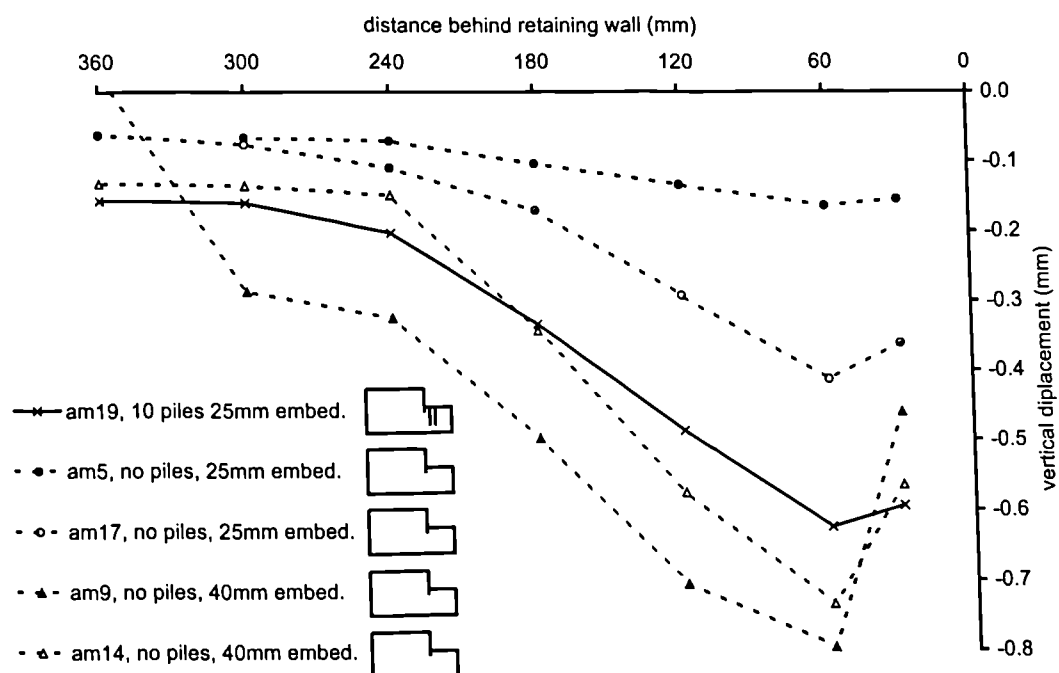


Figure 4.32 Comparison of settlements behind the retaining wall in test AM19 with those seen in deep and shallow embedded walls without piles

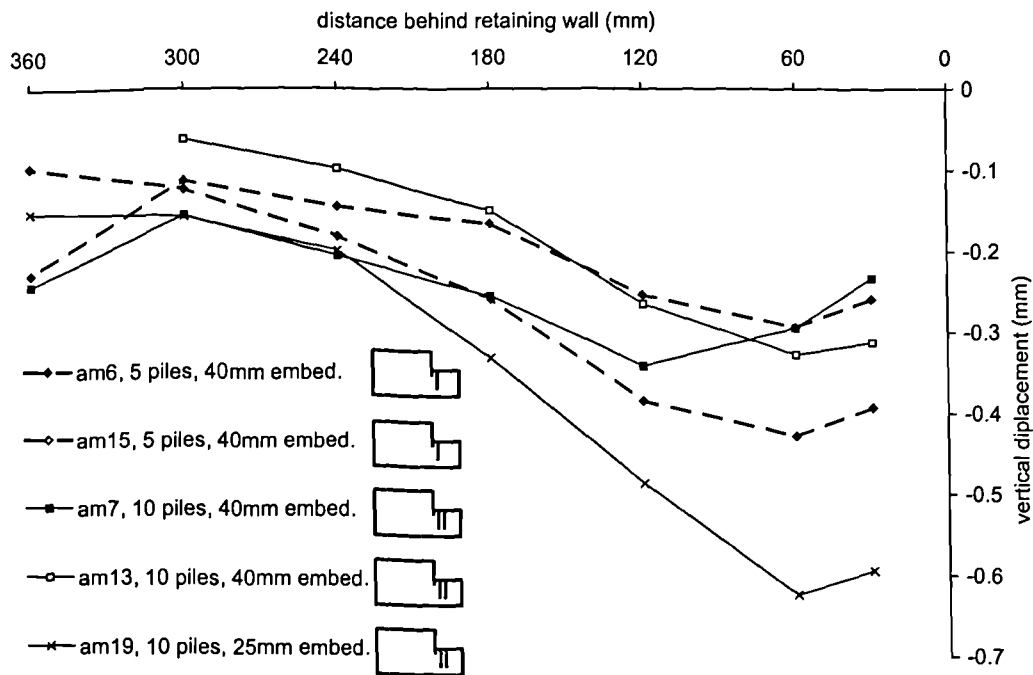


Figure 4.33 Comparison of settlements behind the retaining wall in test AM19 with those seen in tests on more deeply embedded walls with piles

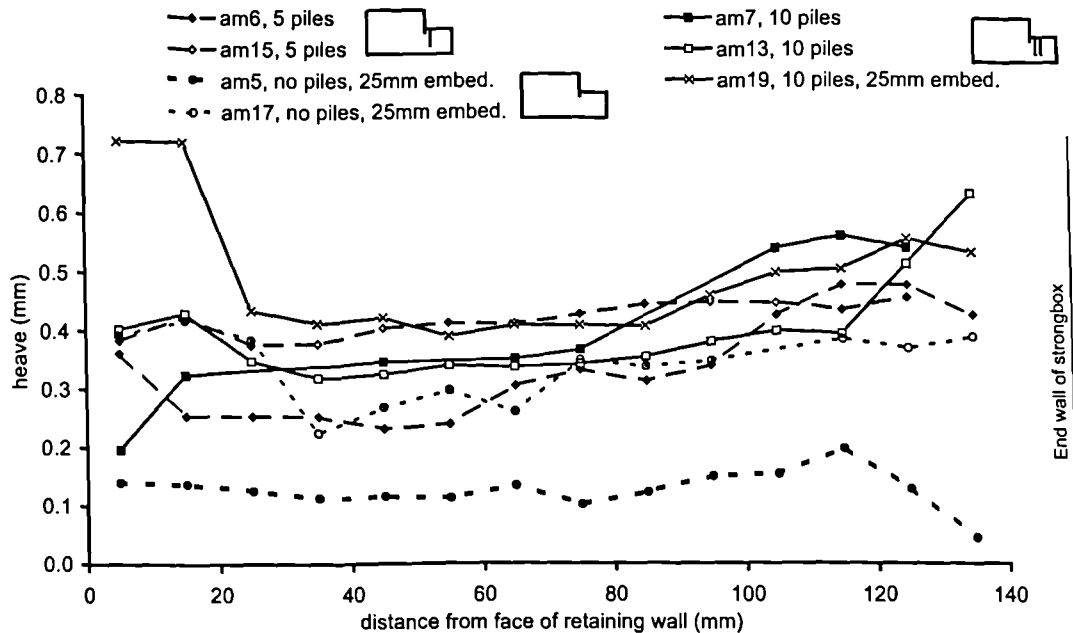


Figure 4.34 Comparison of heave measured at excavation formation level in test AM19 with that measured in tests on more deeply embedded walls with piles and shallow embedded walls without piles

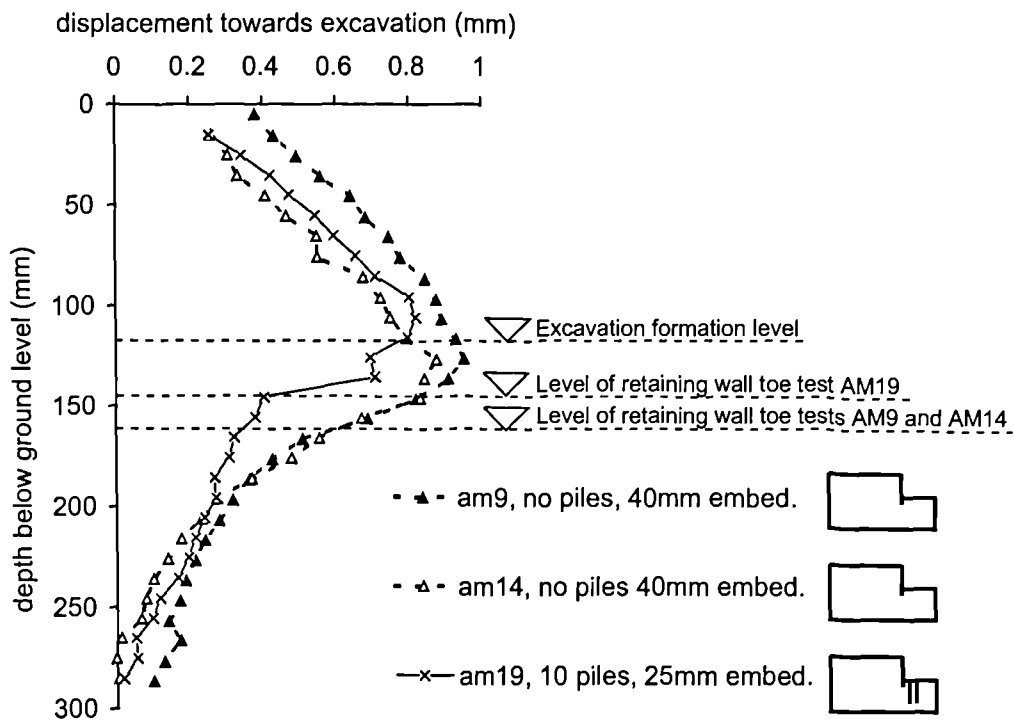


Figure 4.35 Comparison of horizontal displacements measured in test AM19 with those measured in tests on more deeply embedded walls without piles.

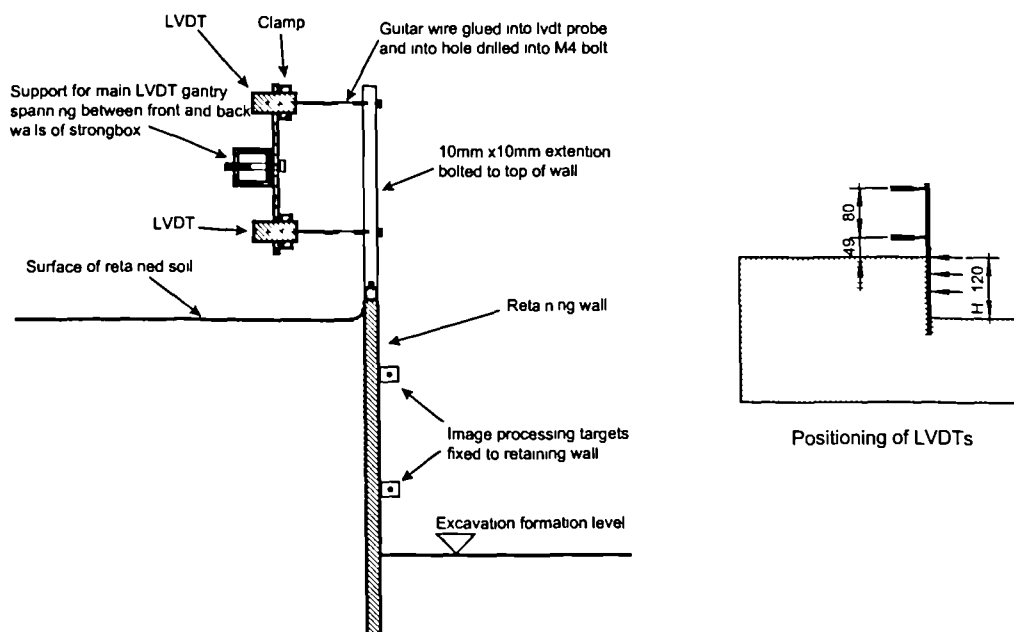
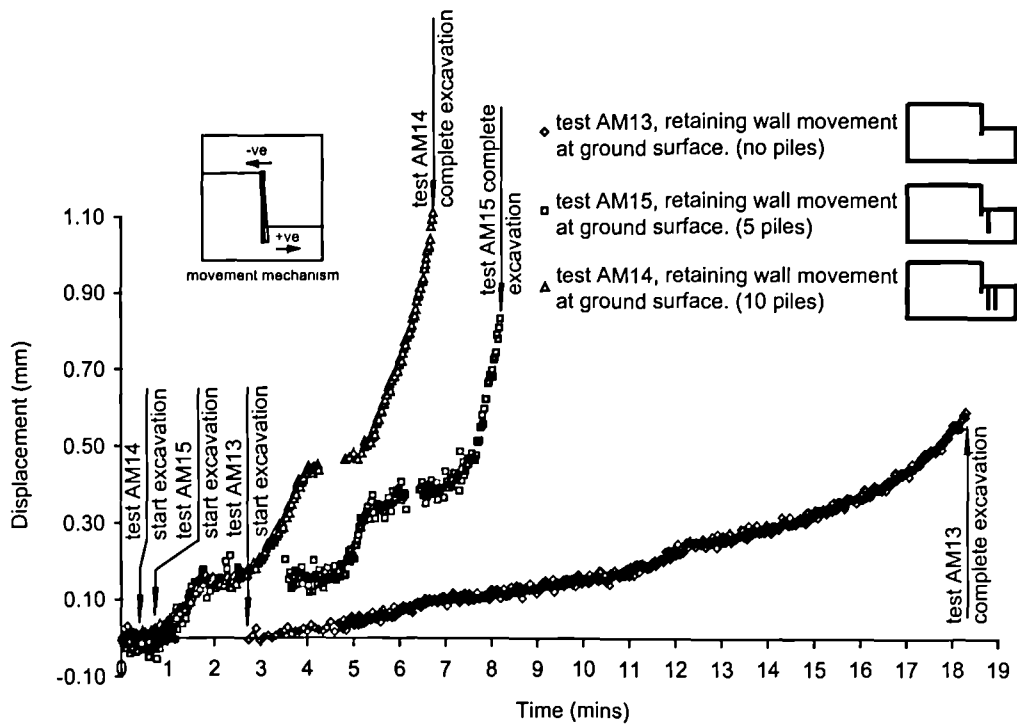
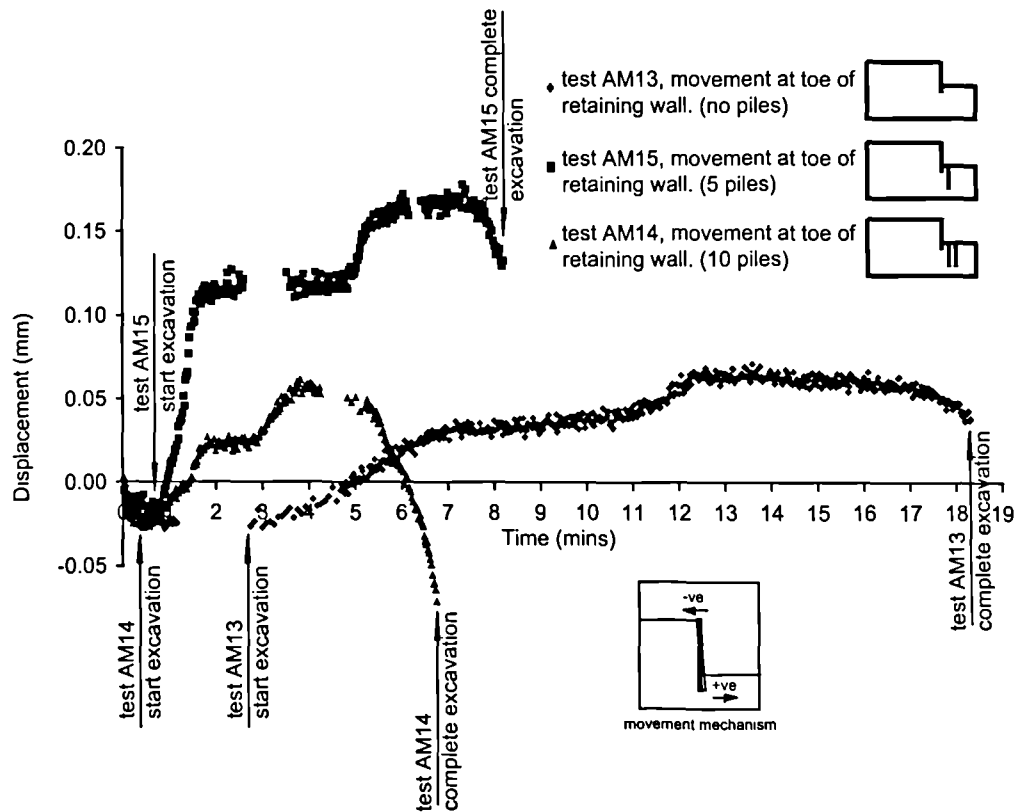


Figure 4.36 Part elevation on model showing arrangement of LVDTs and image processing targets used to measure wall rotation.



a) Displacements at toe of wall.



b) Displacements of wall at retained ground surface.

Figure 4.37 Horizontal wall movement with 40mm embedment walls during simulated excavation stage of typical tests.

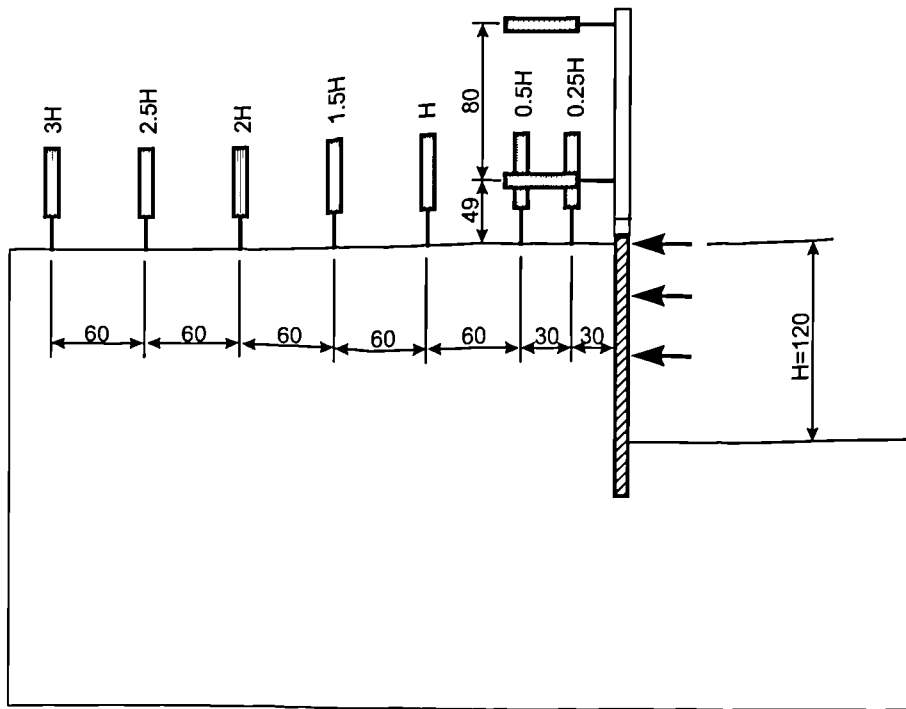
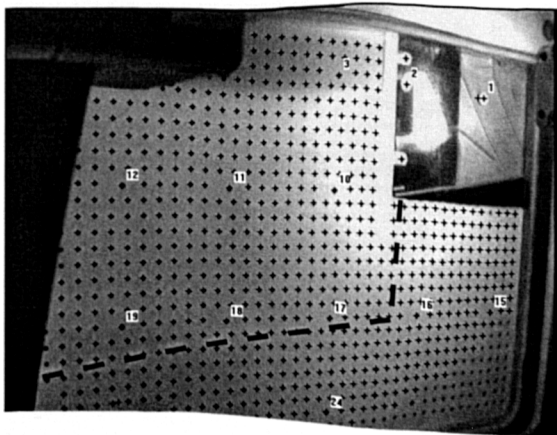
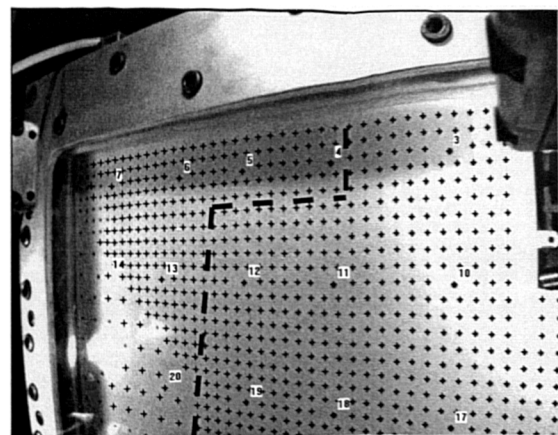


Figure 4.38 Schematic diagram showing positions of LVDTs



a) Image from Toshiba camera



b) Image from Pulnix camera

Figure 4.39 Typical images taken from sequence during test AM15 showing the field of vision of the image processing cameras. A substantial area of overlap between the two cameras in the area behind the retaining wall allowed comparison of displacements measured.

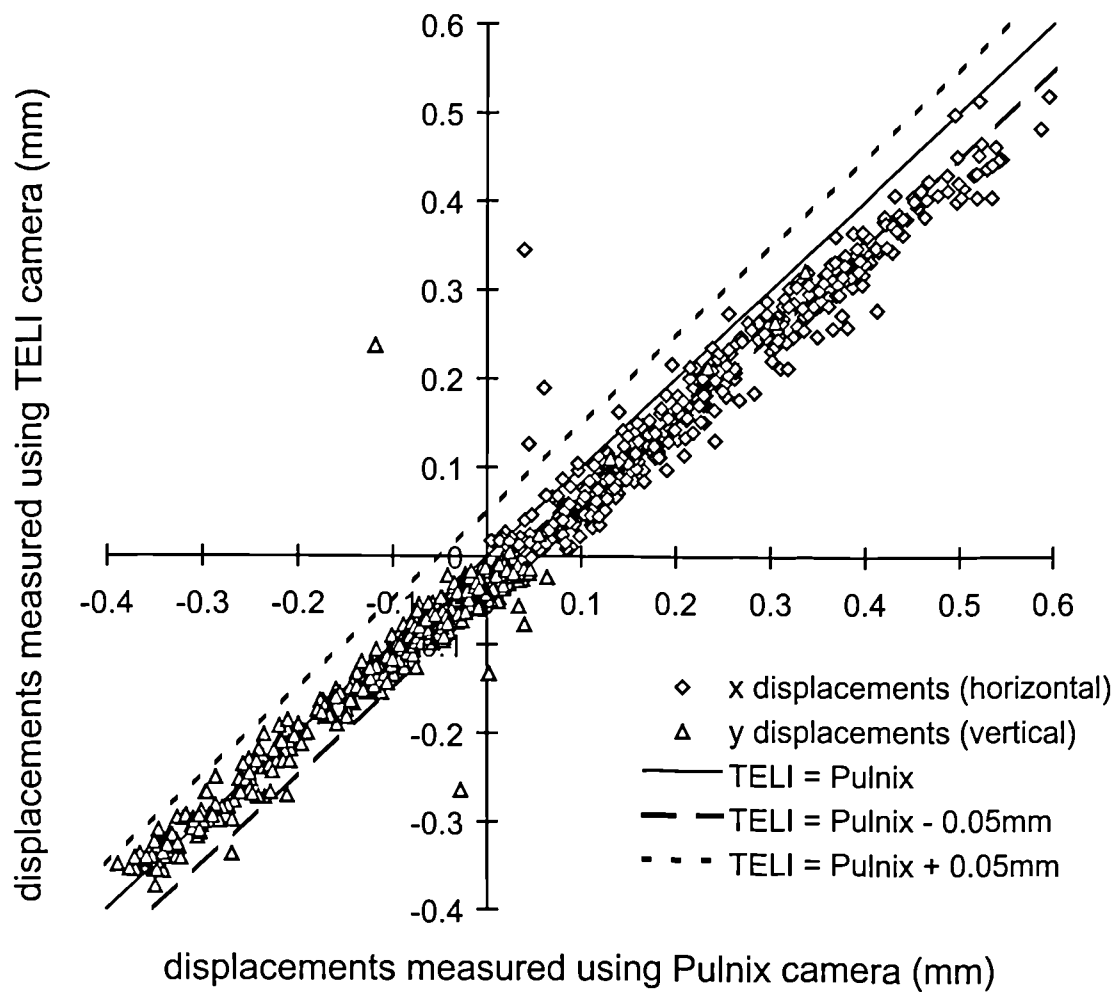
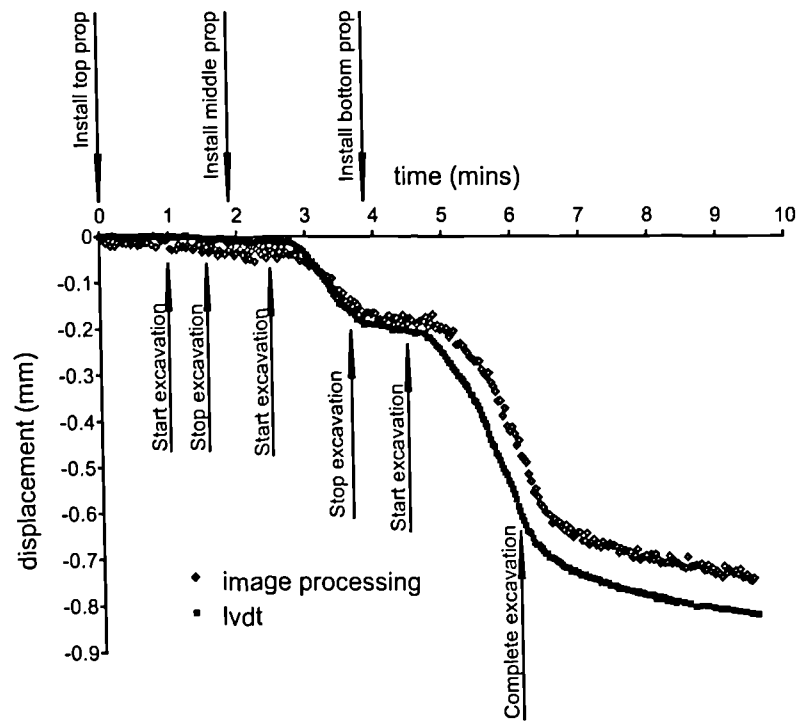
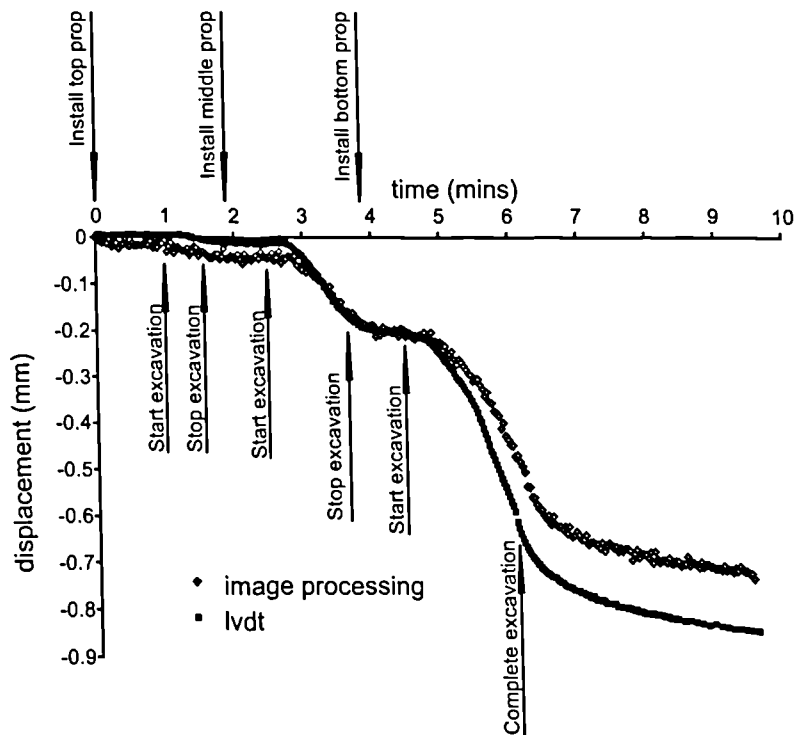


Figure 4.40 Comparison between displacements measured using TELI and Pulnix image processing cameras during test AM17.

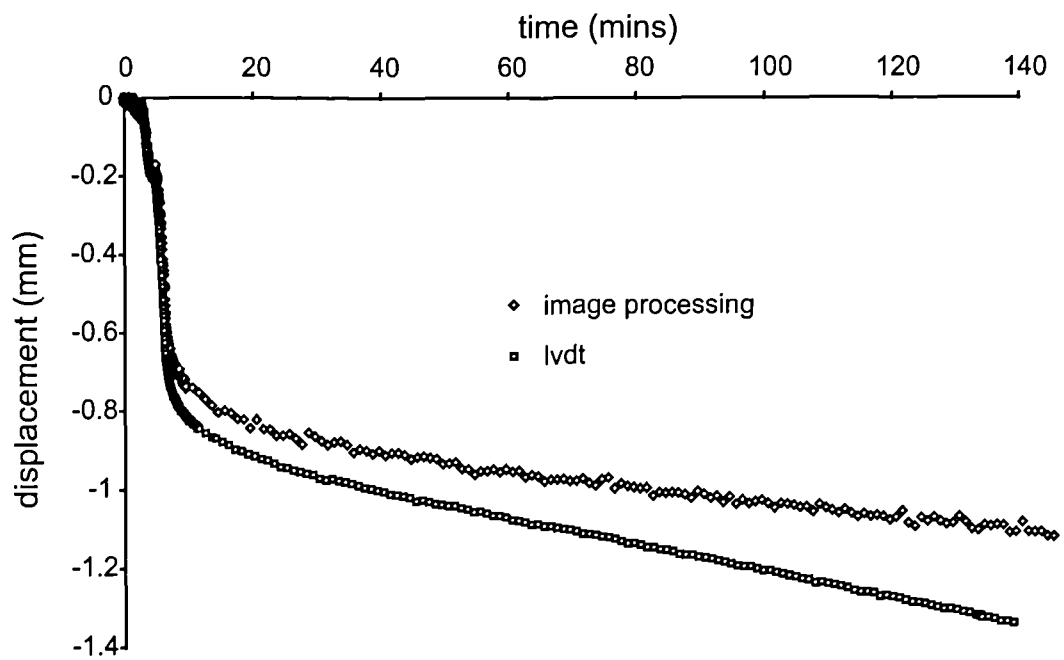


a) 0.25H behind retaining wall

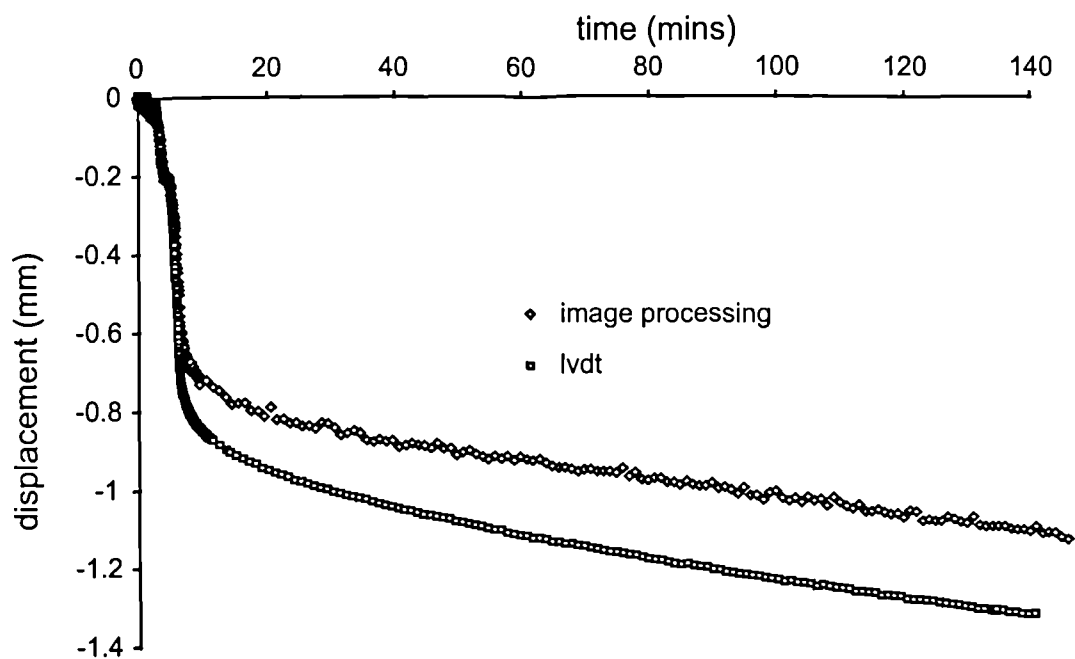


b) 0.5H behind retaining wall

Figure 4.41 Comparison between vertical displacements, measured at the retained soil surface with LVDTs, and with image processing 15mm below the retained soil surface at 0.25H and 0.5H behind the retaining wall during the simulated excavation stage of a typical test (test AM19).



a) 0.25H behind retaining wall



b) 0.5H behind retaining wall

Figure 4.42 Comparison between vertical displacements, measured at the retained soil surface with LVDTs, and with image processing 15mm below the retained soil surface at 0.25H and 0.5H behind the retaining wall during and subsequent to the period of the simulated excavation stage of a typical test (test AM19).



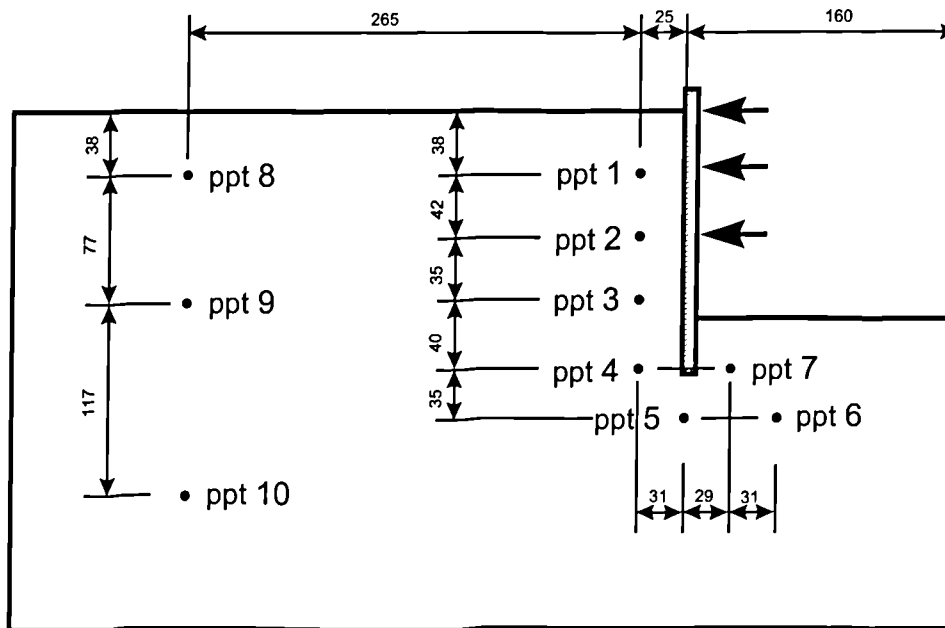


Figure 4.43 Positions of Druck PDCR81 pore pressure transducers

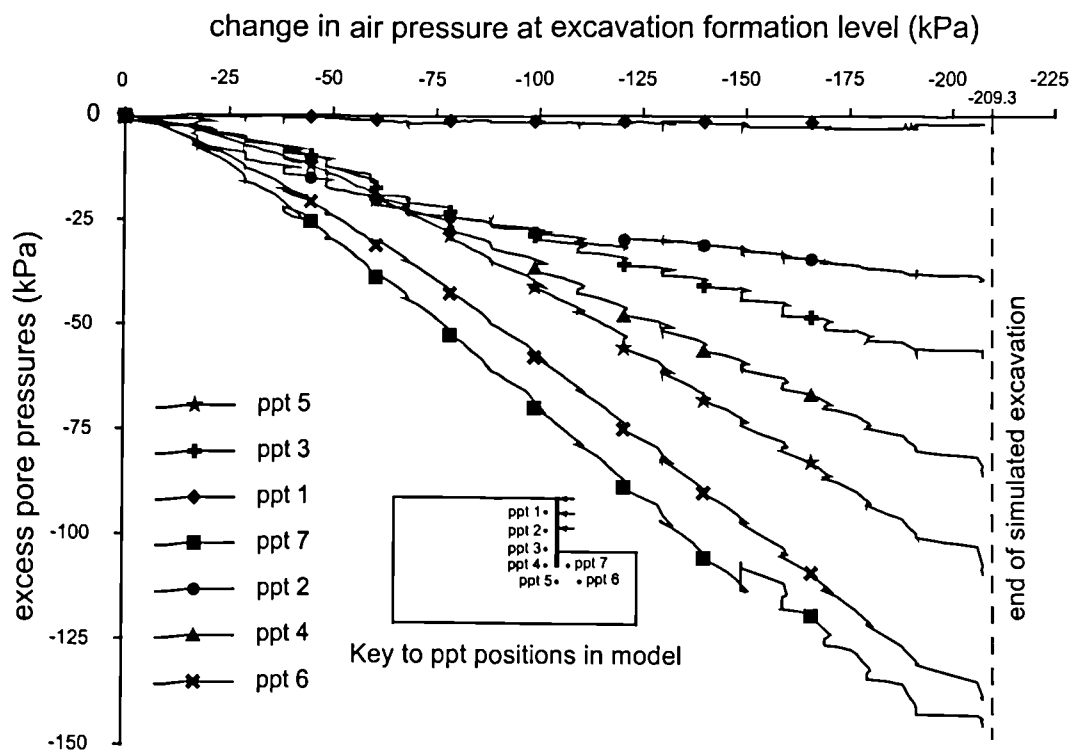


Figure 4.44 Excess pore pressures measured during simulated excavation stage of test AM13.

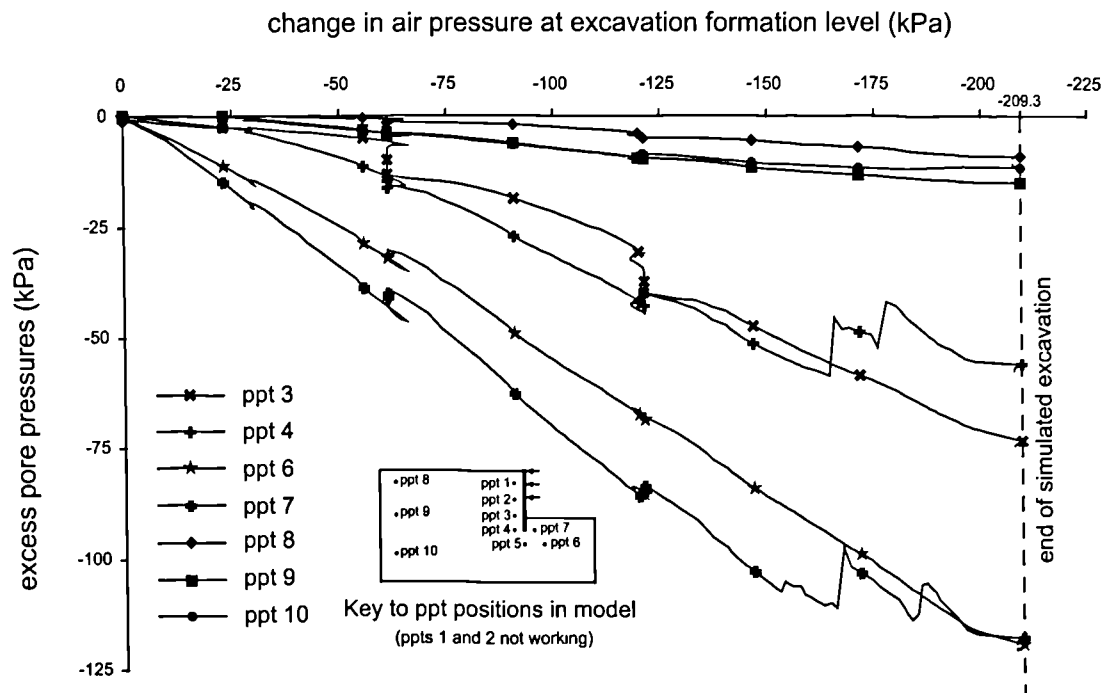


Figure 4.45 Excess pore pressures measured during simulated excavation of test AM19

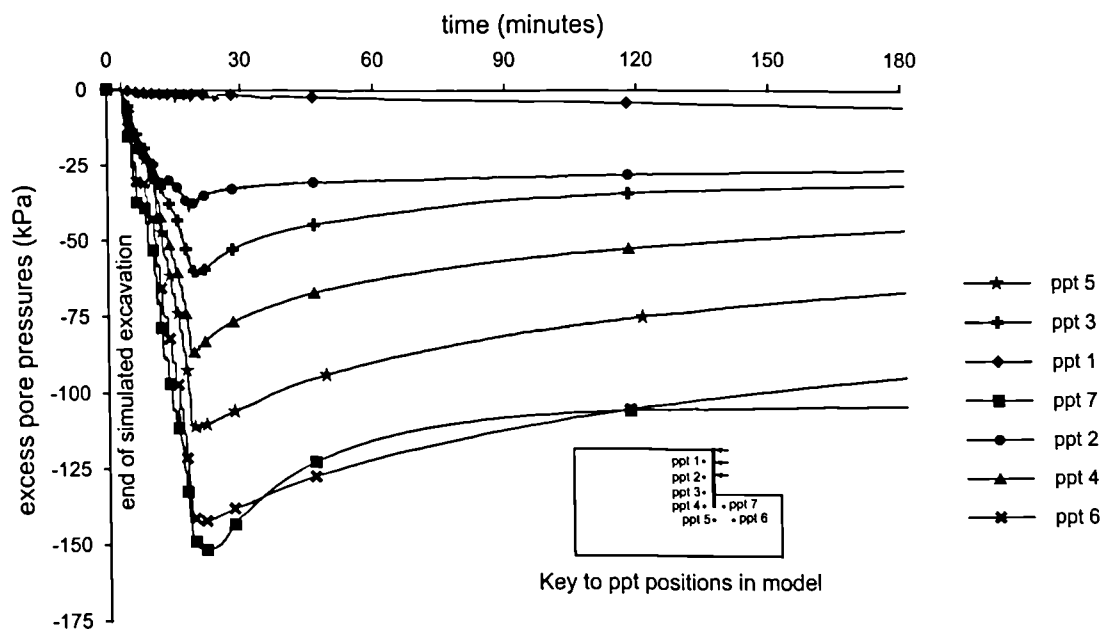
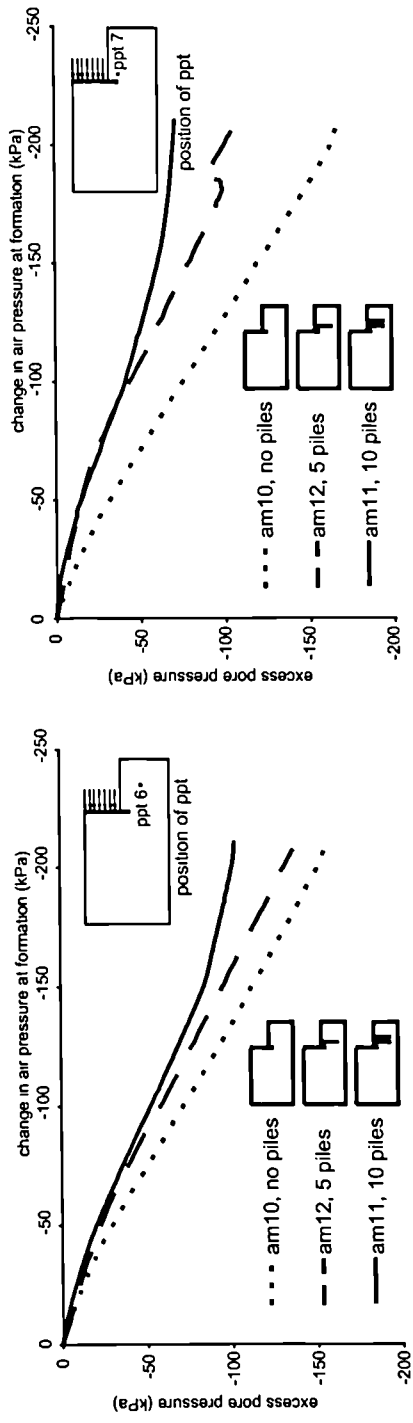
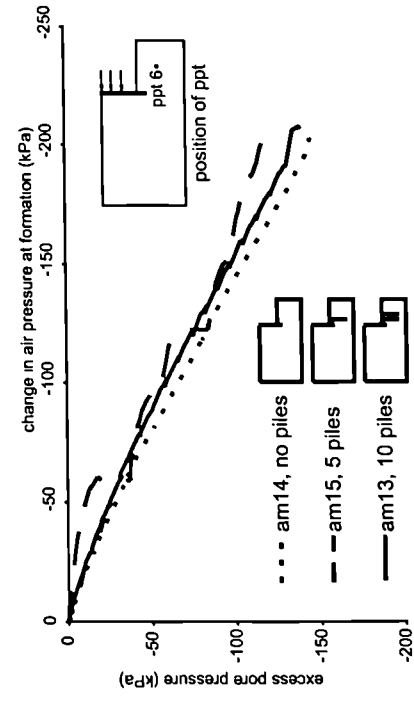


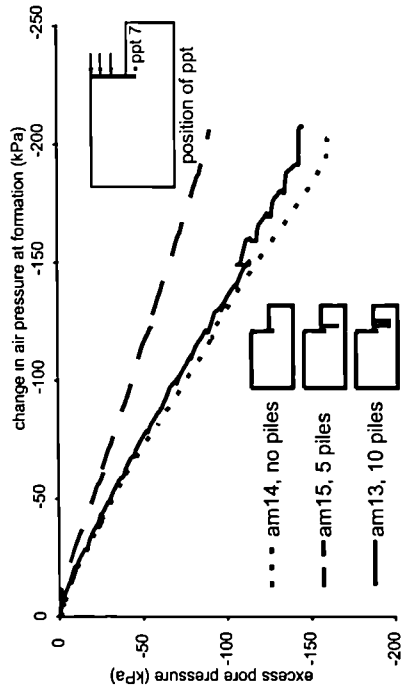
Figure 4.46 Dissipation of excess pore pressures following simulated excavation during test AM13



a) very stiff lateral restraint to retaining wall (ppt6)



c) propped retaining wall (ppt6)



b) very stiff lateral restraint to retaining wall (ppt7)

d) propped retaining wall (ppt7)

Figure 4.47 Response of pore pressure transducers below excavation formation level during reduction of the supporting air pressure during the simulated excavation stage of two sets of tests using; very stiff propping (a and b); conventional propping (c and d).

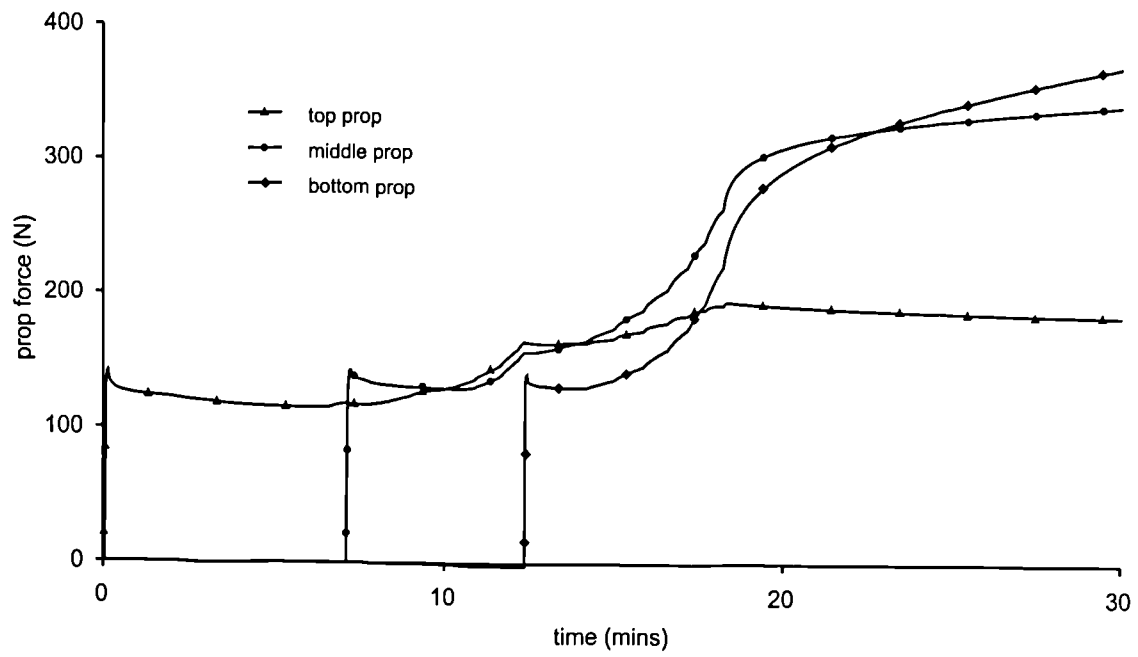


Figure 4.48 Development of prop forces during simulated excavation stage of a typical test (test AM13)

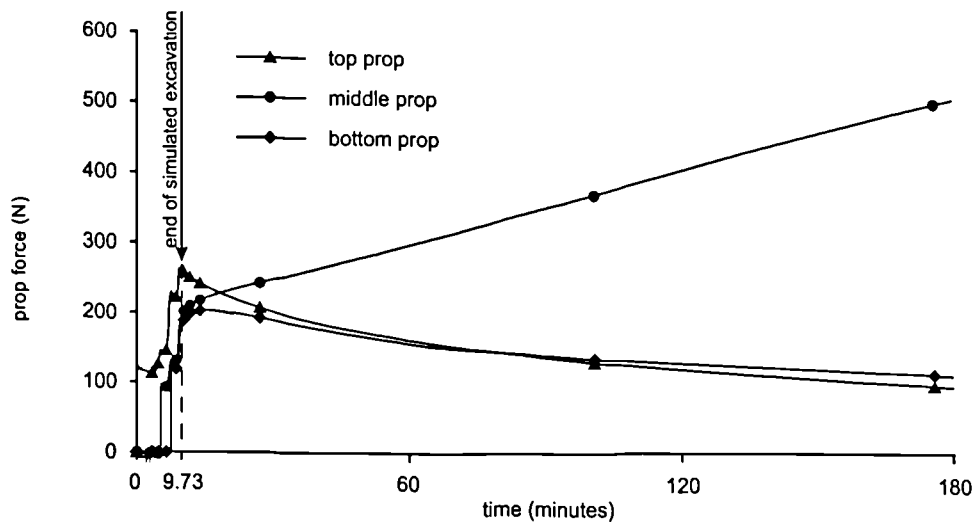


Figure 4.49 Prop forces measured in test AM7. The magnitude and variations shown are typical for all tests

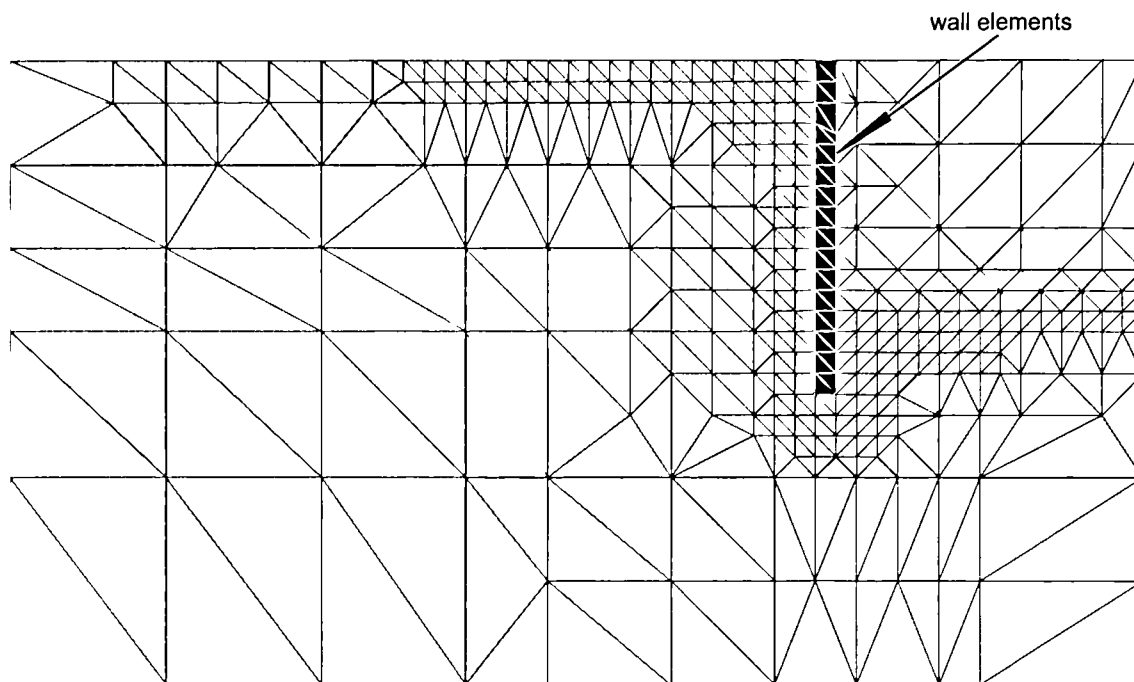


Figure 5.1 Primary mesh used in preliminary finite element analyses.

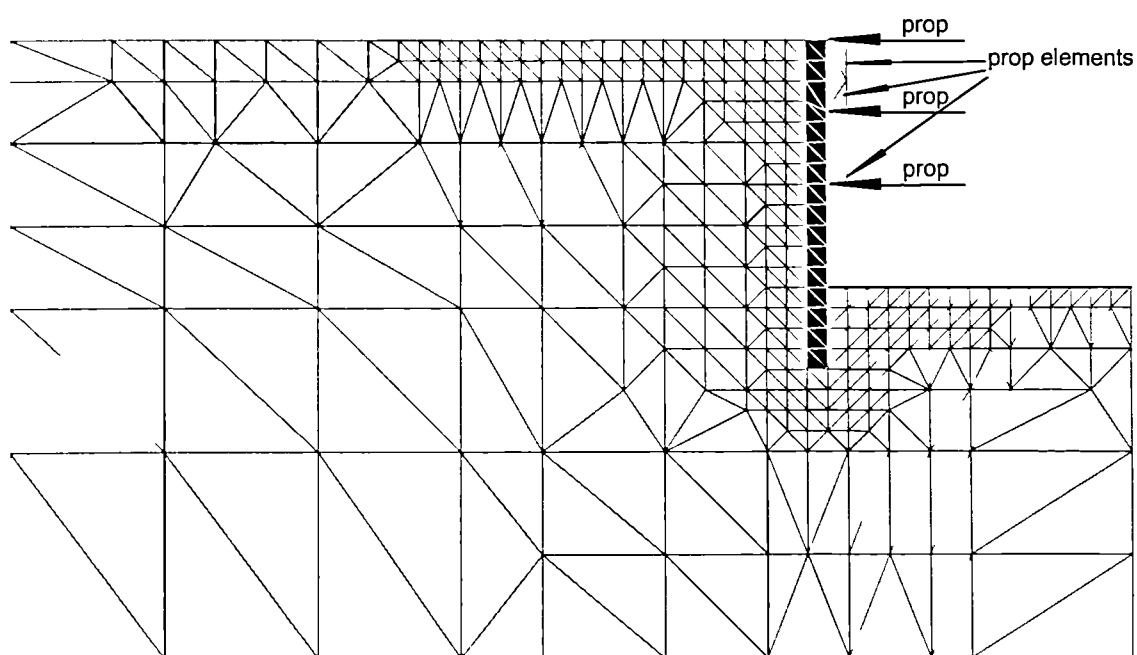


Figure 5.2 Secondary mesh used in preliminary finite element analyses.

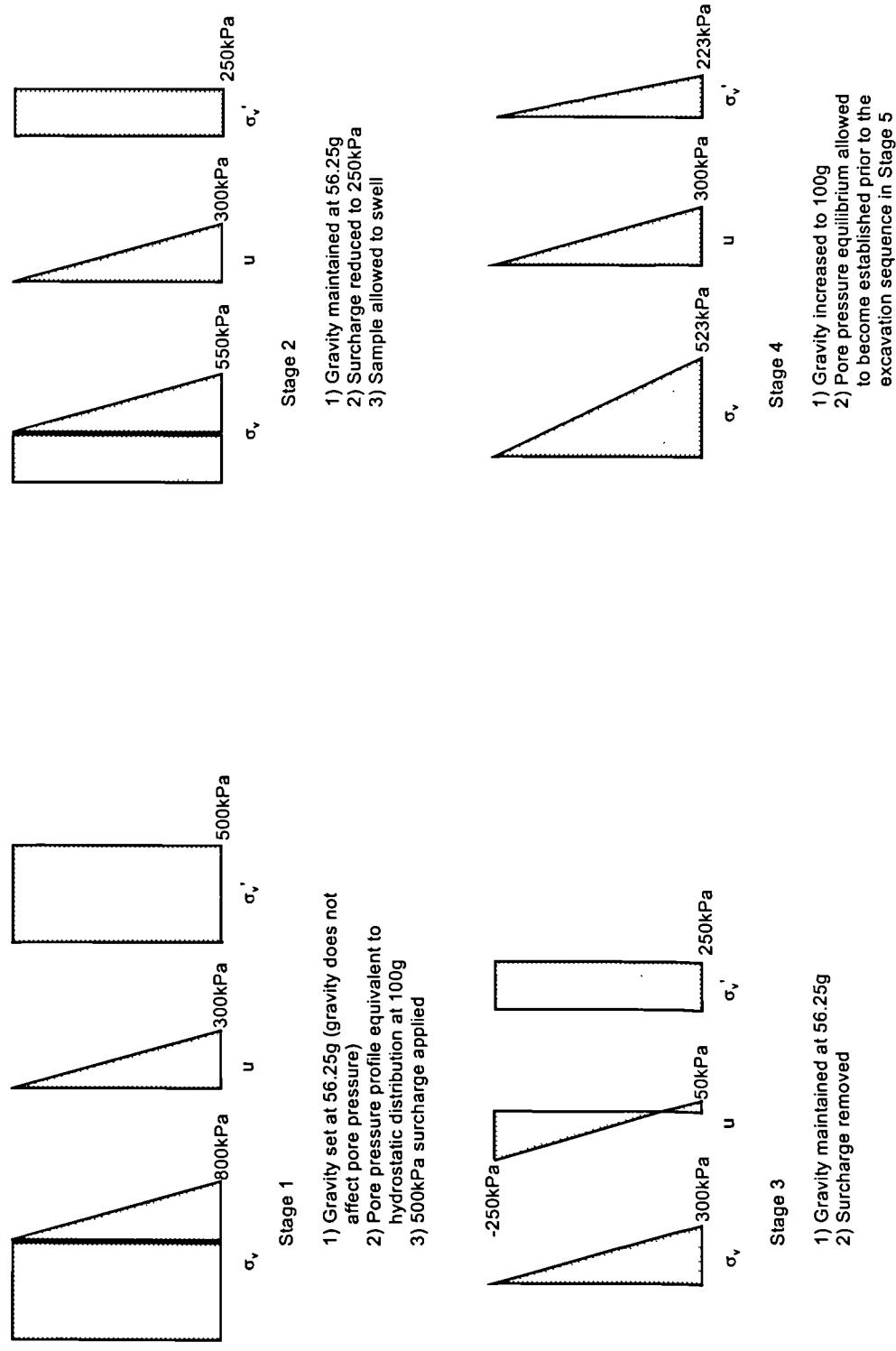


Figure 5.3 Key stages in modelling the stress history of the sample prior to the excavation sequence showing how the true effective stress is maintained throughout the analysis by gravity manipulation and the imposition of an artificial hydrostatic pore pressure distribution.

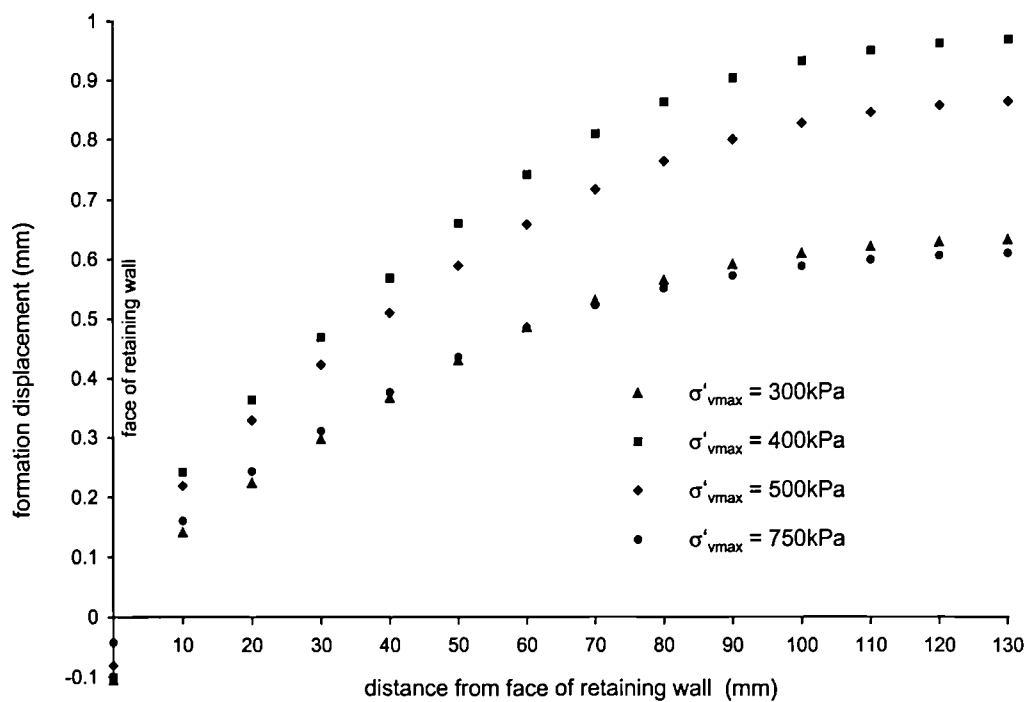


Figure 5.4 Finite element analyses predictions of excavation formation displacement for a range of preconsolidation pressures.

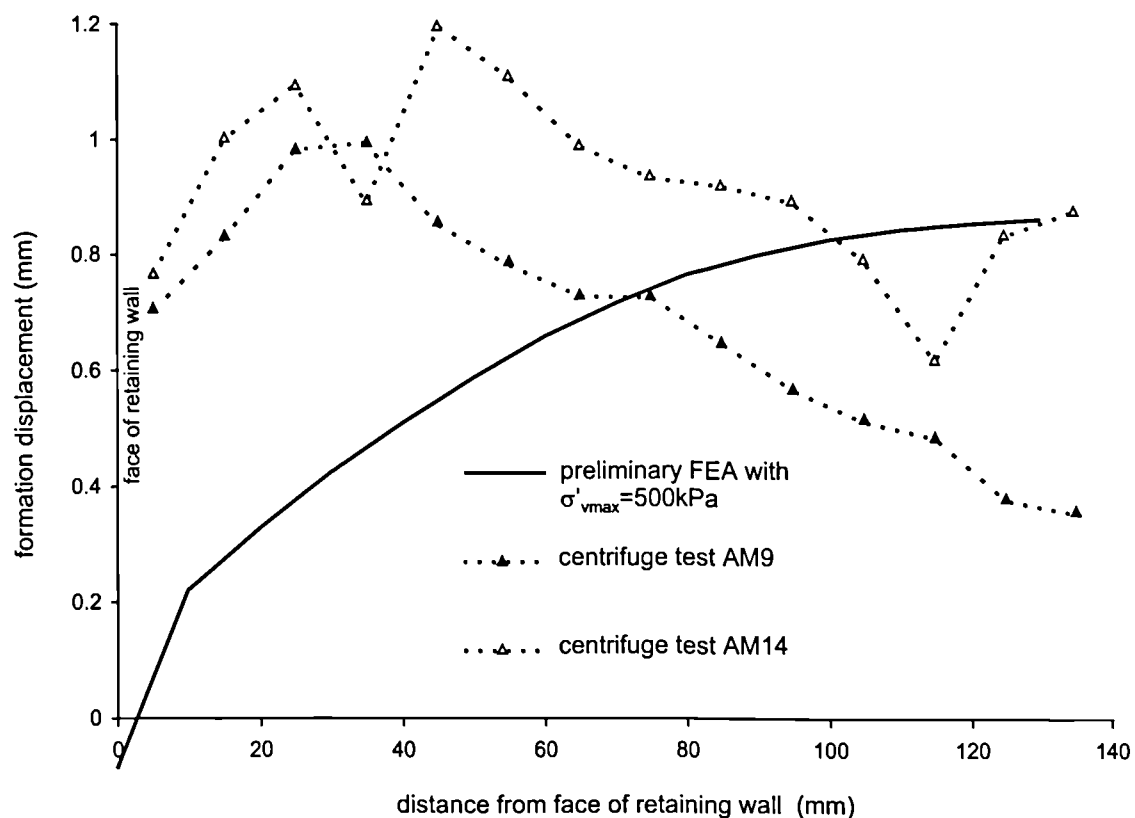
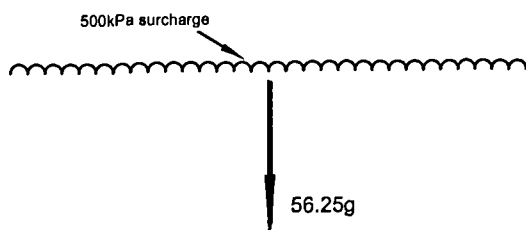
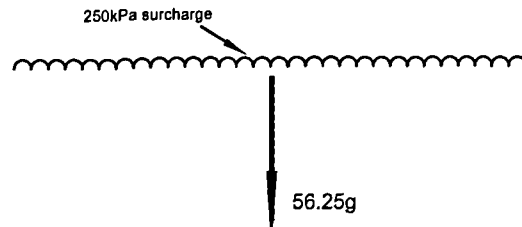


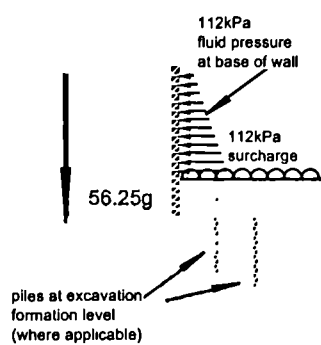
Figure 5.5 Comparison of formation displacement predicted by preliminary finite element analyses with results of centrifuge test AM9 and test AM14.



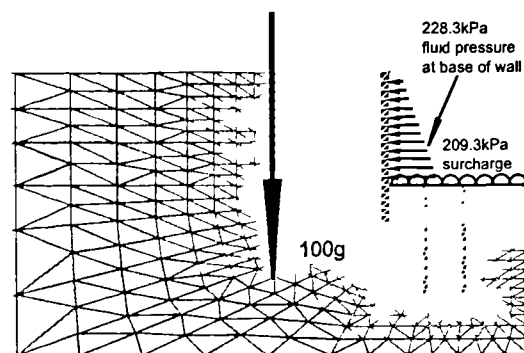
Stage 1 Maintain gravity at 56.25g and consolidate under surcharge loading of 500kPa.



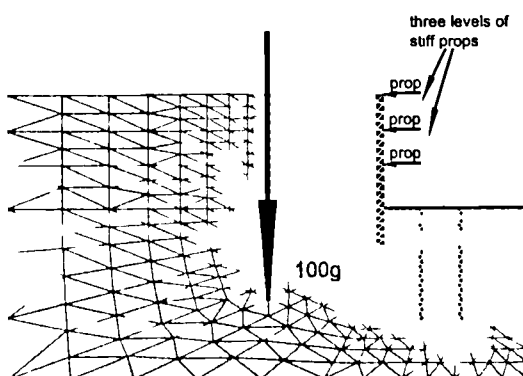
Stage 2 Maintain gravity at 56.25g. Swell to 250kPa by reducing surcharge loading.



Stage 3 Remove surcharge. Substitute wall and pile elements. Remove the soil elements in the area of the excavation. Replace soil elements with pressures equivalent to calculated stresses acting at base of wall and at excavation formation level with gravity maintained at 56.25g.



Stage 4 Increase gravity to 100g and increase support stresses. Allow consolidation of excess pore pressures.



Stage 5 Remove pressures at excavation boundaries and place props. This sequence carried out from top down with successive levels of props in place prior to excavation beneath.

Figure 5.6 Typical sequence of events modelled in finite element analyses.



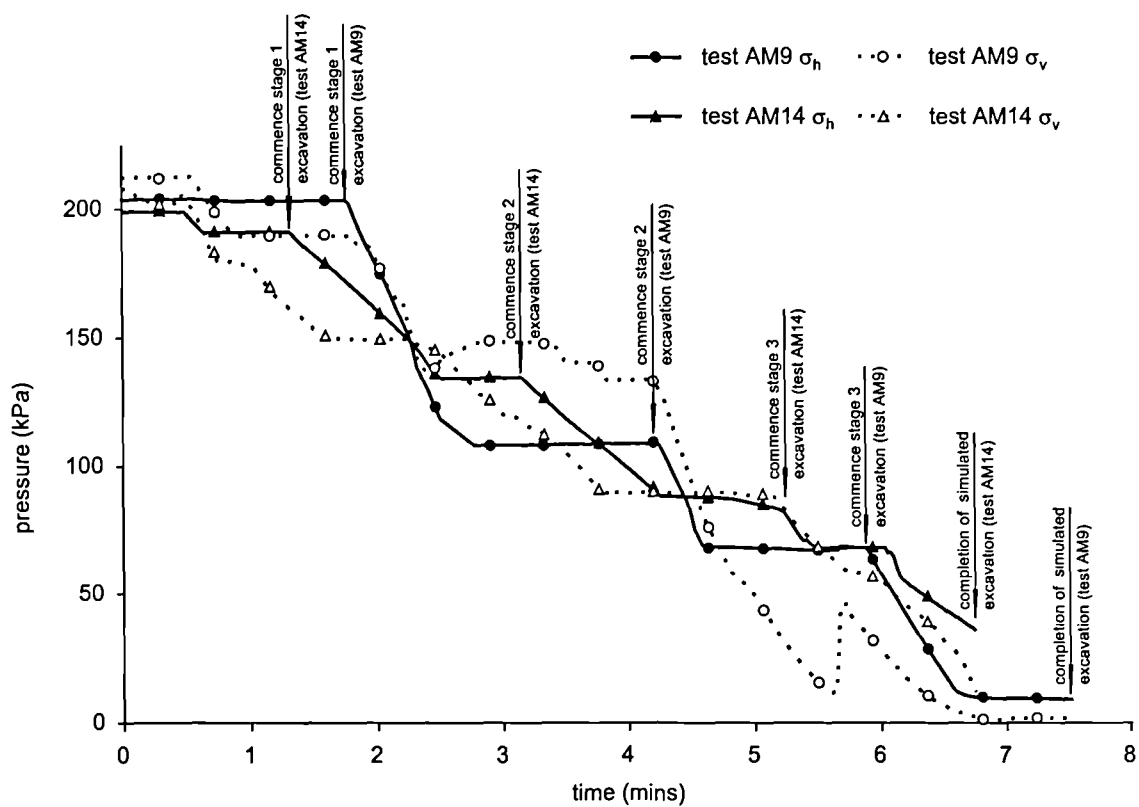


Figure 5.7 Variation in excavation support pressure during centrifuge model tests AM9 and AM14.

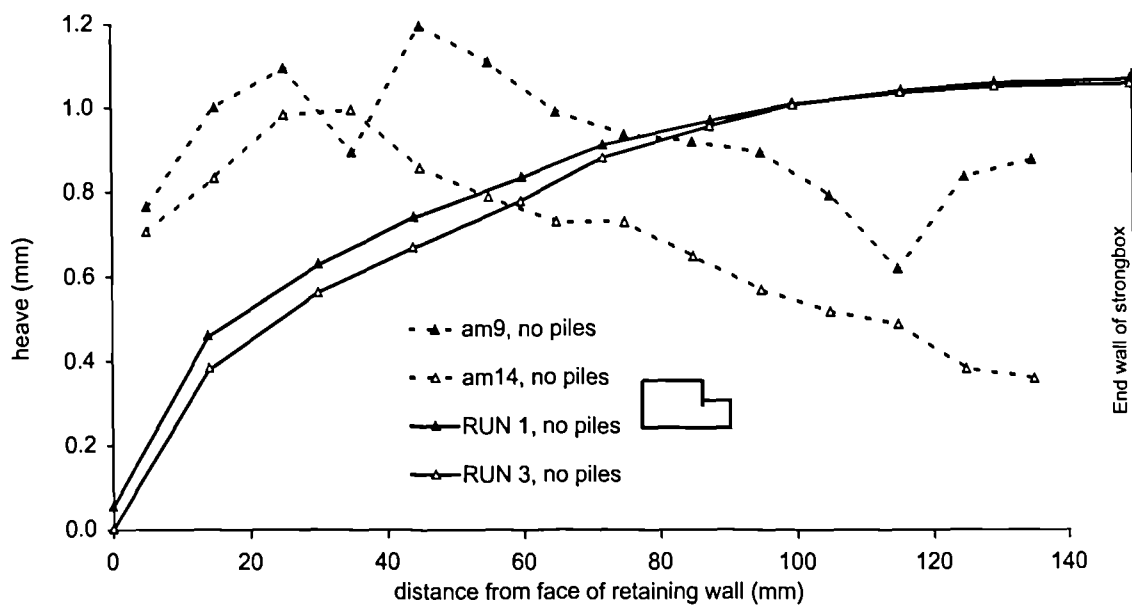


Figure 5.8 Comparison of heave at excavation formation level in FEA and centrifuge tests in which piles were not modelled.

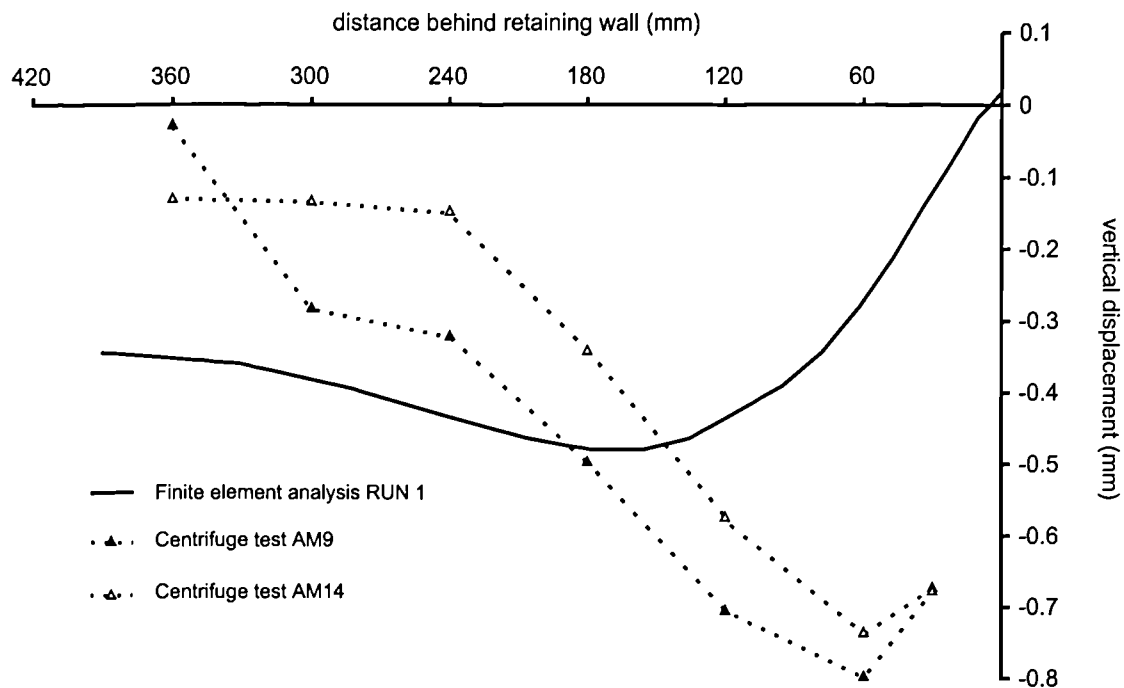


Figure 5.9 Comparison of settlement behind retaining wall at completion of simulated excavation between centrifuge model tests AM9 and AM14 and finite element analysis RUN1.

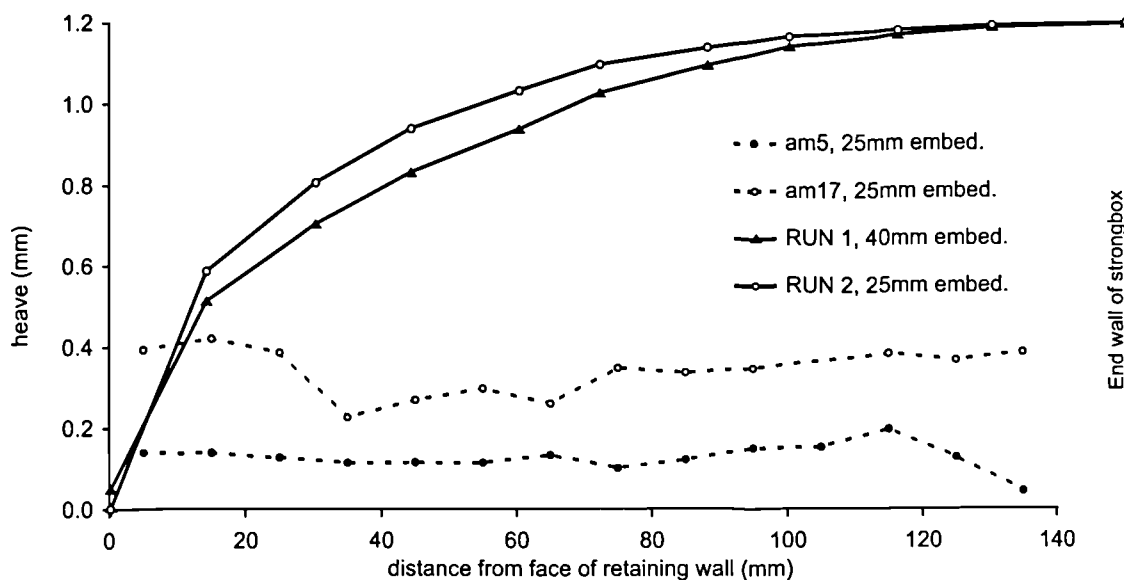


Figure 5.10 Comparison of formation displacements at end of excavation for centrifuge tests on shallow embedded walls and FEA on deep and shallow embedded walls.

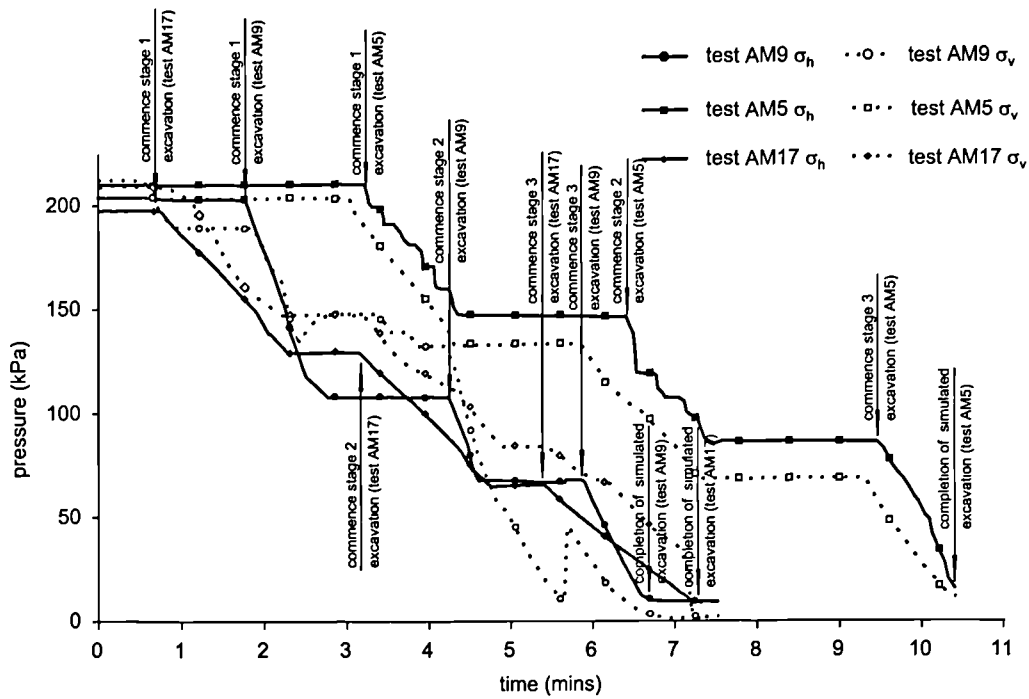


Figure 5.11 Variation in excavation support pressure during centrifuge model tests AM9, the excavation sequence of which was used in the FEA, and centrifuge model tests AM5 and AM17 on shallow embedment walls.

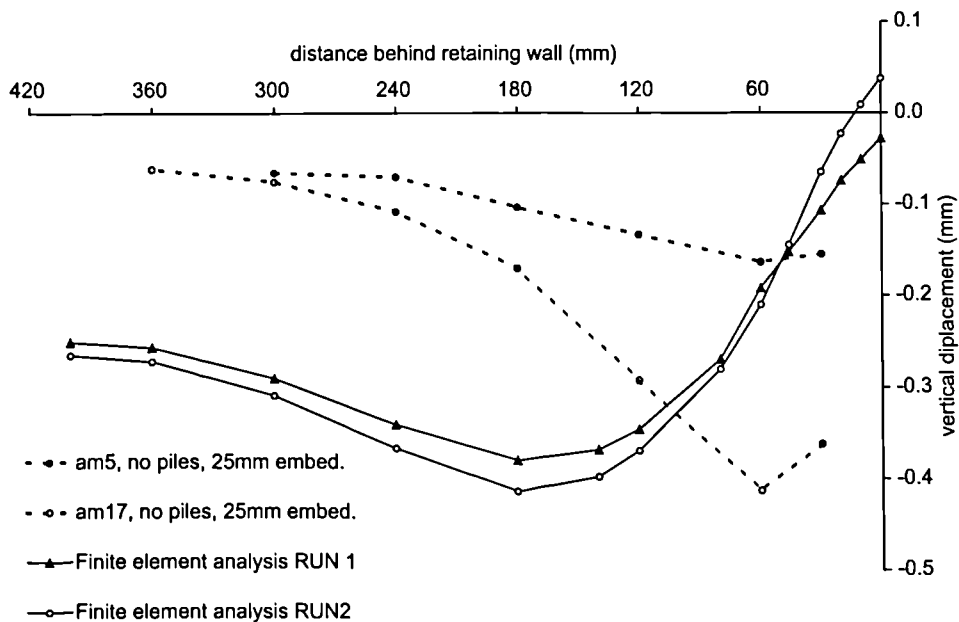


Figure 5.12 Comparison of settlement behind retaining wall at completion of simulated excavation between centrifuge model tests AM5 and AM17, with shallow embedded walls, and finite element analyses RUN1 and RUN2.

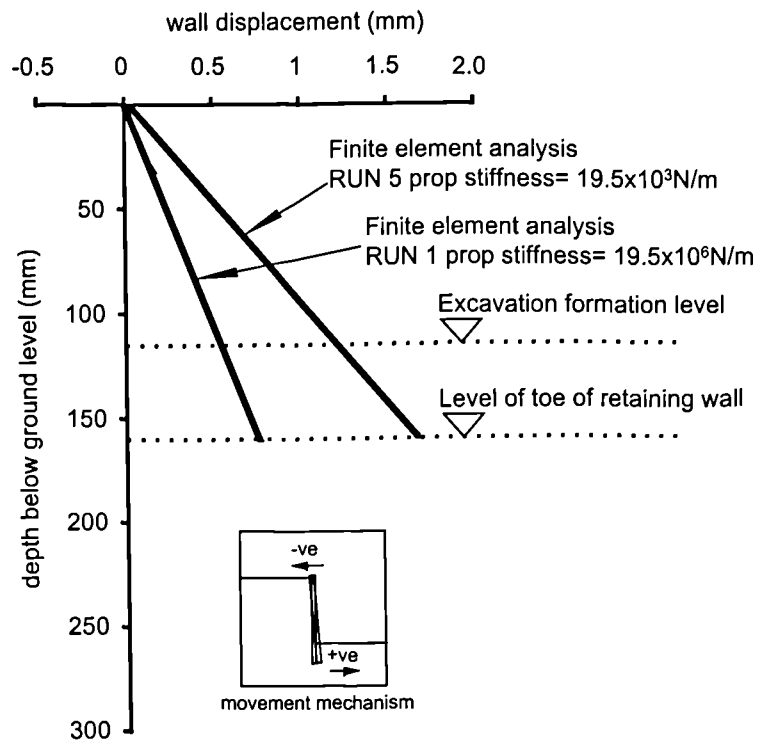


Figure 5.13 Comparison of wall displacement predictions between finite element analyses RUN 1 and RUN 5 in which prop stiffness was varied.

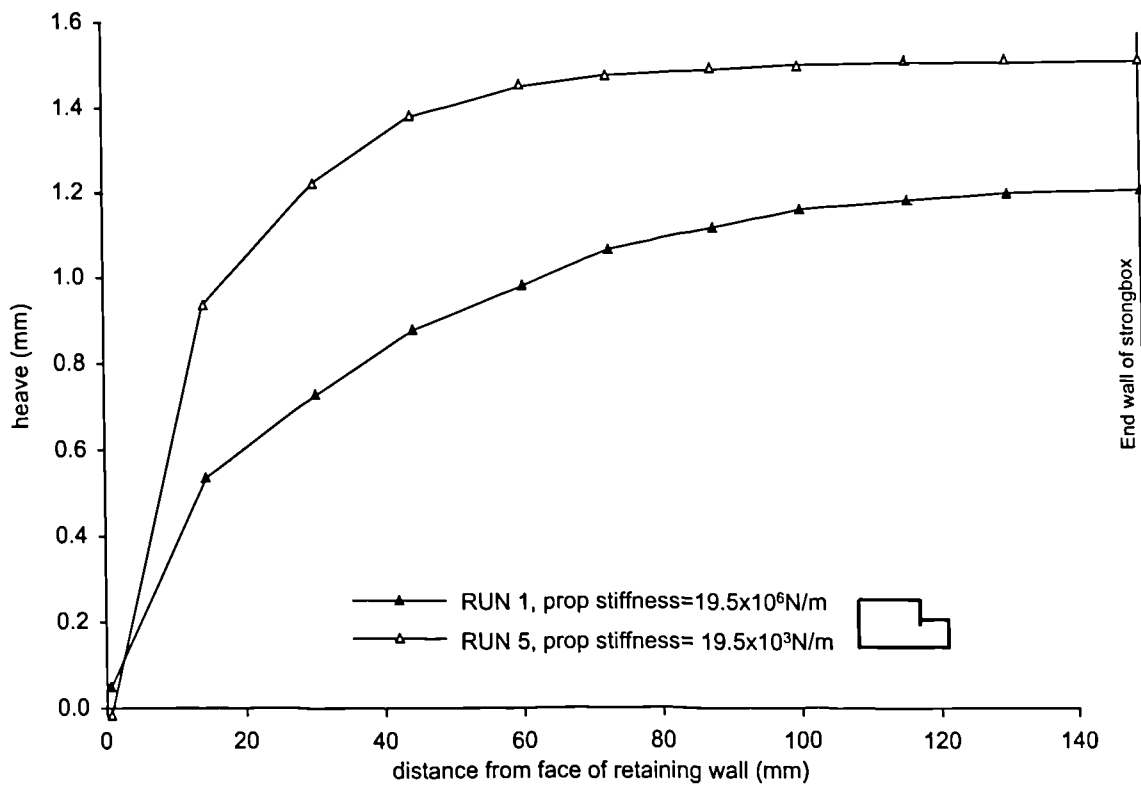


Figure 5.14 Comparison of displacement at excavation formation level between finite element analyses RUN 1 and RUN 5 in which prop stiffness was varied.

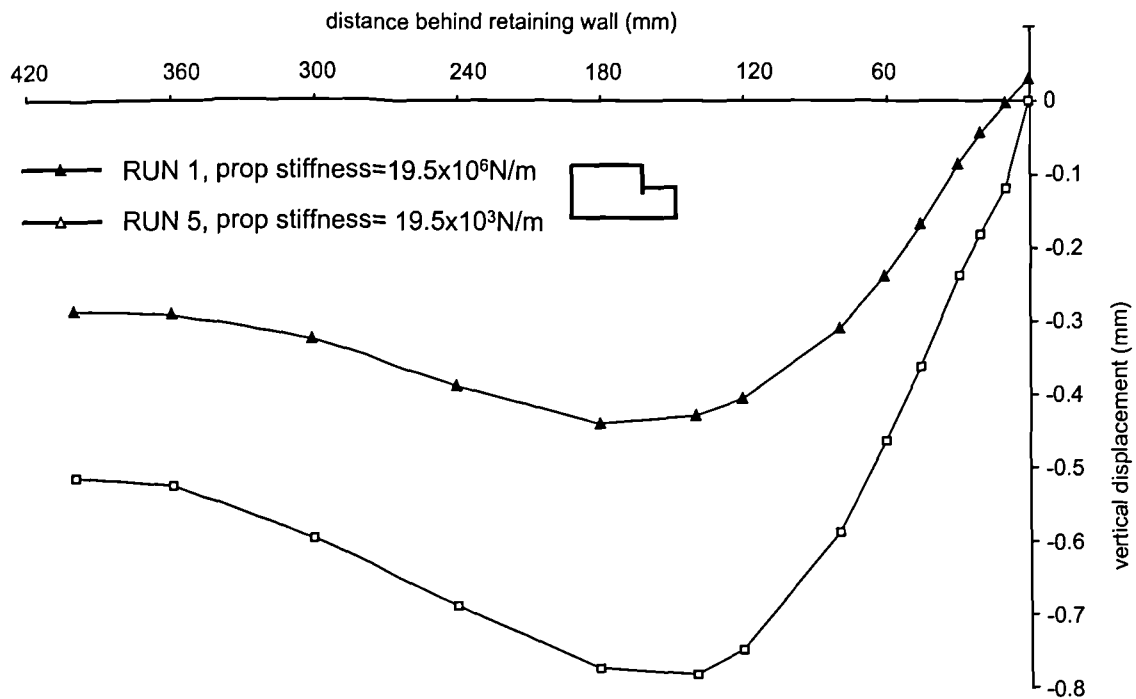


Figure 5.15 Comparison of displacement retained ground surface between finite element analyses RUN 1 and RUN 5 in which prop stiffness was varied.

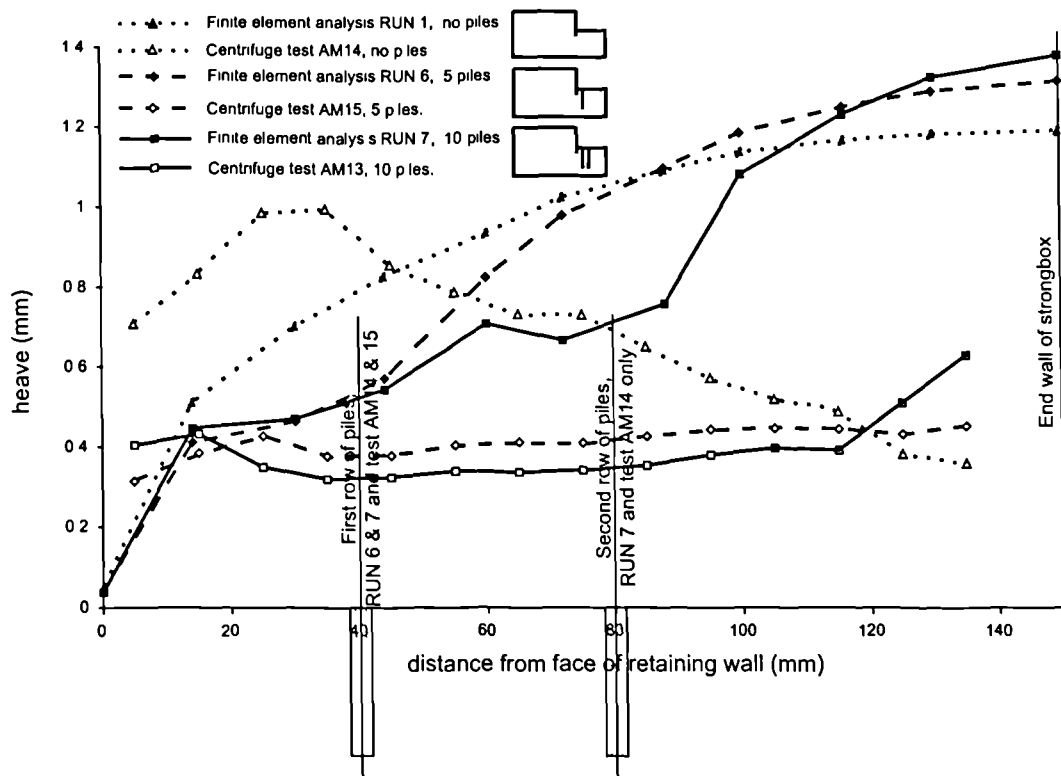


Figure 5.16 Comparison of heave measured in centrifuge model tests with and without piles with that predicted by FEA.

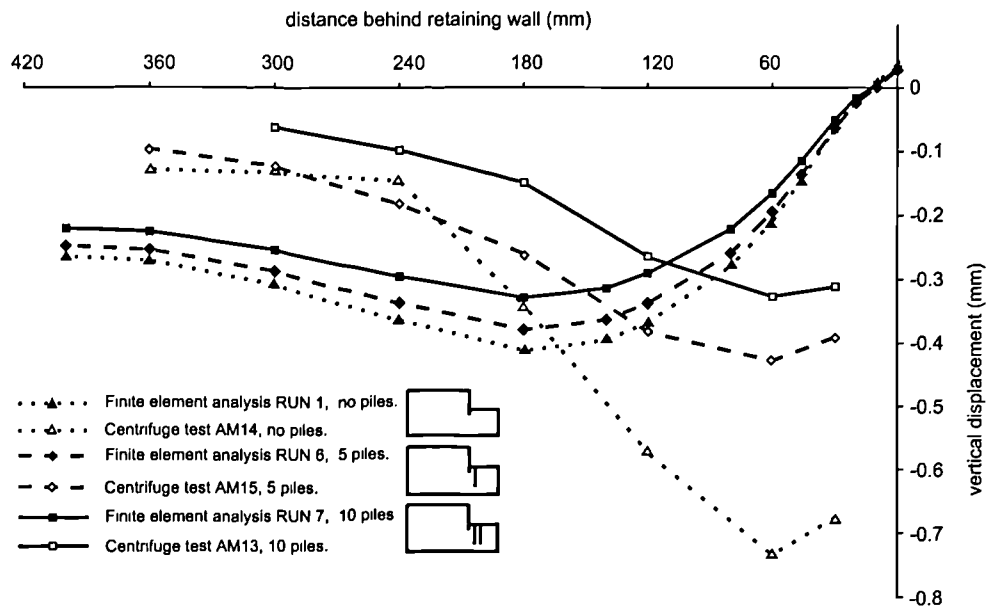


Figure 5.17 Comparison of settlement behind retaining wall at completion of simulated excavation between centrifuge model tests AM13, AM14 and AM15 and finite element analyses RUN1, RUN6 and RUN7.

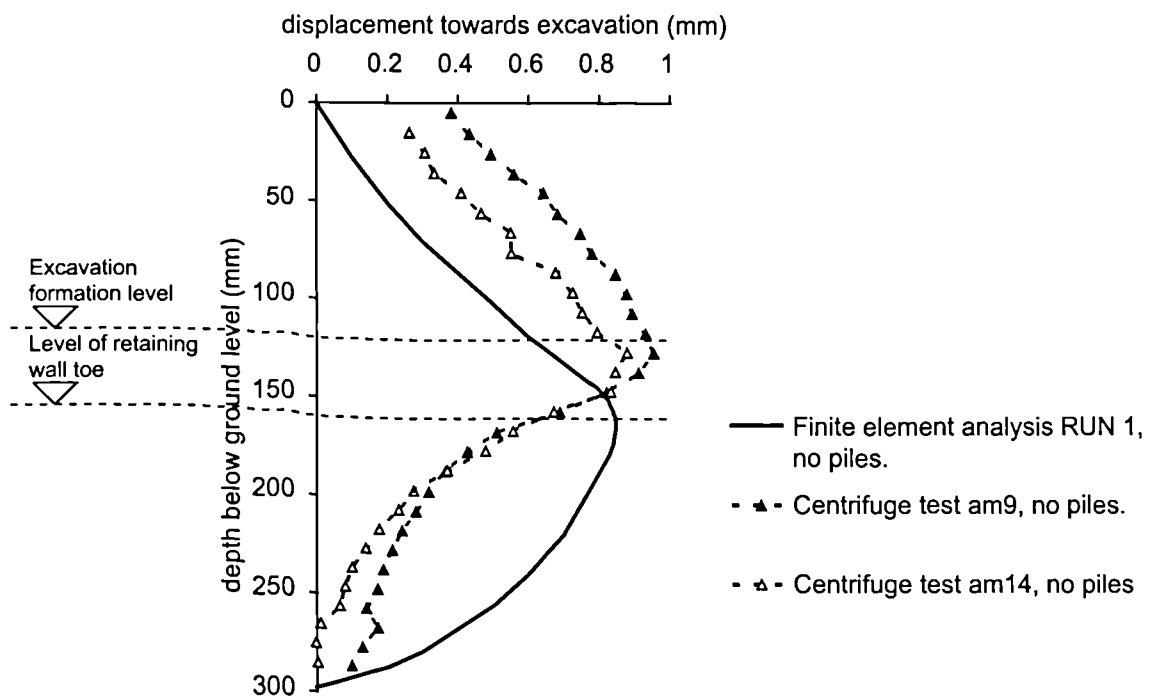
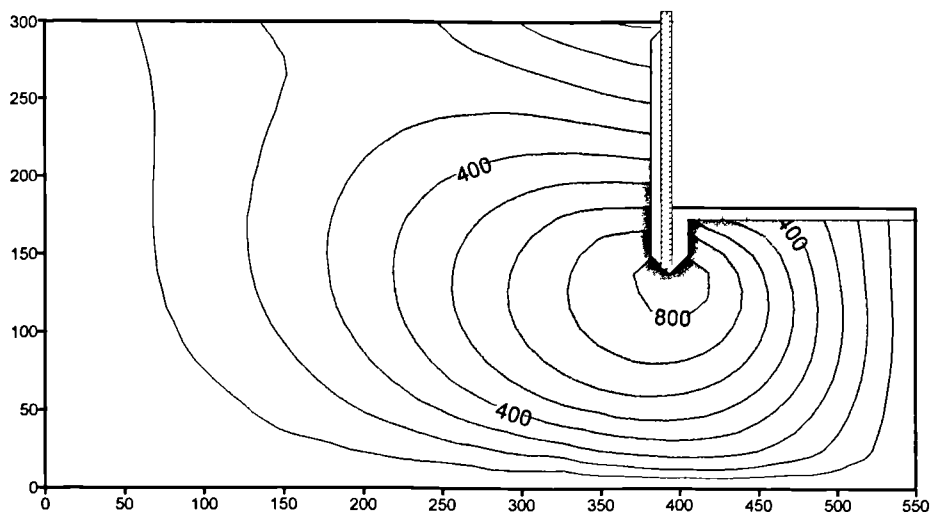
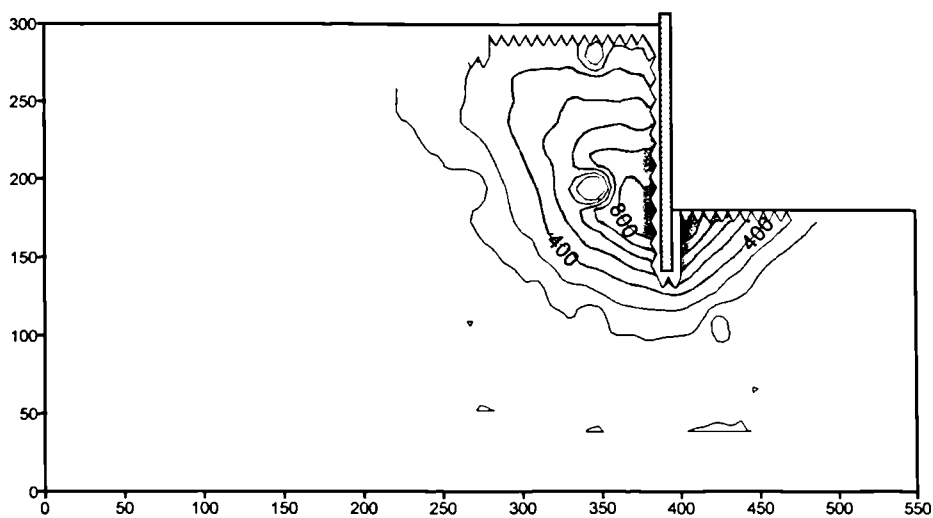


Figure 5.18 Comparison between the finite element analysis RUN 1 prediction of horizontal displacement behind the retaining wall and that measured using image analysis in centrifuge test AM9 and AM14.



a) Contours of horizontal displacement from finite element analysis RUN 1.



b) Contours of horizontal displacement from centrifuge test AM14 at completion of simulated excavation.

Figure 5.19 Comparison between contours of horizontal displacement in finite element analysis and centrifuge test. (Displacement in  $\mu\text{m}$ )

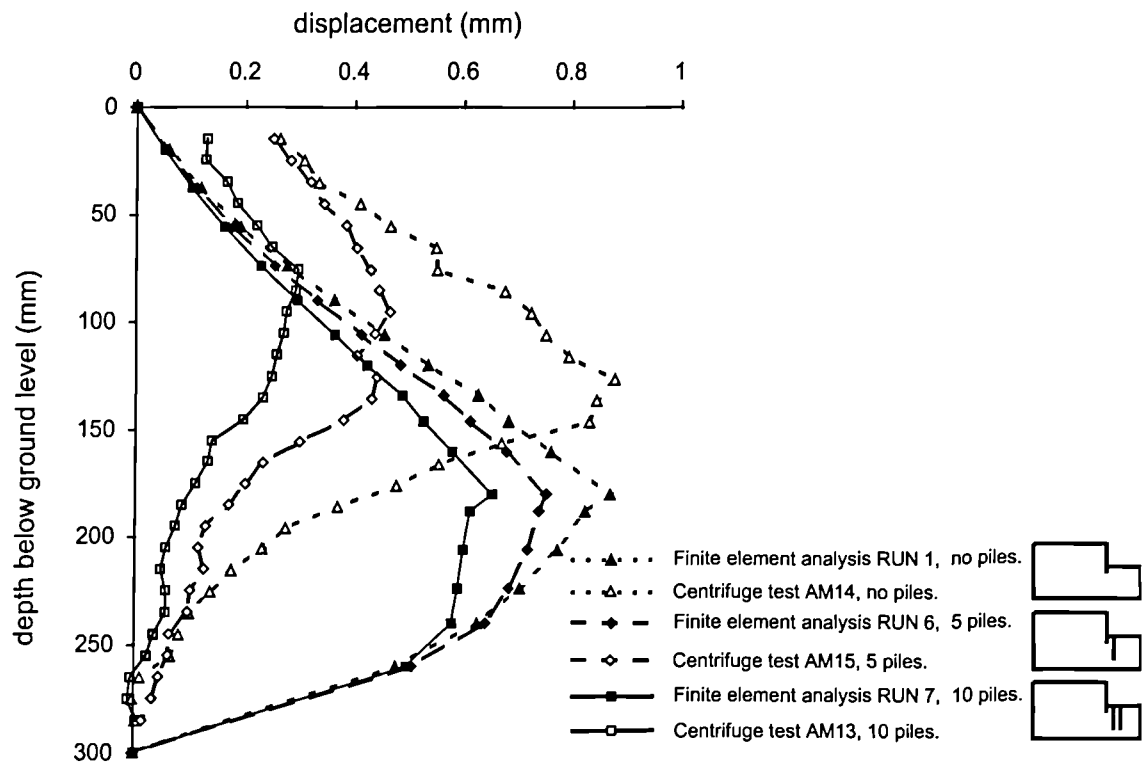


Figure 5.20 Comparison of horizontal displacements measured behind the retaining wall in centrifuge model tests with FEA predictions of wall displacement and displacement below the wall for tests with varying numbers of piles.

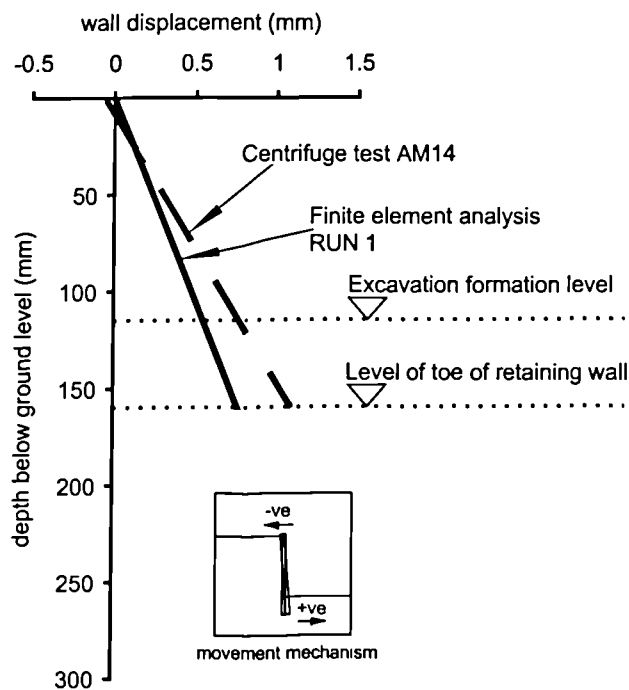


Figure 5.21 Comparison of wall displacement predicted by finite element analysis RUN 1 and centrifuge test AM14.



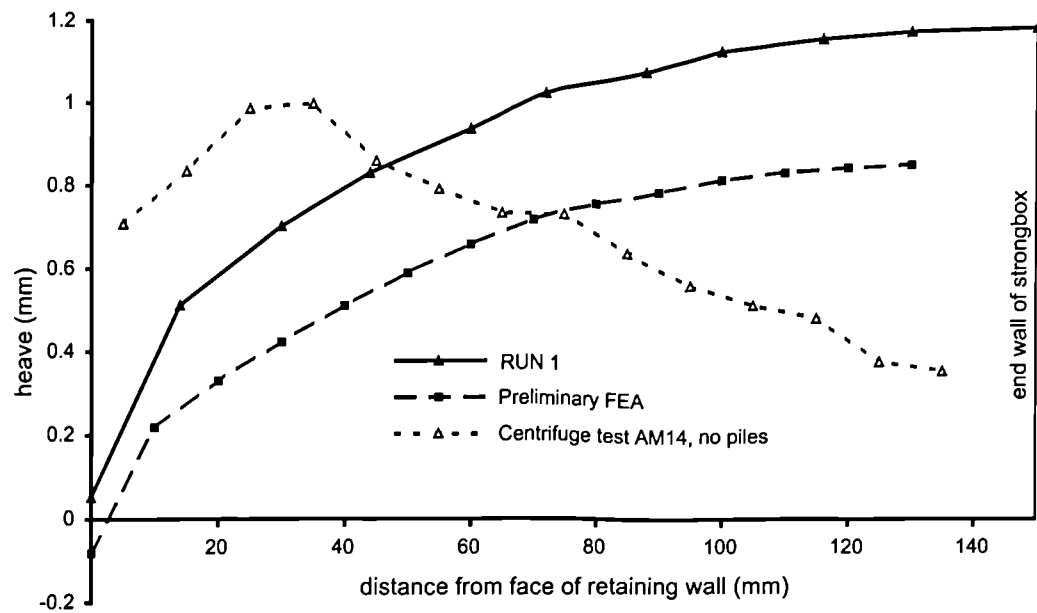


Figure 5.22 Comparison of heave in centrifuge model test AM14, in which no piles were used, with the predictions of preliminary finite element analyses carried out prior to model testing and a more detailed analysis.

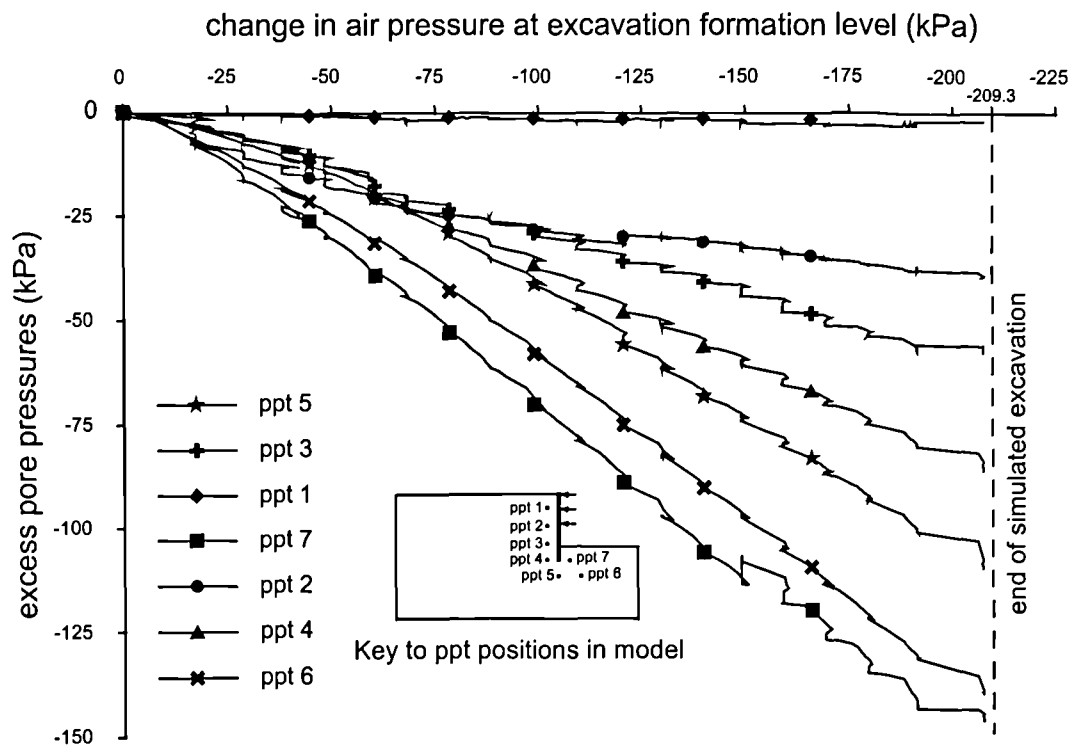


Figure 6.1 Generation of excess pore pressures during the simulated excavation stage of a typical test (AM13).

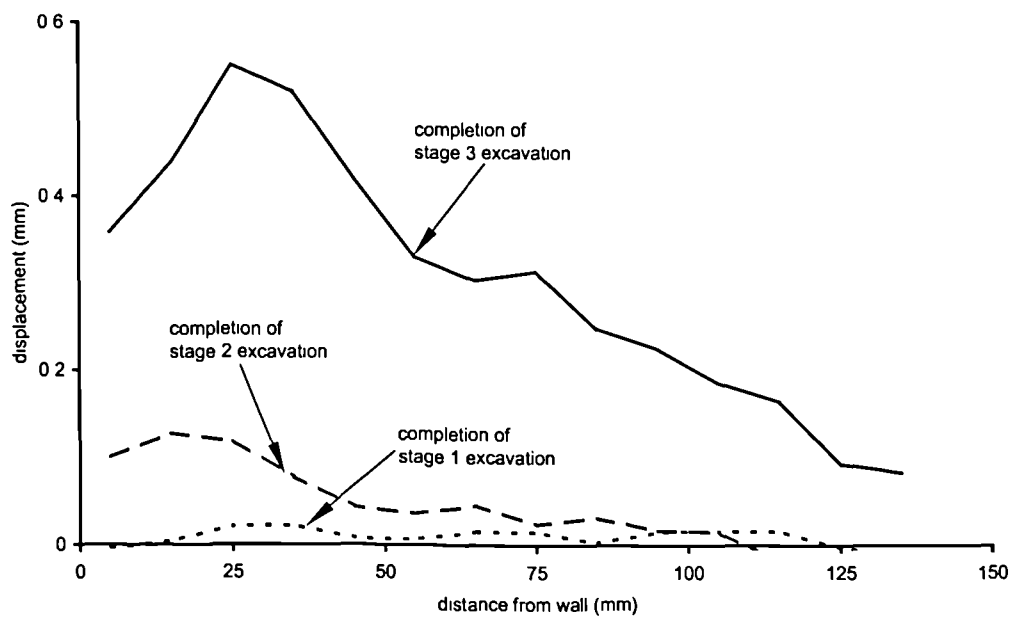


Figure 6.2 Development of excavation formation displacements during the simulated excavation stage of a typical test (AM14).

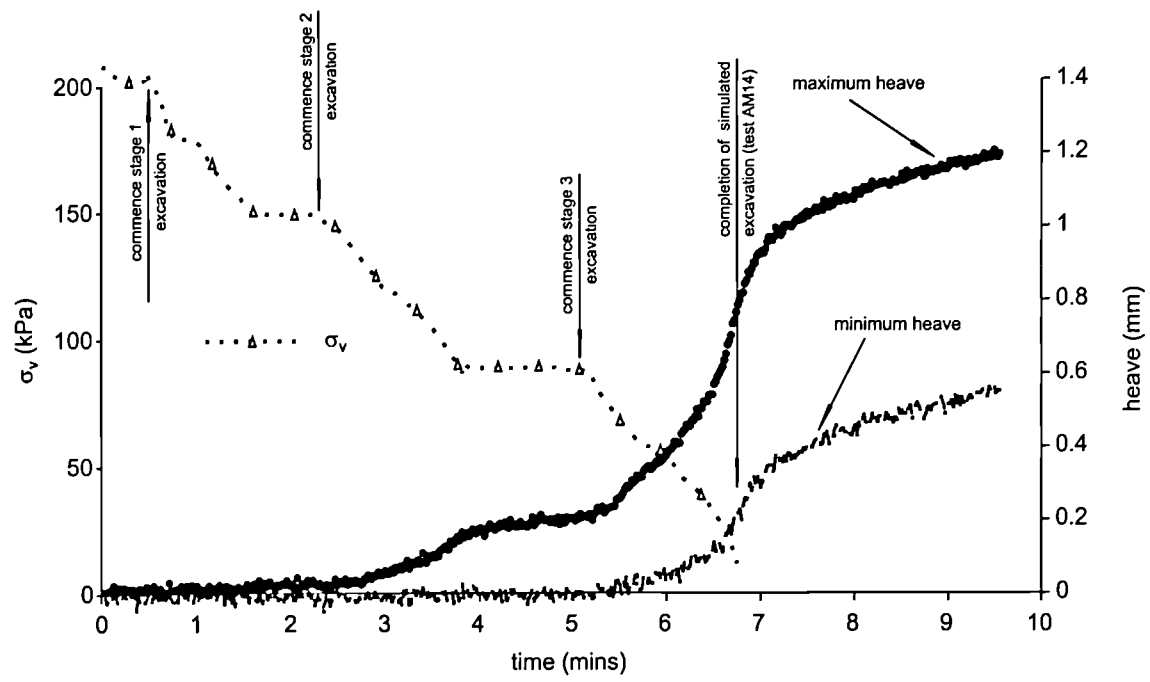
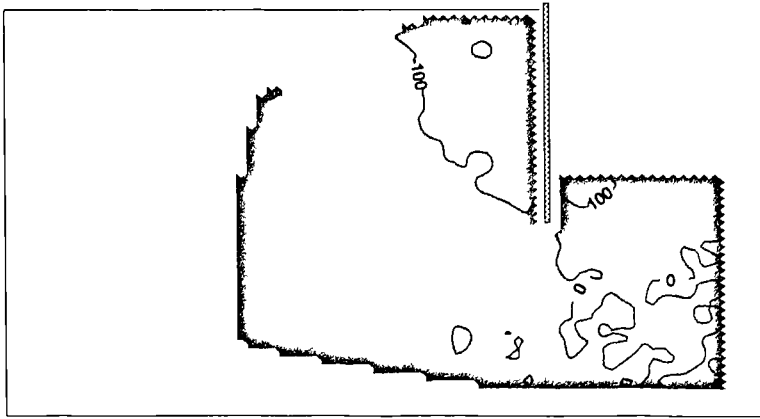
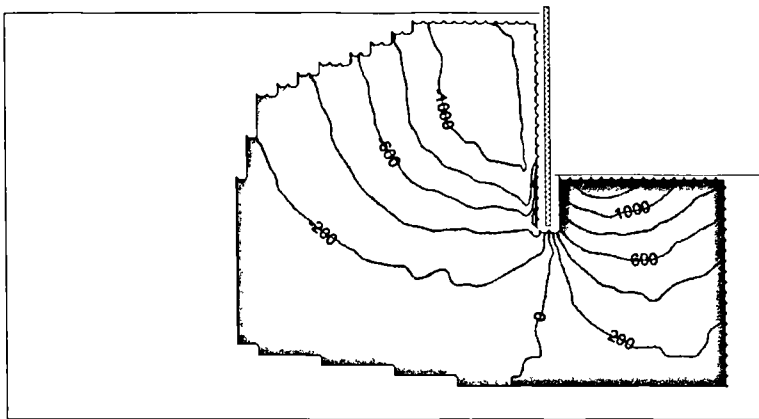


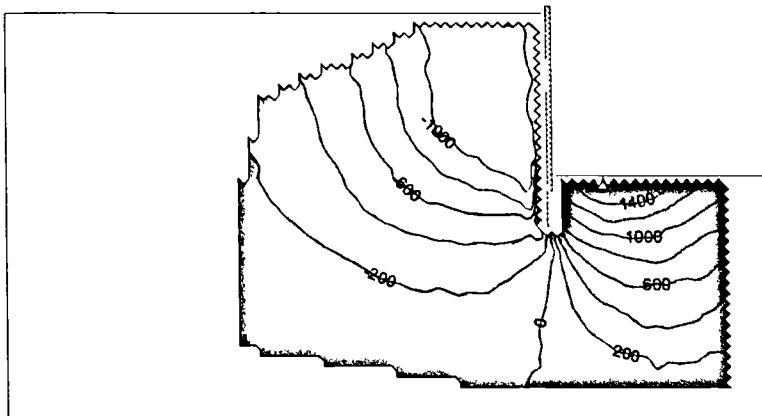
Figure 6.3 Development of heave during simulated excavation in test AM14.



- a) At completion of simulated excavation. A small amount of heave is well established over a substantial depth beneath the excavation.



- b) After 15 minutes. Softening at formation level has resulted in large increases in heave in front of the retaining wall toe. Displacements at ground level have increased dramatically.



- c) After 30 minutes. Heave and settlements have increased but at a much reduced rate.

Figure 6.4 Contours of vertical displacement at key stages during test AM14 (displacements in  $\mu\text{m}$ )

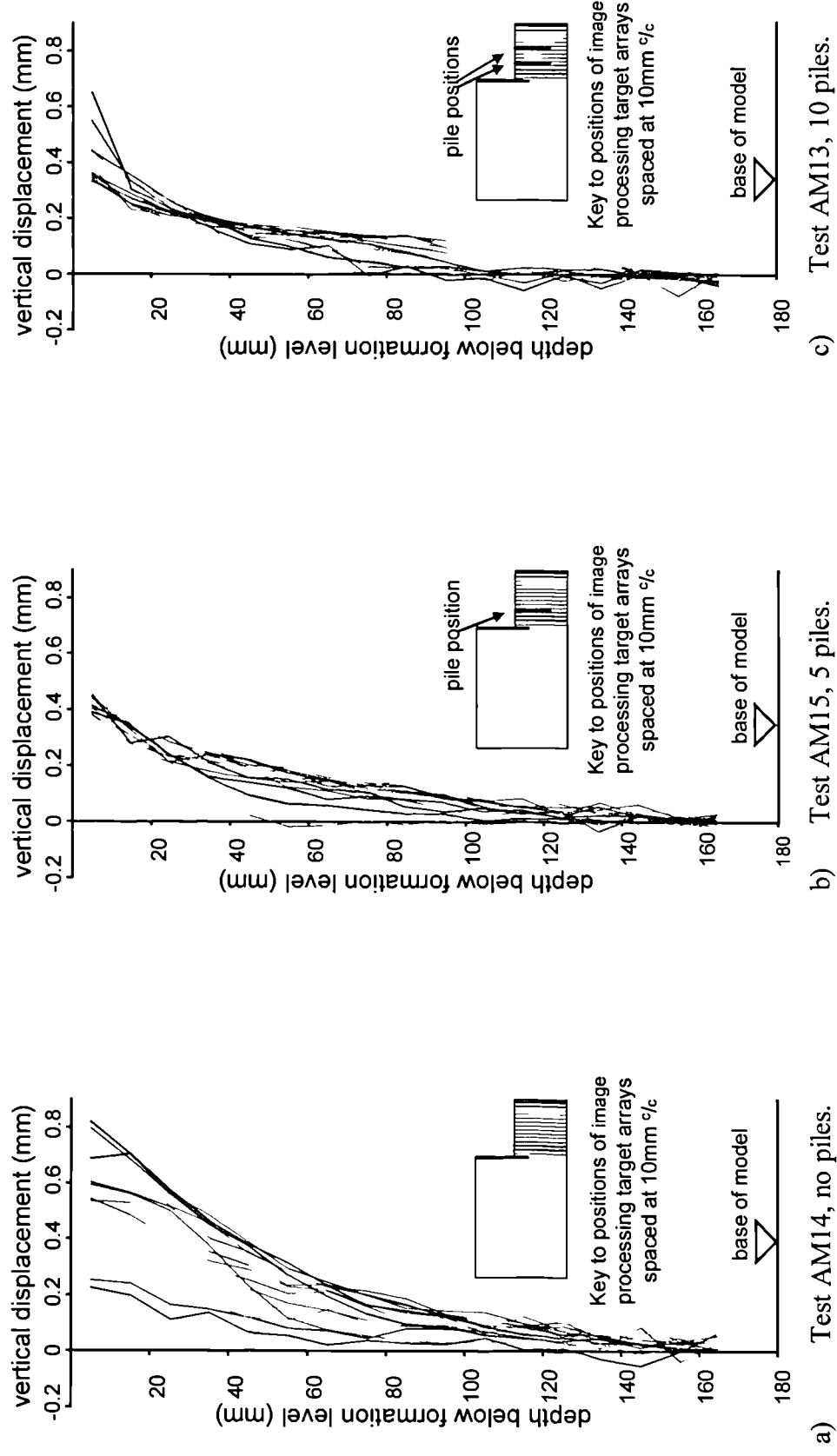


Figure 6.5a-c Comparison of vertical displacements in the soil below excavation formation level in tests AM13, AM14 and AM15, measured using image processing on completion of the simulated excavation.

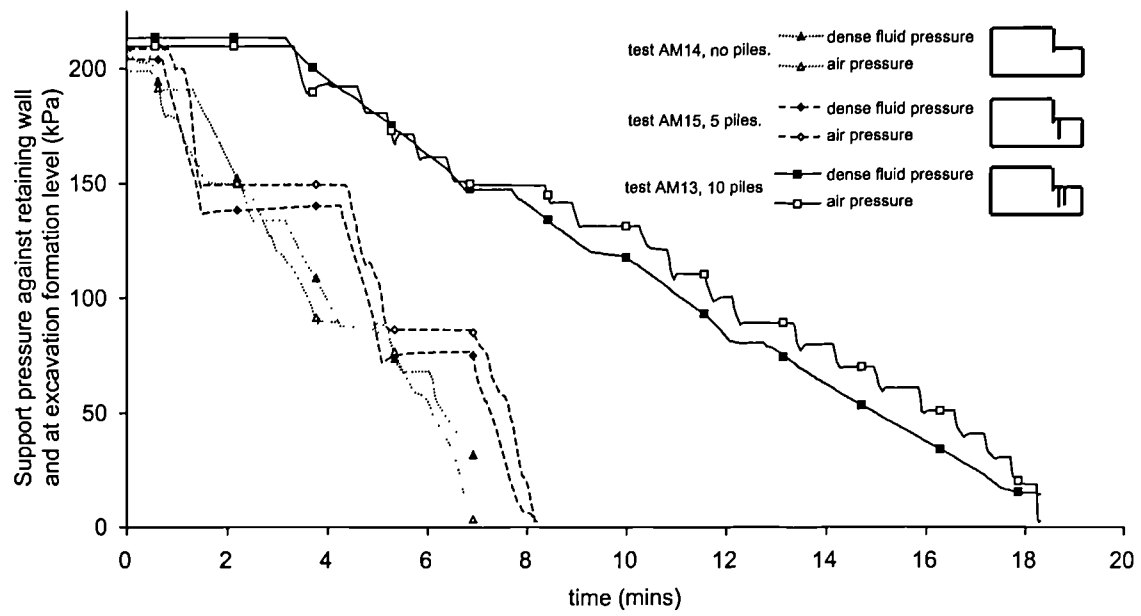
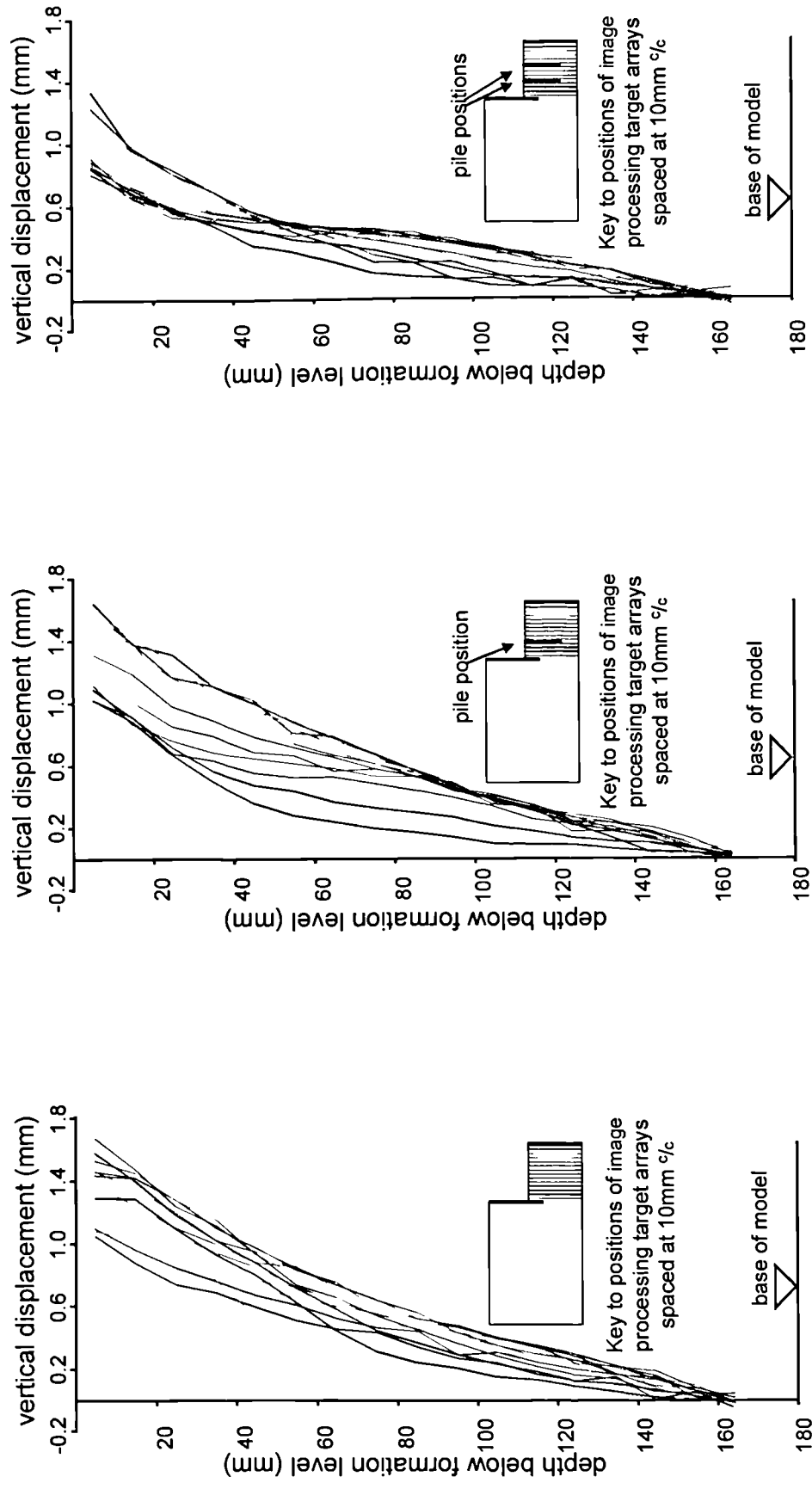
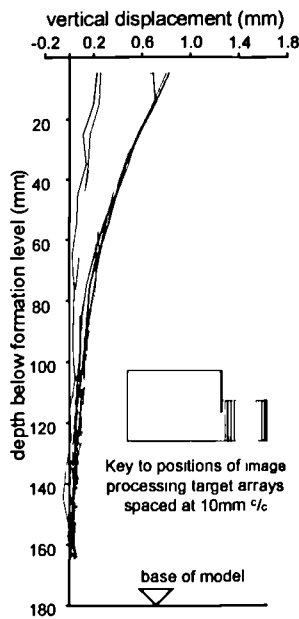


Figure 6.6 Relative times for the simulated excavation stage of tests AM13, AM14 and AM15.

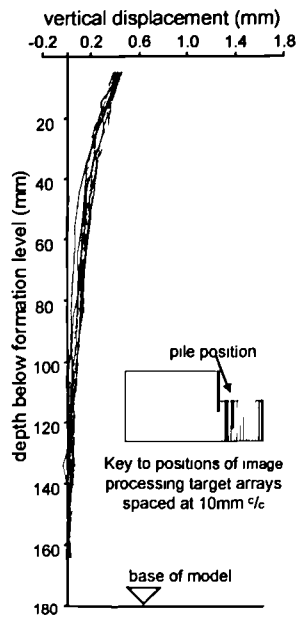


a) Test AM14, no piles. b) Test AM15, 5 piles. c) Test AM13, 10 piles.

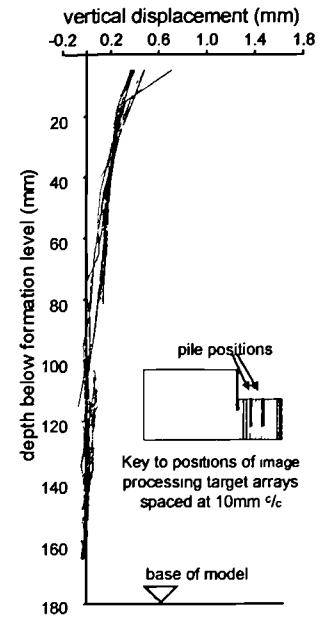
Figure 6.7a-c Comparison of vertical displacements in the soil below excavation formation level in tests AM13, AM14 and AM15, measured using image processing 20 minutes after completion of the simulated excavation following some consolidation.



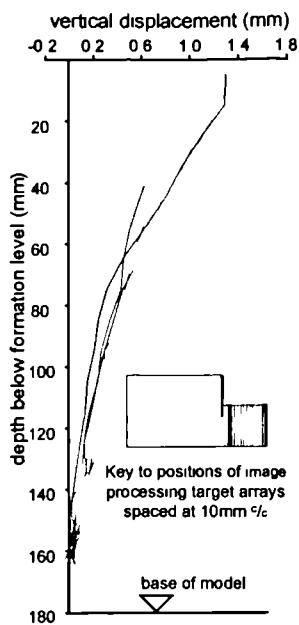
a) Test AM14, no piles.



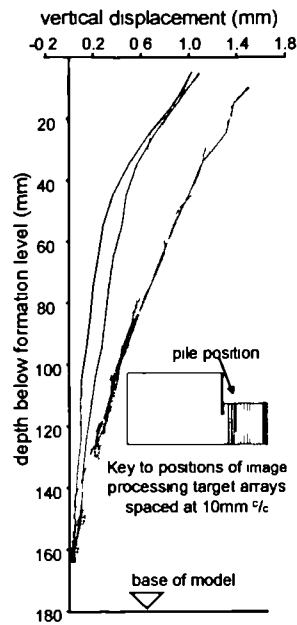
b) Test AM15, 5 piles.



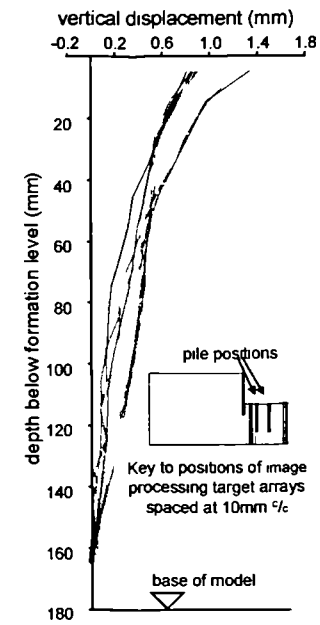
c) Test AM13, 10 piles.



d) Test AM14, no piles.



e) Test AM15, 5 piles.



f) Test AM13, 10 piles.

Figure 6.8a-f Comparison between displacements beneath excavation formation level in tests with and without piles immediately after completion of simulated excavation and 20 minutes later when some consolidation had taken place.



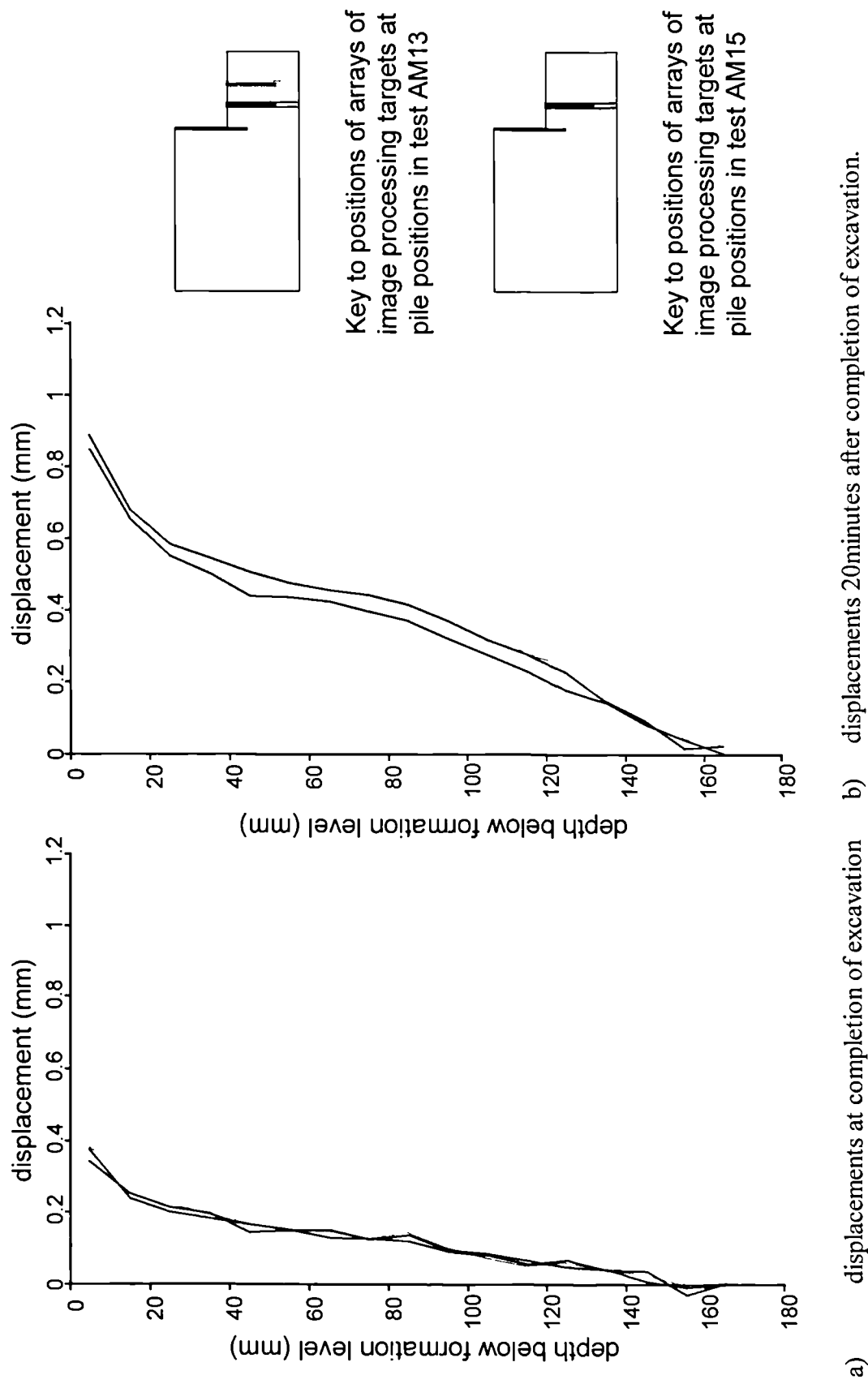
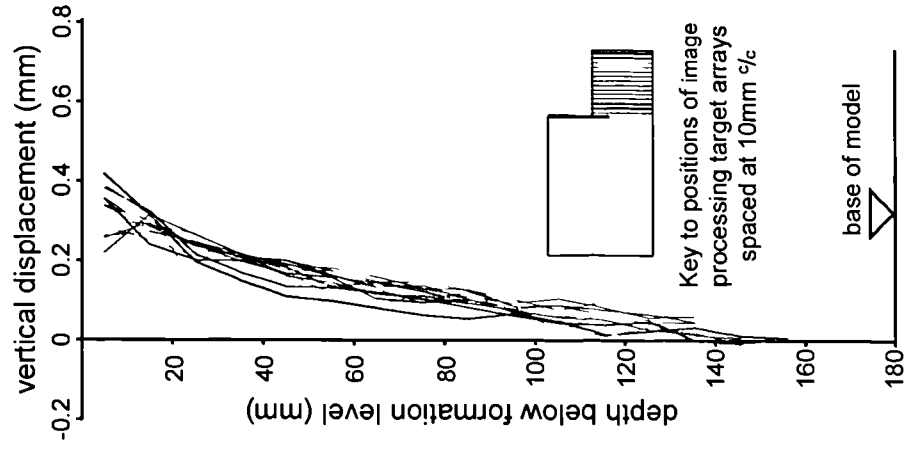
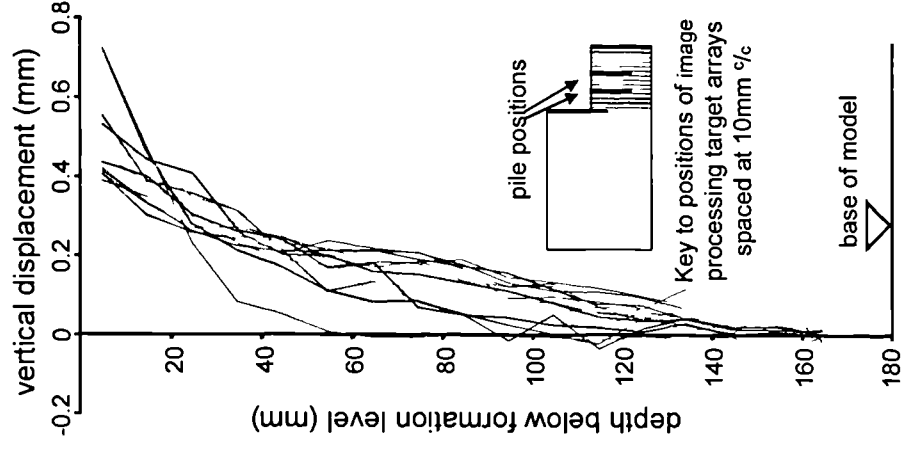


Figure 6.9a-b Comparison of vertical displacements at pile positions in tests AM13 and AM15.



a) Test AM17, no piles



b) Test AM19, 10 piles

Figure 6.10a-b Comparison of vertical displacements in the soil below excavation formation level in tests AM17 and AM19, measured using image processing on completion of the simulated excavation.

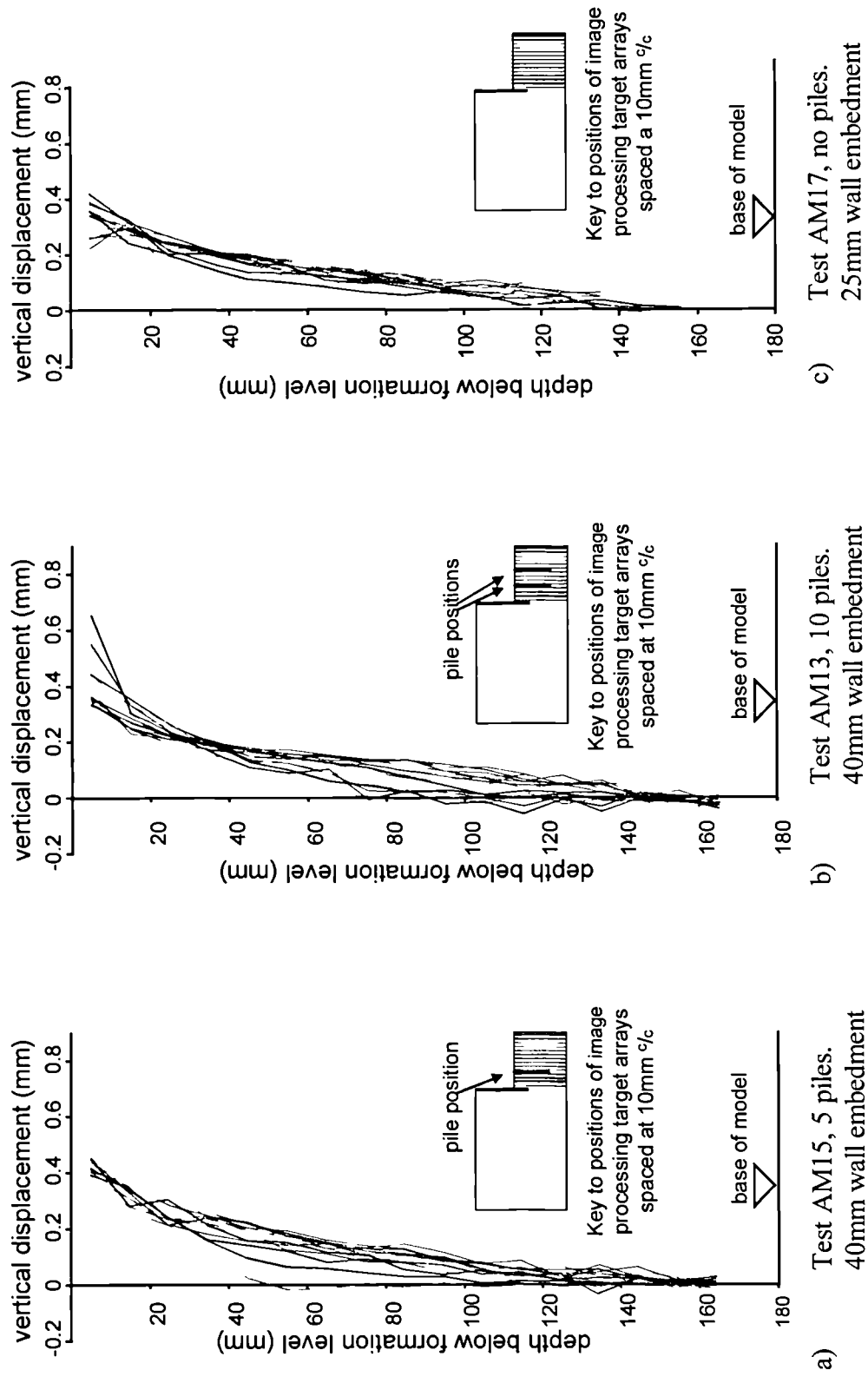


Figure 6.11a-c Comparison of vertical displacements below excavation formation level in tests AM15 AM13, (with 40mm wall embedment) and test AM19, (with 25mm wall embedment), measured using image processing on completion of the simulated excavation.

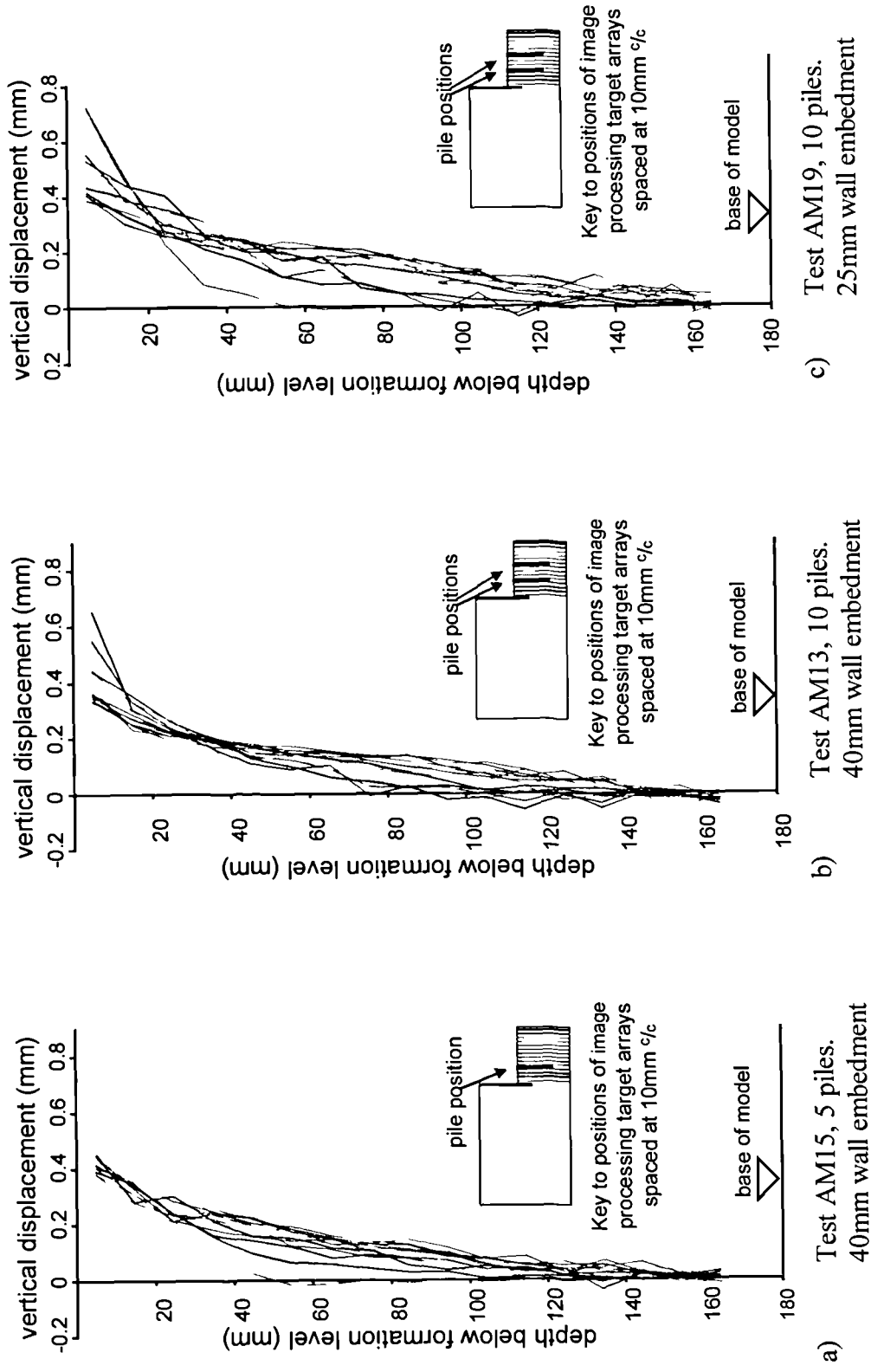
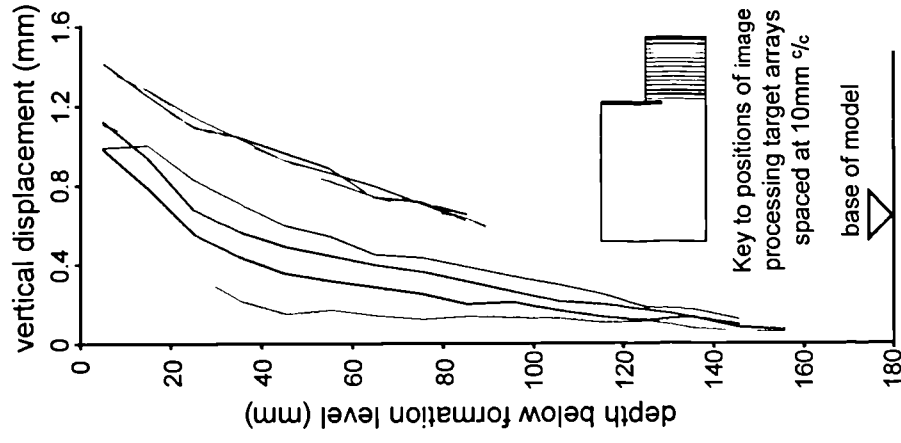
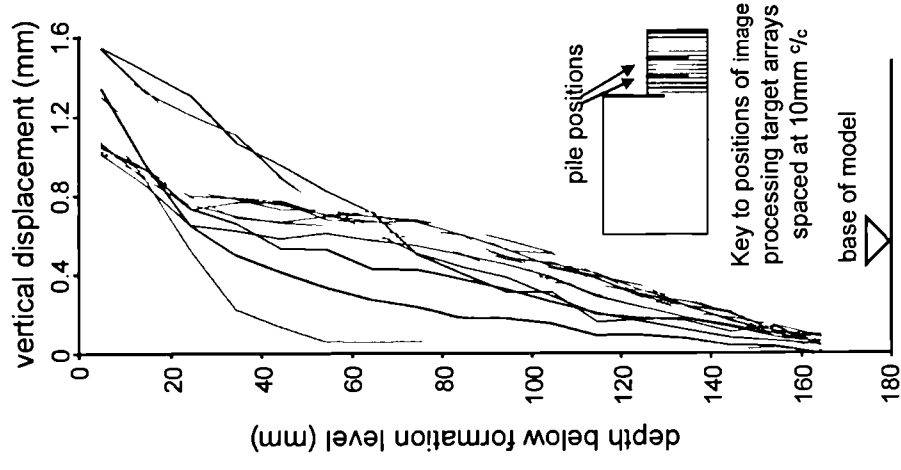


Figure 6.12a-c Comparison of vertical displacements below excavation formation level in tests AM15 AM13, (with 40mm wall embedment) and test AM19, (with 25mm wall embedment), measured using image processing on completion of the simulated excavation.

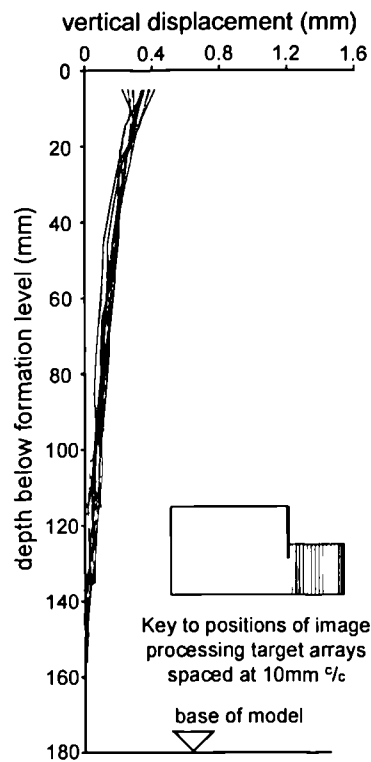


a) Test AM17, no piles

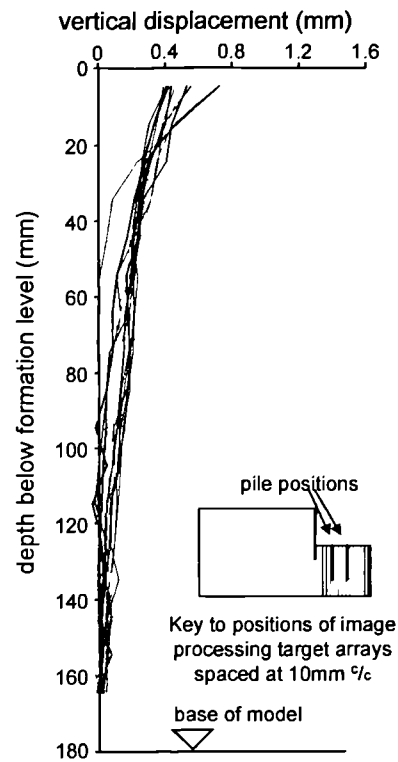


b) Test AM19, 10 piles

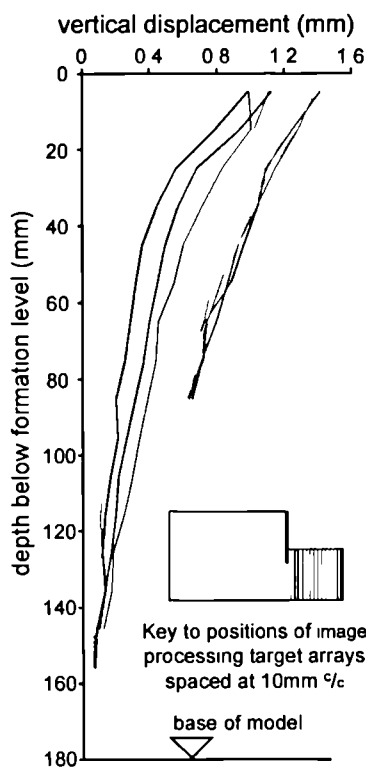
Figure 6.13a-b Comparison of vertical displacements in the soil below excavation formation level in tests AM17 and AM19, measured using image processing 20 minutes after completion of the simulated excavation.



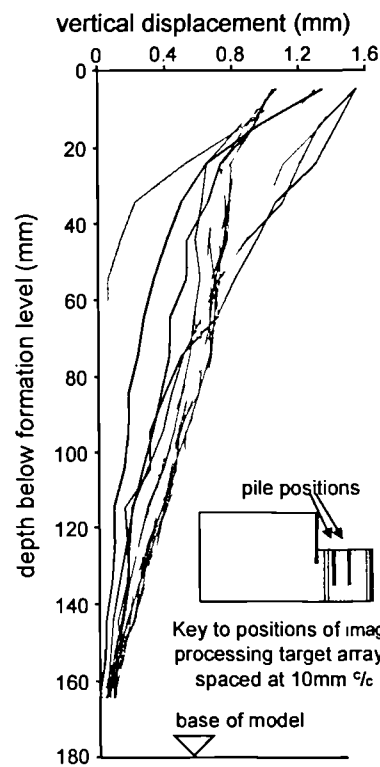
a) Test AM17, no piles



b) Test AM19, 10 piles



c) Test AM17, no piles



d) Test AM19, 10 piles

Figure 6.14a-d Comparison between displacements beneath excavation formation level in tests with and without piles immediately after completion of simulated excavation and 20 minutes later when some consolidation had taken place. (25mm wall embedment depth).

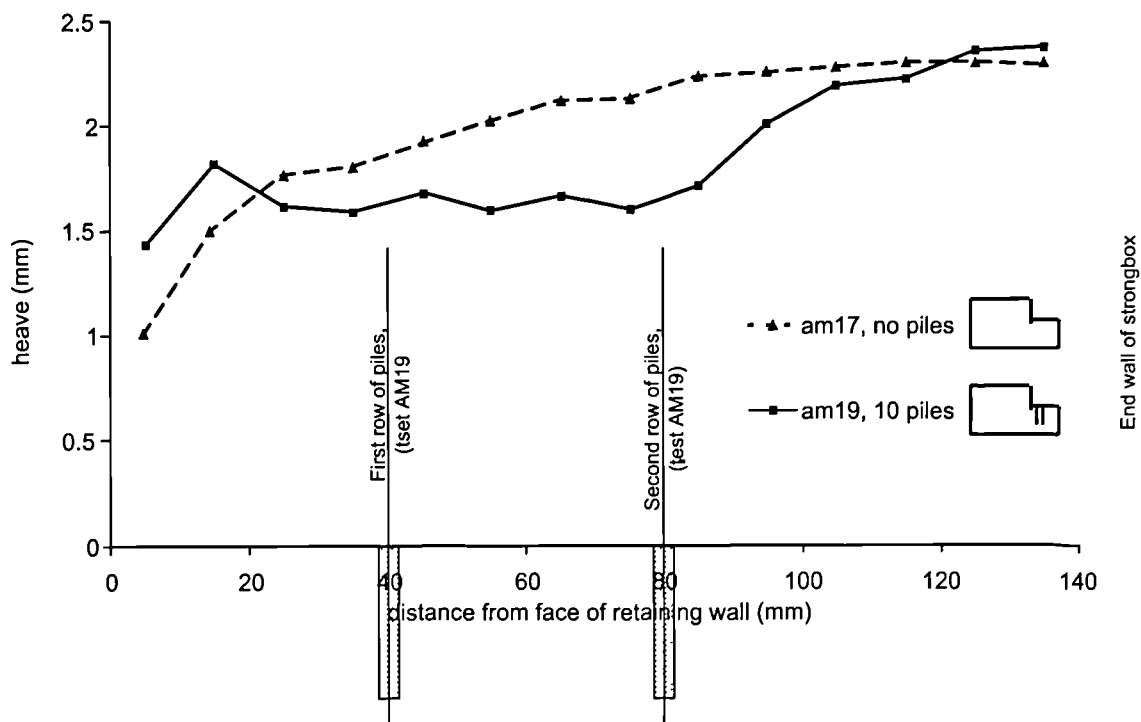


Figure 6.15 Comparison of excavation formation displacements between tests AM17 and AM19 following a 60 minute period of consolidation after the simulated excavation stage of the test.

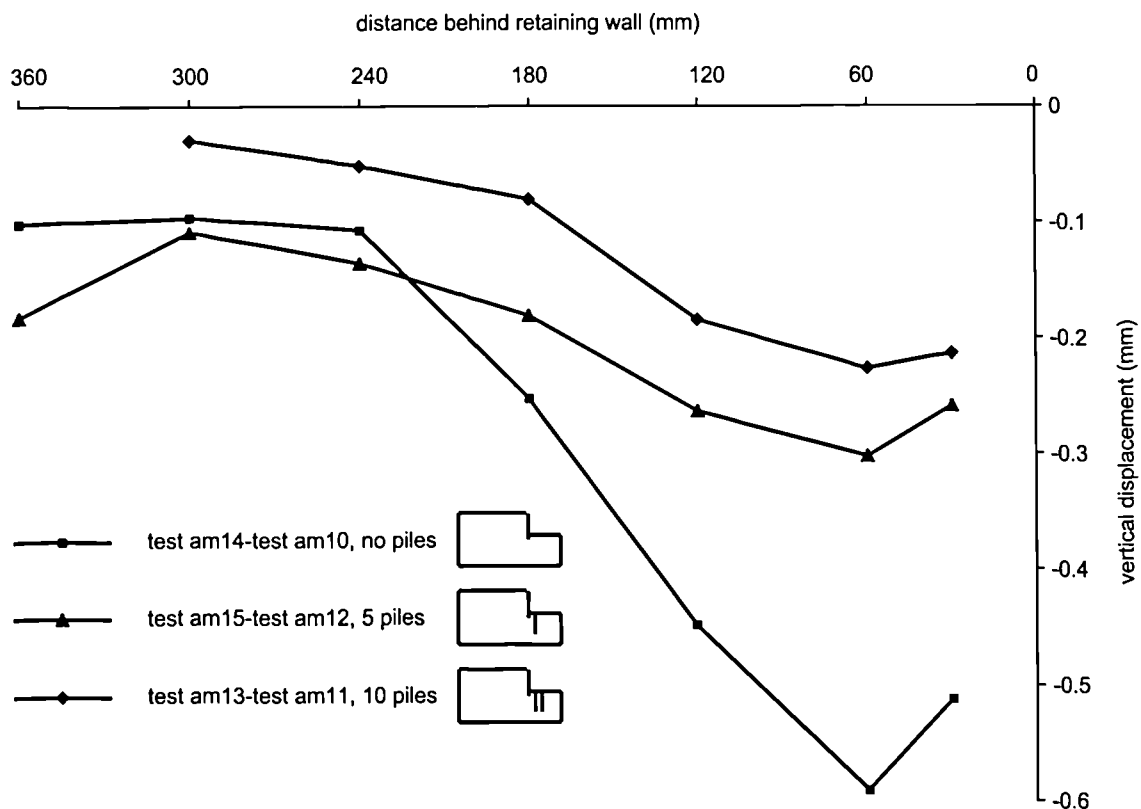


Figure 6.16 Comparison of approximate retained surface settlements attributable to horizontal movement of the retaining wall at the end of the simulated excavation stage of typical tests.

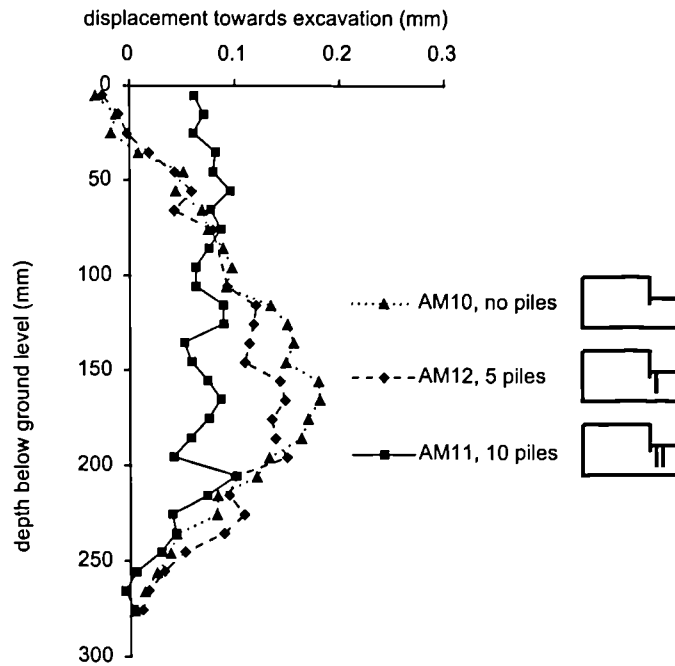


Figure 6.17 Horizontal displacements of retaining wall at the end of simulated excavation in tests AM10, AM11 and AM12 in which the retaining wall was effectively fixed horizontally owing to the use of modified apparatus.

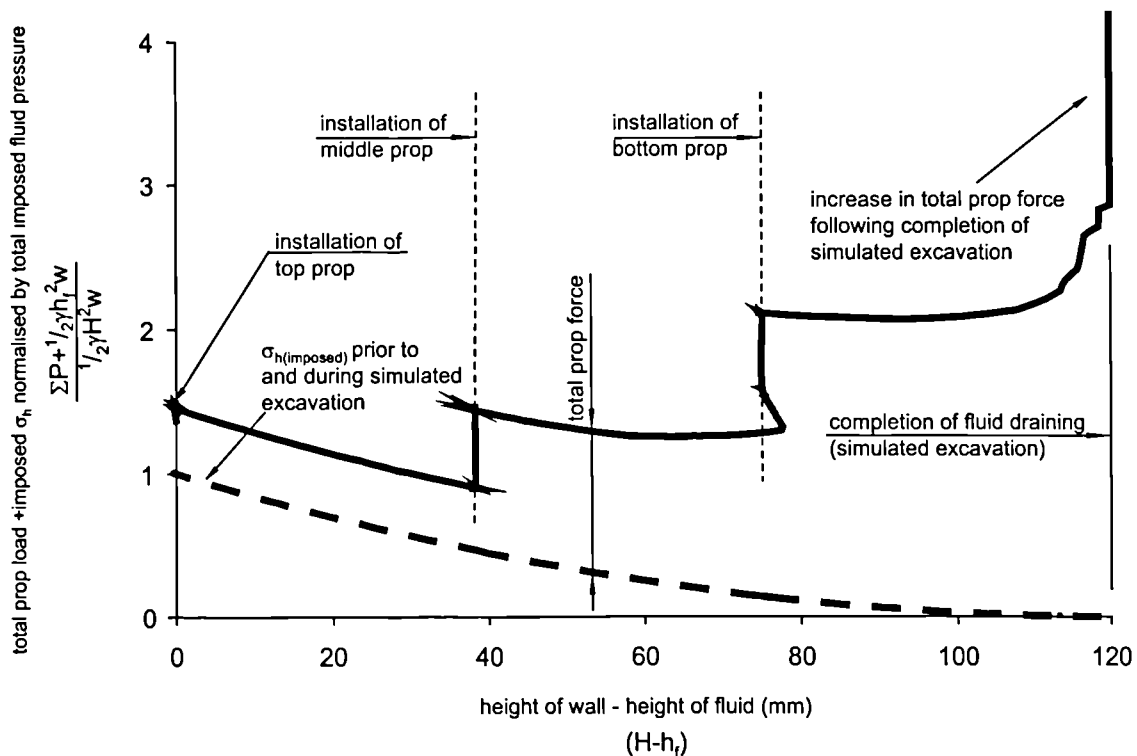


Figure 6.18 Variation of total retaining wall support pressure normalised by total imposed fluid pressure with reduction in height of fluid in a typical test (test AM15). Also shown, to demonstrate the development of the total prop force, is the reduction in fluid pressure during the simulated excavation stage of the test.



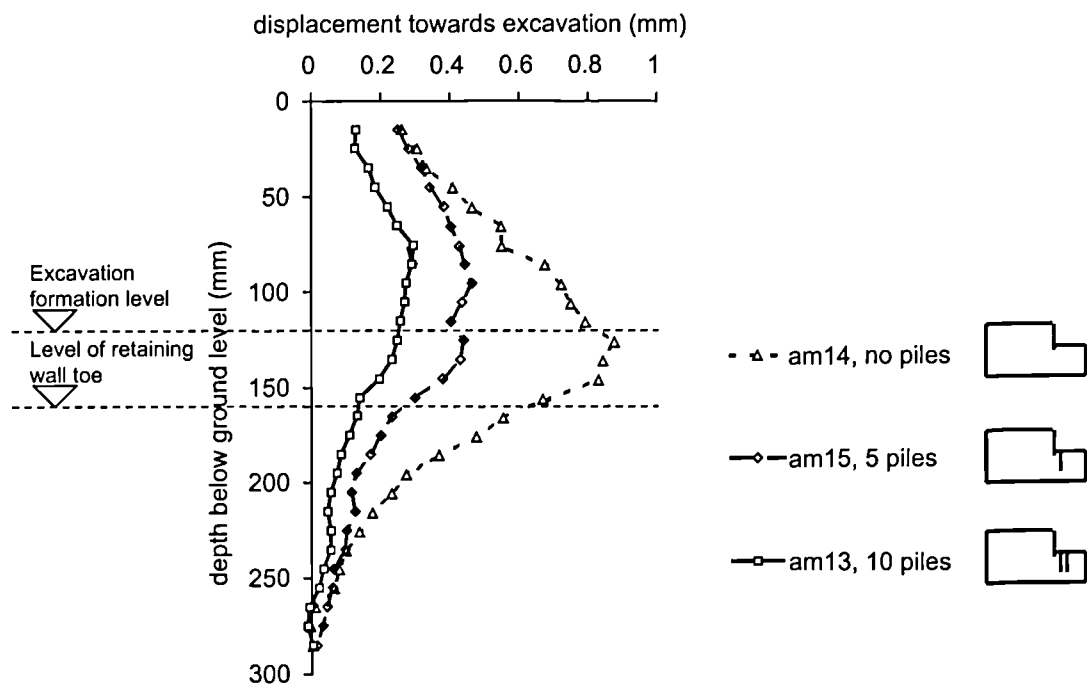


Figure 6.19 Comparison of horizontal displacements behind the retaining wall measured using image processing at completion of the simulated excavation stage of test AM13, AM14 and AM15.

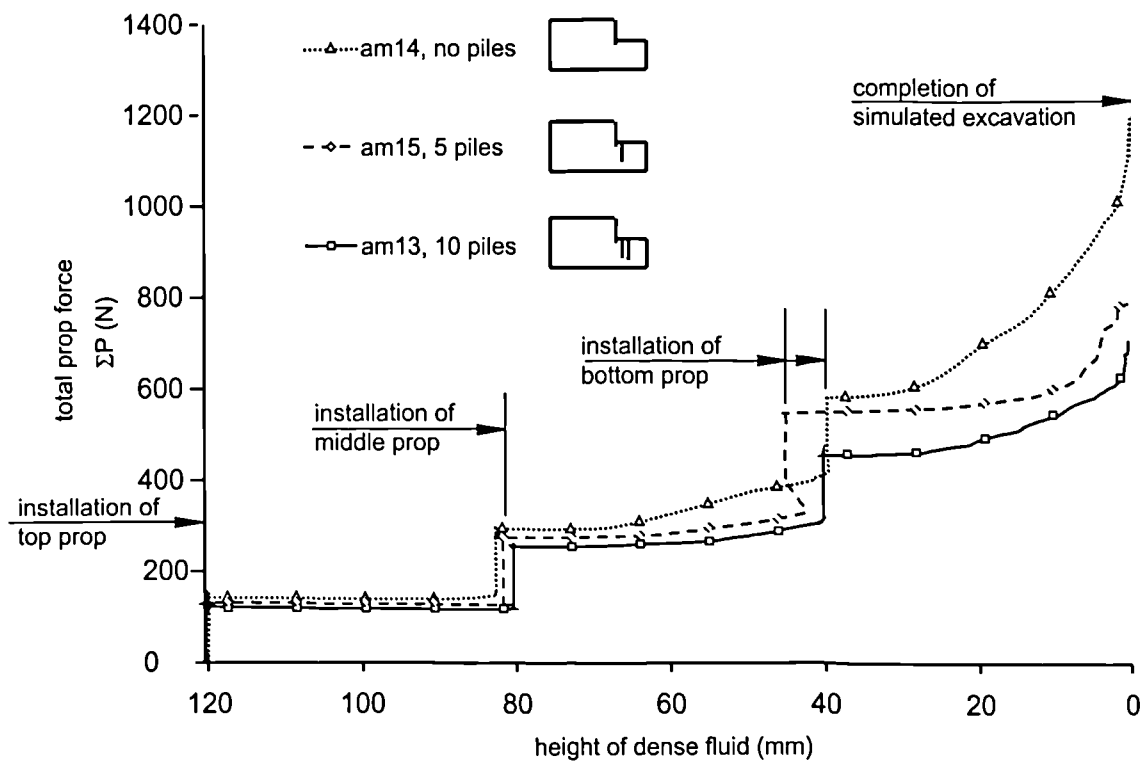


Figure 6.20 Comparison of development of total prop force during simulated excavation in tests AM13, AM14 and AM15.

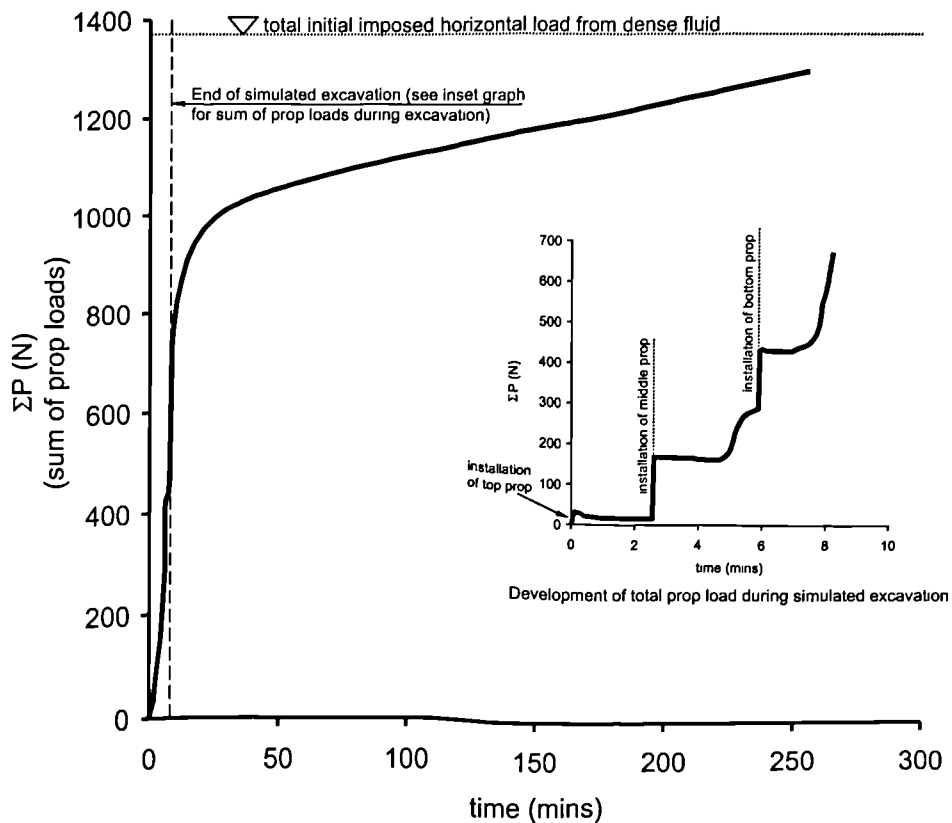


Figure 6.21 Development of total prop load during and after the simulated excavation stage of a typical test (test AM15).

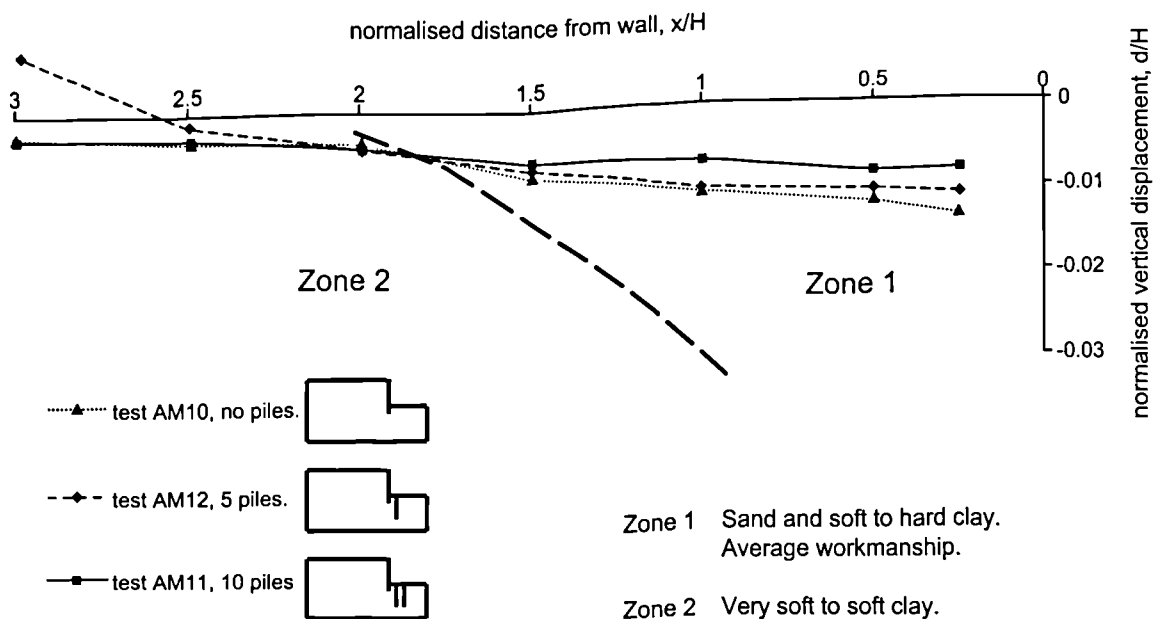


Figure 6.22 Normalised settlement behind the retaining wall at the end of simulated excavation in tests AM10, AM11 and AM12 shown in the context of expected settlements for excavation in various soils from field monitoring data by Peck (1969).

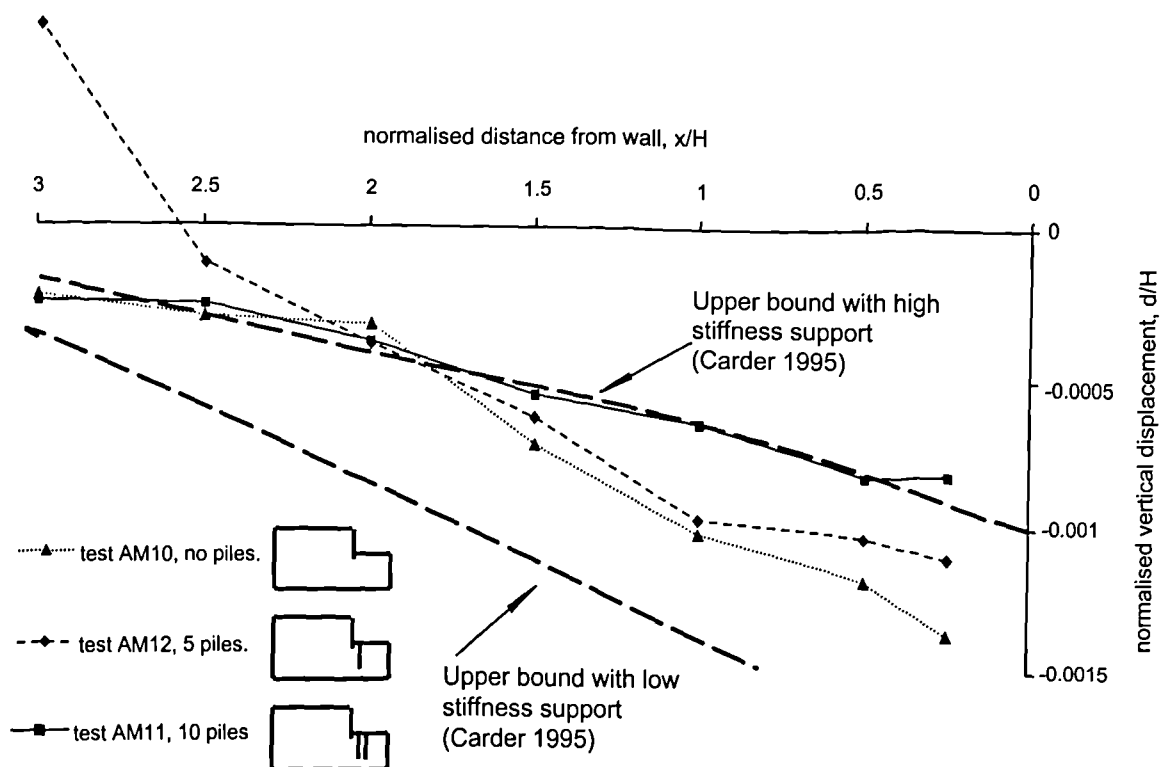


Figure 6.23 Normalised settlement behind the retaining wall at the end of simulated excavation in tests AM10, AM11 and AM12 shown in the context of expected settlements for excavation in stiff clay from field monitoring data by Carder (1995).

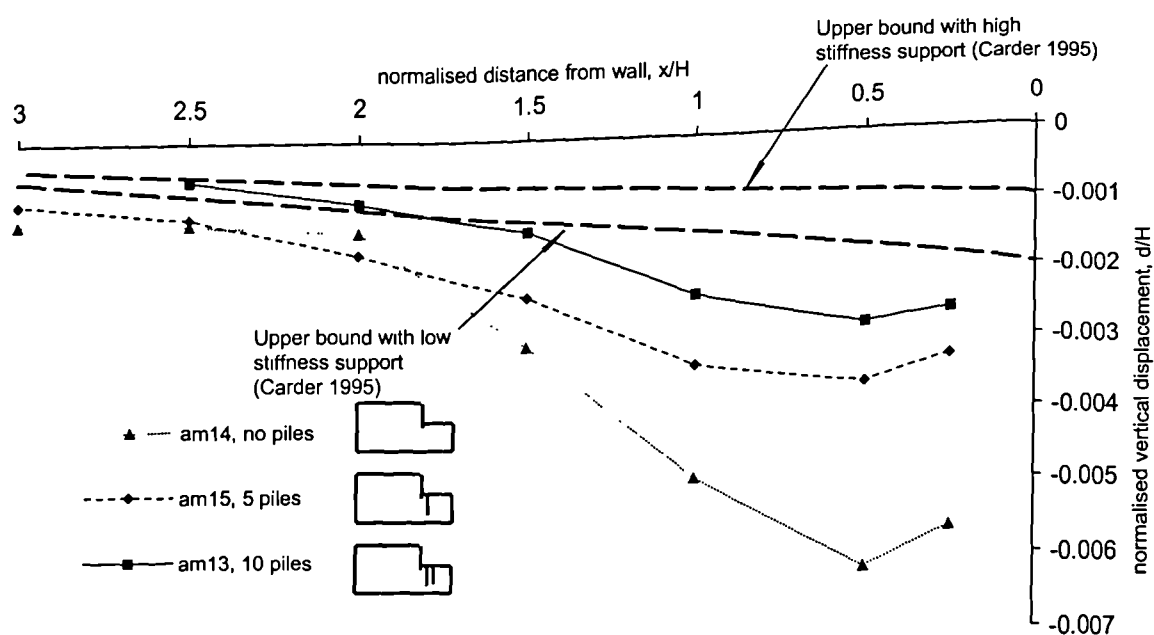


Figure 6.24 Normalised settlement behind the retaining wall at the end of simulated excavation in tests AM13, AM14 and AM15 shown in the context of expected settlements for excavation in stiff clay from field monitoring data by Carder (1995).

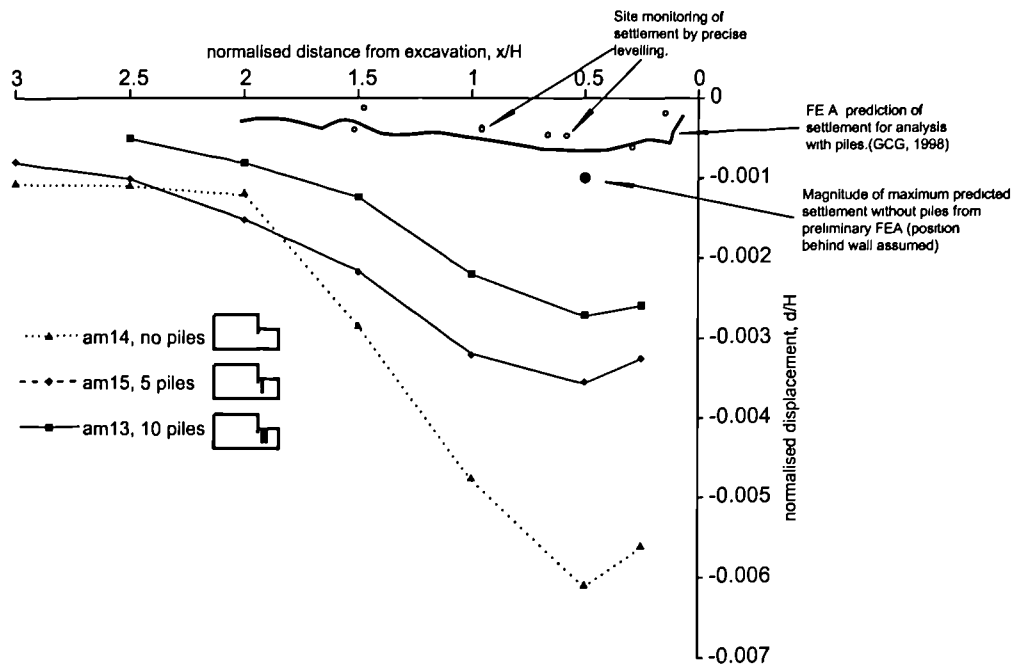


Figure 6.25 Comparison of normalised displacements in centrifuge model tests with predicted and measured normalised displacements at the site of the former Knightsbridge Crown Court.

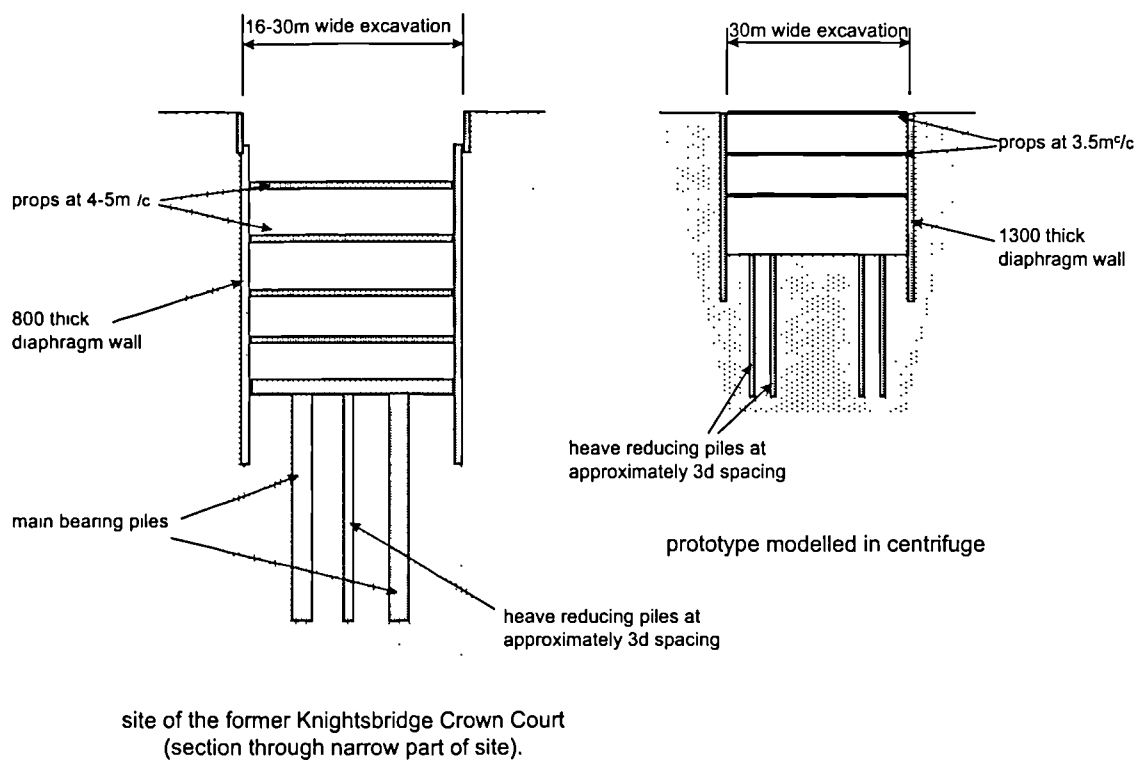


Figure 6.26 Relative geometry of the basement at the site of the former Knightsbridge Crown Court formed using top down construction and the centrifuge model.

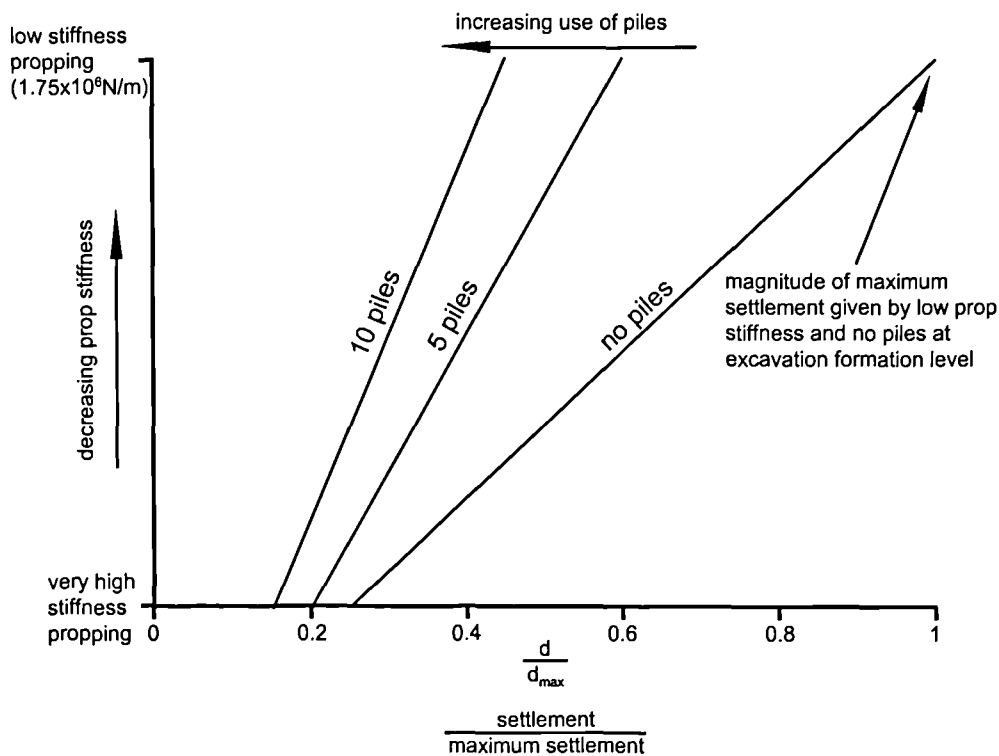


Figure 7.1 Trend lines showing the influence of piles on the magnitude of maximum settlement at ground level upon completion of excavation as suggested by results of centrifuge tests.

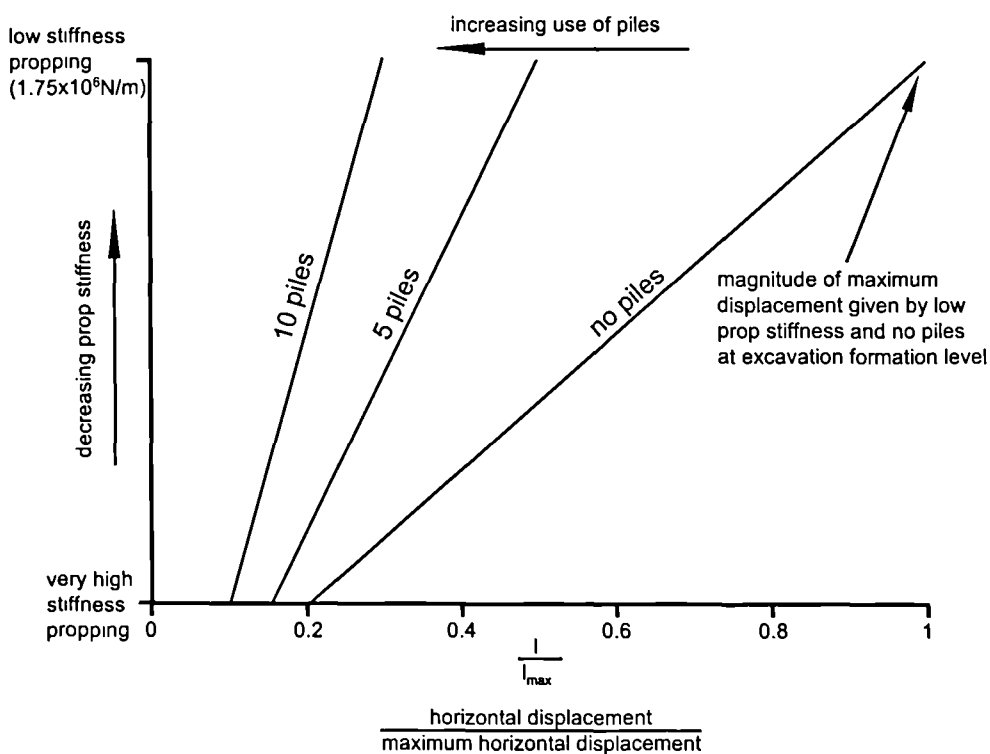


Figure 7.2 Trend lines showing the influence of piles on the magnitude of maximum horizontal displacement behind the retaining wall upon completion of excavation as suggested by results of centrifuge tests.